The study of the dissolution and solubility kinetics of thin polymer films for resist materials

Buley, Jill Marie

Award date:
1993

Awarding institution:
University of Bath

The Study of the Dissolution and Solubility Kinetics of Thin Polymer Films for Resist Materials

Submitted by Jill Marie Buley
for the degree of Ph.D.
of the University of Bath
1993

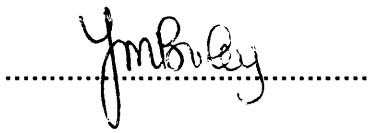

ProQuest LLC
789 East Eisenhower Parkway
P.O. Box 1346
Ann Arbor, MI 48106-1346

Declaration

The work presented in this thesis was carried out in the School of Chemistry, University of Bath between October 1988 and September 1991. Unless otherwise stated, it is the work of the author and has not been submitted for any other degree.

signed 

J M Buley

Acknowledgements

I would like to thank my supervisor, Dr Gareth Price for his guidance and encouragement throughout this work.

I am indebted to the SERC for financial support, to the University of Bath for the provision of research facilities and to Prof. R.S. Davidson at City University for the use of his UV equipment.

Thanks are also due to Dawn and Tony for all their enthusiastic help during their final year projects, and to both the staff and students of the Chemistry department for making my time at Bath an enjoyable experience.

My appreciation goes to the technical staff, Joe, Les and Mike in the workshop, and particular thanks to Mike Harriman for his helpful discussions and support during the construction of the quartz crystal microbalance.

My grateful thanks to Nick for his help with proofreading and for all the support he gave me during my studies at Bath.

Finally I would like to acknowledge Dow Corning for their provision of the time and resources to complete this thesis.

To Mum and Dad

Abstract

Thin polymer films used as resists play an essential part in the fabrication of microcircuits. The resist operates by undergoing some chemical change during irradiation which changes its solubility characteristics, allowing development of the image. Solvent development is controlled by both kinetic factors such as penetration into the polymer and diffusion into the solution, and thermodynamic interactions between polymer and solvent. The work described in this thesis describes the modification of a piezoelectric quartz crystal microbalance to measure each of these phenomena. The results show that all of the factors important in resist development can be monitored and have provided vital information in optimising the performance of particular systems. The use of the QCM method has enabled the measurement of thermodynamic parameters in terms of Flory-Huggins parameters. Volume fraction activity coefficients and interaction parameters have been determined for a series of solvents with PDMS (to validate the method) and polystyrene and PMMA (for use in characterising dissolution phenomena).

The QCM technique has also been adapted for use in the solution phase, enabling the monitoring of changes in polymer dissolution and solubility during development. Hence, an understanding of the parameters that affect the resolution of resists has been gained. This work has concentrated on the effect of polymer molecular weight and its distribution, the type of developing solvent and its temperature and UV irradiation on the dissolution characteristics of a number of polymer/developer systems. The results for PMMA as a model but commercially relevant system, were shown to be comparable to those of other workers and several discrepancies in literature have been clarified. Also, it has been demonstrated that a range of effects fundamental to the dissolution process can be studied. The results

have been extended to both positive (e.g. polystyrene, poly(4-chlorostyrene), poly(phenylmethylsilane)) and negative resists (e.g. poly(vinyl cinnamate)) and yielded information on two major aspects of resist development; swelling and dissolution. The relative rates of these two stages have been investigated to enable the determination of the predominant diffusion mechanism of the resist systems.

The two experimental techniques have allowed correlation of the observed dissolution behaviour with thermodynamic properties so that the behaviour of a particular polymer/solvent system can be predicted. The use of the QCM method in both the vapour and solution phase has been shown to be extremely useful for the determination of the optimum developing conditions of a wide range of systems in a rapid, convenient and economic manner.

Contents

Chapter One

1.0 Introduction

Thin polymer films are used extensively in the semiconductors industry and are an essential part of the production of very large scale integrated circuits (VLSI), particularly in the development of smaller component sizes. VLSI fabrication requires a method for forming accurate and precise patterns, usually on silicon substrates. These patterns are defined by lithographic processes in which the desired pattern is first generated in a resist layer (usually a polymeric thin film) and then transferred *via* processes such as etching into the underlying surface.

During the solvent development of the resist material, the solvent penetration and polymer dissolution are controlled by both kinetic and thermodynamic polymer/solvent interactions. Kinetic factors, such as the diffusion of the solvent into the polymer structure, the relaxation response of the polymer and subsequent diffusion of the polymer molecules into the solvent must be considered. The mobility of the solvent molecules into the polymer is primarily related to their molecular size and the thermodynamic compatibility gives an indication of the strength of the interactions between the polymer and solvent molecules.

The purpose of this study was to use the quartz crystal microbalance (QCM) to obtain information on the dissolution properties of thin polymer films, with the aim of investigating the molecular processes involved in the thermodynamics and kinetics of polymer solution. Such information will prove useful in the understanding of the effect of solvent developing conditions on the ultimate resolution of the resist.

1.1 Photoresist Technology

Microcircuit fabrication requires a method for forming accurate and precise patterns, usually on silicon substrates, to produce the desired electrical characteristics of the circuit and polymeric materials play an important role in the fabrication of these patterns. The definition of the pattern in the resist layer is achieved by exposing the resist to some suitable form of patterned radiation such as ultraviolet light, electrons, x-rays or ions (usually through a mask). The resist contains radiation-sensitive groups which chemically respond to the incident radiation forming a latent image of the circuit pattern, which can subsequently be "developed" by exposure to a suitable solvent to dissolve away either the irradiated (for a positive resist) or unirradiated areas (for a negative resist) of the polymer to leave exposed metal. The areas of resist remaining after development must now protect the underlying substrate during the variety of additive and/or subtractive processes encountered in semiconductor processing. A schematic diagram of the photolithographic process is shown in Figure 1.

1.1.1 Resist Requirements

The performance of a resist depends on a large number of processing variables which makes the determination of the performance of a photoresist more difficult. Variables such as substrate preparation, temperature and time of pre- and post-exposure bake, degree of exposure, developer composition and time and method of development can affect the resolution obtainable.

Resist requirements for microfabrication are similar irrespective of exposure technology. Application of a polymer for high energy radiation

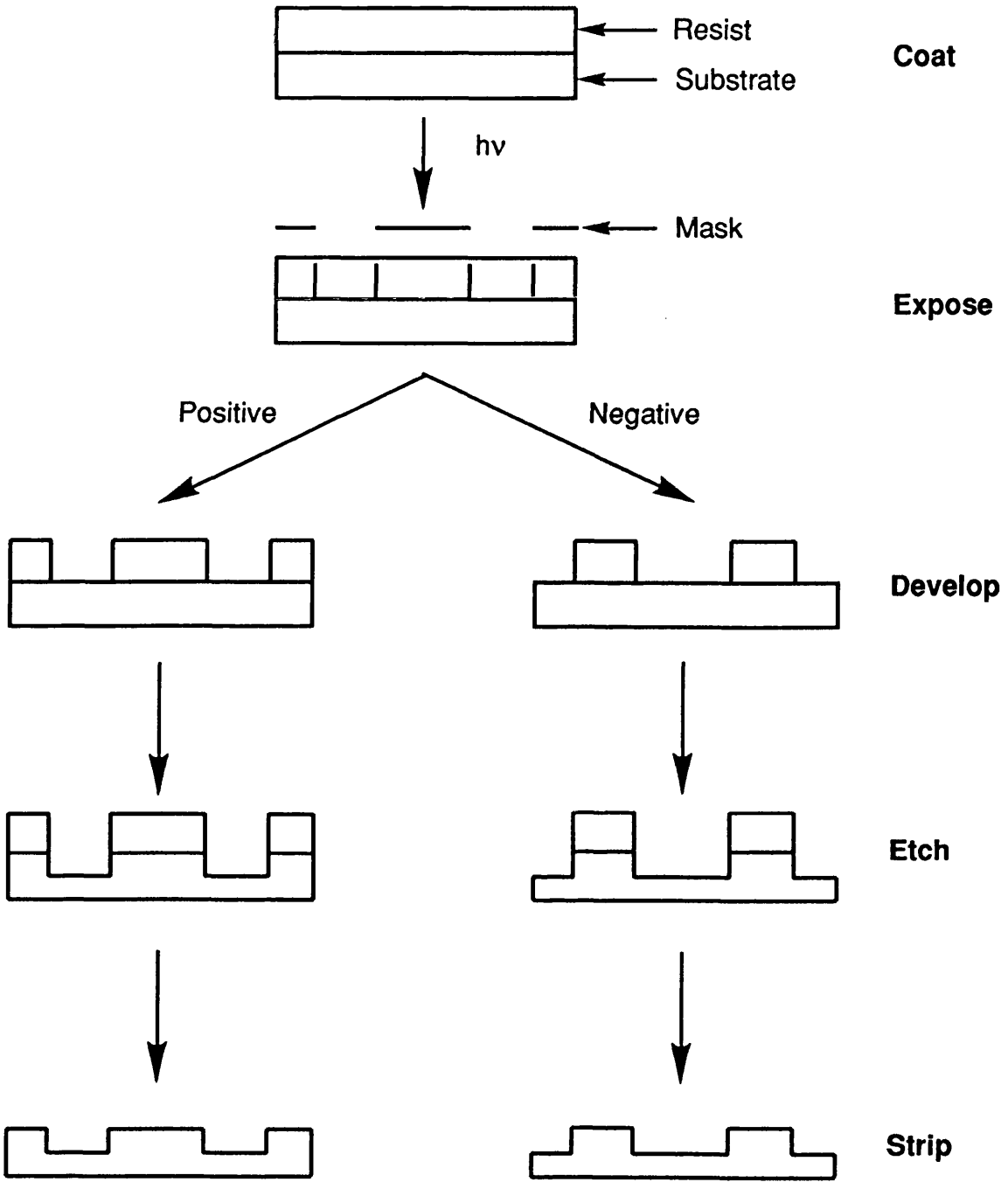

Figure 1: Schematic Representation of the Photolithographic Process Sequence

lithography depends on various parameters such as solubility, adhesion, etch resistance, radiation sensitivity and resolution. Schnabel and Sotobayashi have discussed the effects of these parameters in more detail in a comprehensive review of the different types of polymers that have been considered as resist materials[1]. Solubility in volatile organic solvents is a necessary requirement, since films are normally deposited on a substrate by spin-coating from solution and quick evaporation of the solvent will give a more even film. The resist must be able to withstand the etching environment during the pattern transfer process[2] and must possess adequate adhesion to the substrate (e.g. silicon dioxide and silicon nitride) which will withstand all processing steps. Poor adhesion will lead to marked undercutting (see Figure 2), loss of resolution and possibly complete destruction of the pattern[3].

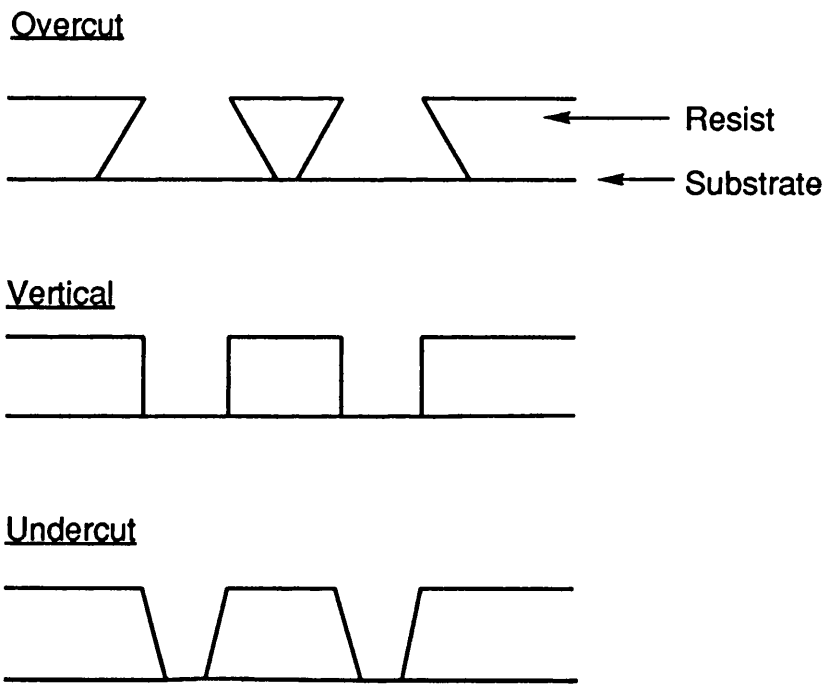

Figure 2: Types of Resist Profiles

In an undercut profile, the shape of the resist is dominated by the dose and reflected exposure rays, while in the overcut profile, the developer dominates the resist profile and removes part of the unexposed film. Etch resistance refers to the ability of the resist to withstand the etching environment during the pattern transfer process[2]. The most common method of pattern transfer is wet chemical etching, which places emphasis on the adhesion and chemical stability of the resist.

Sensitivity and contrast are two very important lithographic parameters of a resist and must be optimised when considering design features that must be incorporated into the resist. They are determined primarily by the chemical composition, molecular parameters and physical properties of the polymer. The sensitivity of a resist is conventionally defined as the input incident energy required to achieve the desired chemical response in the resist. The contrast of a resist is the pattern attainable with a given resist for a particular processing condition. For negative resists, it is related to the rate of cross-linked network formation and, for a positive resist, to both the rate of degradation and the rate of change of solubility. The radiation sensitivity of polymers is generally determined by measuring the thickness of resist layers (d_N) after development as a function of dose[4]. Figure 3 shows exposure curves commonly obtained with positive and negative resists.

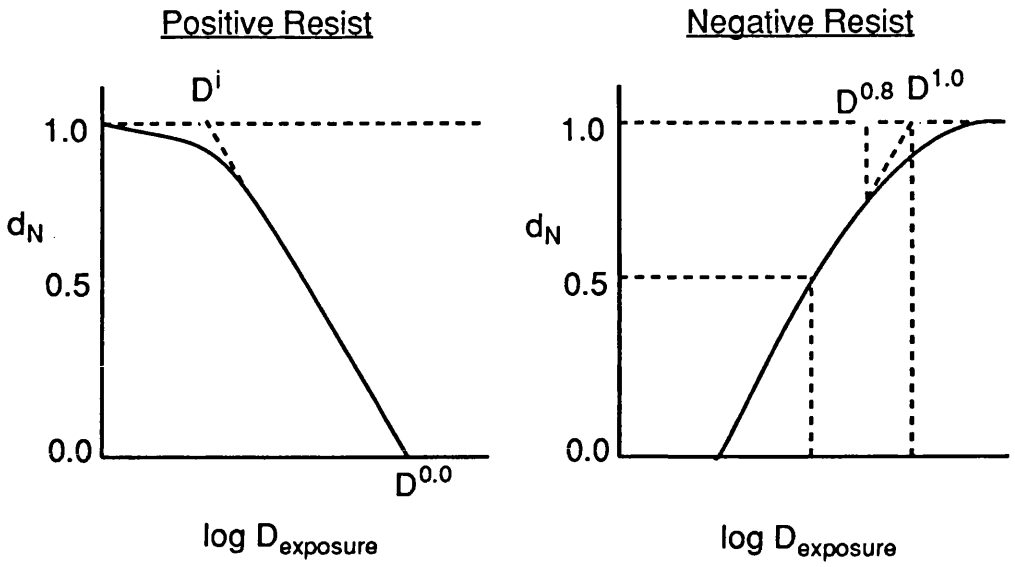

Figure 3: **Schematic Diagram of the Exposure Curves for Positive and Negative Resists**

In the case of positive resists, the dose required to remove, upon development, 100% of irradiated polymer, is a measure of the radiation sensitivity. The corresponding measure for negative resists is the dose required for obtaining 50% of the original resist layer. The contrast factors can be derived from the linear portions of the exposure curves (see Figures 3 and 4).

$$\gamma = \left[\log \frac{D^{0.0}}{D^i} \right]^{-1} \qquad \text{Positive Resist}$$

$$\gamma = \left[\log \frac{D^{1.0}}{D^{gel}} \right]^{-1} \qquad \text{Negative Resist}$$

Figure 4: **Measurement of Contrast for Resist Systems**

The pattern resolution attainable with a given resist, for a particular set of processing conditions, is determined in a large part by the resist contrast. A flow chart detailing a typical resist process is shown in Figure 5.

Reichmanis and Thompson[5] have recently published a review on resist materials for microlithography, which discusses the various lithographic technologies available and the different resists and processes that are being developed for these technologies.

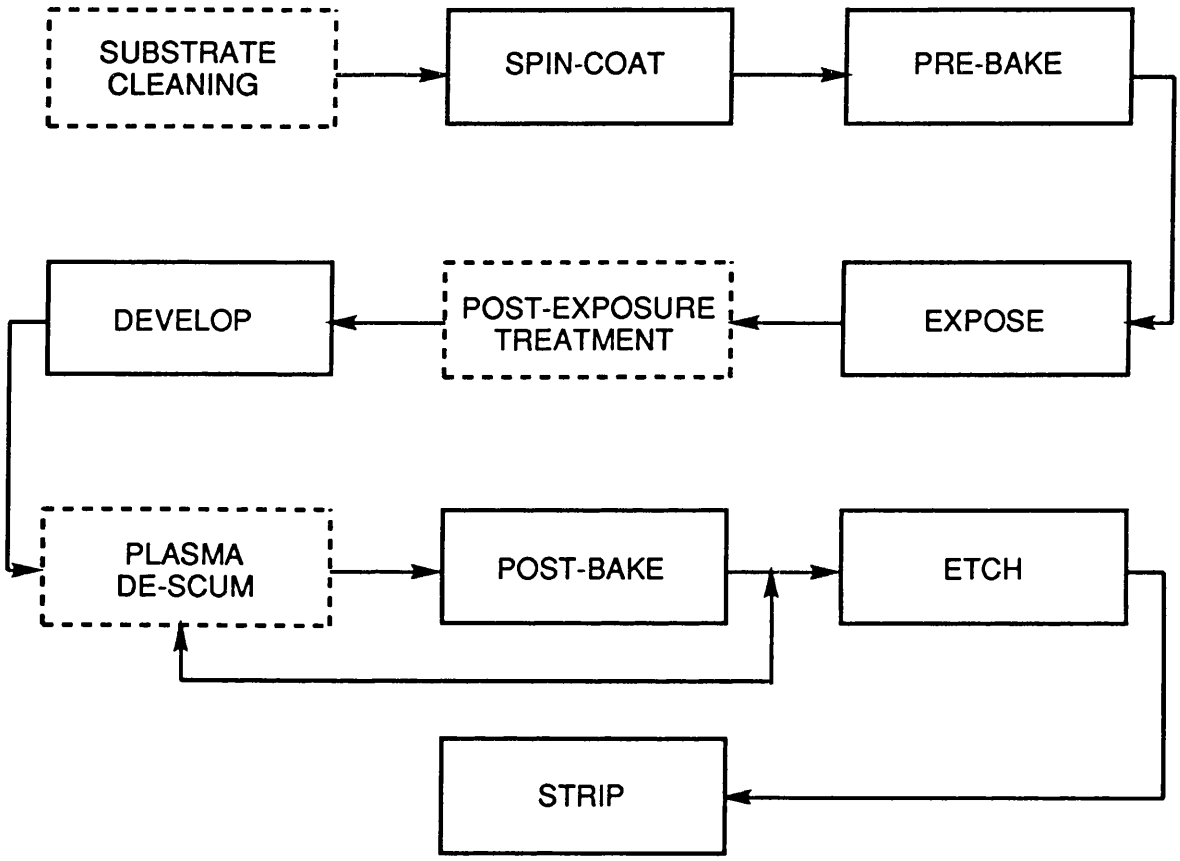

Figure 5: Flow Chart for a Typical Resist Process

1.1.2 Types of Resist Materials

There are a number of publications which give comprehensive reviews on the types of materials that are used as resists and the technologies involved in the microelectronics industry[6,7,8,9]. In his review, Pethrick has made an attempt to predict the changes in microlithographic technology that may occur in the next decade[10].

Resists can be categorised into two types, negative and positive resists depending on the solubility change upon irradiation of the material.

1.1.2.1 Negative Resists

Polymer resists that become less soluble after exposure to radiation are termed negative resists and during development in a suitable solvent, the exposed regions of polymer remain whilst unexposed polymer is removed. The insolubilisation can be brought about by a number of means such as an increase in molecular weight due to polymerisation or cross-linking, or a change in polarity due to formation of more polar groups or more non-polar functional groups.

Current research on negative resists tends to concentrate on the incorporation of radiation sensitive cross-linkable groups into the main chain or side chain to promote cross-linking. The major families of negative resists are primarily the vinyl carbon backbone systems with reactive side chains such as styrenes, halogens and epoxy groups[11].

Taylor and co-workers[12] first reported that the incorporation of a halogen into methacrylate and acrylate polymers resulted in a thousand-fold

increase in their sensitivity to radiation induced cross-linking. This finding has been applied to styrene-based resists by Thompson and co-workers who found improved resist sensitivity when using chlorine substituted styrenes[13]. Generally, the chlorine containing polymers have higher sensitivity and glass transition (T_g) than polystyrene whilst retaining resolution[14]. The chlorine content of the resists can be used as a control of the sensitivity and contrast of the resist system with the contrast decreasing and sensitivity increasing with increased chlorine content[15,16]. Chlorostyrene, chloromethylstyrene and a number of other polystyrenes have been copolymerised with polymers such as siloxanes and polyvinylnaphthalene with enhanced sensitivities having been observed[17]. The incorporation of silicon atoms into the backbone *via* polydimethylsiloxane (PDMS) produces a highly sensitive resist. The high sensitivity of PDMS is due to the weak silicon-carbon bond (140 - 180 kJ mol^{-1}) and the formation of two radicals for efficient cross-linking[8].

In polystyrene-based resists the contrast increases with decreasing molecular weight. However, the lower sensitivity of the lower molecular weight chlorostyrenes is often traded for higher resolution. Swelling upon development can be evident, but may be suppressed by a good choice of developer.

The capacity of the epoxy moiety to undergo efficient cross-linking reactions has been utilised in the resist industry. Hirai and co-workers[18] first reported the use of epoxidised 1,4-polybutadiene as a high resolution (1 μm), highly sensitive electron beam resist, and this sensitivity has since been confirmed by Feit and co-workers[19]. Unfortunately, the contrast of the resist was low and hence did not achieve wide usage. However, this initial work has encouraged the use of epoxy groups to provide radiation

sensitivity in polymer systems, such as the copolymer of glycidyl methacrylate and ethyl acrylate[20].

A simple photodimerisable resist is poly(vinyl cinnamate) made by the esterification of poly(vinyl alcohol) with cinnamoyl choride[21]. Upon irradiation in the deep UV region, the cinnamate groups can dimerise to yield a truxillate as shown in Figure 6. If cinnamates from two chains are involved the cyclic product represents a cross-link. Copolymers of poly(vinyl cinnamate) may be prepared to address particular fabrication requirements, and other photodimerisable groups may be attached such as naphthyl acrylate, styryl acrylate or furan acrylate to improve sensitivity[22].

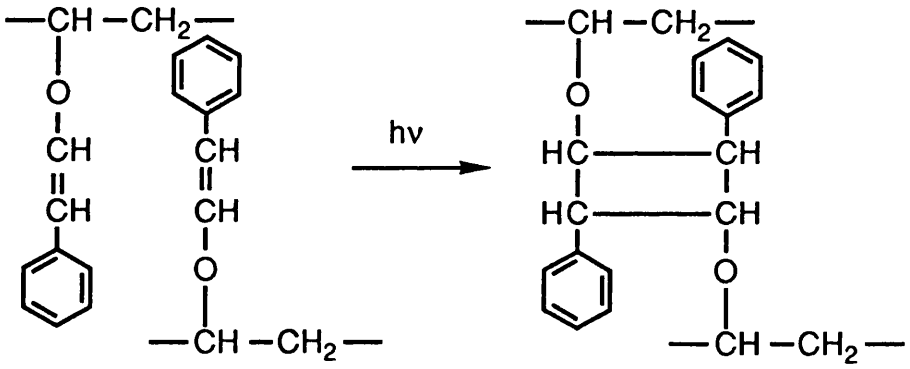

Figure 6: UV-Induced Dimerisation of Poly(vinyl cinnamate)

Negative resists have seen continuing use in the manufacture of circuit boards and microelectronic devices because of their high chemical resistance, good image reproduction qualities and low cost. The sensitivity of negative resists is generally greater than that of positive systems since an average of only one cross-link per chain is required to achieve an insoluble cross-linked network[23]. Most positive systems require several events per chain to affect differential solubility. Since polymer dissolution occurs first by

swelling of the matrix followed by chain disentanglement (see Section 1.2.1), the resolution of many materials is inferior to that in positive systems. However, Novembre and Bowden have shown that by careful selection of developer solvents, high resolution patterns can be obtained in several negative-acting resists[24].

1.1.2.2 Positive Resists

Materials that exhibit enhanced solubility after exposure to radiation are known as positive resists. The enhanced solubility can be brought about by either chain scission or by dissolution-inhibition mechanisms. Positive resists are used widely in the production of VLSI devices because of their high resolution.

The "classic" positive resist that undergoes chain scission upon radiation is polymethylmethacrylate (PMMA)[4,25] as shown in Figure 7. Its popularity in the resist industry is due to a number of factors such as degradation by chain scission without cross-linking, dissolution in several solvents (especially ketones) without appreciable swelling, good adhesion to substrates and good resistance to acidic and alkaline etch solutions.

PMMA was first reported as an electron-beam resist by Hatzakis[25] and is still considered to be one of the highest resolution materials available. Since this first report, the performance of PMMA as a resist has been improved by chemical and physical modifications and these have been reviewed by Moreau[26]. The accepted mechanism of radiation induced cleavage of PMMA involves scission of the polymer backbone which results in a reduction in polymer molecular weight and enhanced solubility of the exposed regions[27]. The sensitivity of PMMA can be improved by increasing

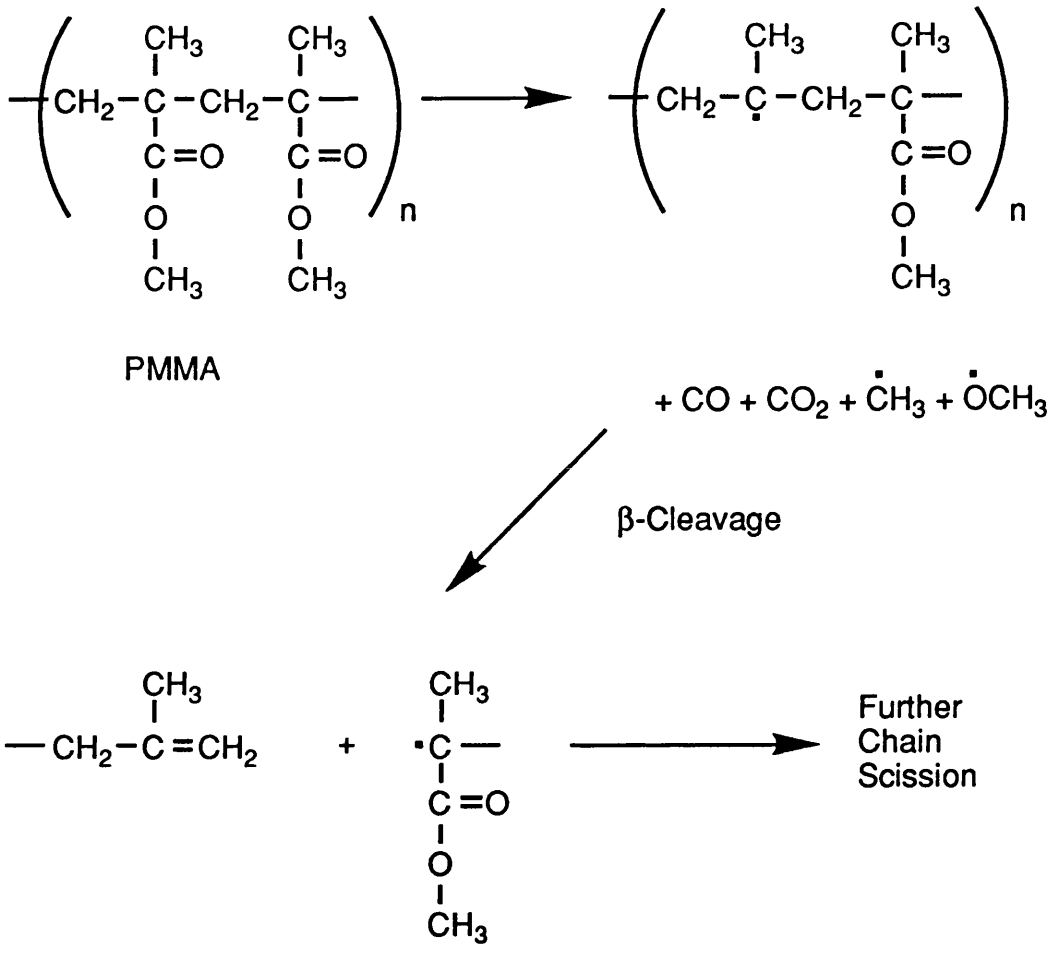

Figure 7: UV-Induced Chain Scission of PMMA

the molecular weight and narrowing the polydispersity with a practical upper limit of about 700000 in number average molecular weight (M_n) without coating difficulties. The efficiency of main chain cleavage can be further improved by replacement of the methyl group with electronegative functionalities, such as chlorine or cyano groups, or by the introduction of bulky groups to provide steric hindrance and hence weaken the main chain. The copolymerisation of the methacrylate with more radiation sensitive components can also improve the sensitivity of the resist.

The dissolution-inhibition resists are typically composed of three components: a novolac resin (phenolformaldehyde), a

diazonaphthoquinone sulphonate ester and a dilute aqueous base. The alkali-soluble resin is rendered insoluble through incorporation of a hydrophobic, radiation-sensitive material. Upon irradiation, the hydrophobic moiety may be either removed or converted to an alkali-soluble species, allowing selective removal of the irradiated portions of the resist by an alkali developer solution. Although the basic components of all dissolution-inhibition resists are the same, changes in the substitution pattern on the novolac resin and/or photo-active compounds lead to changes in resist performance. One deficiency of the novolac resins is their low glass transition temperature which usually ranges from 70 to 120°C, as thermal stability is required to withstand the pre- and post-baking treatment.

A number of organosilicon materials have been investigated as polymer resists and more recently research has begun on the polysilane derivatives[28,29]. Polysilanes are a class of polymers in which silicon atoms constitute the main chain with organic groups in the side chain. All the high molecular weight polysilane derivatives absorb strongly in the UV spectral region, and the position of this absorption is a function of both the nature of the side chain and the molecular weight of the polymer. Irradiation of the polysilanes leads predominantly to chain scission, but the ratio of chain scission/cross-linking is dependent upon the side group. Because of their high silicon content, the polysilanes provide an excellent etch barrier to developing conditions. A number of reviews have appeared in the literature on the use of soluble polysilanes in microlithography[30,31,32].

1.1.3 Application of Resist Materials

The first process in the semiconductor manufacturing sequence involves the coating of the substrate with the resist material. The objective of this step is to obtain a uniform, adherent, defect-free polymer film over the entire substrate. There are several methods by which a support may be coated with a photoresist, and the chosen method depends largely on the uniformity requirement and the thickness of the coating desired[33].

Spin coating is a technique whereby a thin coat of photoresist (0.1 - 5 μm) is applied to one side of a small section of a substrate and is used where a fair degree of uniformity is desirable. Usually the substrate is flooded with a resist solution and then rapidly rotated at a constant speed between 1000 and 10000 revolutions per minute until the film is dry. Fundamental properties which govern film uniformity and thickness include polymer composition, molecular weight, solution concentration (i.e. viscosity), solvent properties and the angular velocity and acceleration of the spinner. Thompson and co-workers discuss the effect of these parameters in more detail[13] and Moreau gives a comprehensive examination of the physics involved in spin coating[26].

Other methods used for the coating of resist materials include spray, dip and roller coating. Spray coating is used to apply very heavy or thick coatings, whilst dip coating provides the most uniform coatings and is used for large-scale production and the treatment of large areas. The resulting thickness of resist is again dependent on the viscosity of the photoresist and to the speed at which the substrate is withdrawn from the coating solution. Roller coating is used for the uniform application of very thin coatings to rigid surfaces, but is not practicable for the coating of small surfaces. Comparison

of all the available coating techniques shows that spin coating prevails as the most dynamic, uniform process capable of the resolution of film thickness required for high resist performance. A comprehensive review of the parameters involved in coating is given by Elliot in his review of integrated circuit fabrication technology[34].

After coating a resist film from solvent, the polymer film contains 1 to 3% residual solvent and may contain built-in stresses caused by the shear forces encountered during the coating process. Prior to exposure, the resist film is baked at a temperature above the T_g (i.e. where the polymer chains are mobile) and the boiling point of the solvent to remove the residual solvent and any stresses formed during coating. Residual solvents will adversely affect both subsequent exposure and developing cycles, and stress in the film may result in loss of adhesion or erratic developing during subsequent processing. During pre-baking, the polymer flow relieves any built-up stress, closes pinholes, planarises the film, and by the formation of an insoluble surface layer produces a desirable induction effect upon dissolution in a developer. Pre-baking therefore ensures that the resist film has uniform properties across the substrate[35].

1.1.4 Development of Resist Materials

Once a resist has been applied to a substrate and irradiated, the next step in resist production is the development[13]. The object of the development step is to remove the exposed or unexposed resist region at a faster rate than the background and in a reproducible manner. It has a great influence on pattern quality and requires more process time than any other step. There have been new developments in this stage of the lithographic process such as Reactive Ion Etching (RIE) and plasma etching[13] which

involves dry etching environments[36]. Dry development has been reviewed extensively by Taylor[37], and advances in these development processes have been taken into account in the design of organic resist materials[38]. However, the solution development of images still remains the most common method for the production of microcircuits. Since development is a major variable in achieving good photoresist geometries, it must be carefully determined and monitored to optimise the process. During the development process, there should be no reduction in original film thickness, minimum developing time (< 1 minute), minimum distortion and swelling and faithful reproduction of the required dimensions. A number of variables can affect the development time such as pre-bake conditions, developer concentration, developer temperature, resist thickness and the amount of mixing. Generally all these variables are fixed except developer concentration and temperature and these are usually used to adjust the development time.

Since differences in development rates play such a crucial role in determining ultimate circuit density, further improvements in VLSI technology depend upon a clear understanding of photoresist dissolution at the molecular level.

1.2 Dissolution of Polymers

1.2.1 The Theory of Dissolution of Polymers

The dissolution of glassy polymers in principle occurs exactly like small molecule dissolution in that the polymer/polymer interactions between the monomer units of the polymer chains are replaced by polymer/solvent interactions between the monomer units and the solvent molecules[39]. However, there are differences in the individual phases of the dissolution process. In the case of a monomeric solid, each solvated molecule is immediately free to move away from the undissolved monomer and into the solvent. Each solvated monomer unit in the bulk polymer though, has a limitation imposed on its mobility because of its covalent bonding to the polymer backbone. After solvation, it can only move away to the extent of the length of the solvated portion of the chain. Only when the other monomer units belonging to the same chain are similarly solvated is the entire chain free to move away from the bulk polymer.

The process of dissolution of a polymer by a liquid consists basically of two stages[39]. First, the small more intrinsically mobile liquid molecules, driven by their chemical potential gradient, diffuse into the polymer matrix to form a gel. Then, swelling and loosening of the interpenetrating and highly immobile chain-like polymer molecules occurs in response to the build-up of internal pressure resulting from the absorption of liquid. As the polymer matrix swells, the mobility of the absorbed liquid molecules typically increases due to plasticisation or the increase in the polymer molecules' segmental mobility, and the penetration tends to auto-accelerate. Finally, as the polymer molecules become separated, they acquire sufficient intrinsic mobility to diffuse away into the surrounding liquid.

The diffusion and relaxation processes are complicated and a number of studies of these processes have been made, but no firm conclusions as to the mechanisms of solution on a molecular level have been reached[40,41,42,43]. Advances have been made in the development of models to predict the transport of penetrants in glassy polymers based on free volume theories and diffusivity and viscous flow parameters[44].

If the response of the polymer matrix to the penetration by the liquid were simply passive, offering no mechanical resistance to liquid absorption, the overall process would be governed solely by random walk diffusion and could be described by Fick's law. Fickian behaviour for diffusion in polymers is described by Case I diffusion and is concentration gradient controlled. The solvent penetration obeys the generalised Fick equation, where the diffusion coefficient (D) normally increases with solvent concentration (c).

$$\frac{\partial c}{\partial t} = \nabla [\, D(c)\, \nabla c \,]$$

However, the response of the polymer matrix to liquid absorption must be taken into account, and then non-Fickian behaviour (Case II diffusion) is observed. The swelling of the glass in gel formation involves large scale segmental motion, the magnitude of which is relaxation controlled. This relaxation process is related to slow redistribution of available free volume by the segmental motions in the relaxing polymer. This affects solvent penetration rates, making them time and sample thickness dependent. Figure 8 indicates the typical solvent concentration profiles observed for the two contrasting diffusion mechanisms.

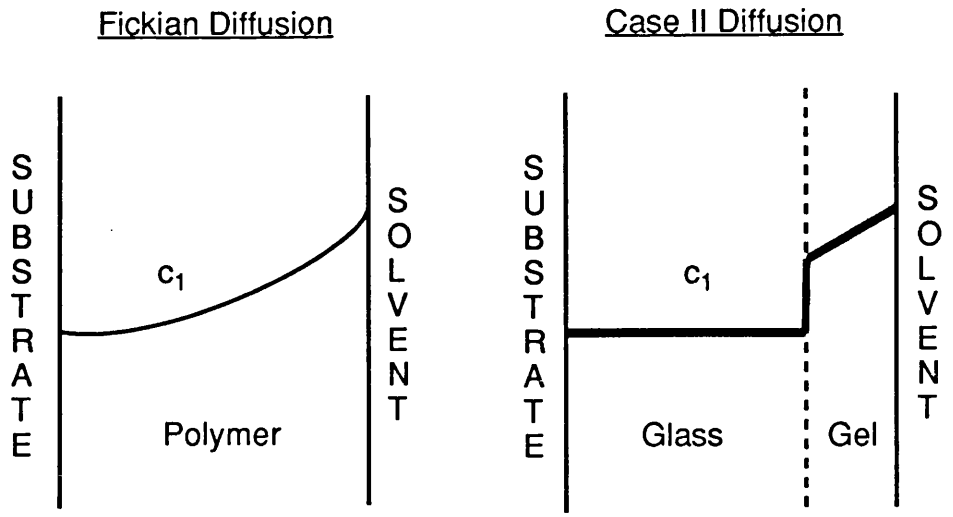

c_1 = Solvent concentration with respect to polymer

Figure 8: Concentration Profiles for the Limiting Cases of Diffusion

The diffusion process can be related to the amount of solvent absorbed, M_t, per unit area at time t.

$$M_t = kt^n$$

where k and n are constants depending on polymer/solvent system.

Fickian diffusion leads to initial direct proportionality between total weight uptake and $t^{1/2}$, while Case II diffusion exhibits an upward sigmoidal curvature. Case II swelling can be characterised by the solvent boundary advancing at constant velocity, the weight gain being directly proportional to time and a uniform solvent concentration behind the advancing front. Vrentas and Vrentas have recently considered the theory of Fickian diffusion in glassy polymer-solvent systems[44]. A number of reviews of non-Fickian sorption in glassy polymers are available[39,45,46,47].

The transition between the two types of diffusion can be seen from system to system and also, in changes in temperature and concentration in a given polymer/solvent system[39]. This has been shown for the transport of methanol in PMMA sheet where a transition from Case II to Fickian transport is seen from ambient temperatures to the boiling point of methanol[48]. Vrentas and co-workers have suggested that the dimensions of the sample may affect the diffusion process[49]. The effect of film thickness and sample history on the parameters describing transport in glassy polymers has also been studied by Hopfenberg[50]. For the n-alkane adsorption by microspheres, spheres, films and sheets of polystyrene, it was found that absorption in submicron microspheres is controlled by Fickian diffusion whereas films (approx. 75 μm) and spheres (approx. 184 μm diameter) sorb according to Case II absorption kinetics.

Ueberreiter and Asmussen[42,51] have related the dissolution rate (s) to the diffusion coefficient for the penetration (D) of the solvent into the polymer by:

$$s = \frac{D}{l}$$

where D is the diffusion coefficient and l is the thickness of swollen layer. The diffusion coefficient has been shown to be related to temperature by:

$$D = D_o \exp^{(-E_a/RT)}$$

where E_a is the activation energy of diffusion.

Typical values for the activation energy for the diffusion of solvents in polymeric solids range from 20 to 80 kJ mol^{-1}. As the size of penetrant increases, the diffusion coefficient decreases but the activation energy increases. The diffusion coefficient is constant over a large range of molecular weight. It has been shown that above a limiting molecular weight, for the dissolution of polystyrene in toluene, although the dissolution rate increases and the thickness of the swollen layer decreases, that D is independent of chain length. This is because the diffusion process involves the "jump" of solvent molecules from one monomer unit to another and therefore will not be affected by chain length.

The overall shape of the solvent molecule will mainly influence the diffusion coefficient while interacting polar groups or the polarity of the solvent molecule should determine the thermodynamic suitability.

1.2.2 Factors Affecting Dissolution Rate

Several factors can affect the rate of dissolution including:

1. Molecular weight
2. Molecular weight distribution
3. Thermal history of polymer
4. T_g of polymer and solvent composition in gel layer,
5. Tacticity of polymer
6. Formation of gaseous products within the polymer film
7. Type of developing solvent and solvent temperature

It is well known that the equilibrium solubility of polymers is dependent upon their molecular weight[52]. This is related to the decrease in

entropy of mixing with increasing molecular weight of polymer in solution. However, high molecular weight positive resists are preferable to those of low molecular weight as increased sensitivity can be obtained[53]. In the high molecular weight resist, for a given area and thickness of resist, there would be fewer molecules and thus fewer scission events would be required to obtain sufficient degradation for complete development.

Ueberreiter and Asmussen have studied a homologous series of polystyrenes in a number of solvents and found that the following relationship held over a wide range of molecular weight (M)[54].

$$s = kM^{-A}$$

where k and A are constants for a particular polymer/solvent system.

The amount of swelling of the polystyrene was found to increase with the square root of molecular weight and increased abnormally above a M_n of 150000, due to strong entanglement of large macromolecules. The diffusion of solvent molecules into the polymer was found to be controlled by the gradient of the chemical potential and dependent on the size and chemical constitution of the solvent molecules. The swollen layer acted as a resistance for the diffusion of the molecules by the diminution of the concentration gradient in this region. They also obtained the following dependence of swollen surface layer (δ) on temperature.

$$\delta = \delta_o \exp^{(-E_a/RT)}$$

Harris[55] found that removal of very high molecular weight molecules from PMMA resists led to considerable improvement to the dissolution rate of

PMMA in solvents. At a given weight average molecular weight (M_w) or M_n, samples of high polydispersity PMMA have been shown to have a higher dissolution rate than those of low polydispersity[56]. Removal of very high molecular weight molecules, which are dominant in determining intrinsic velocity, is found to lend considerable improvement to the rate of dissolution of PMMA in solvent and quality of spin coated films. Harris has concluded that the optimum distribution of PMMA for use as a resist, is one which contains little or no molecules with weights below 50000 or above about 600000.

Lai and Shepherd[53] have studied the effects of the molecular weight distribution on the sensitivity of PMMA as a positive electron resist using methyl ethyl ketone/isopropanol (i.e. MEK/IPA) developer mixtures. The molecular weight and molecular weight distribution were found to have a significant effect on the sensitivity of PMMA. With decreasing spread in molecular weight distribution, the number of scission events for critical exposure is decreased i.e. the sensitivity increases with decreasing heterogeneity.

Solvent mobility in polymeric matrices is strongly affected by its local environment and hence, is very strongly influenced by polymer architecture and by the thermal and mechanical history of the polymer. Gipstein and co-workers[57] have found that the solubility of isotactic PMMA is much greater than that of the syndiotactic and atactic forms. This very high solubility rate of isotactic PMMA is attributed to a low T_g (i.e. 40°C) and greater degree of free volume, and it was found that the molecular weight dependence is stronger for the low T_g than for the higher T_g syndio- and atactic forms.

The effect of heat treatment on the dissolution rate of PMMA has been studied by Greeneich[58] and a strong dependence of the dissolution rate on the pre-bake temperature and time was found. Ouano[59] has made a detailed study on the effect of residual solvent content on dissolution rate of PMMA, and interpreted the relationship between dissolution rate and solvent content in terms of the free volume theory. At high solvent concentrations, the PMMA chain segments may have enough mobility to facilitate solvent diffusion through the polymer matrix, however, as the solvent concentration is reduced, the solvent will reach a concentration whereby it must diffuse through a glassy matrix, thereby reducing the solvent loss dramatically.

Deckmann and Dunsmuir[60] in their evaluation of PMMA as an electron resist, have shown that the sensitivity and contrast of the resist can be altered by pre-baking either above or below the glass transition temperature. Sensitivity improvement was shown to be caused by solvent trapped in the network of the resist pre-baked below T_g. The trapped solvent pre-swells the polymer network so that small perturbations to the molecular weight distribution of the PMMA cause it to become soluble in the developer.

Ouano[59] and Cooper[61] have studied the dissolution rates of exposed and unexposed PMMA samples and found much faster dissolution rates for the exposed samples. Ouano postulated that the formation of microporosity upon irradiation (i.e. by the formation of gaseous products such as CO, CO_2, and CH_4 and radicals such as $^{\bullet}OCH_3$ and $^{\bullet}CH_3$) would open up the polymer structure, hence increasing the diffusion coefficient of the solvent.

The molecular size of the solvent is also found to have a great effect on the solubility of resists, as the diffusion rate of the solvent into polymeric resists is very strongly dependent on the free volume between the highly interpenetrating chains of the polymer. Ueberrieter and Asmussen[42] found that the solubility rate of a polymer was closely related to the penetration rate of the solvent. This was demonstrated by the strong dependence of the solubility rate of polystyrene on the solvent molecular weight of a homologous series of alkyl acetates. A sharp drop in solubility rate of the polymer was found between propyl and butyl acetate which was attributed to a change in the diffusion mechanism of the solvent from a relatively "unhindered" to a highly "hindered" diffusion process.

Normally the suitability of a solvent is discussed in thermodynamic and kinetic terms, where the kinetic influence is reflected in the value of the diffusion coefficient while the thermodynamic suitability influences the thickness of the swollen layer[39,62,63]. The solvent mobility is primarily related to its molecular size whereas thermodynamic compatibility is associated with the strength of the interactions between structural groups of both polymer and solvent molecules. An appropriate measurement of thermodynamic compatibility is given by the solubility parameter, δ[64]. The Flory-Huggins interaction parameter, χ can give another measure of polymer compatibility[52] (see Section 1.4.1). For a good solvent, there is a preferable interaction between the polymer and solvent and the chains are extended and this is reflected in low χ value ($\chi < 0.5$). By contrast, in a poor solvent, polymer chains are coiled to prevent interaction with the solvent, with high χ values ($\chi > 0.5$) obtained. In intermediate solvents, the chains are in an unperturbed state and these are known as theta solvents.

The development of resists often involves the use of solvent/non-solvent systems with the non-solvent acting as a moderator[33]. In their dissolution/swelling studies of PMMA in MEK/IPA and methyl isobutyl ketone (MIBK)/methanol mixtures, Manjkow and co-workers[65] have observed a sharp transition between complete solubility and almost total insolubility, and found a temperature dependence of the position of this transition. The addition of small amounts of low molecular weight non-solvent has been found to increase the rate obtained with a higher molecular weight solvent[66,67]. The increase in dissolution rate may be attributed to the small size of the molecule penetrating rapidly into the polymer structure[39].

1.2.3 Experimental Methods for Polymer Dissolution

Traditional methods for the determination of resist film thicknesses as a function of time in the developing solvent, tend to rely on the repeated development of a resist for various pre-determined times, followed by quenching in a non-solvent and baking to drive off the developer before measuring the remaining film thickness[40].

One of the simplest methods for polymer dissolution rate measurements is the "Dip and Dry" method[40,58]. Pieces of resist-coated wafers are immersed in a developing solvent and removed after a measured development time, dried and baked for a short time. The thickness of the remaining film is then measured using techniques such as diamond stylus measurements, interferometry and ellipsometry. However, the method is tedious and is prone to errors due to the presence of induction periods and failure to stop dissolution immediately when desired.

Ueberreiter and co-workers[68] were amongst the first workers to have made a study of the rate of dissolution of polymers using the "Dip and Dry" technique. They investigated the dissolution process by using pellets of a solid glassy polymer immersed in flowing solvent and a micrometer stage-equipped microscope to study solvent penetration and pellet dissolution rates. They suspended carbon black of very fine particle size in the pellets and observed the surface layer of the polymers *via* the microscope. By using refractive index measurements, solvent penetration was monitored by the rate at which the solvent (and carbon black) front advanced into the pellet, dissolution rates were calculated from the rate at which the polymer/solvent boundary receded.

Ouano and Carrothers[59] extended Ueberreiter's technique to more closely simulate photoresist dissolution by using pressure-moulded or cast film samples in a holder that ensured a one-dimensional dissolution process. They developed a microscopic technique that utilised the optimum angle of illumination microscopy (i.e. critical angle microscopy) rather than dyes to follow moving layer boundaries. By this method the effect of polymer tacticity, T_g, thermal history of the polymer and solvent swelling power on dissolution dynamics could be monitored. Qualitative measurements of the dissolution rate of polymer films could be made by following the "Dip and Dry" procedure.

More recently, several *insitu* monitoring techniques for photoresist development have been reported. Konnerth and Dill[69,70] have developed a very high speed scanning spectrophotometer to measure the relative reflectivity of the resist sample as a function of wavelength. However, these techniques require a complex method for converting relative to absolute reflectivity to determine film thickness.

A laser endpoint detection system based on interferometry principles has been developed[71]. The intensity of reflected light oscillates periodically as the film thickness of polymer on a reflecting substrate decreases. The period of oscillation is a function of the indices of refraction of the solvent, polymer and wafer as well as the wavelength of the light. The change in intensity can be used to interpret the dissolution of the film. However, complications arise when the film swells or the formation of a surface transition layer occurs. The systems only provide data to within an integer multiple of one-half of a wavelength and so the resolution is not sufficient for detailed kinetic studies. However, in some cases a transition layer can be measured during laser interferometry, and Krasicky and co-workers[72] have studied the dissolution process of PMMA in MEK and detected a transition layer.

An ellipsometer (psi-meter) has been developed by Flack and co-workers for the *insitu* measurement of resist film thickness in developer solutions[73]. A psi-meter is a single element rotating polariser ellipsometer which modulates the polarisation of an incident laser beam and measures the intensity fluctuations of the reflected light. This technique has also been employed by Greeneich to monitor photoresist thickness as a function of time. Unfortunately, the method relies heavily on complex calculations.

There are several other techniques which can be used to measure dissolution rates and thin film processes[74] including refractometry, NMR[75], low frequency capacitance and critical angle microscopy[59]. Rodriguez and co-workers[67] give a review on the methods for dissolution rate measurements.

Recently a group from IBM have published details of the construction[76] and operation of a quartz crystal microbalance (QCM) for the characterisation of dissolution kinetics of thin films[77,78]. The monitor is capable of resolving such fine detail as the periodic modulations in photoresist dissolution rates due to standing wave interference effects during exposure. The QCM was found to be a good method for monitoring polymer dissolution as it is a highly accurate, sensitive and continuous process and thin films can be measured hence simulating the conditions used in the industrial processing of resist films. The use of the QCM in the vapour and liquid phase is described in the following sections.

1.3 Quartz Crystal Microbalances (QCM)

1.3.1 Theory of the QCM

The QCM utilises the piezoelectric effect of certain types of quartz crystals which show a characteristic resonant vibration frequency in an electric field. The piezoelectric effect was discovered in 1880 by Pierre and Jacques Curie[79] and is observed when pressure exerted on a small piece of quartz produces an electrical potential between the deformed surfaces. The application of a voltage produces the converse effect by causing physical displacements of the quartz at a resonant frequency.

This resonant vibrational frequency has been shown by Sauerbrey[80] to change in direct proportion to the mass of any layer of material coating the crystal. He exposed a torsional beam microbalance and a quartz plate to the same depositing flux and showed that a shift in resonance frequency was proportional to the deposited mass within ±2%. Sauerbrey's theoretical predictions have since been confirmed and extended by Oberg and Lingensjo[81], Behrdt and Love[82], Warner and Stockbridge[83], EerNisse[84], Miller and Bolef[85] and Lu and Lewis[86].

The resonant frequency of the crystal is dependent upon the physical dimensions of the plate and the thickness of the electrodes upon it. Heising[87] has established that the orientation of the quartz crystal with respect to crystallographic axes has an important effect on the resonant frequency. The mode of vibration that is most sensitive to the addition or removal of mass for a quartz crystal resonator is the high frequency thickness-shear mode (see Figure 9).

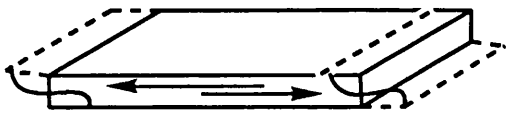

Figure 9: The Fundamental Thickness-Shear Mode of Vibration

To make a quartz crystal plate oscillate in the thickness-shear modes, the plate must be cut to a specific orientation with respect to the crystal axes. The cuts belonging to the rotated Y-cut family such as AT and BT-cuts are representative. For the purpose of monitoring thin-film deposition processes, almost all commercial QCMs use AT-cut quartz crystals oscillating in the fundamental thickness-shear mode. The AT-cut (see Figure 10) is commonly chosen because its resonance frequencies are nearly temperature independent in the neighbourhood of room temperature. Brice[88] gives a review on the types of crystals suitable for quartz resonators and the factors affecting their performance.

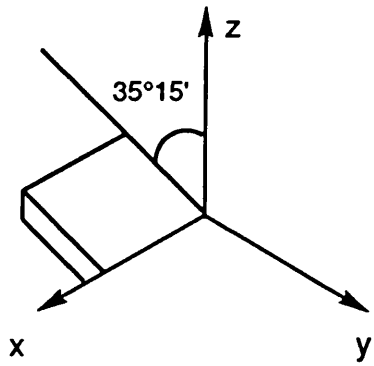

Figure 10: AT-Cut Quartz Crystal Plate

Schumacher[89] has recently considered the interfacial phenomena at the solid/liquid junction such as the influence of solid deposits, surface

roughness, surface stress on the resonant frequency of the crystal and found that these factors can greatly contribute to the resolution obtained.

Prior to 1970, most quartz crystal monitors employed the following equation proposed by Sauerbrey[90], to determine the deposited mass:

$$\frac{\Delta F}{F_q} = \frac{- m_f}{m_q}$$

where ΔF is the resonant frequency shift, F_q is the original resonant frequency, m_f is the areal density of deposited film and m_q is the areal density of the quartz plate.

The original derivation of this equation was not mathematically rigorous, and derivations with more sound theoretical justifications have since been given by Warner and Stockbridge[83], using a perturbation analysis to the loaded quartz resonator and by Miller and Bolef[85], based on the model of a one-dimensional acoustic composite resonator. Up to a limit of $m_f/m_q = 0.01$, they found that Sauerbrey's equation is a useful approximation because the deposited mass or thickness is linearly proportional to the change of frequency. Further work on higher mass loadings led to the insertion of the frequency constant N into the Sauerbrey's equation[77].

$$\Delta F = - \left(\frac{F_q^2}{N \rho_q} \right) m_f$$

where ρ_q is the density of quartz crystal (2650 kg m^{-3}), N is the frequency constant ($F_q t_q$) and t_q is the thickness of quartz crystal resonator.

By extending the analysis of the acoustic composite resonator by Miller and Bolef, Lu and Lewis[86] demonstrated experimentally that the following theoretically valid equation is highly accurate for a mass load as high as m_f/m_q of about 0.7. They have used a one-dimensional acoustical composite resonator model to study the behaviour of a quartz-crystal resonator with large mass loads, and the film thickness (t_f) and mass of polymer coating can be calculated from the following equation:

$$\rho_f t_f = -\left[\frac{(F_c - F_q)\,\rho_q v_q}{2F_q^{\,2}}\right]$$

Where ρ is the material density, v is the shear wave velocity in the material, f and q denote the film and quartz crystal respectively and F_c is the mechanical resonant frequency of deposited film if it were isolated. For materials with a spatially uniform density, the area density of the polymer film is equivalent to the product of thickness and density. However, the mass must be uniformly distributed and completely cover the quartz crystal, and the area covered by the deposited material should be known precisely.

Lu and Lewis have further shown that, if the added mass is limited to a small area and to an arbitrary location on the crystal surface, the mass induced frequency shift will depend on the position of the deposited mass. The sensitivity of detection of the crystal is inversely proportional to the square of the electrode diameter and thickness of the crystal[91]. The amplitude of the oscillation of the crystal is a maximum at the centre of the electrodes and near zero at the edges where the electrical connections are clamped as demonstrated by Ullevig and co-workers[92]. In the general case, the relationship between differential sensitivity and the radius is a bell-

shaped function. This indicates the importance of ensuring the complete coverage of the crystal when coating.

The current most widespread application of the QCM is in thin film science and technology i.e. as a thickness monitor for deposited thin solid films. Piezoelectric quartz crystal resonators have a sensitivity to mass changes of 10^{-12} g under optimum conditions. This sensitivity has led to a variety of different commercial and research uses. Such applications include the use of piezoelectric crystals for the detection of moisture in hydration studies, the selective gas detection in chromatography, the measurement of solubility of vapours in polymers and the study of the corrosion of metals. Further applications of the QCM in both the gas and liquid phase are detailed in the following sections.

1.3.2 Applications of the QCM

1.3.2.1 QCM Measurements in the Gas Phase

The concept of measuring mass using the frequency to deposited mass relationships of Sauerbrey has been exploited extensively in the design of selective sensors for the gas phase. Recent reviews by Guilbaut[93] and Alder[94], identify the current uses and areas of research for the QCM.

The QCM has been used as a detector for chromatography owing to the mass sensitivity, simplicity and ruggedness, all of which recommend it for portable and on-site remote operation[95]. King, in 1964, was the first to use the quartz crystals in this fashion, by using gas chromatography stationary phases on the crystal coating material to improve the selectivity for certain

groups. A universal mass detector based on a resonating piezoelectric crystal for liquid chromatography was developed by Schulz and co-workers[96].

Polymer coated crystals have been used routinely for measuring vapour solubilities of a wide variety of plastics and elastomers[97,98]. Equilibrium between vapour and rubber is almost simultaneous mainly because the film is so thin. The data produced is precise, allowing the observation of subtle changes in the polymer. This rapid equilibrium has led to the extensive use of QCMs in the area of surface science. Ognjanovic and co-workers[99] have recently developed a new method of interpreting data from the QCM technique which enables the study of the variation of surface concentration of 1-iodo-n-hexane on polystyrene with respect to time at the vapour/polymer surface. Good agreement was obtained between the QCM data and Rutherford backscattering techniques, with the QCM offering distinct advantages such as increased sensitivity and the capability of collecting swelling data continuously with time.

Levenson[100] has produced a brief survey of the QCM surface science applications which include the chemisorption of gases on thin films, in molecular studies of gas/surface interactions and in physical adsorption.

Hlavey and Guilbaut[101] have reviewed the application of the piezoelectric quartz crystal in different areas of analytical chemistry. The review details the usefulness of the piezoelectric crystal as a sorption detector in polymer research. Further reviews have been published on the use of piezoelectric crystals for mass and chemical measurements[94,102,103].

1.3.2.2 QCM Measurements in the Liquid Phase

Studies of the effects of liquids on quartz crystal resonators have only appeared recently in the literature. In comparison with the use of piezoelectric detectors in the gas phase, only a small number of studies of the operation of these sensors in liquid have been described.

Adsorption measurements using a crystal are more difficult to obtain in a liquid than in the gas phase as there are greater energy losses at the crystal/liquid interface, which makes it more difficult for the crystal to maintain a stable oscillation. The frequency shift of the crystal is proportional to the ratio of the kinetic energy of the deposit to that of the bare crystal[83]. If the deposit forms a distribution of droplets rather than a uniform film, then the influence of viscous effects is increased.

The dampening, D of the crystal resonator is defined as the reciprocal of the quality factor Q.

$$D = \frac{1}{Q} = \frac{\text{Energy dissipated per cycle}}{\text{Time averaged energy store in the resonator}}$$

For an air-backed quartz transducer, a quality factor of about 15 is obtained if it is radiating into water but this is increased to 100, if air is substituted as the load, hence it can be seen that a large dampening effect is observed with water as the load[104].

Because of the problems associated with the dampening effect of viscous liquids, most of the research associated with the use of the QCM in the liquid phase has centred round the QCM circuitry and crystal mounting.

Konash and Bastiaans[105] have made attempts to overcome the dampening problem. They produced a novel flow cell design in which the method of crystal mounting appears to have compensated for the increase in energy loss by allowing the liquid to come into contact with only one face of the crystal. They observed changes in the resonance frequency of the crystal when different liquids passed through the cell, and attributed these changes either to density differences or to surface adsorption. They managed to achieve stable adsorption exclusive of density effects. They found however, that the sensitivity was poor and that the coating on the crystal became saturated with analyte and, in addition, was gradually removed by solvent action.

Recently, several groups have adapted the QCM for solution work with concurrent electrochemical experimentation[106]. This instrumentation can measure both the mass change and the charge passed at an electrode surface. Such measurements have been applied to the study of metal deposition[107,108], ion fluxes in polymer films[109,110,111] and several other interfacial phenomena[112,113].

Deakin and Melroy[114] have reported the application of the QCM to the *insitu* study of the oxidation of aluminium in a solution of ethylene glycol and ammonium pentaborate. They found that they could quantitatively study the growth and dissolution of thick, passive oxide films. However low concentration solutions had to be used as the viscosity of the solvent at higher concentrations causes the oscillation of the crystal to cease.

Nomura and co-workers[115] have made an examination of the change of frequency obtained when a quartz crystal was immersed in solvent mixtures. They found that the change in oscillation frequency

depended on the density and viscosity of the solvents, whilst the solvent flow had little effect on frequency change. They found good agreement between measured and calculated frequency changes when the crystal was immersed in organic solvents. However the oscillation frequency is quite sensitive to stresses caused by mounting and the changes in the hydrostatic pressure of the fluid. They have also studied the dependence of crystal frequency on temperature[116] and found that between 20 and 27°C, the transistorised oscillator gave a pronounced decrease in frequency of 1 kHz.

The shift of resonance frequency of a crystal when brought in contact with a viscous liquid was calculated by Kanazawa and Gordon[117].

$$\Delta F_L = \frac{F_0^{1.5} (\eta_L \rho_L)^{0.5}}{\pi \mu_Q \rho_Q}$$

where F_o is the oscillation frequency of the blank crystal, η_L and ρ_L are the viscosity and density of the liquid, and μ_Q and ρ_Q are the shear modulus and density of quartz, respectively.

In their study of the frequency changes resulting from metal deposition and from oxide formation, Bruckenstein and Shay[118] have shown that the mass sensitivity of the QCM can be the same in the fluid as in vacuum. They have considered some of the experimental aspects of the use of the QCM in solution[119]. The employment of reference and indicator crystals has helped to compensate for liquid density changes[108]. *Insitu* electrogravimetric studies of sub-monolayer and many monolayer thick electrodeposited and electrosorbed films have been measured by this technique. The high sensitivity of the QCM technique has also made it a

useful tool in the study of the swelling behaviour and stability of Langmuir-Blodgett films in the aqueous phase[120].

Recently, the QCM has been applied as a "biosensor" in which an immunological reaction that occurs at an interface of a transistor results in an output of an electrical signal[121,122]. The antigenic component is immobilised on an auxiliary thin film or directly on the crystal surface, and the antibody in solution is detected by reaction with the immobilised antigen.

Hinsberg and co-workers have introduced a method for the measurement of dissolution kinetics of thin films using a piezoelectric crystal attached to a microbalance[78]. In a later paper, Hinsberg and Kanazawa[76] published details of construction and operation of the QCM for the characterisation of dissolution kinetics of thin films. The instrument allows the accurate characterisation of etching behaviour of very thick and rapidly dissolving films and can be used to examine photoproduct effects on resist dissolution[77]. By adapting the design of a QCM from the literature, we have been able to construct a QCM dissolution apparatus capable of monitoring polymer dissolution, and have used this monitor to study the factors affecting polymer dissolution.

1.4 Thermodynamics of Polymer Solutions

In the previous sections, we have introduced the theory and methods of study of the dissolution kinetics of polymer/solvent systems. In order to correlate the factors that affect the dissolution kinetics with the diffusion of solvent into the polymer structure, we need the ability to measure the polymer/solvent interactions. Hence an understanding and an experimental method to measure the thermodynamics of polymer solutions is required.

1.4.1 The Theory of Thermodynamics of Polymer Solutions

Solutions of high polymers and other large molecules show striking departures from the laws of ideal solutions. Experimental measurements of the activities of low molecular weight substances in polymer solutions showed, as early as the 1930's, that polymer solutions are far from ideal. Meyer and Lühdemann[123] first suggested that deviations from ideality of polymer solutions were due to the length and consequent number of conformations of the polymer chains. Fowler and Rushbrooke[124] introduced the concept of a rigid lattice whose lattice sites are occupied either by polymer or solvent segments. Huggins[125] and Flory[126] extended the lattice method to athermal mixtures of monomers and chain polymers, and the relationships derived from this theory have been used in this thesis.

From the point of view of thermodynamics, the properties which are of particular interest are the activity coefficient, γ and the Flory-Huggins interaction parameter, χ. The activity coefficient can be defined as a measure of deviation of a solution from ideality and can be expressed in a modified form of the Raoults Law expression.

$$\gamma_1 = \frac{P_1}{(P_1^{o} x_1)}$$

where P_1 is the equilibrium pressure of component 1 over the solution, P_1^{o} is the saturated vapour pressure of the component at the temperature of the solution, x_1 is the mole fraction of the component in solution and γ_1 is the activity coefficient of component 1 in the solution.

The use of mole fraction (x) is inconvenient in polymer solution calculations because the molecular weight of the polymer is very large compared to that of the solute, and hence as a result the mole fraction of the polymer in solution is usually very small even though the weight fraction may be close to unity. Calculation of the mole fraction requires precise knowledge of the polymer molecular weight, which is often difficult to determine accurately. Concentration scales which are convenient to use when determining thermodynamic properties of polymer solutions include volume fraction (Φ), segment fraction (Ψ), weight fraction (W) and site fraction (Θ). In this work, volume fractions have been used throughout. The solvent and polymer are denoted by the subscripts 1 and 2 respectively.

$$\Phi_1 = \frac{x_1 V_1}{x_1 V_1 + x_2 V_2}$$

where V_1 is the molar volume of the solute.

The interaction parameter is a measure of the interaction between the polymer and the solvent and it is related to the solubility of the polymer in the solvent. Solubility is governed by the free energy of mixing. For solution to take place at constant temperature and pressure, there must be a negative change in this free energy.

$$\Delta G < 0$$

Hence, using the Gibb's equation:

$$\Delta G = \Delta H - T\Delta S$$

$$\text{then } \Delta G^m = \Delta H^m - T\Delta S^m < 0$$

Where ΔG^m is the Gibbs free energy of mixing, ΔS^m is the entropy of mixing, ΔH^m is the enthalpy of mixing and T is the temperature.

The entropy value in the equation can be determined from a lattice model (i.e. we assume that solution can be represented by a three dimensional lattice) using the Boltzmann equation:

$$\Delta S = \underline{k} \ln W$$

where $\underline{k}$ is the Boltzmann constant and W is the number of ways of arranging a system.

If pure solvent, each site of the lattice is occupied by a solvent molecule, whilst if a polymer/solvent system, each site can contain either a polymer segment or solvent molecule.

$$\Delta S_m = -k (x_1 \ln\Phi_1 + x_2 \ln\Phi_2)$$

where x is the mole fraction and Φ is the volume fraction ($\Phi_1 + \Phi_2 = 1$ for a binary system).

The enthalpy of mixing arises from differences in interaction energies between polymer segments and solvent molecules. Flory's treatment states that w_{aa} is the interaction between solvent molecules, w_{bb} is the interaction between polymer segments and w_{ab} is the interaction between polymer and solvent.

The energy change upon mixing would be:

$$w = w_{ab} - 0.5(w_{aa} + w_{bb})$$

For n_1 solvent molecules, rn_2 polymer segments (where r is the number of sites occupied by polymer):

$$\Delta H^m = (n + rn_2)\, \Phi_1\, \Phi_2\, w$$

$$\text{or } \Delta H^m = RT\, \Phi_1\, \Phi_2\, \chi$$

where χ is the interaction parameter characterising the energy interactions.

However, free energies of mixing are difficult to measure, therefore the free energy is related to some colligative property of the solvent, for example, vapour pressure or osmotic pressure.

Using partial molar functions and Raoult's Law, the Flory Huggins expression becomes:

$$\ln a_1 = \ln\Phi_1 + (1-1/r)\Phi_2 + \Phi_2^2\chi$$

Where r is the ratio of the molar volume of the polymer to the molar volume of the solvent i.e. V_2^o/V_1^o and a_1 is the thermodynamic activity of the solvent.

Activity coefficients on a volume fraction basis are therefore given by:

$$\gamma_1^v = a_1/\Phi_1 = \exp[(1-1/r)\Phi_2 + \chi\Phi_2^2]$$

The interaction parameter consists of an enthalpy term and an entropy term:

$$\chi = \chi_H + \chi_S$$

The Flory Huggins model has three main disadvantages in that it contains a series of mathematical approximations, assumes no volume change on random mixing and only mixing or combinatorial entropy effects are considered, which means that such things as polarity are not considered.

The interaction parameter has been used as a measure of the "quality" of a solvent for a given polymer/solvent system. It is usually regarded as an empirical parameter defined as a "residual free energy" so that it accounts for enthalpic and all entropic contributions apart from the combinatorial term. Generally, a value of χ greater than 0.5 indicates a poor solvent interaction for the polymer/solvent system whilst conversely a value less than 0.5 indicates a stronger interaction. More comprehensive treatments of the thermodynamics of polymer solutions have been proposed[52] but for a working model the Flory Huggins theory is sufficient for our studies.

1.4.2 Experimental Techniques used to Determine Thermodynamic Properties of Polymer Solutions

Numerous techniques have been used to determine thermodynamic parameters of polymer solutions, and these include:

1. Vapour pressure lowering
2. Isopiestic sorption
3. Gas liquid chromatography
4. Osmotic pressure
5. Sedimentation-diffusion equilibrium
6. Vacuum microbalances
7. Sorption by thin films coated on piezoelectric crystals

Comprehensive reviews of these techniques have been produced by Orwoll[127] and Bonner[128].

1.4.2.1 Vapour Pressure Lowering

Vapour pressure lowering experiments involve the direct measurement of the difference in vapour pressure between a solution and pure solvent. The experiments can be carried out using essentially two methods: the null method[129] and the differential method of Jessup[130]. The absolute pressure above a solution of known composition is measured, usually by balancing it against air or nitrogen with a null manometer, and the balancing pressure is then measured with a mercury manometer or electronic Bourdon gauge. From the weights or volumes of the solvent and polymer used, the composition of the solution can be determined. Solvent may be added as a known weight of fluid into the polymer-containing vessel

or by distillation onto the polymer from a calibrated tube, the level of which is read before and after distillation.

Baxendale and co-workers[129] have carried out a thorough comparison of the differential method and the null method of determining solvent partial pressures. Bawn and co-workers[131] have used a similar process to study polystyrene sorption in toluene and MEK at different temperatures.

1.4.2.2 Isopiestic Sorption

The isopiestic sorption method has many variations and in broad terms, a polymer/solvent solution is allowed to come to equilibrium with the same pure solvent of known partial pressure. The known partial pressure is generated by maintaining a sample of pure solvent at a temperature lower than that of the solution or by making a solution of known composition for which the partial pressure/concentration relationship is known. Gee and Orr[132] produced one of the earliest examples of the isopiestic method.

A different type of isopiestic device was used by Van der Waals and Hermans[133], and Bonner and Prausnitz[134]. This type of device involves the suspension of the polymer sample on a pan by means of a sensitive quartz spring. Sakwada and co-workers[135] provided a third variation of the isopiestic method which was used for the study of water sorption by polyvinyl alcohol. The apparatus is similar to the quartz spring device except that only one constant temperature bath encloses both solvent and polymer solution compared to two individual baths for the other methods.

1.4.2.3 Gas-Liquid Chromatography (GLC)

In 1969, Smidsrod and Guillet[136] were the first workers to use GLC to measure thermodynamic properties such as activity coefficients and enthalpies of solution. Since then a considerable amount of work has been done by other workers using GLC to measure thermodynamic properties of polymer systems[137,138,139].

In this method, polymer is loaded onto a chromatographic column and it becomes the stationary phase in a GLC experiment. The low molecular weight diluent in the vapour phase acting with a carrier gas such as helium, are injected into the column. The polymer has a tendency to absorb the diluent. This tendency is a function of the interaction parameter and it is measured in terms of the retention volume.

Where the thermodynamic parameters of a solute in a polymer have been determined at zero solute concentration, the activity coefficient is known as an "infinite-dilution" activity coefficient and a review of the determination of infinite-dilution activity coefficients has been produced by Guillet[140]. Conder and Purnell[141,142,143] have developed the mathematical basis for the use of GLC at infinite solvent concentrations and the method was shown to produce results which agreed with traditional static methods. Brockmeier and co-workers[144,145,146] were the first to demonstrate that GLC could be used to determine the partial pressure of a solute in a polymer solution at concentrations up to 50% by weight.

Finite concentration GLC involves the equilibration of the chromatograph column (packed with the polymer-coated substrate), with a mixed carrier-solvent vapour stream of known constant composition. This is

followed by the injection of a small quantity of solvent as in a conventional experiment. Finite concentration GLC has been used by Aspler and co-workers[147] to study the effect of water on a cellulose derivative and also the interaction of organic vapours with hydroxypropylcellulose.

1.4.2.4 Osmotic Pressure

Many workers have used the osmometer to study the thermodynamics of polymer solutions[91,148]. This method involves the measurement of solution virial coefficients and a typical equilibrium time is around 24 hours. However, the viscosity of the solutions sets a limit to the maximum concentrations. Performing this method in solutions of up to 30% concentration has only been achieved in a few cases. Rehage and Meys managed to achieve this percentage of concentration using a system of polystyrene in toluene and cyclohexane respectively[149].

1.4.2.5 Sedimentation-Diffusion Equilibrium

The sedimentation-diffusion equilibrium method operates on the theory that in an ultracentrifuge there is such a distribution of molecular species, that the centrifugal forces are balanced by differences in the activities. This provides a method in principle that is a simple technique for the determination of the activities and chemical potentials in polymer solutions. Pederson[91] and Drucher[150] first demonstrated that the balance between these two effects could be used to determine activity coefficients in binary solutions. An exact theory of the thermodynamics of the ultracentrifuge equilibrium was later proposed by Young and co-workers[151]. Further theories which were closer to ideality have been advanced by Shulz[152] and other workers[153,154,155,156]. Scholte[157]

has used this method to study polystyrene with toluene and cyclohexane at different temperatures and concentrations.

1.4.2.6 Vacuum Microbalances

This method involves the isothermal measurement of the absorption of the vapour of a volatile liquid into a thin film of an involatile liquid spread on an inert particulate solid. Thin films are used to reduce the time to reach equilibrium.

There are three types of microbalance which have been used to study the thermodynamic properties of liquid mixtures. The types include the quartz spring balance, commercial electronic beam balance and the magnetic suspension balance. The magnetic suspension balance combines the advantages of both the quartz spring balance and the commercial beam balance in that its performance is not affected by the organic vapours studied and it provides a high load to precision ratio. Ashworth and Price[158,159] have used the three balances to study polydimethylsiloxane (PDMS) solutions, in particular, the sorption of benzene and cyclohexane on PDMS at 25°C.

1.4.2.7 Piezoelectric Sorption Detector

King[95], Bonner and Chang[160] have shown that a piezoelectric crystal can be used to study the thermodynamics of polymer solutions. When the quartz crystal is coated with a viscous polymer liquid, it can be used to detect the sorption of solutes by the polymer. The frequency of the crystal changes in response to a change in mass on the surface of the crystal and these responses can be used to calculate the appropriate

thermodynamic parameters. Crystals of this type have been shown to be sensitive up to mass changes of 10^{-9} g[95]. The frequency increases as mass increases when the crystal is placed in a dense medium, such as a liquid or compressed gas.

Bonner and Chang have investigated nitrogen sorption by low density polyethylene at 125°C and pressures up to 2000 psi. Their experiment was performed at both continuous flow and static conditions and equilibration times of fifteen minutes were obtained. The sorption of organic vapours by polystyrene has been studied by Saeki and co-workers[161] using AT-cut crystals with a 10 MHz base frequency. Equilibrium times of three to ten minutes were obtained using an acceptable tolerance of frequency change of ±5 Hz.

1.4.2.8 Comparison of the Experimental Methods

The choice of experimental technique to employ in the determination of activity coefficients and interaction parameters for a particular polymer/solvent system is driven by a number of factors. These include the required accuracy of the results, the range of concentration to be studied, the length of equilibrium time, the range of temperature to be studied and size of sample.

Vapour pressure lowering experiments can be highly accurate but the thermodynamic parameters determined can be substantially in error if the solvent is impure or not properly degassed. The method becomes very inaccurate at very small vapour pressures and a long time is required before equilibrium is attained. The osmotic pressure and sedimentation techniques use dilute polymer solutions and hence are not applicable.

The GLC technique becomes more inaccurate at higher concentrations of solvent because larger injection volumes have to be used and this strains the theory on which the calculations are based. The chromatographic peaks become more spread out at large vapour concentrations, which makes the measurement of the retention times less precise. Infinite dilution GLC has been shown to be a reproducible, accurate and rapid method of determining activity coefficients and interaction parameters of solutes in polymers[139] with reproducibility of results of 1 - 2%[128]. In their finite concentration GLC study of decane sorption by polyethylene at 185°C, Brockmeier and co-workers[144,145,146] have found agreement between these experimental values with those at infinite dilution. However, there are systematic differences between GLC results and extrapolated results of finite concentration studies carried out using static methods. The reason for this difference has not yet been resolved, although some efforts towards resolution have been reported[162]. Typically, GLC results can be determined over the course of a day, comparing well with the vacuum microbalances, although some polymers may require a week for an isotherm to be obtained by this method, particularly if bulk polymer is used rather than a polymer spread onto a solid support. The concentration range open to study by GLC is limited by the requirement that the saturator temperature must be below that of the column such that for a column at 25°C, the highest usable saturator temperature is approximately 23°C.

The vapour sorption techniques can, in principle, be used at solvent pressures up to saturation, although because small temperature fluctuations can cause large changes in solvent partial pressures and the long length of time required to reach equilibrium this is not practicable. The use of vacuum microbalances is usually restricted to temperatures around ambient, although quartz spiral microbalances have occasionally been used at

elevated temperatures. However, unlike GLC where the results are less accurate for high concentrations, vapour sorption results are more accurate at higher concentrations.

The time required to determine the absorption isotherm for the piezoelectric sorption method is fairly rapid because of the use of thin polymer films. An experimental precision of less than 2% has been obtained for the piezoelectric sorption detector. Bonner and Chang[160] found good agreement between their results and those of Lundberg and co-workers[163] within an experimental precision of 1%. Saeki and co-workers found reasonable agreement between their results and those of other workers using more traditional methods[131,148,164], but disagreement was found for solutions of chloroform and benzene in polystyrene at low solvent concentrations. The restriction of using ambient temperatures found for the vacuum microbalances does not apply to the piezoelectric sorption apparatus or to GLC methods since an oil bath or conventional gas chromatograph oven could be used.

The sample size required for polymer/solvent measurements varies according to the experimental method used. The electronic vacuum microbalance and GLC apparatus requires 0.2 - 2 g of polymer whereas only 50 - 100 mg of sample is required for the operation of the quartz spiral microbalance. Sub-milligram amounts of polymer are required for the piezoelectric sorption detector.

The piezoelectric sorption detector can therefore offer many advantages when determining activity coefficients and interaction parameters. These include the possibility of measuring thermodynamic parameters over a wide range of temperatures and pressures. The

measurement of these parameters at finite concentrations can be made rapidly as equilibrium is attained quickly when small amounts of polymer are used and the experimental data obtained has very high precision. The piezoelectric sorption detector combines the advantages of the vacuum microbalances and finite concentration GLC. It involves trivial data reduction and does not require any of the assumptions needed for GLC analysis.

1.4.3 Thermodynamic Properties of Polymer/Solvent Systems

A large database of values of thermodynamic parameters for polymer/solvent systems has been compiled by Orwoll as part of his 1976 review[127]. This review has been used as a preliminary source of the thermodynamic parameters of the polymer/solvent systems studied in this thesis.

1.4.3.1 Polydimethylsiloxane (PDMS)/Solvent Systems

A number of investigations have been reported on the thermodynamic properties of PDMS with various organic solvents hence making it ideal for testing our apparatus. A comparison of results between different groups is possible for benzene and hexane. Chahal and co-workers[165], using a vapour sorption technique, have determined the Flory-Huggins interaction parameter for the sorption of hexane and benzene in PDMS at 20°C finding a linear decrease in the value of χ with increasing solvent concentration. Flory and Shih[166] have since repeated the measurements and found good agreement with the results obtained by Chahal.

Sugamiya[167] have used osmotic pressure measurements in the calculation of χ for a series of n-alkanes with PDMS over a 5 - 30 wt% concentration range. Included in their results are data for the sorption of n-hexane on PDMS at 20 and 50°C. The value of χ was found to slightly increase with temperature, but varied little over the measured concentration range.

Summers and co-workers[168] used GLC techniques in their measurement of thermodynamic parameters of PDMS/hydrocarbon systems

over a wide temperature range, and the solvents included benzene and hexane. Good agreement between their GLC results and the vapour sorption measurements of Chahal and co-workers[165] was found.

Ashworth and Price have used both the magnetic suspension balance[158] and GLC[169] in the measurement of the variation of χ with concentration for benzene in PDMS at 25°C and found excellent agreement with the work of Flory and Shih. Ashworth and Price have continued their study by the determination of the vapour sorption of chloroform at 30°C at infinite dilution and compared these results with those obtained by GLC in a previous study on the same polymer[170]. Price and Guillet[171] have applied the technique of gas chromatography to the study of polymer solution thermodynamics of hexane and benzene in PDMS. Comparison of the GC results with those of other workers using sorption techniques gave good agreement[172].

As far as the author is aware, there are no literature results for the measurement of the thermodynamic parameters of PDMS/solvent systems using the piezoelectric sorption technique.

1.4.3.2 Polystyrene/Solvent Systems

Many studies, both at infinite dilution and at finite solute concentrations, have been made for polystyrene. Because of the numerous data available, it is again possible to make some comparisons between the data of various workers with our experimental results.

Baughan[164] has presented χ at 20°C for a wide variety of mixtures of polystyrene with both polar and non-polar diluents at relatively low values of

solvent concentration. Several vapours ranging from those of liquids in which polystyrene dissolves (e.g. benzene, dioxane) to those of liquids in which it will only swell (e.g. cyclohexane, nitromethane) were measured. Schulz and Flory, using a sedimentation technique, have found that the interaction parameter for the system polystyrene/cyclohexane increases with increasing solvent concentrations[173].

Bawn[131] has used vapour pressure lowering techniques to study the vapour sorption of MEK on polystyrene at different temperatures (25, 60 and 80°C). The dependence of activity coefficient on the weight fraction of solvent was independent of temperature whilst the interaction parameter increased with increasing solvent concentration. Bawn and co-workers[174] have shown little temperature and molecular weight dependency in the values of activity coefficient for the sorption of chloroform on polystyrene at 25 and 50°C. However the rate of attainment of equilibrium was markedly different. Flory and Hocker[175] have investigated the thermodynamic properties of polystyrene with MEK at 25°C using high pressure osmometry.

Saeki and co-workers[161] have determined the activity coefficients of benzene, cyclohexane and chloroform in binary solution with polystyrene at 23.5°C using a piezoelectric sorption apparatus. Good agreement was found between the results of Baughan and those of Saeki for the polystyrene/cyclohexane system. However at low solvent concentrations, disagreement was found between the results for benzene and chloroform and previously published results. No other studies of polystyrene/solvent systems have used the piezoelectric sorption apparatus.

1.4.3.3 Poly(4-chlorostyrene)/Solvent Systems

There is very little vapour/liquid equilibrium data available for the sorption of solvents by poly(4-chlorostyrene). The most relevant work is that of Corneliussen and co-workers[176]. In their study of the thermodynamic properties of solutions of polar polymers using isopiestic techniques, they have measured the interaction parameter as a function of volume fraction for poly(4-chlorostyrene) in toluene at 22°C. They found that the introduction of polar side groups into a non-polar polymer skeleton causes a continuous transition between the properties of the pure non-polar and pure polar polymers.

1.4.3.4 Polymethylmethacrylate (PMMA)/Solvent Systems

As far as the author is aware, there has been no systematic studies of the effect of solvent concentration on the thermodynamic parameters of PMMA.

1.5 Summary

In this introductory Chapter, we have given an overview of the technology and processes involved in the development of polymer resist systems with implication to the overall resolution of the resist and hence we have shown the need for the further understanding of the solubility/dissolution kinetics of polymers. We have described the experimental techniques available for the study of polymer dissolution and shown that the QCM technique could be developed as a possible method for the detailed study of resist development.

We have shown methods for the measurement of the thermodynamic parameters for the interaction of solvent with the polymer structure, and described the necessary theory for the understanding of the thermodynamics of polymer solutions.

We will now present the experimental techniques used in the determination for both the solution and dissolution kinetics.

Chapter Two

2.0 Experimental

As discussed in Chapter 1, the development of the resist is one of the most important steps in photolithography, and there are many factors that affect the overall resolution of this process. In an attempt to gain an insight into the dissolution characteristics of resist materials, our QCM technique will be applied in the liquid phase and furthermore, its use in the vapour phase will enable a correlation of the observed dissolution with the thermodynamics of resulting polymer solutions.

By the use of the QCM under liquids, we will demonstrate a technique that is a quick and accurate method for the study of polymer solutions and dissolution. Exposure of a layer of polymer on a crystal to solvent in this way initially results in a weight gain due to solvent absorption, followed by a weight loss as polymer dissolves away from the surface. Monitoring of the solvent action as a function of time and suitable deconvolution of the results allows calculation of the rate of penetration of solvent into the polymer and the rate of polymer dissolution.

The use of the QCM in the vapour phase proved to be a viable method for the determination of thermodynamic properties of polymer solutions. The quartz crystal was coated with a thin polymer film and allowed to sorb solvent vapour at a series of pressures hence allowing the measurement of the thermodynamics of solution under conditions very similar to those in practice.

The following sections will describe our choices of apparatus and experimental set-up for the above applications. Both the kinetics and thermodynamics studies were performed concurrently, however as literature

precedence suggested that liquid phase measurements were more complex than those in vapour, initial experience of the use of the QCM was gained for the vapour phase.

2.1 Vapour Sorption Apparatus

For the measurement of the thermodynamic properties of polymer solutions, a method of accurately controlling and measuring the solvent vapour pressure of the system is fundamentally important. Hence, a suitable vacuum system incorporating the QCM apparatus needed to be assembled, which would enable the simultaneous measurement of both the solvent vapour pressure and frequency change of the polymer coated crystal.

2.1.1 Development of Apparatus

The vacuum system was designed to admit solvent vapour into the QCM apparatus and monitor the uptake of solvent at a series of known vapour pressures. Schematic diagrams of the vacuum system and QCM apparatus used in the measurement of the polymer/solvent interactions are shown in Figures 11 and 12.

Basic pumping on the system was provided by means of an Edwards rotary vacuum pump and this was backed with an Edwards mercury diffusion pump, with a liquid nitrogen trap. The pressure in the pumping line was monitored using Edwards "Pirani" and "Penning" meters. The sorption apparatus was designed for operation from $1x10^{-5}$ Torr to atmospheric. The pressure in the sorption chamber was measured with a M.K.S. Instruments "Baratron" 270 capacitance pressure gauge operated with a 1000 Torr head. This allowed determination of pressures up to atmospheric to a precision

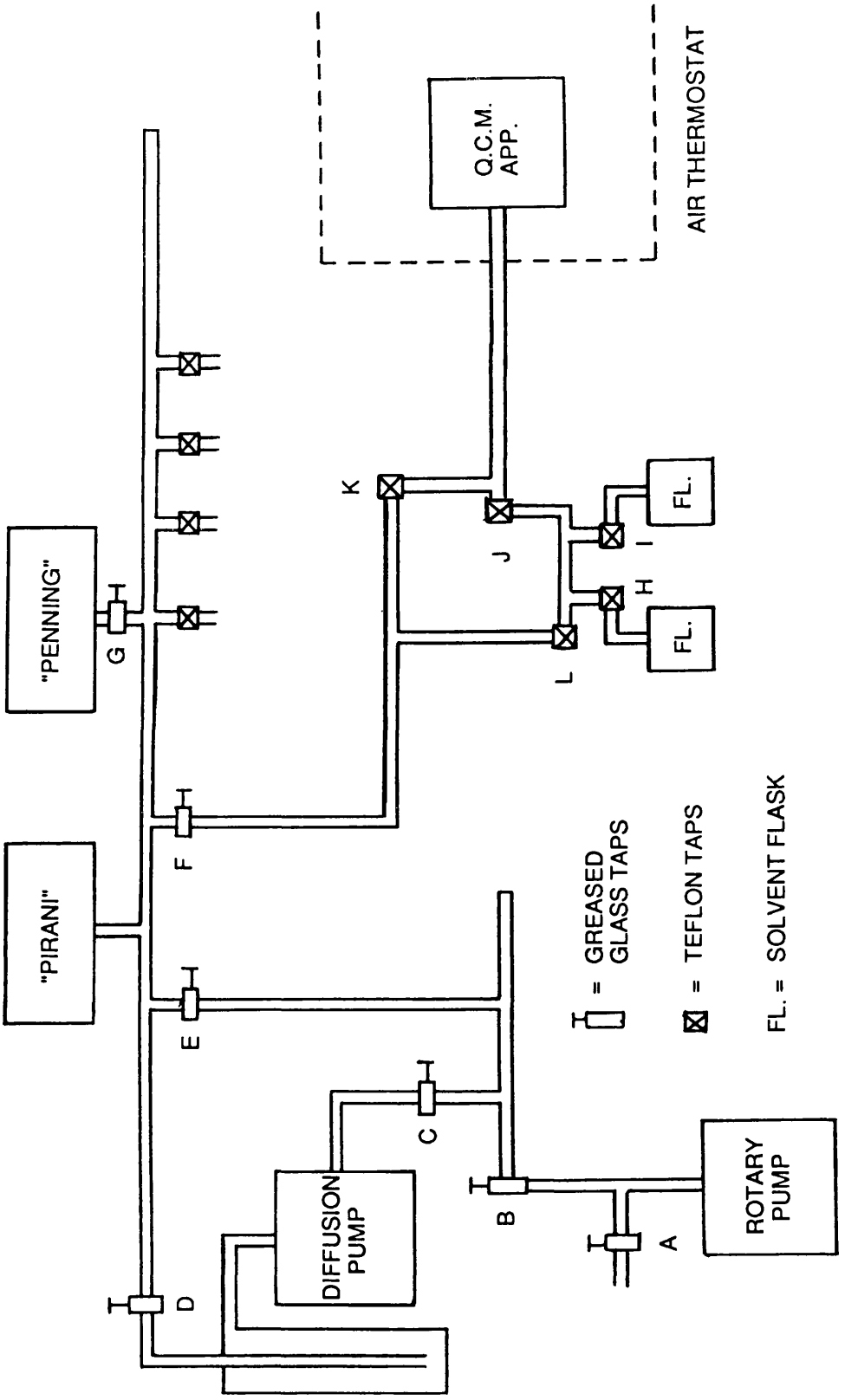

Figure 11: Schematic Diagram of the Vacuum System

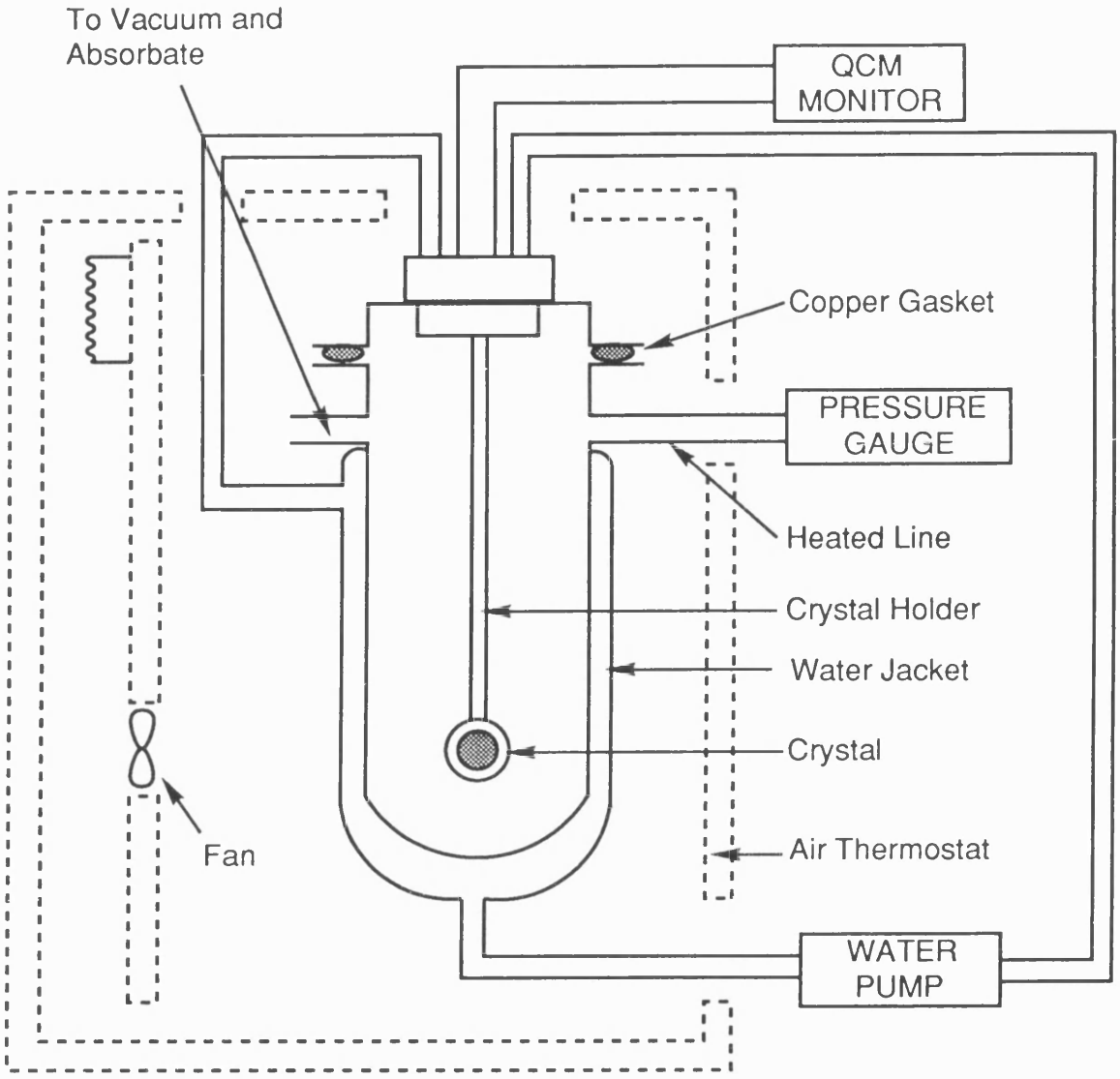

Figure 12: Schematic Diagram of the Vapour Sorption Apparatus

of ±0.01 Torr over an operating temperature range of 0 - 45°C. The gauge was connected to the sorption vessel by means of a glass line which was maintained at a temperature greater than the sorption vessel by means of heating tape and a Variac controller. This prevented condensation of solvent prior to entry of the sorption vessel.

Taps A - F in Figure 11 were greased, ground glass taps and the remainder were "teflon" greaseless taps to prevent any sorption of solvent by

grease present. The main pumping line led to the absorption chamber through tap K where the quartz crystal holder was situated, a subsidiary line incorporating taps L and J led to the solvent reservoirs. Two solvent flasks were utilised so that the solvent could be distilled over to purify and degas it. The upper vacuum line was added to the apparatus to perform other solvent distillations and degassing when required.

A commercially available Edwards FTM5 thin film deposition monitor was used to monitor the frequency of the quartz crystal. This monitor uses the QCM principle outlined in Section 1.3.1, and is designed to display the thickness of films up to 1 mm covering the crystal to a resolution of ±0.1 nm after being programmed with the density of the covering material and hence a rate of deposition/removal of ±0.1 nm s^{-1} can be measured. Alternatively the base resonant frequency of the crystal and the subsequent frequency of the loaded crystal can be displayed with a resolution of ±1 Hz, and the monitor was used in this mode for this work.

The AT cut, 6 MHz base frequency quartz crystals (diameter 14 mm, electrode diameter 7 mm, thickness 0.5 mm) were supplied by Edwards. The crystal was supported by a holder fitted with heating/cooling coils and this holder was placed in a jacketed glass vessel, as shown in Figure 12, which was connected to the vacuum system.

A number of designs for sealing the system were used in the course of this study. Early work with greased ground glass flanges and/or rubber gaskets showed that solvent vapour was rapidly absorbed, either by the grease or rubber, hence invalidating the results. Therefore, the crystal holder was sealed to the jacketed vessel by means of a coupling incorporating a copper gasket, which eliminated the use of grease or rubber,

hence minimising the solvent sorption problem. An additional mount was also designed so that two crystals could be accommodated in the jacketed glass vessel. In this case, the conventional crystal mount was dispensed with and the crystals were supported using thin wires which were soldered to a metal plate at the top of the sorption vessel, and connected to a switch enabling the monitoring of the frequencies of both crystals. The metal plate was attached to the sorption vessel as for the original mount.

The sorption vessel was maintained at a constant temperature by a Grant W14 circulating water bath capable of ±0.01°C control, which was connected to the water jacket of the vessel and the heating/cooling coils of the crystal holder, all the tubing to and from the bath being insulated. The sorption vessel was also enclosed in an air thermostat constructed from wood and perspex, with the use of perspex at the front of the vessel allowing the observation of the system during an experiment, and polystyrene blocks were used to further insulate the system. The temperature of the air surrounding the sorption vessel was maintained at approximately 0.2°C higher than that of the vessel, and a heating mat in conjunction with a circulating fan was used to heat the enclosure. This air thermostat insulated the sorption vessel from any external fluctuations of temperature. The vessel temperature was monitored by means of a mercury in glass thermometer (25 - 50°C operating range, accurate to ±0.1°C). This was calibrated with reference to a platinum resistance thermometer.

2.1.2 Procedure

The original crystal frequency (i.e. uncoated crystal) was recorded in air and the crystal coated with the polymer being studied. The coating was applied by adding dropwise *via* a syringe, a dilute polymer solution (approximately 0.1 - 1.0 wt%) onto the top face of the crystal. A commercially available spin-coater was then used to spread the polymer solution evenly over the crystal surface to produce a thin film. (N.B. The speed of the coater could be adjusted to allow for viscosity differences between polymer samples.) After allowing the solvent to evaporate, the crystal was replaced in the holder and the frequency measured. During the course of the study, the effect of pre-baking the spin-coated crystal was studied to ensure that all the solvent had evaporated prior to measurements. The coated crystals were pre-baked at 140°C for twenty minutes and the frequency was then measured.

The crystal was placed in the sorption vessel, and the unit sealed. It was then evacuated by means of the rotary pump until a pressure of <0.1 Torr was achieved, at which point the mercury diffusion pump was switched on. Evacuation of the system prior to a sorption experiment minimises changes in the measured frequency due to the sorption of water or air, and allows the pressure zero to be obtained. When the crystal frequency had stabilised (usually overnight), it was recorded at the measured pressure.

Before commencing each experiment, the leak rate of the system was measured to ensure any leaks in the system had been minimised and that they would not have a great effect on the actual readings. For this, the pumps were isolated from the sorption vessel by closing Taps K and J and the pressure change in the vessel over a known period of time recorded.

Hence, a leak rate was found, enabling us to establish that any frequency and pressure changes were due solely to the absorbate and not attributable to the absorbing of air upon the breakdown of vacuum A high leak rate ($>1x10^{-3}$ Torr min^{-1}) could not be tolerated, and leaks present in the system had to be eliminated or minimised.

Prior to each run, the solvent to be used was degassed. The solvent flask was attached to tap H with the tap closed and the flask was placed in liquid nitrogen to freeze the solvent. Taps K and J were closed and Tap H carefully opened to evacuate the solvent, any change in pressure was monitored by the "Penning" and "Pirani" gauges. Tap H was then closed and the liquid nitrogen removed to allow the solvent to return to room temperature. The degassing procedure was repeated until no change in pressure was observed. Taps K and J could then be opened. Any solvent first used in a run was distilled at least twice to remove impurities before degassing was performed. After the leak rate test and solvent degassing, the system was again evacuated.

After sufficient evacuation (i.e. when no further change in the vacuum was observed and the pressure was less than 0.01 Torr), the pumps were again isolated from the sorption vessel by closing taps K and L and a small amount of solvent vapour (≈5 - 20 Torr) was admitted into the vessel *via* taps H and J and then the taps were closed. The frequency change due to the absorption of the solvent onto the crystal was monitored by the FTM5 until equilibrium had been reached. The equilibrium position was taken as the time when the pressure and frequency had reached constant or near constant values (±1 Hz). The time taken to attain this position varying according to the solvent, polymer coating and pressure. The resulting frequency, vapour pressure and the temperature of the air thermostat were

recorded. More solvent vapour was then admitted into the vessel and the procedure repeated until the sorption isotherm had been obtained. As each solvent approached the solvent vapour pressure, the solvent had to be gently heated so sufficient could be admitted into the sorption vessel.

On completion of the sorption isotherm, the solvent flask was again placed into liquid nitrogen to freeze the solvent. Taps J and H were re-opened and the solvent desorbed from the crystal back into the solvent flask. Once the removal of solvent from the sorption vessel was complete, taps J and H were closed and taps K and L opened so that the system could be evacuated.

It was observed with higher solvent concentrations that there was significant desorption of vapour from the polymer film. After initial admittance of solvent vapour, the frequency of the crystal decreased as expected, but at equilibrium the frequency had increased to above that of the initial decrease at that particular pressure. This was thought to be caused by the solvent condensing out onto the polymer and quartz crystal, and illustrates the need to ensure that equilibrium conditions have been attained.

Several sets of sorption data were obtained to ensure reproducibility of results. For each system, a control run was performed on an uncoated crystal to ensure that observed frequency changes were due to absorption by the polymer and not quartz crystal absorption.

2.2 Dissolution Kinetics Apparatus

The commercial FTM5 QCM unit used in the vacuum studies was not suitable for use in the solution mode, as the monitor "failed" (i.e. oscillation of the crystal ceased) as soon as liquid was placed on the faces of the crystal. The failure was due to the oscillator circuit not driving the crystal oscillator sufficiently to overcome the viscous effect of the liquid because of the poor Q factor. Therefore an oscillator circuit was built in the laboratory, which was operable under such solution conditions.

2.2.1 Development of Apparatus

Initially an oscillator circuit based on that published by Hinsberg and co-workers[76] was built, but this was found to be inoperable (a number of design faults were found) and failed as soon as the crystal was immersed in solution. The transistorised Pierce-Miller oscillator circuit of Benje and co-workers[177] (similar to that proposed by Nomura[115]) was then constructed, which was more successful than the original circuit, but did not give the required stability for solution studies.

Finally a circuit based on the oscillator design of Bruckenstein and Shay[119] was constructed. This set-up utilises two quartz crystals, a "reference" crystal and a "working" crystal, with separate oscillator circuits. The reference crystal is canned to exclude it from external influences, which gives extra frequency stability, and only the frequency difference between the two crystals is measured. The circuit diagram can be found in Figure 13. With a few modifications to the layout of the circuit and the addition of a variable capacitor to the working crystal circuit for more frequency control, a stable frequency reading could be observed for the crystal under solution.

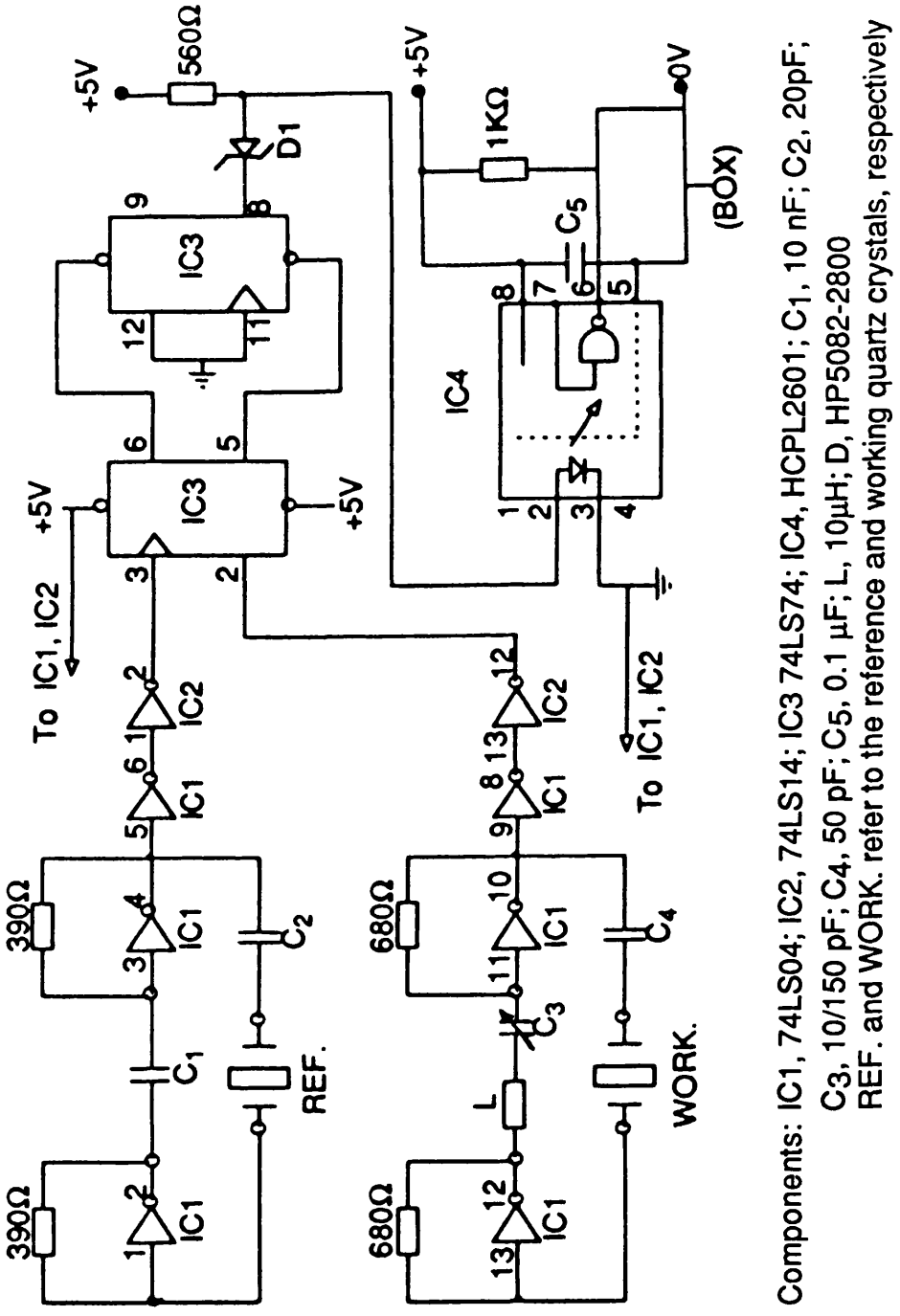

Figure 13: Schematic Diagram of the Electrical Circuit used in the Construction of the Quartz Crystal Microbalance

The crystals used were AT cut, 10 MHz base frequency quartz crystals, which had a diameter of 14 mm and thickness 0.5 mm and were supplied by Euroquartz Ltd (Crewkerne). The crystal circuits and optocoupler circuit were driven independently by 5V power supplies. The frequency difference between the working and reference crystals was monitored using a Racal Dana 1030 frequency counter (resolution ±0.1 Hz) which was interfaced to an Elonex PC88C microcomputer, *via* a Metrabyte IEEE interface card, where subsequent data treatment was performed. Measurements were made at one second intervals, each being the average of ten separate readings. To give signals of the required stability, the apparatus (i.e. crystal holder and oscillator circuit) was contained in an aluminium box which acted as a Faraday cage. A computer program was written to enable the crystal frequency difference and the time elapsed to be stored on disc for further manipulation, and this program can be found in Appendix 3.

Once a viable oscillator circuit had been constructed, the flow cell for the dissolution studies was built. Initially flow across only one face of the crystal was considered. A solvent impermeable material which is an electrical insulator was required for its construction and PTFE was chosen because of its inertness, and stainless steel piping was chosen for the solvent inlet and outlet.

The initial cell design utilised "O" rings to clamp the crystal between two PTFE pieces, and the solvent was flowed across one face of the crystal. A Watson-Marlow 502 peristaltic pump was used to flow the solvent across the crystal face using flow rates of 5 - 40 ml min^{-1}. "Homemade" butyl "O" rings (made from butyl sheeting) were used since butyl rubber was found to be less reactive towards MEK and MIBK (which are typical developing

solvents in the resist industry) than commercially available "O" ring material. The electrical contact between the crystal and oscillator circuit was made *via* aluminium wire with silver-loaded epoxy glue making a permanent connection between the crystal and wire. This cell design gave satisfactory results but was prone to leakage of solvent from the crystal cavity and was difficult to thermostat when temperature control was required. It was also found that resolution was reduced due to the clamping of the crystal.

A more simple cell design, with both sides of the crystal exposed to the developing solvent, was then constructed. The crystal was placed in a crystal holder such as that used on electronic circuit boards and this holder was then soldered to the input of the oscillator circuit. A metal rod was fixed to the holder so that the height of the crystal could be adjusted. This design involved no "O" rings or clamping of the crystal so that there would be no constraint on the solvent used and the crystal could be interchanged with great ease.

A schematic diagram of the kinetic apparatus used with the second cell design is shown in Figure 14. The apparatus consisted of a glass vessel containing the developing solvent (capacity ≈150 ml) which was magnetically stirred to achieve equilibrium conditions of temperature and composition in the solvent. The temperature control of the beaker was maintained by circulating thermostatted water from a water bath (Grant W14 circulating bath). The solvent in the vessel was hence thermostatted to ±0.1°C and the temperature of the solution was monitored using a mercury in glass thermometer (range 0 - 50°C, accurate to ±0.1°C).

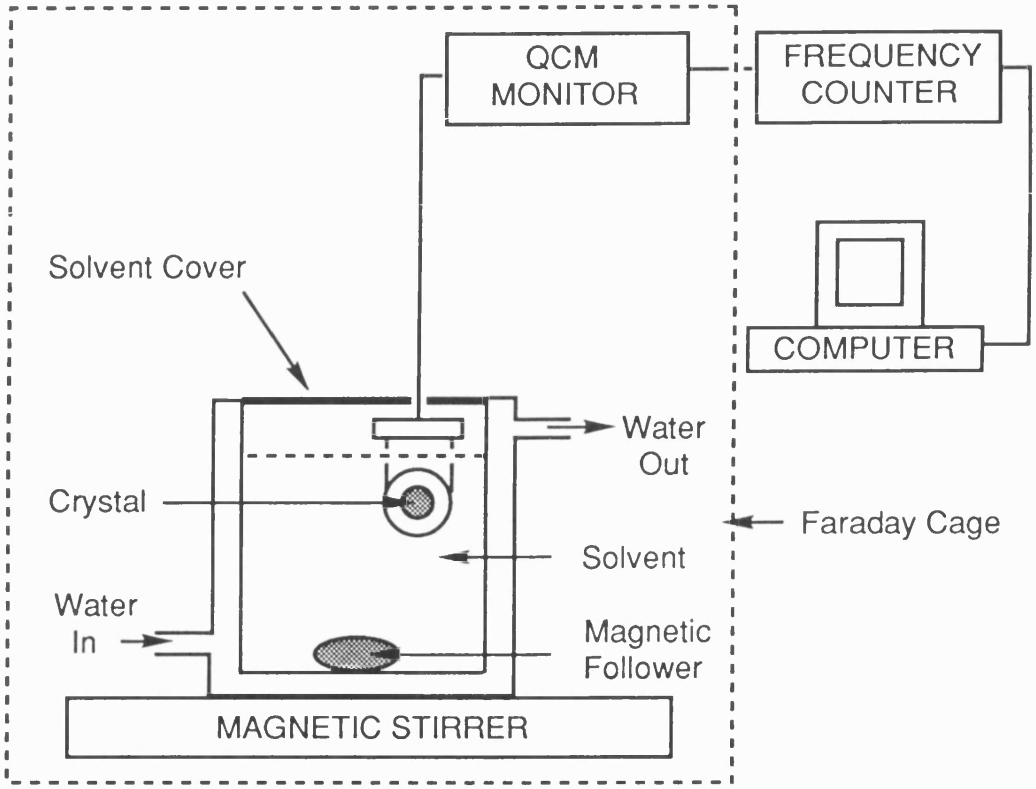

Figure 14: Schematic Diagram of the Kinetic Apparatus

2.2.2 Procedure

Before starting a series of experiments, the crystals were cleaned (by soaking the crystals overnight in chloroform and using cotton wool to clean the surface). The resonance frequency of each of the uncoated crystals was then recorded in air before being coated with polymer. The coating solutions used were approximately 1 wt% polymer in solvent. The coating was applied by immersing the crystal in the polymer solution and allowing the solvent to evaporate. "Dip coating" was used instead of spin coating as the crystal needed to be coated on both sides. The crystals were then pre-baked above the glass transition temperature of the polymer to remove the remaining solvent and to anneal the film.

The coated crystal was placed in the crystal holder and its resonant frequency allowed to stabilise before being recorded. The crystal was then rapidly immersed into the developing solvent and the frequency change followed with time until no further change was noted. On completion of the run, the crystal was cleaned with chloroform and re-immersed in the developing solvent and the frequency measured, thus enabling the calculation of the remaining film thickness.

2.3 Materials

2.3.1 Solvents

Solvents of the best available grade supplied by the Aldrich chemical company were used throughout the study and were shown by GLC to be at least 99 mole% pure. Methyl, ethyl, n-propyl and n-butyl acetates were distilled over potassium carbonate to remove any traces of acetic acid and the methanol was distilled from calcium hydride. Prior to use in the thermodynamic studies, the solvents were distilled over a number of times, using the two solvent flasks attached to the apparatus, in order to purify and degas the solvent.

2.3.2 Polymers

2.3.2.1 Polymethylmethacrylate (PMMA)

The PMMA sample (see Figure 15) used in the thermodynamic studies and the initial kinetic studies was a polymer supplied by BDH Ltd having a M_n of 56000 and a polydispersity (γ) of 2.0 as measured by Gel Permeation Chromatography (GPC). ^1H NMR spectroscopy showed it to be primarily atactic.

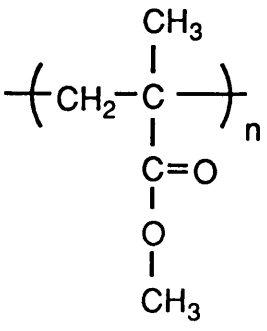

Figure 15: PMMA

For the molecular weight studies, narrow polydispersity samples from Polymer Laboratories Ltd were used. The molecular weights quoted are those supplied by the manufacturers for GPC calibration purposes (as shown below in Table 1). Unless otherwise stated, PMMA will refer to the wide polydispersity sample; where the standards have been used, it will be explicitly stated.

M_n	γ
6100	1.11
10300	1.06
22200	1.07
34500	1.04
67000	1.04
107000	1.10
330000	1.11
820000	1.04
1400000	1.07

Table 1: Molecular Weight Distributions of PMMA Standards

2.3.2.2 Polystyrene and Poly(4-chlorostyrene)

The polystyrene was a secondary standard with a M_W of 430000 and γ of 3.1 obtained from the Aldrich chemical company (Figure 16). For the molecular weight studies, a polystyrene standard with a M_W of 675000 and γ of 1.05 from the Polymer Laboratories was also used.

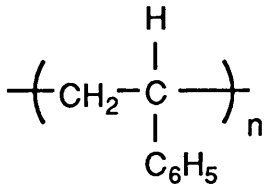

Figure 16: Polystyrene

The poly(4-chlorostyrene) was prepared by a radical polymerisation process using a 0.1 wt% azobisisobutyronitrile initiator with a 50% solution of inhibitor free 4-chlorostyrene (supplied by Aldrich chemical company) in toluene[178]. It had a M_n of 60000 and a γ of 1.88 as measured by GPC using polystyrene calibration standards.

2.3.2.3 Poly(phenylmethylsilane)

The wide polydispersity poly(phenylmethylsilane) polymer (Figure 17) was prepared *via* a Wurtz-type coupling of the methylphenyldichlorosilane monomer heated at reflux in toluene with a sodium dispersion. Full details of the preparation can be found in Reference 179. (The monomer and solvents were supplied by the Aldrich chemical company.) The sample had a M_n of 9600 and a γ of 6.2 as determined by GPC using polystyrene calibration standards.

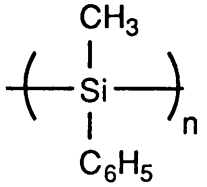

Figure 17: Poly(phenylmethylsilane)

For the molecular weight studies, this wide polydispersity polysilane sample was separated into a range of molecular weights by either preparative GPC or fractional precipitation with methanol and the resulting molecular weight distributions measured by GPC (Table 2).

Separation Method	M_n	γ
Prep. GPC	29300	1.9
	18400	1.4
	7500	1.4
Fractionation	53700	5.8
	34500	1.9
	14500	1.4
	9600	1.2

Table 2: Molecular Weight Distributions of Poly(phenylmethylsilane)

2.3.2.4 Polydimethylsiloxane (PDMS)

The PDMS sample (Figure 18) was a DC 200 silicone fluid obtained from Dow Corning Ltd. It had a M_w of 26000.

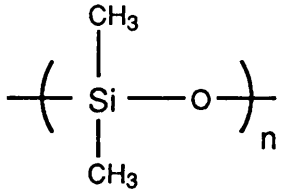

Figure 18: Polydimethylsiloxane

2.3.2.5 Poly(vinyl cinnamate)

The poly(vinyl cinnamate) (Figure 19) was supplied by the Aldrich chemical company.

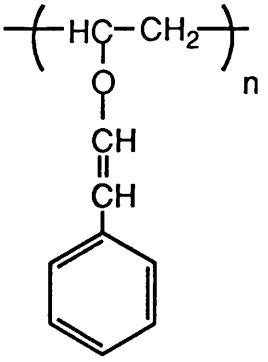

Figure 19: Poly(vinyl cinnamate)

2.4 Ultra-Violet Exposure Experimental Method

To illustrate the potential application of some of our polymer samples to photoresist systems, we exposed some polymer samples to UV irradiation to determine the effect of exposure on the dissolution characteristics of the polymer films. The initial studies on the wide polydispersity PMMA sample were performed at the Chemistry Department of City University using a medium pressure mercury lamp (Hanovia, 500W). As the preliminary studies gave promising results, the PMMA sample and poly(vinyl cinnamate) sample were exposed to a high intensity deep UV lamp (UVA Associates, 200W, with output peaks at 254 and 313 nm) at the University of Bath. A metal box was constructed which allowed the sets of crystals to be exposed to the irradiation at a constant distance whilst giving adequate shielding to the user during the exposure and removal of the crystals. Prior to exposure, both the lamps were allowed to warm-up over a 15 - 30 minute period and the crystals were turned over halfway through the irradiation to ensure the even exposure of the sample (i.e. only one side of the crystal could be exposed at one time). The dissolution kinetics of these samples was then measured.

2.5 Conclusion

The following chapters will illustrate some results using both the vapour sorption and dissolution kinetics apparatus and will give some preliminary results for the effect of UV exposure on the dissolution of polymer films.

Chapter Three

3.0 Development of Experimental Techniques

The aim of the work in this chapter was to establish that the experimental techniques, for both the dissolution and vapour sorption apparatus, would give accurate and reproducible results compared with existing experimental methods.

3.1 Dissolution Kinetics - QCM Apparatus

The following sections outline the data reduction used to obtain information from the raw frequency data about the dissolution kinetics of the polymer systems.

3.1.1 Data Reduction

As previously stated in Section 1.3.1, the mass change of a polymer can be related to the frequency change by Sauerbrey's relationship:

$$F = \frac{-(F_o^2).\ M_p}{AN\rho_q}$$

where F is the frequency of the loaded crystal, F_o is the fundamental resonant frequency, A is the active area of the uncoated crystal, ρ_q is the density of quartz, N is the "Frequency Constant" of the quartz crystal and M_p is the mass of coating.

Using the above equation and introducing the density of the polymer, ρ_p, the frequency can be transformed into the film thickness, T_f using the following equation (assuming uniform coating):

$$T_f = \left[\frac{(N\rho_q)}{F_o^2\rho_p}\right]\Delta F$$

The initial film thickness of the polymer coating can be calculated from the difference between the frequency of the coated crystal and that of the uncoated crystal whilst resonating in air. When initially immersed in liquid, the coated crystal exhibits a decrease in oscillation frequency. The magnitude of this shift is related to the viscosity and density of the liquid. To compensate for this change in frequency, the crystal is immersed in the developing liquid prior to coating, to enable the measurement of the crystal frequency in solution before coating (F_u). The frequency of the coated crystal upon immersion in the liquid is measured (F_c), and the difference between F_c and F_u indicates the frequency change (ΔF_{liquid}) due to the coating whilst resonating in the liquid medium.

$$\Delta F_{liquid} = (F_c - F_u)$$

Within experimental error, and by treating the film as a rigid layer, the film induced frequency shift in solvent is the same as that of the bare crystal. This results in the effects of solvent and film on the frequency shift being additive and can be treated independently.

The changes in frequency of the crystal (ΔF) during development of the film are stored with the corresponding development times by the computer and can be displayed as a series of frequency/time curves. The

results for a series of polymer films can then be normalised to the same initial thickness by displaying throughout the development the percentage of film remaining with respect to time.

$$\Delta F_t = -(F_o - F_t)$$

$$\% \text{ film remaining} = \left(\frac{F_u - F_{c.t}}{F_u}\right) . 100$$

From the normalised curves, the dissolution/swelling rates of the polymer films may be obtained by measuring the slope of the % film remaining/time curves. The data was imported from the BASIC computer program directly into a speadsheet to enable easy data manipulation.

$$\text{Dissolution rate} = \left(\frac{\% \text{ film removed}}{\text{time}}\right) . T_f$$

In cases where no swelling occurred, the rate of dissolution was taken as the initial slope of the percentage of film remaining versus time plot. In systems showing concurrent swelling and dissolution, the two curves were deconvoluted to measure rates of both processes. For the purposes of this work, the dissolution rate is measured at the end of any induction or swelling period.

3.1.2 Feasibility Studies of Dissolution Kinetics Apparatus

As an introduction to our work and to serve to illustrate our methods, initial studies from the literature were performed on PMMA. This polymer has been studied by other workers and it is also in commercial use as a positive photoresist. The usual developing solvent for PMMA is a mixture of MEK and IPA, and this system was used for our initial feasibility studies. Precise comparison of our results with those of other workers is not possible since the dissolution rate in a solvent depends on a large number of factors including the exact structure and thermal history of a particular polymer sample, which makes it difficult to work on identical samples to those used for the literature studies.

All the PMMA samples used in this work were pre-baked in an oven at 160°C for 1 hour to remove remaining solvent and to anneal the polymer film.

3.1.2.1 Effect of Film Thickness on Dissolution Measurements

Figure 20 shows the results for the dissolution of PMMA (M_n 56000, γ 2.0) at three different initial film thicknesses in a 60:40 v/v mixture of MEK and IPA at 25°C, plotted as functions of both film thickness and frequency change. For the film of starting thickness 0.42 μm, the total change in frequency for complete dissolution is 11.7 kHz. Since the uncertainty in measuring the frequency is less than ±10 Hz, we can measure the film thicknesses with a resolution of approximately ±0.1 nm. The results also show that, within the limits studied, the rate of dissolution given by the slopes of the curves is independent of the film thickness.

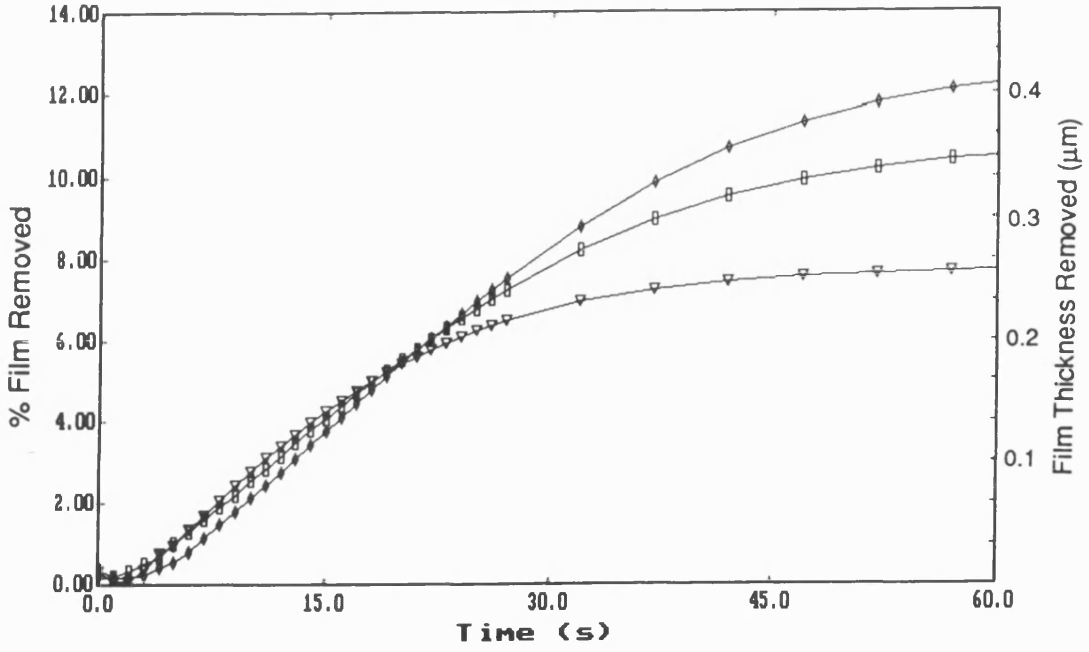

Figure 20: Effect of Film Thickness on the Dissolution of PMMA in 60:40 v/v MEK/IPA at 25°C

The shape of the dissolution curves indicate that a brief induction period occurs before rapid dissolution starts, and as the last layers of polymer are removed from the crystal surface a slowing down in the dissolution rate is observed. These observations are related to the initial penetration of the solvent and swelling of the surface layer before dissolution occurs and to the adhesion of the last layers of the polymer to the substrate. Both of these features will be studied in more detail during the course of this thesis.

3.1.2.2 Reproducibility of Dissolution Measurements

To illustrate the reproducibility of our measurements, four separate experiments were performed on different days and with different quartz crystals for the dissolution of PMMA in MEK at 25°C. The films were approximately 1μm in thickness and have been normalised to the same initial thickness. The results are displayed in Figure 21 as the percentage of the film remaining with development time. No swelling of the film was observed, and all four films had been completely removed after a development time of 75 s. The dissolution curves are very similar and calculation of dissolution rates gave 2.422 ± 0.017 μm min^{-1} with the four runs agreeing to within ±1%.

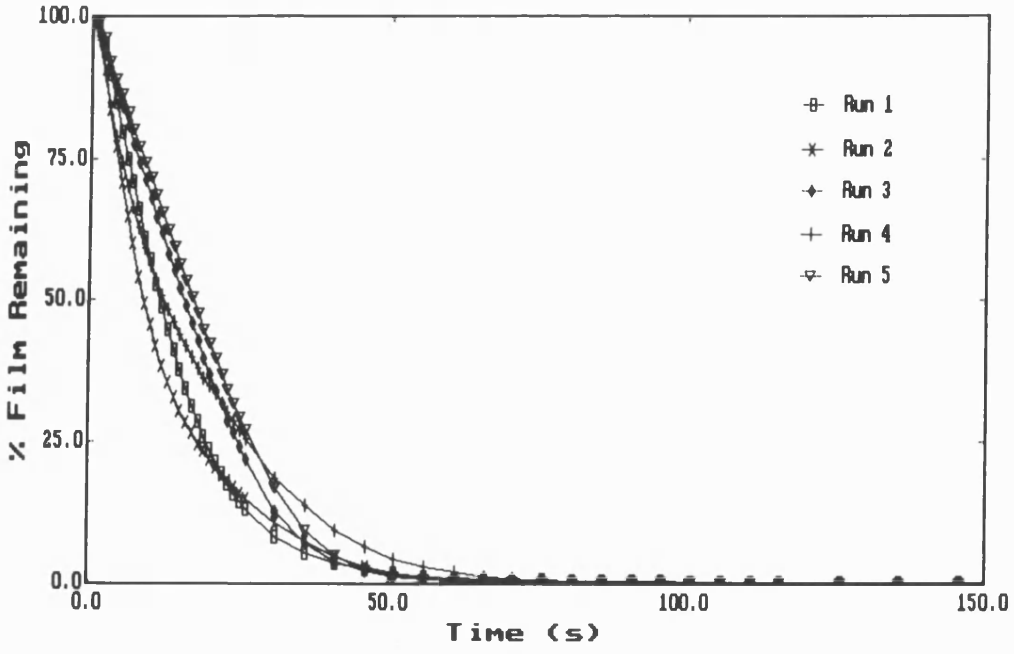

Figure 21: **Reproduciblity of Dissolution Rate Measurements for PMMA in MEK at 25°C**

3.1.2.3 Effect of Temperature on Crystal Resonant Frequency

An uncoated crystal was exposed to a developing solution of 100% MEK over the temperature range 16 - 53°C, and the effect of solution temperature on the resonant frequency can be seen Figure 22.

The frequency change was recorded once a steady frequency had been attained. The resonant frequency of the crystal increased linearly with temperature with a maximum frequency change observed of 500 Hz between 16 and 53°C. This change in base frequency due to temperature, illustrates the importance of recording the frequency of the uncoated crystal (F_u) in the solvent at the required developing temperature.

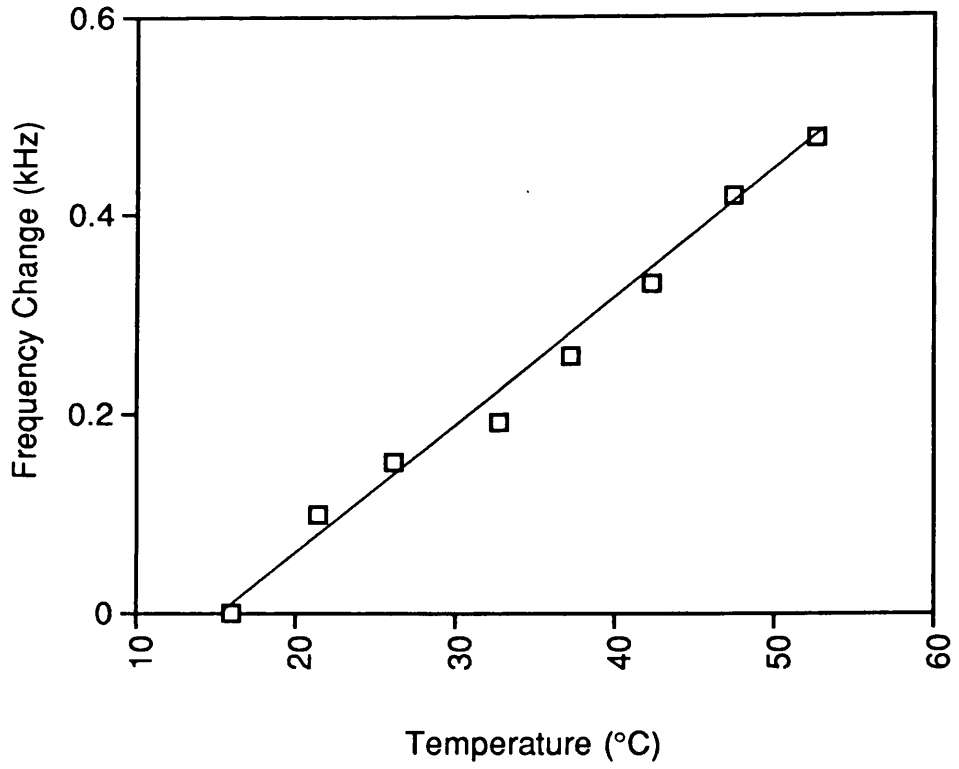

Figure 22: Effect of Temperature on an Uncoated Crystal in MEK

3.1.2.4 Measurement of Swelling and Dissolution Kinetics

A series of 1μm thick PMMA coated crystals were developed in both good solvents and non-solvents at 25°C to show the capability of the dissolution apparatus to monitor both dissolution and swelling processes. It has already been shown in Section 3.1.2.2, that MEK is a good solvent for PMMA with complete dissolution of a 1μm film within 75 s. Figure 23 shows that both tetrahydrofuran and MIBK have similar solvent power to that of MEK, with no swelling of the film observed and complete dissolution within 100 s. PMMA is observed to swell in dichloromethane with a 5% weight increase within 300 s and no dissolution of the film. No swelling or dissolution (i.e. weight change) is observed for the "development" of a PMMA sample in cyclohexane. Both toluene and 3-methyl-2-butanone also show a combination of dissolution and swelling of the PMMA films with an initial 10% increase in weight observed before dissolution becomes the predominant process.

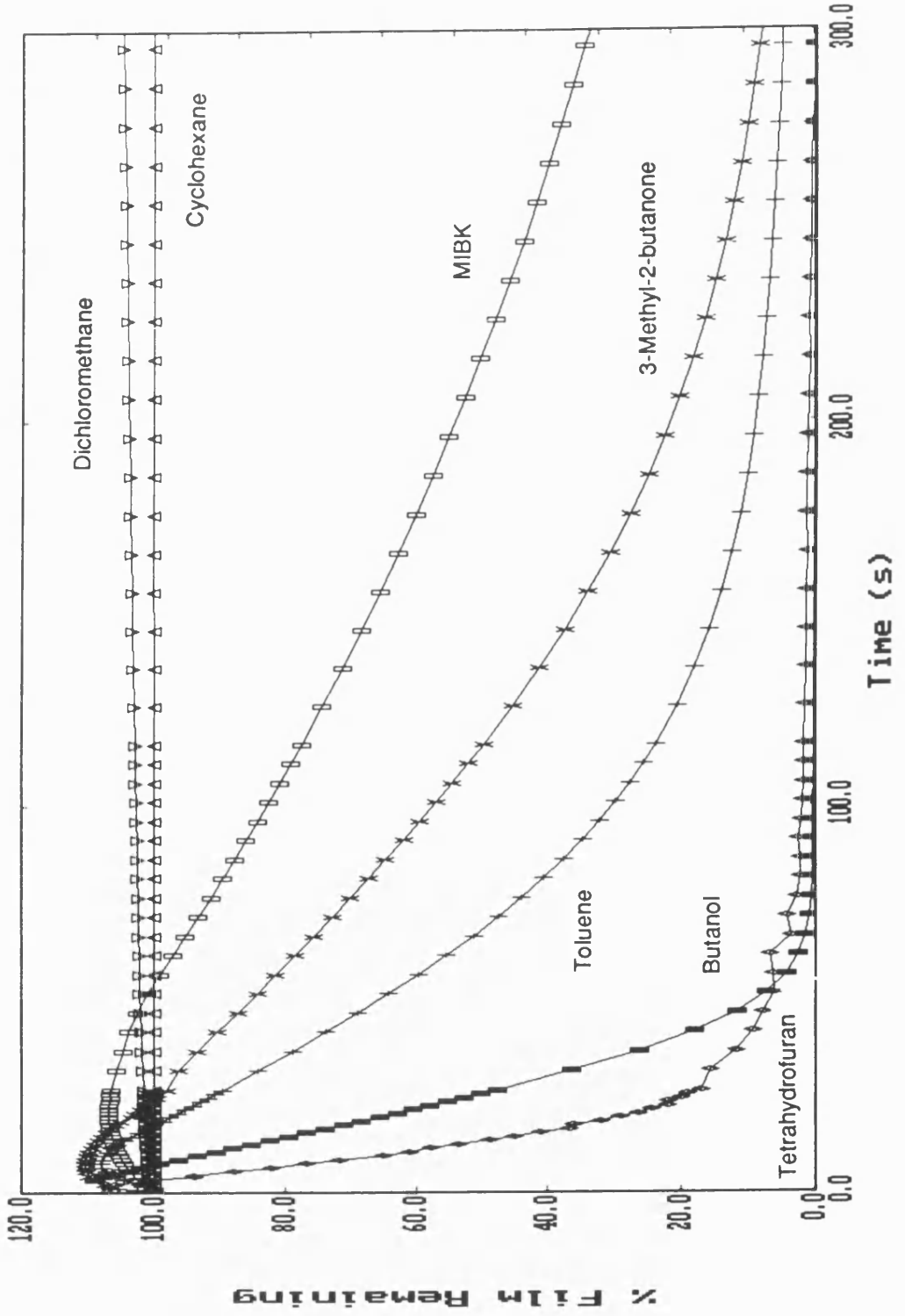

Figure 23: Dissolution of PMMA in a Series of Solvents at 25°C

3.2 Vapour Sorption - QCM Apparatus

The aim of this section was to demonstrate that our recently designed and constructed vacuum apparatus could utilise the QCM to successfully determine various thermodynamic parameters of polymer solutions.

3.2.1 Data Reduction

The following data reduction method was used to obtain the volume fraction activity coefficients and Flory-Huggins interaction parameters from the vapour sorption data obtained for the polymer/solvent systems studied.

Using Sauerbrey's relationship (as outlined in Section 1.3.1), the weight fraction of solvent (w_1) sorbed by the polymer can be calculated using:

$$w_1 = \frac{m'}{m' + m_o} = \frac{\Delta F'}{\Delta F' + \Delta F_o} \qquad : w_1 = 1 - w_2$$

Where $\Delta F'$ is the frequency decrease due to the solvent mass ($\Delta m'$) sorbed by the polymer on the crystal and ΔF_o is the frequency decrease due to the initially applied polymer coating of mass Δm_o.

Hence the volume fraction of solvent (Φ_1) can be calculated from:

$$\Phi_1 = \frac{\Delta F'/\rho}{\Delta F'/\rho + \Delta F_o/\rho_p} \qquad : \Phi_1 = 1 - \Phi_2$$

The saturated vapour pressure of the solvent at the solution temperature P_1^o is calculated using the following equation:

$$\ln P_1^o = A - \frac{B}{(T + C)}$$

where A,B and C are the Antoine vapour pressure equation coefficients. The values of A,B and C and second virial coefficients for the solvents used in this study and the literature sources are given in Appendix 1.

At equilibrium between the solvent vapour phase and the polymer/solvent solution phase, the fugacity of solvent in the vapour phase equals the fugacity of solvent in the liquid phase. Hence, the volume fraction activity coefficient ${}^v\gamma_1$ of the solvent at a given solution temperature is given by[134]:

$$\ln {}^v\gamma_1 = \ln\left(\frac{P_1}{P_1^o\Phi_1}\right) + \frac{(V_1^o - B_{11})(P_1^o - P_1)}{RT} + \frac{1}{2}\left(\frac{B_{11}}{RT}\right)^2 \cdot (P_1^{o2} - P_1^2)$$

Where P_1 is the partial pressure of solvent above the polymer solution, P_1^o is the saturated vapour pressure of solvent at the solution temperature T, B_{11} is the second virial coefficient of the solvent, V_1^o is the molar volume of solvent and R is the gas constant.

As shown in Section 1.4.1, the polymer/solvent interaction parameter can be obtained from the Flory-Huggins expression:

$$\ln {}^v\gamma_1 = \ln \Phi_1 + \left(1 - \frac{1}{r}\right)\Phi_2 + \Phi_2^2 \chi$$

The values of Φ_1 and Φ_2 represent the volume fractions of solvent and polymer respectively, r is the ratio of the molar volume of the polymer to that of the solvent and χ is the Flory-Huggins polymer/solvent interaction parameter.

BASIC computer programs "FHUGGINS" and "CONSTANT" have been written to calculate volume fraction activity coefficients and interaction parameters and can be found in Appendix 3.

3.2.2 Estimation of Errors

The QCM sorption method of determining activity coefficients and interaction parameters is open to large errors caused by the limitations of the design of the system.

The main errors in this study were in the measurement of the frequency decrease due to the coated polymer, the resolution of the FTM5 and the temperature control of the air thermostat. The errors were determined by changing the effect of each of the factors in turn, and recalculating the parameters.

The QCM sorption method is much more susceptible to deviation at low solvent concentrations. At low solvent concentrations (i.e. $\Phi_1 < 0.05$), an error in measured frequency change of ±1 Hz, could cause a deviation of the calculated activity coefficient of 1%, and an error as great as 30% in interaction parameter. At higher concentrations, the overall frequency change is much greater and thus the effect of an error of ±1 Hz will not be as great. For a typical system, a solvent volume fraction of 0.3, a 1 Hz change could cause an error of approximately 5% in the measurement of interaction

parameter. In the measurement of the frequency change due to the polymer coating, an error of 10% in the measurement of ΔF_0 will have little effect on the value of activity coefficient and volume fraction of solvent, but an error in Flory-Huggins interaction parameter of up to 3% can occur. A greater accuracy in determining the activity coefficients and interaction parameters could be obtained by applying thicker polymer films. However, for our sorption studies, if the coating was too thick then the crystal "failed" either due to lack of contact with the electrodes or due to failure of the FTM5 monitor (which has a certain operating range).

The control of temperature *via* the air thermostat was another source of error as the heating mat and circulating fan were unable to maintain the desired temperature stability. The fan was on continuously whilst the heating mat was controlled by the relay and would cut in and out during the experiment according to any temperature fluctuations of the surroundings.

When the fan cut in, the temperature of the air thermostat would surge up to a maximum of 0.4°C and when it cut out, the temperature would drop by 0.4°C before the relay turned the heating mat back on. The set-point of the relay had been adjusted to minimise the temperature surges observed. The greatest variation in the temperature inside the sorption vessel would have been ±0.1°C which translates into an error of ≈0.5% in the activity coefficient over the measured concentration range. The greatest error was observed in the measurement of χ, where the effect of a temperature change could produce an error as large as 20% at low solvent concentrations and 7% at higher concentrations. It was found that temperature fluctuations had negligible effects on the solvent fraction.

These possible errors must be taken into account when interpreting the experimental data. For the initial vapour sorption studies, error bars have been added to the Figures (Y ±3%, X ±5%) to give an indication of the precision of our results.

3.2.3 Feasibility Studies of the Vapour Sorption Apparatus

3.2.3.1 Solvent Sorption on an Uncoated Crystal

To illustrate the importance of maintaining a very low leak rate in the vacuum system, an uncoated crystal was subjected to varying pressure of air over the range 0 - 400 Torr at 50 Torr intervals at 30°C and the subsequent change in frequency was monitored, and the results are shown in Figure 24.

An air pressure of 400 Torr produced a frequency change of 35 Hz, and a linear relationship was found between change in frequency and air pressure. This emphasizes the requirement of a leak-tight system, particularly if small changes in frequency are to be measured, to ensure that any change in frequency can be attributed to the admittance of solvent rather than leaking of air into the system.

Hexane vapour was admitted into the sorption vessel whilst fitted with an uncoated crystal and the resulting frequency change was monitored at 20 Torr intervals over the pressure range 0 - 140 Torr at 30°C.

The frequency of the uncoated crystal changed linearly with solvent pressure as shown in Figure 24. The initial experiment indicates the importance of running a blank crystal in the required solvent before measuring the frequency change of a coated crystal. Any sorption of solvent

by the vacuum system can be eliminated by subtracting the frequency changes observed with the blank crystal from those of the coated crystal. The change in ΔF from hexane and air may be related to the difference in density of the two media.

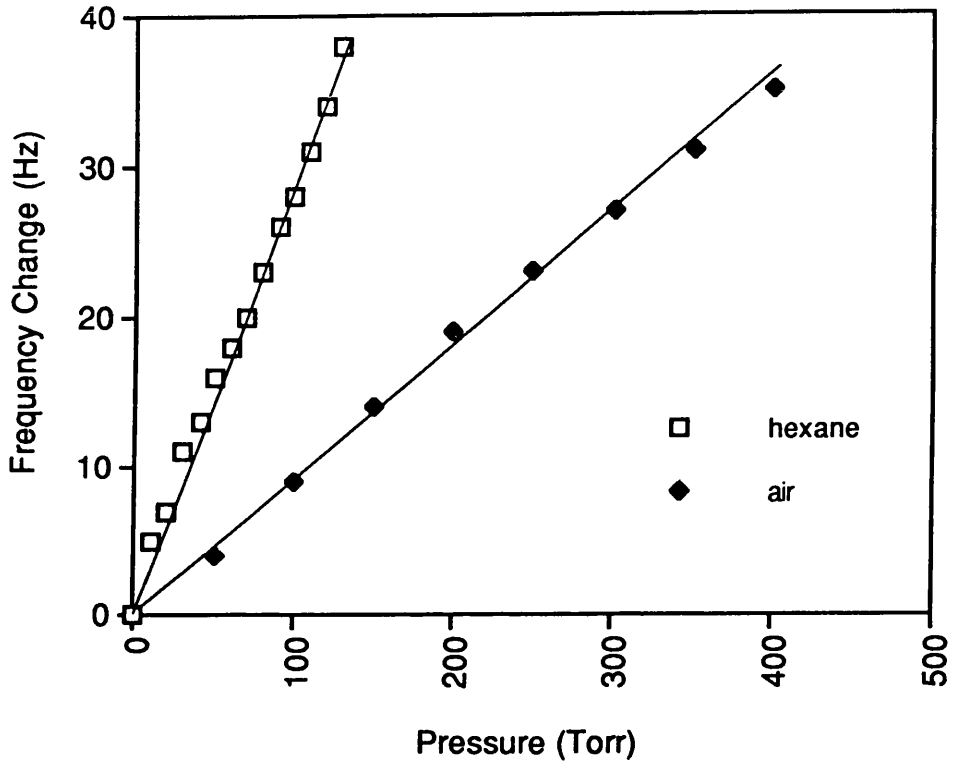

Figure 24: Solvent Sorption of an Uncoated Crystal at 30°C

3.2.3.2 Sorption of Benzene, Chloroform and Hexane on PDMS

As outlined in Chapter 1, PDMS is one of the most thoroughly studied polymers for which vapour liquid equilibria data is available hence allowing a comparison between performance of the QCM technique and that of other methods. It is also one of the few high molecular weight polymers available as a liquid at room temperature, allowing easier coating of the crystal.

To establish the validity of our sorption method, volume fraction activity coefficients and Flory-Huggins interaction parameters for benzene, chloroform and hexane in PDMS solutions at 30°C have been determined, and compared with literature data obtained by other vapour sorption measurements[159] (Figures 25 to 30). The same PDMS sample was used in both this work and that of reference 159. Each solvent system was run over as wide a solvent pressure range as possible, and repeated to ensure reproducibility. The results for the sorption of PDMS with benzene, hexane and chloroform have been directly compared with the results of Ashworth and Price as they have shown good reproducibility of their results with those from the literature.

Agreement between the volume fraction activity coefficients determined by the QCM method and that of Price[159] using a vapour sorption technique has been determined to within an average of ±2.6% for the various solvent systems studied. This agreement is well within the experimental error quoted by previous literature values. There is a greater deviation in the results at lower solvent concentration, which is probably due to differences in measurement procedures between the methods, and also less accuracy in making small Φ_1 and ${}^{v}\gamma_1$ measurements.

There is less agreement between the experimental values of interaction parameter and the literature values, than observed with the activity coefficients. The measurement of interaction parameters is more susceptible to variations in experimental conditions than are the activity coefficients. This can be clearly seen by consideration of the data obtained from the sorption of benzene on PDMS. The activity coefficients (Figure 25) obtained from the two experimental runs show good reproducibility, but the

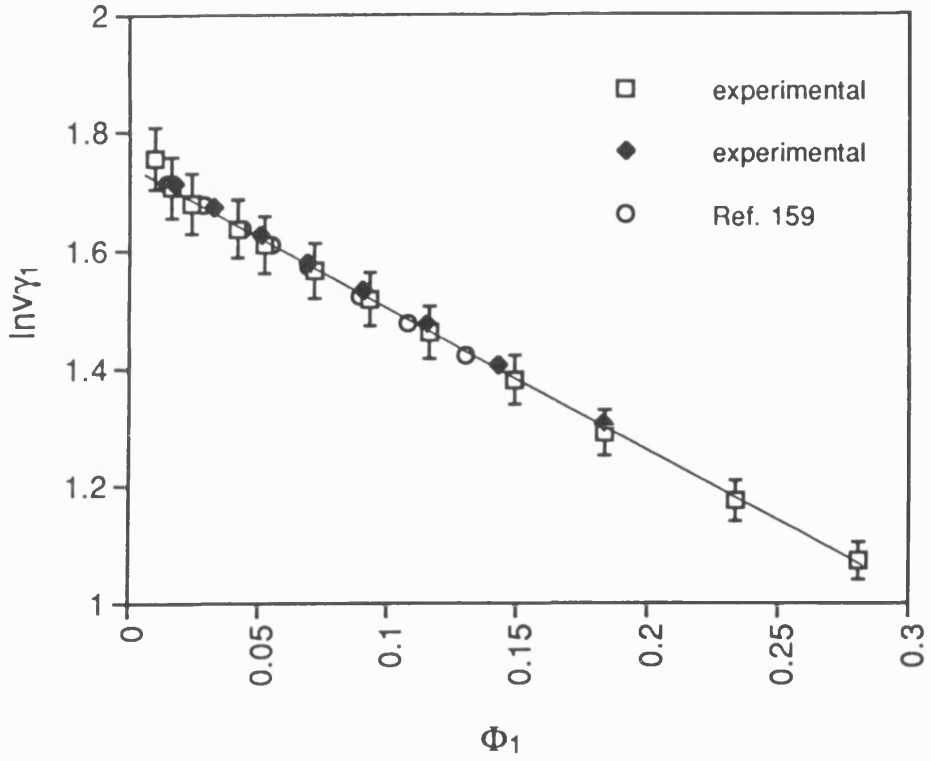

Figure 25: Sorption of Benzene on PDMS at 30°C

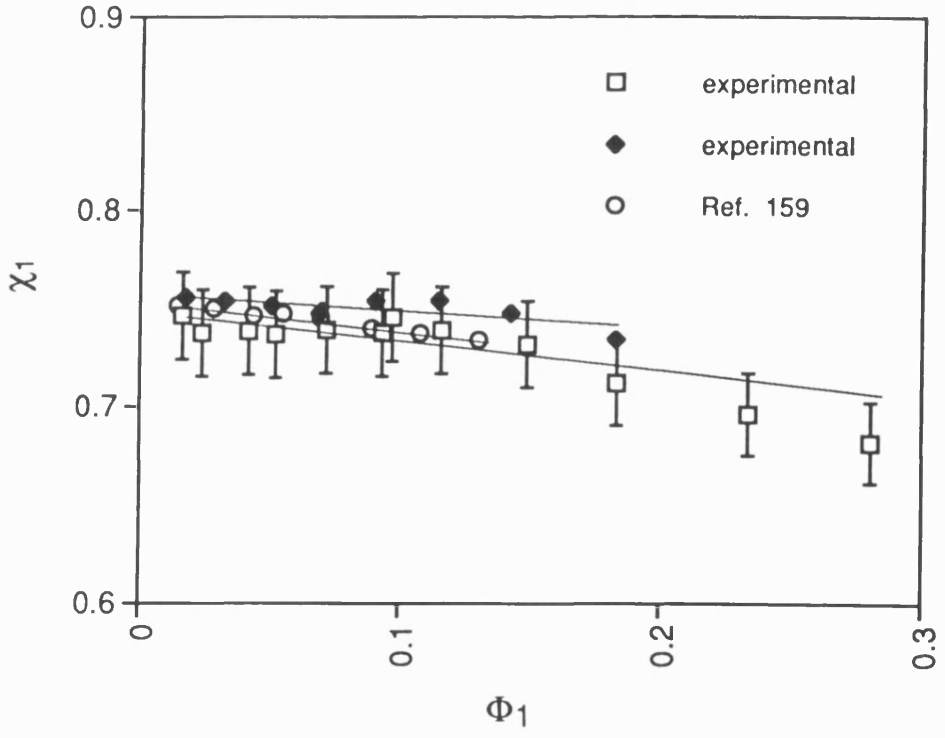

Figure 26: Sorption of Benzene on PDMS at 30°C

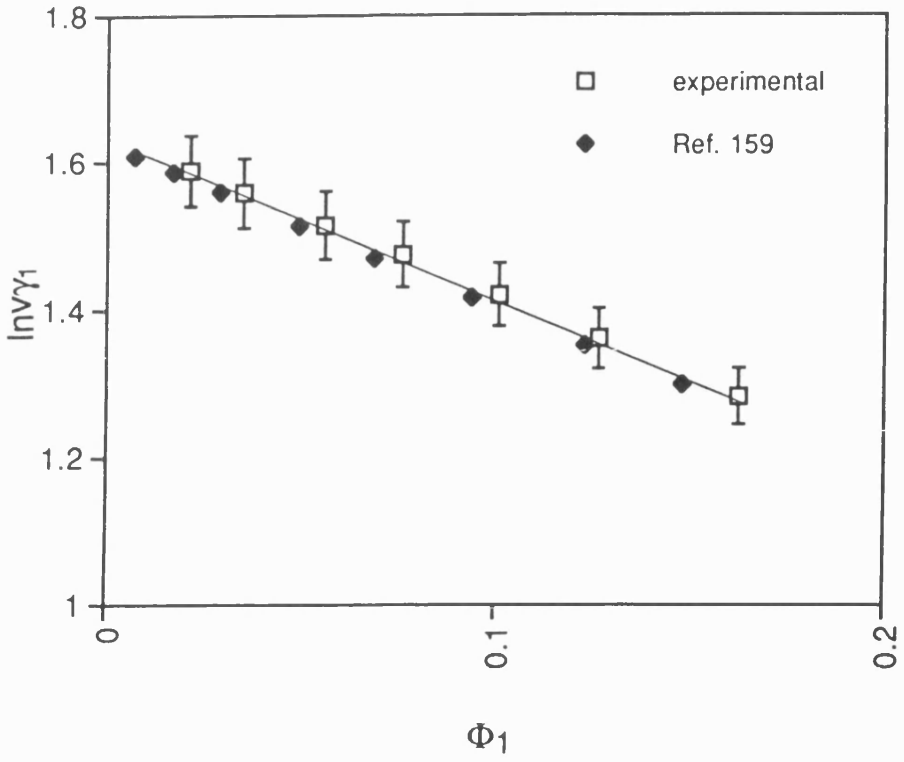

Figure 27: Sorption of Chloroform on PDMS at 30°C

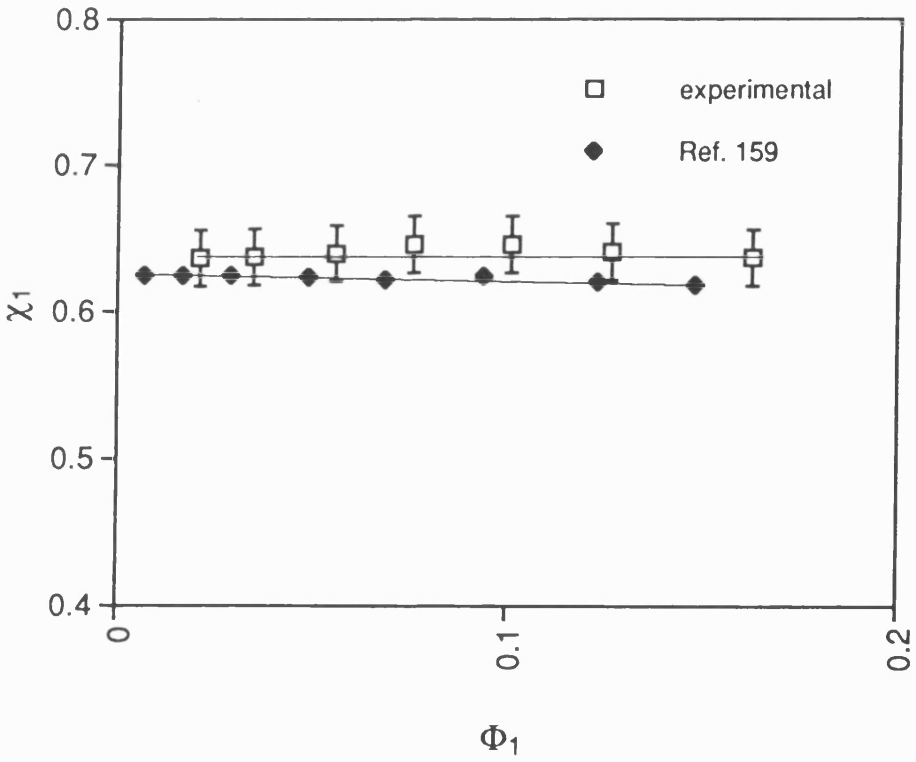

Figure 28: Sorption of Chloroform on PDMS at 30°C

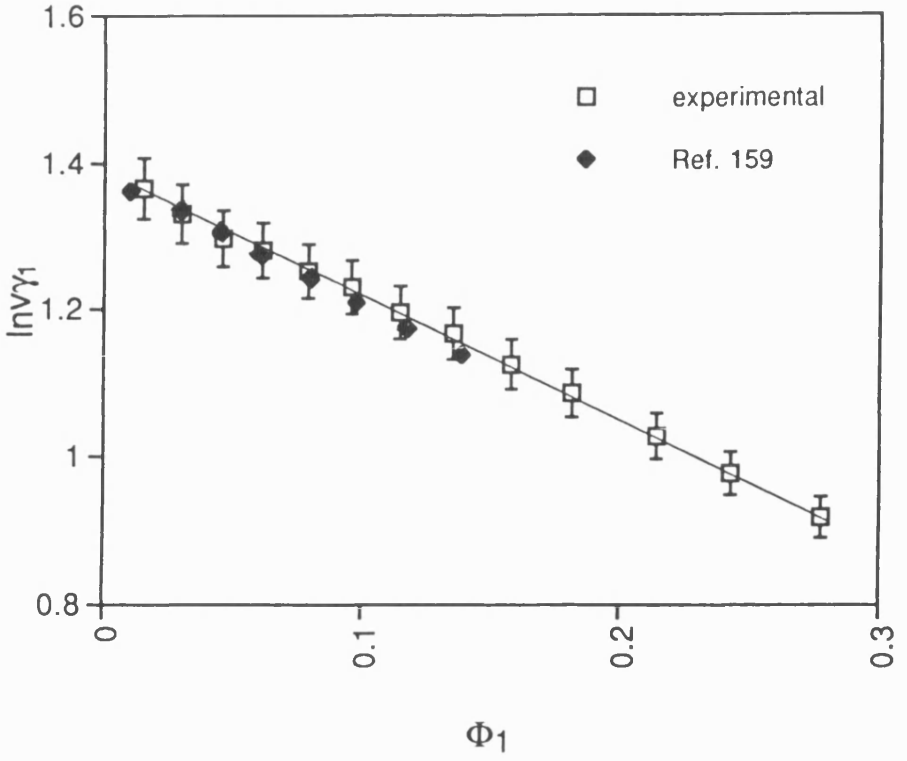

Figure 29: Sorption of Hexane on PDMS at 30°C

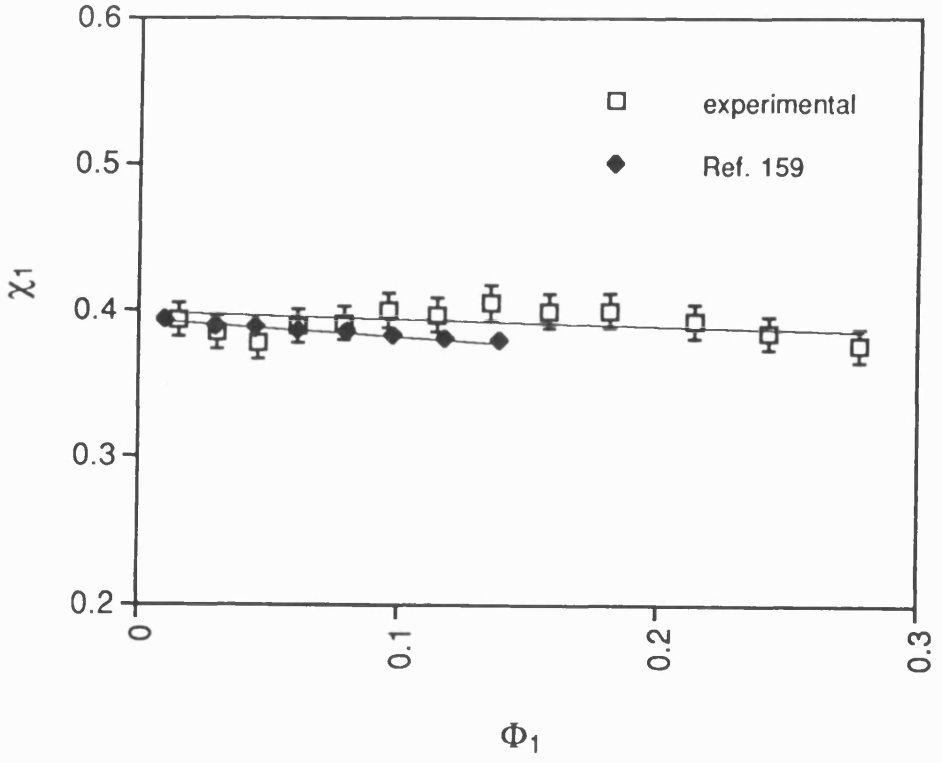

Figure 30: Sorption of Hexane on PDMS at 30°C

values of interaction parameter (Figure 26) show much greater deviation, even though the same experimental data was used for the calculation of both parameters.

3.3 Conclusion

In this preliminary results chapter, our initial studies of PMMA have illustrated that the QCM technique is a rapid and simple method for studying polymer dissolution. With our technique we have demonstrated that both concurrent dissolution and swelling characteristics can be reproducibly monitored in a series of solvents. We will show in subsequent chapters that this technique can be used to study the effect of some of the factors which determine the development resolution of resist systems.

In our thermodynamics studies, we have shown the importance of maintaining a low leak rate in the vacuum system, and how the Flory-Huggins interaction parameter is very prone to experimental error. However, we have shown good reproducibility of our experimental results for the interaction of PDMS in a series of solvents, and agreement with data obtained from more conventional vapour sorption techniques. In Chapter 4, we will demonstrate the reproducibility of our method for other polymer/solvent systems and compare the data with that obtained by other workers using the piezoelectric sorption technique. We will then present some thermodynamic data for systems similar to those used in our dissolution kinetics studies, and attempt to make use of this data to aid in the understanding of the role of polymer/solvent interactions during resist development.

Chapter Four

4.0 Thermodynamic Data from Vapour Sorption Studies

4.1 Introduction

During the development of photoresist materials, both the solvent penetration and resist dissolution are controlled by kinetic and thermodynamic polymer/solvent interactions. The mobility of a solvent molecule into the polymer structure can be related to its molecular size as will be discussed in Chapter 7, whilst the interactions between the polymer and solvent molecules give an indication of thermodynamic compatibility. As shown in Chapter 1, a measure of polymer/solvent compatibility is given by the Flory-Huggins interaction parameter. To enable a correlation between observed dissolution kinetics and thermodynamic interaction, the activity coefficients and interaction parameters have been measured for a series of polymer/solvent systems close to those used in our dissolution kinetics studies.

In Chapter 3, our initial studies of solvent sorption on PDMS have shown the reproducibility of the QCM method for the determination of thermodynamic parameters with results obtained from other more traditional sorption methods. In this Chapter, these studies have been further continued by the direct comparison of our experimental data for the sorption of solvent on polystyrene with results obtained by other workers using a QCM method[161]. Volume fraction activity coefficients and Flory-Huggins interaction parameters were also measured for a series of PMMA/solvent systems where literature results are not available. This will allow the direct

comparison with the PMMA and polystyrene/solvent systems used in the dissolution kinetics studies.

The sorption apparatus as described in Section 2.1, was set up with a dual crystal holder to allow the monitoring of the change in frequency of a blank crystal whilst measuring the frequency of the polymer coated crystal upon solvent sorption. In the following experiments, the frequency of the uncoated crystal remained constant, indicating that all the frequency changes observed for the coated crystal must be due to solvent sorption by the polymer coating and not the quartz crystal.

Throughout the thermodynamic study, it was observed that after each sorption experiment, the frequency of the coated crystal did not always return to its original oscillating frequency after solvent evacuation. This may be due to the movement of the polymer coating during solvent sorption or insufficient solvent desorption.

Graphs have been plotted to show the thermodynamic parameters measured for the polymer/solvent systems studied. The results are tabulated in Appendix 1.

4.2 Solvent Interactions with Polystyrene

4.2.1 Sorption of Benzene on Polystyrene

The sorption of benzene on polystyrene (M_W 430000, γ 3.1) was measured at 30°C with two quartz crystals coated with different coating thicknesses (ΔF_0 = 1712 and 1990 Hz). Figures 31 and 32 show there is good agreement for both the activity coefficients and Flory-Huggins interaction parameters. The reproducibility of the results obtained with our apparatus for two different crystals was thus clearly demonstrated.

The sorption of benzene with polystyrene has been previously studied by Saeki and co-workers[161], using a piezoelectric sorption detector, and by Baughan[164], using a more conventional weighing method. These studies were carried out at 23.5 and 20.0°C, using polystyrene samples of molecular weight 110000 and 500000, respectively. A comparison of our results with those of both Saeki and Baughan can be seen in Figures 31 and 32. Our experimental results would be expected to deviate from the literature, as our sorption study was performed at a higher temperature using a different molecular weight polystyrene sample. Over the concentration range measured, a linear relationship between the activity coefficient and solvent fraction is observed, with our experimental results higher than those of Saeki and co-workers but of a comparable line of slope. Baughan's values of activity coefficients are also in very good agreement with our experimental data except at high and low concentrations of solvent, where the values of interaction parameter deviate greatly due to the scatter of Baughan's data.

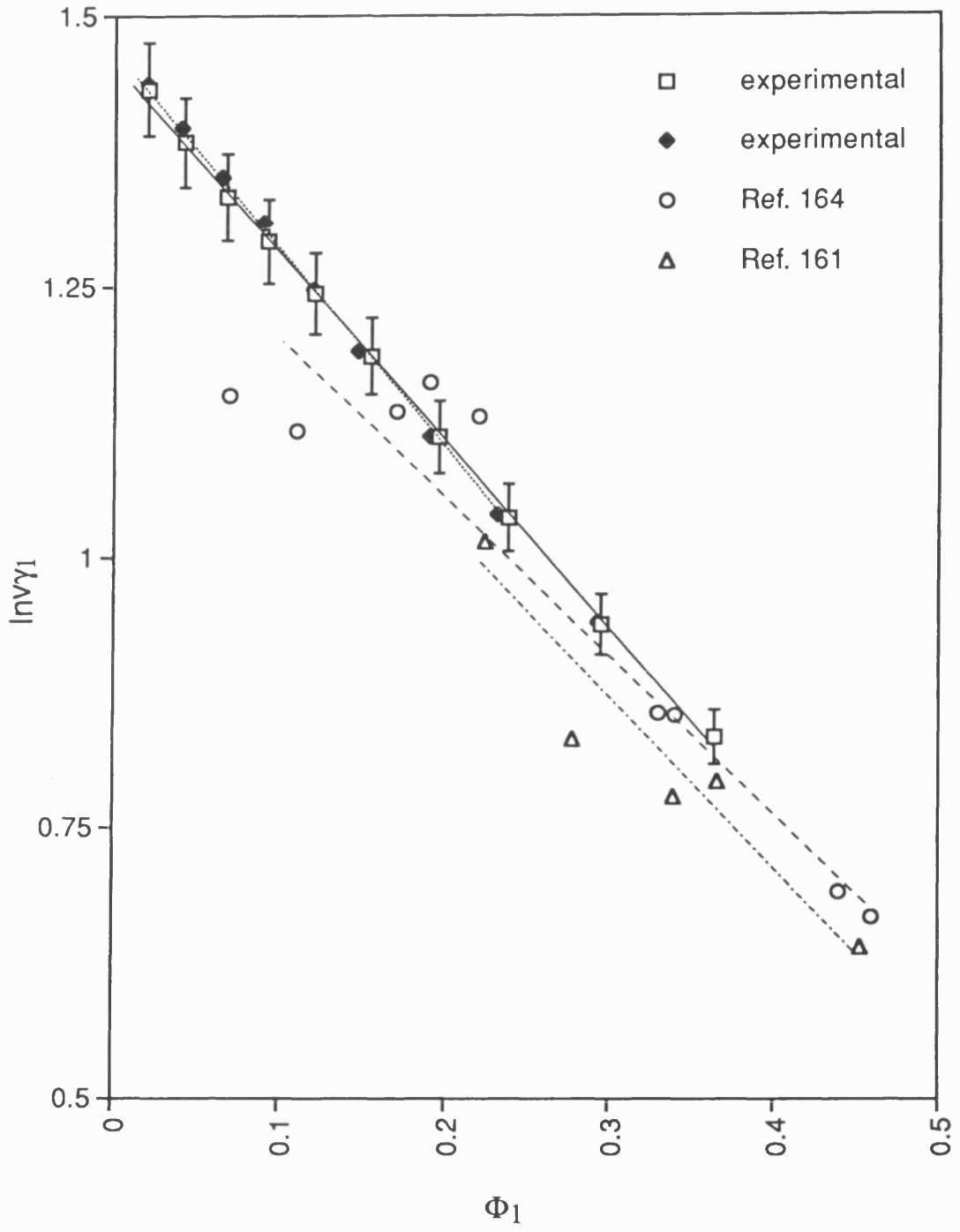

Figure 31: Sorption of Benzene on Polystyrene at 30°C

Activity Coefficient

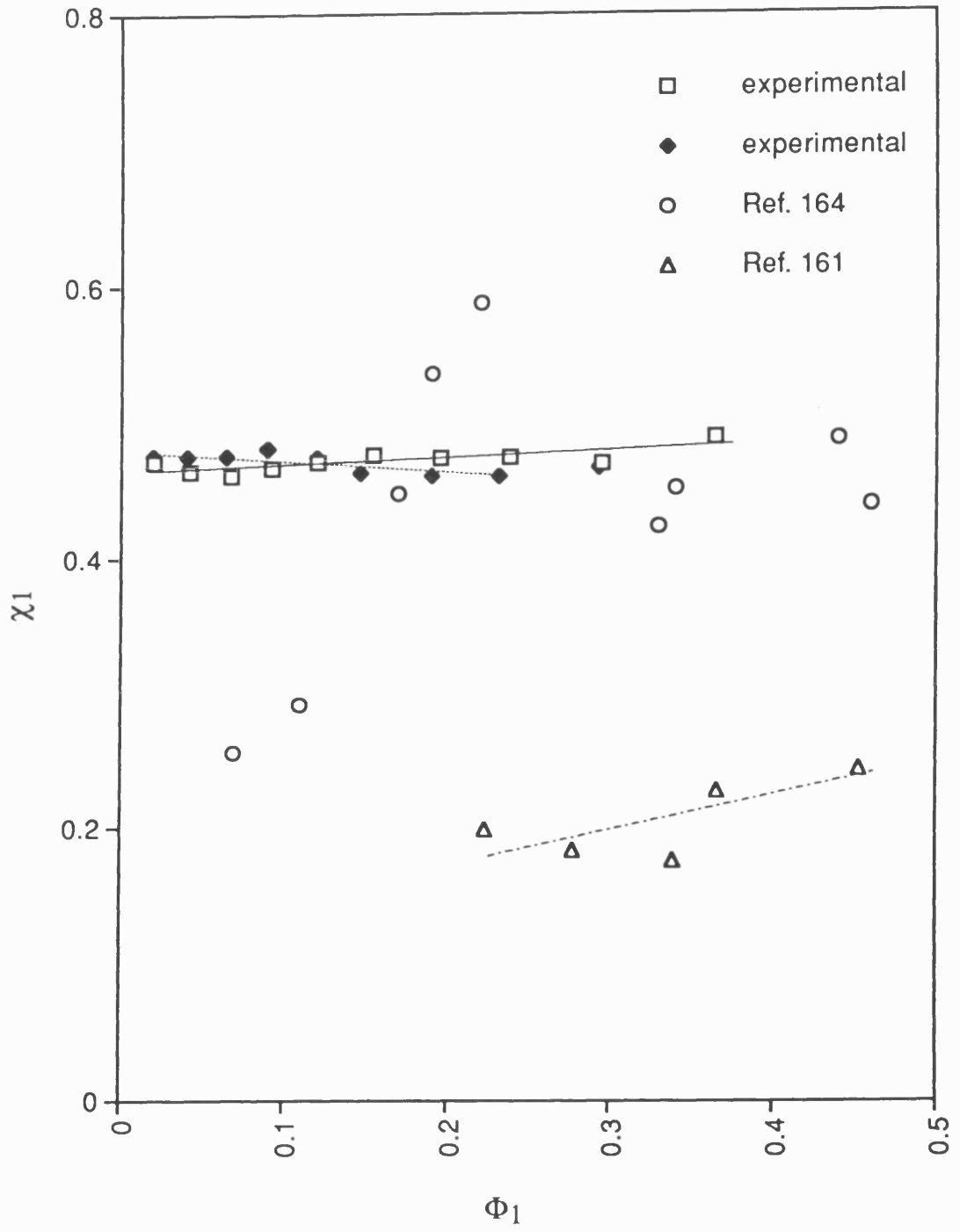

Figure 32: Sorption of Benzene on Polystyrene at 30°C

Interaction Parameter

This observed deviation between the results of Baughan and our experimental data may be due to the different measurement procedures. For example, the polymer films used in the vapour sorption experiments of Baughan were cast from a 3% w/v polystyrene/benzene solution, and the amount of solvent sorbed by the polymer sample is measured by a balance with a precision of ±0.05 mg. In our study, the polymer sample was coated on the crystals from a 0.05% w/w polystyrene/chloroform solution (giving a thinner film), and the weight of the solvent sorbed by the polymer was measured with a precision of ±0.002 mg. Hence, with our thinner coating (i.e. lower equilibration times) and higher precision, we are able to obtain lower experimental error.

Figures 33 and 34 illustrate the effect of changing temperature on the values of γ and χ respectively. For the sorption temperatures (i.e. 25, 30 and 35°C), there is little difference in the slopes for both γ and χ with the values of all the thermodynamic parameters decreasing with increasing temperature. The average values of χ are 0.62, 0.47 and 0.43 at 25, 30 and 35°C respectively, the interaction parameter values indicating poorer solvent interaction at lower sorption temperatures. At all three temperatures, χ was found to be approximately independent of solvent concentration and, as expected, χ and γ were not found to change linearly with sorption temperature (it is often found that χ depends on $1/T$[126]). It is therefore surprising that Saeki has found lower interaction parameter values at a lower sorption temperature.

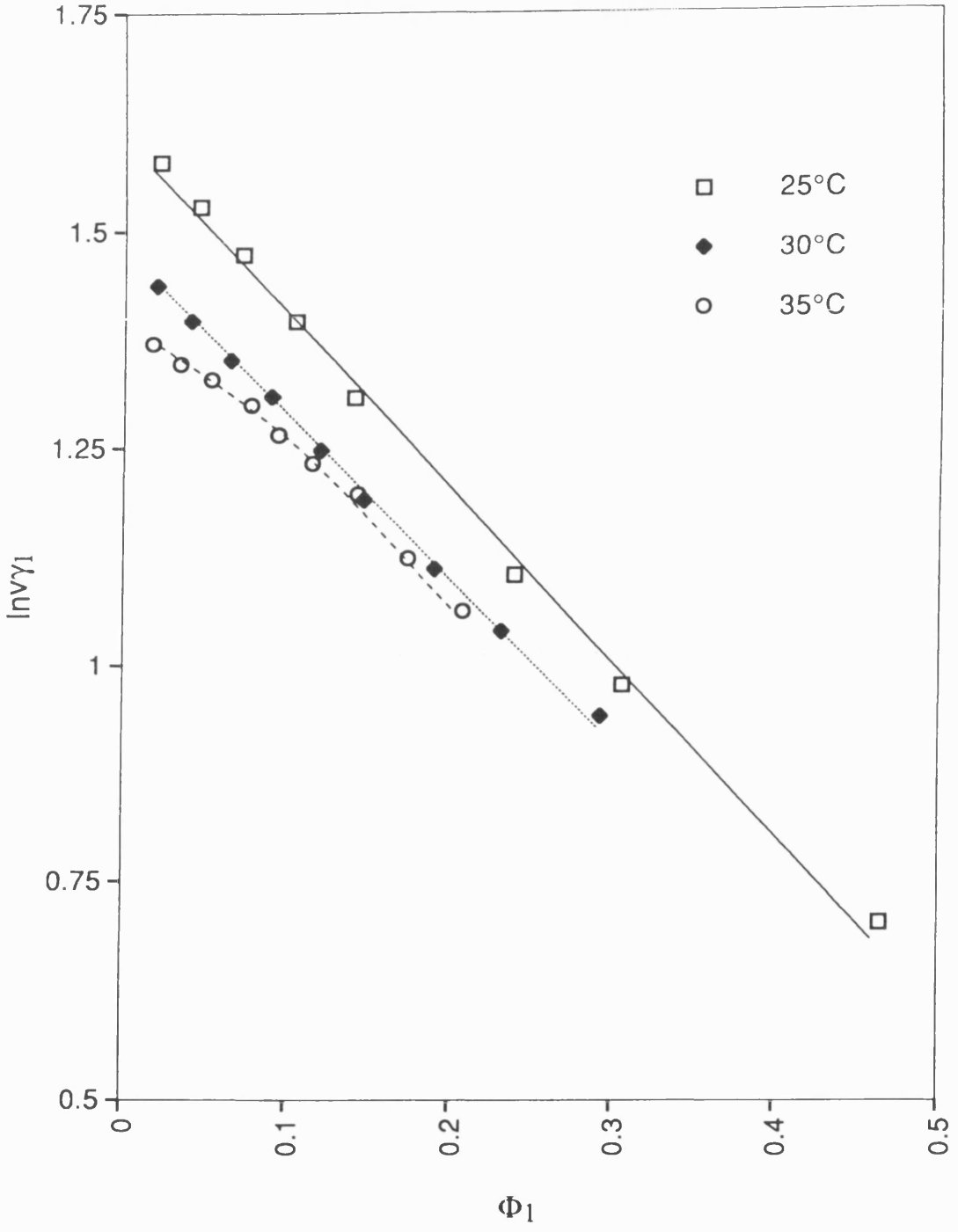

Figure 33: Effect of Temperature on the Sorption of Benzene on Polystyrene - Activity Coefficient

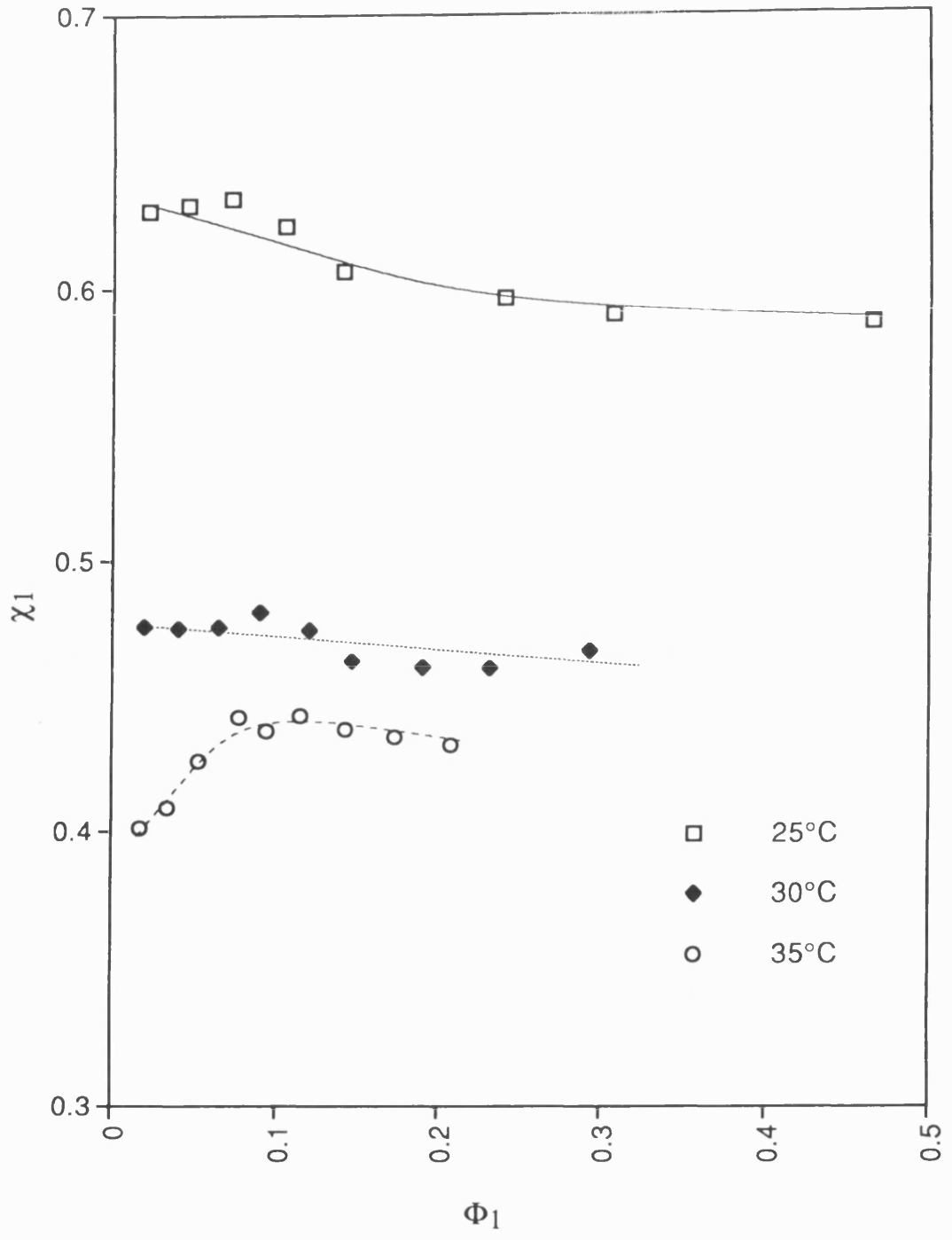

Figure 34: Effect of Temperature on the Sorption of Benzene on Polystyrene - Interaction Parameter

4.2.2 Sorption of Chloroform on Polystyrene

Figures 35 and 36 show the volume fraction activity coefficients and interaction parameters for the sorption of chloroform on polystyrene at 25, 30 and 35°C. The values of activity coefficients and interaction parameters decrease with increasing temperature (i.e. enhanced polymer/solvent interaction). A slight increase in interaction parameter is observed with increasing solvent concentration, however, as the error bars indicate, this may be due to experimental error.

The activity coefficients obtained by Bawn and co-workers[174] using a polystyrene sample (M_n 290000) at 25°C and vapour pressure lowering technique correlate well with the experimental data. Figure 36 indicates that there is a slight deviation in the gradient of the line for χ between the experimental and literature data, however similar dependence of interaction parameter with solvent concentration has been found.

There is great disagreement between our experimental results and those of Saeki and co-workers for their measurement of chloroform sorption on polystyrene (M_w 600000) at 23.5°C[161]. Using a similar measurement technique, Saeki found much lower activity coefficient values which were independent of solvent concentration. For the values of interaction parameter, there was no correlation between our experimental data and that of Saeki except for a similar line of slope for the range of solvent concentration studied. Saeki has obtained negative values of χ which is rather surprising as it would indicate that there are specific interactions between chloroform and polystyrene which is unlikely in this system.

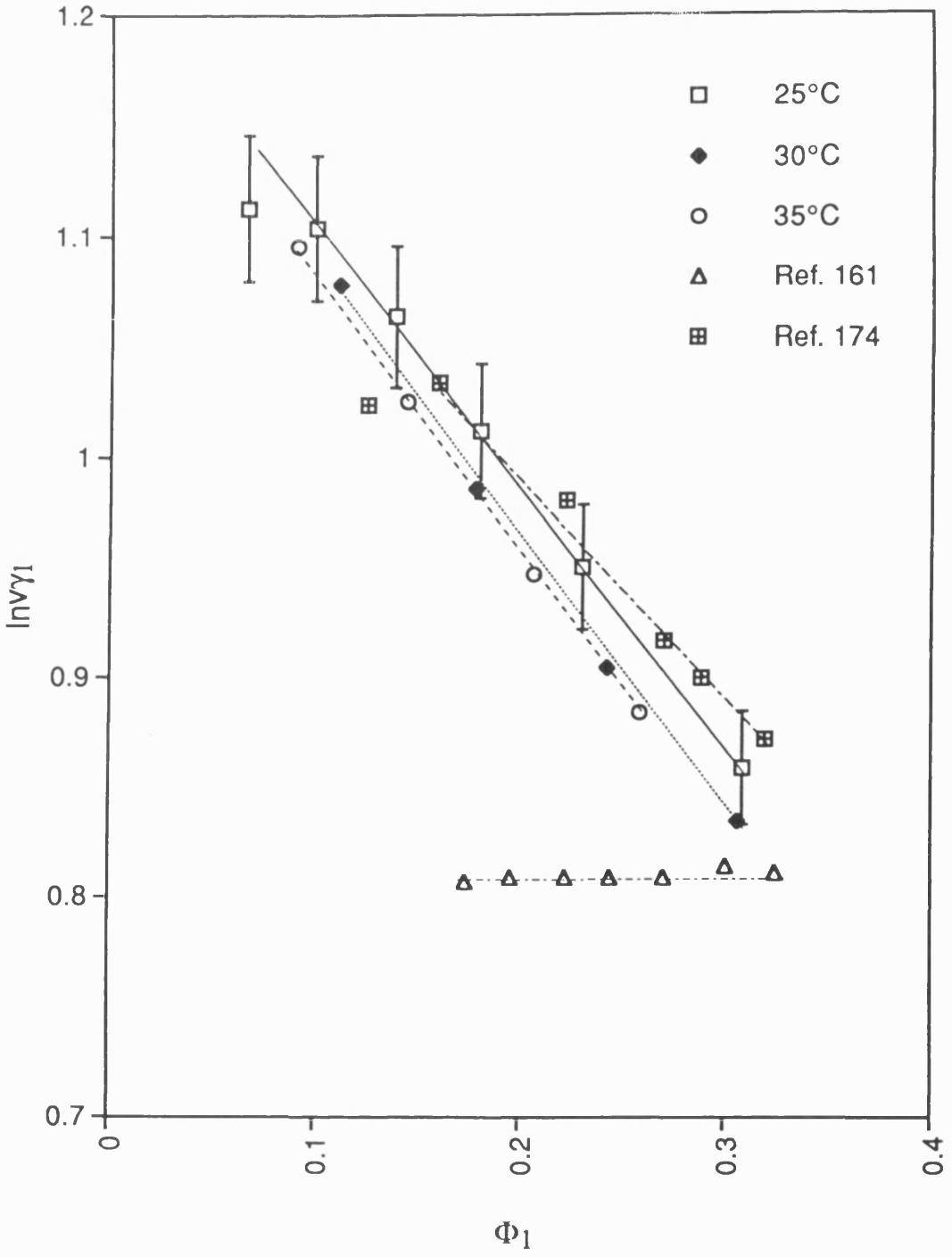

Figure 35: Effect of Temperature on the Sorption of Chloroform on Polystyrene - Activity Coefficient

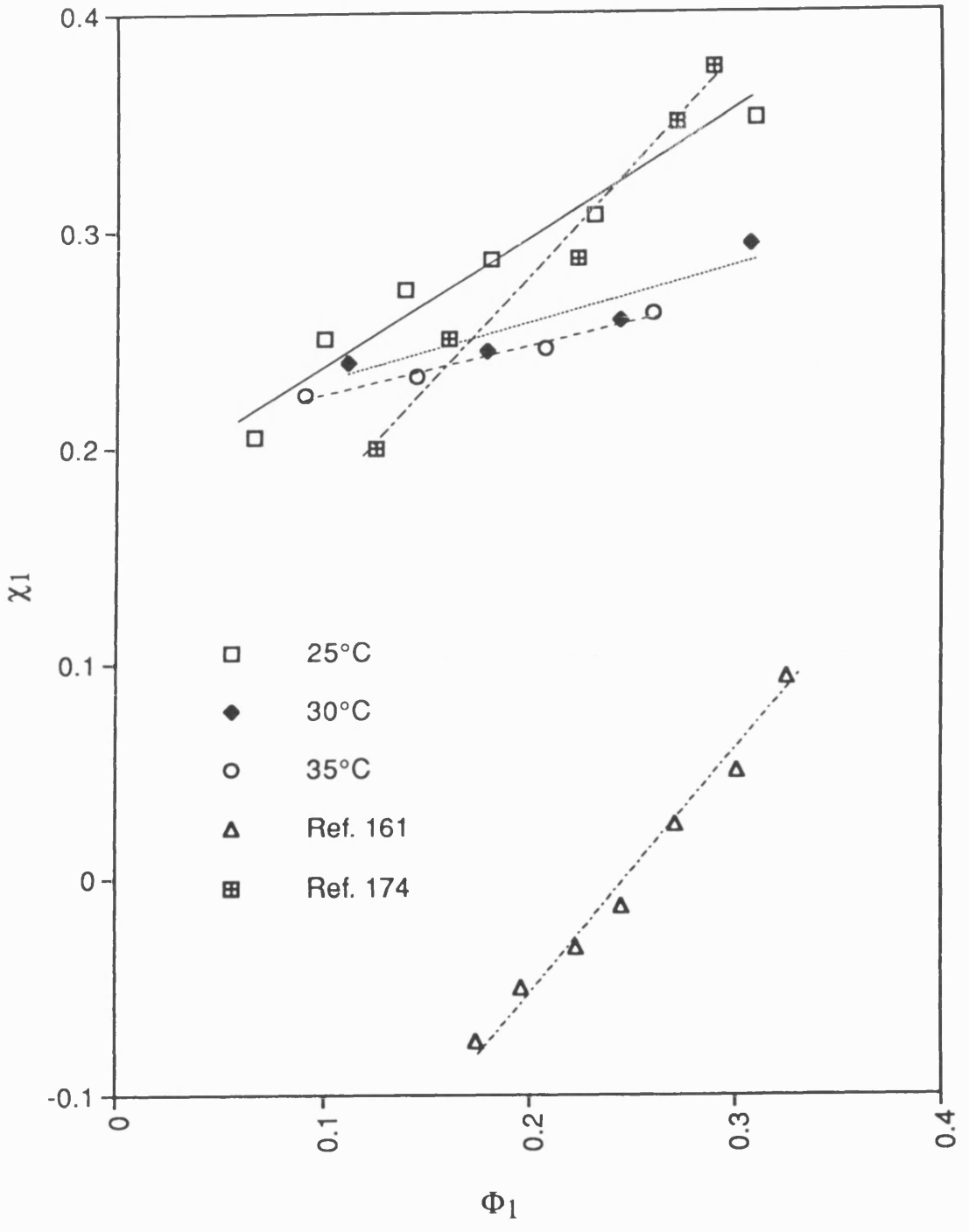

Figure 36: Effect of Temperature on the Sorption of Chloroform on Polystyrene - Interaction Parameter

4.2.3 Sorption of Cyclohexane on Polystyrene

The volume fraction activity coefficients and interaction parameters for the sorption of cyclohexane on polystyrene at 30°C are shown in Figures 37 and 38. Good linear correlation between the activity coefficient and solvent volume fraction was obtained, and comparison of two separate runs, with different quartz crystals, again shows good reproducibility of the results. The deviation between the two sets of interaction parameters is also well within experimental error (as discussed in Chapter 3).

The sorption of cyclohexane on polystyrene (M_n 110000 and 500000) has also been studied by Saeki[161] at 23.5°C, using a piezoelectric sorption detector, and by Baughan[164] at 25.0°C, using a more traditional weighing method. Our results for the activity coefficients and the line of slope correlate well with both sets of literature results, whilst there is deviation in the values of χ. The experimental results show a decrease in interaction parameter (i.e. increased solvent interaction) with increasing solvent concentration. Baughan found higher values of χ but with a similar line of slope, which is not unexpected as both a different molecular weight of polystyrene and lower sorption temperature were used. However, Saeki and co-workers found lower values of interaction parameter which were less dependent upon solvent concentration.

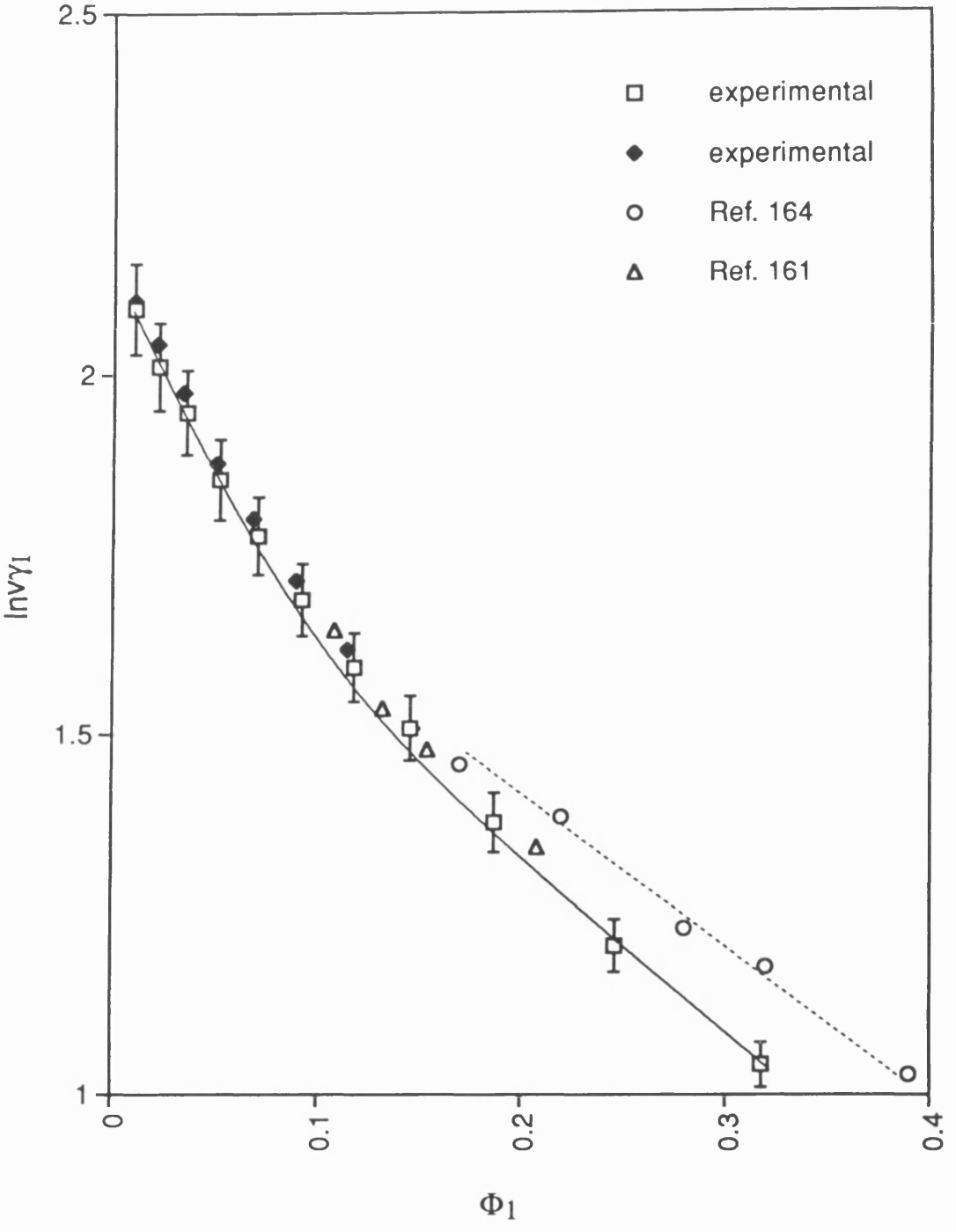

Figure 37: Sorption of Cyclohexane on Polystyrene at 30°C

Activity Coefficient

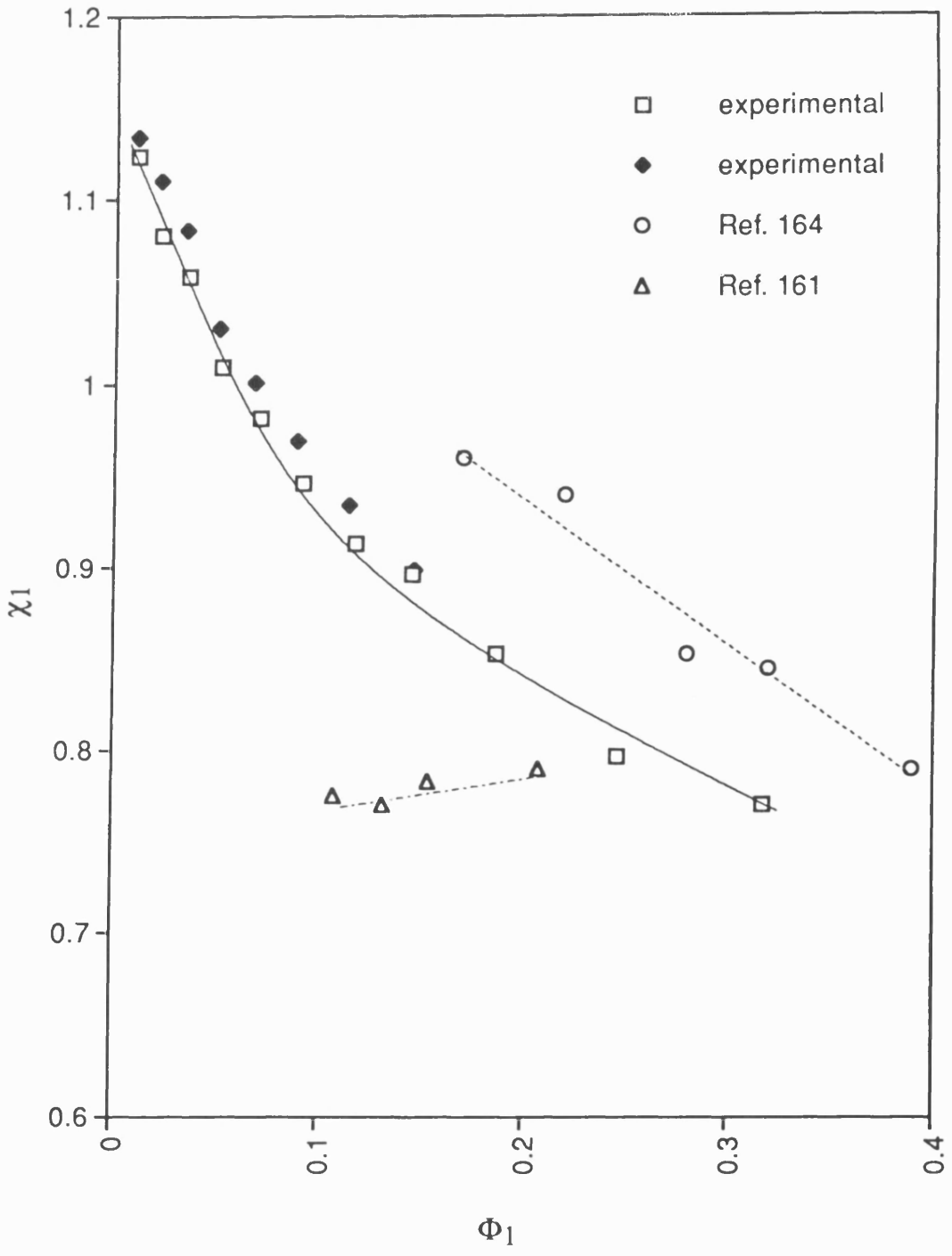

Figure 38: Sorption of Cyclohexane on Polystyrene at 30°C

Interaction Parameter

4.2.4 Sorption of Hexane on Polystyrene

Figures 39 and 40 show the volume fraction activity coefficients and interaction parameters for the polystyrene/hexane system at 30°C. It was very difficult to obtain reasonable reproducibility for this polymer/solvent system, especially at lower concentrations of solvent. There are no literature results for direct comparison with this system. The activity coefficient decreases with increasing solvent concentration, whilst the interaction parameter shows an average value of 1.1 with little variation with respect to solvent concentration. This high value of the interaction parameter is indicative of the poor interaction between the hexane molecules and polystyrene.

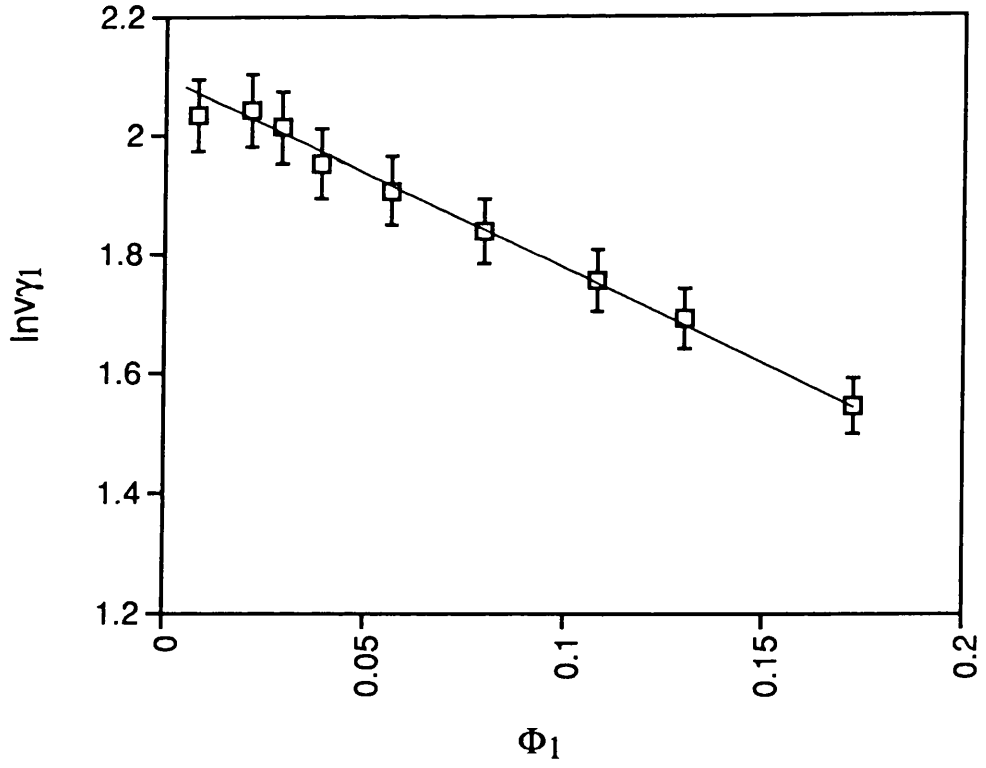

Figure 39: Sorption of Hexane on Polystyrene at 30°C

Activity Coefficient

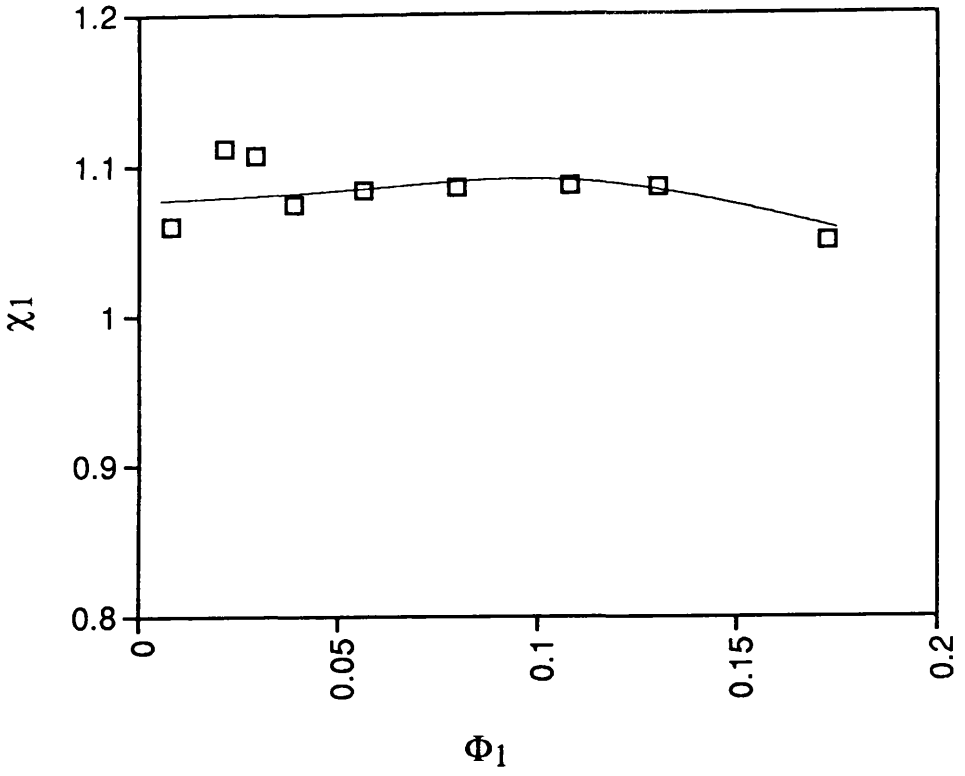

Figure 40: Sorption of Hexane on Polystyrene at 30°C
Interaction Parameter

As we have clearly demonstrated, by comparison with literature, that the QCM vapour sorption technique is a valid method for the determination of γ and χ at a series of sorption temperatures, we have continued our study to include systems comparable to those used in the dissolution kinetics chapters.

4.2.5 Sorption of MEK on Polystyrene

The activity coefficients and interaction parameters for the sorption of MEK on polystyrene at 30°C are shown in Figures 41 and 42 respectively. The activity coefficient and interaction parameter decrease linearly with

increasing solvent concentration. Above the solvent volume fraction of 0.05, the interaction parameter is then found to be virtually independent of solvent concentration, with an average value of 0.8. Good reproducibility between experiments was found for both γ and χ.

Using vapour pressure lowering techniques, Bawn and co-workers[131] have also carried out a study of MEK sorption on polystyrene (M_n 290000) at 25°C. The literature results for χ are lower than those obtained from this study and increase with solvent concentration. It should be noted that Bawn and co-workers used a lower molecular weight sample and sorption temperature, and quoted very little experimental data.

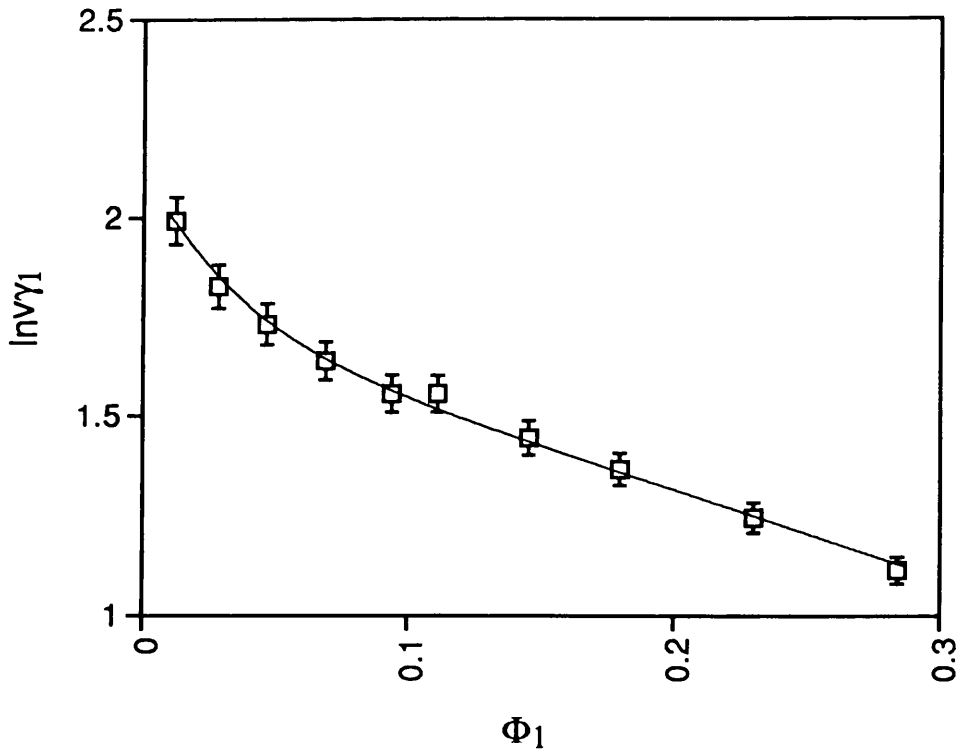

Figure 41: Sorption of MEK on Polystyrene at 30°C

Activity Coefficient

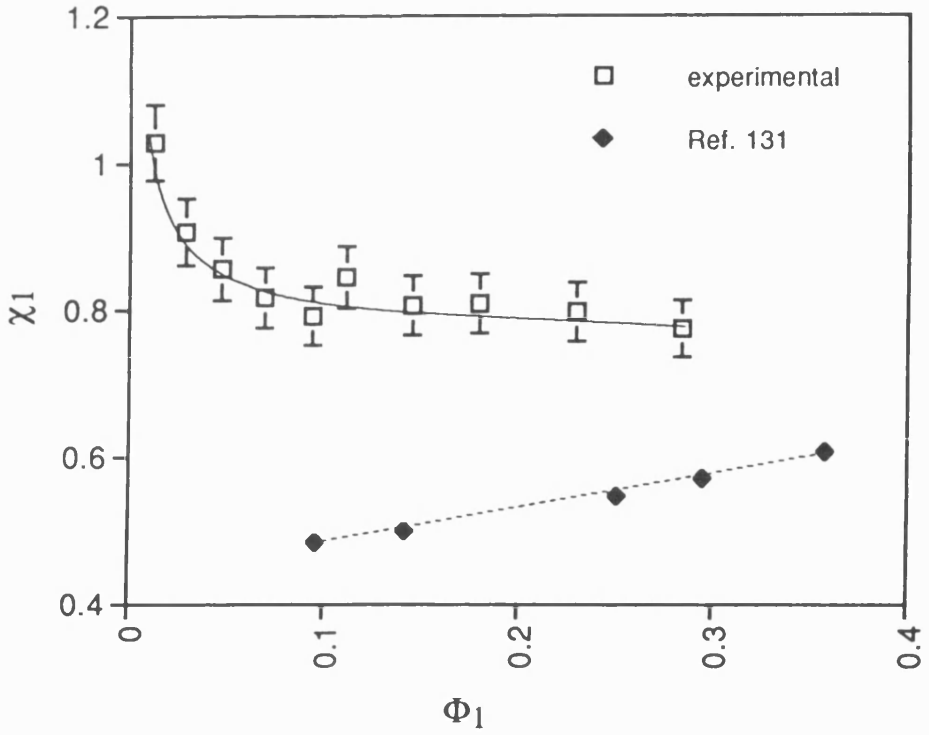

Figure 42: Sorption of MEK on Polystyrene at 30°C

Interaction Parameter

4.2.6 Sorption of IPA on Polystyrene

Using our developed experimental technique, the sorption of IPA on polystyrene at 30°C has been measured. Figures 43 and 44 indicate that at low solvent concentration, both the values of activity coefficient and interaction parameter initially increase until reaching a solvent volume fraction of 0.05, where upon a decrease in activity coefficient and constant value of interaction parameter is observed. The increase in both χ and γ is not linear, and the observed upward slopes may be due to the larger experimental error in measurement that occurs at very low concentrations of solvent ($\Phi_1 < 0.05$). There are no literature values available for the sorption of IPA on polystyrene.

Comparison of the activity coefficients for the sorption of MEK and IPA on polystyrene gives a clear indication of the differences in the polymer/solvent interactions for the two solvents. Both Υ and χ values for IPA sorption are much higher than the respective values for MEK, and the deviation between values increases at higher solvent concentrations. The low values of χ for MEK in polystyrene indicate that it is a good solvent for polystyrene, whilst the high values of χ for IPA sorption indicate that the alcohol is a poor solvent. It would therefore be expected that mixtures of MEK and IPA will give an intermediate value of χ.

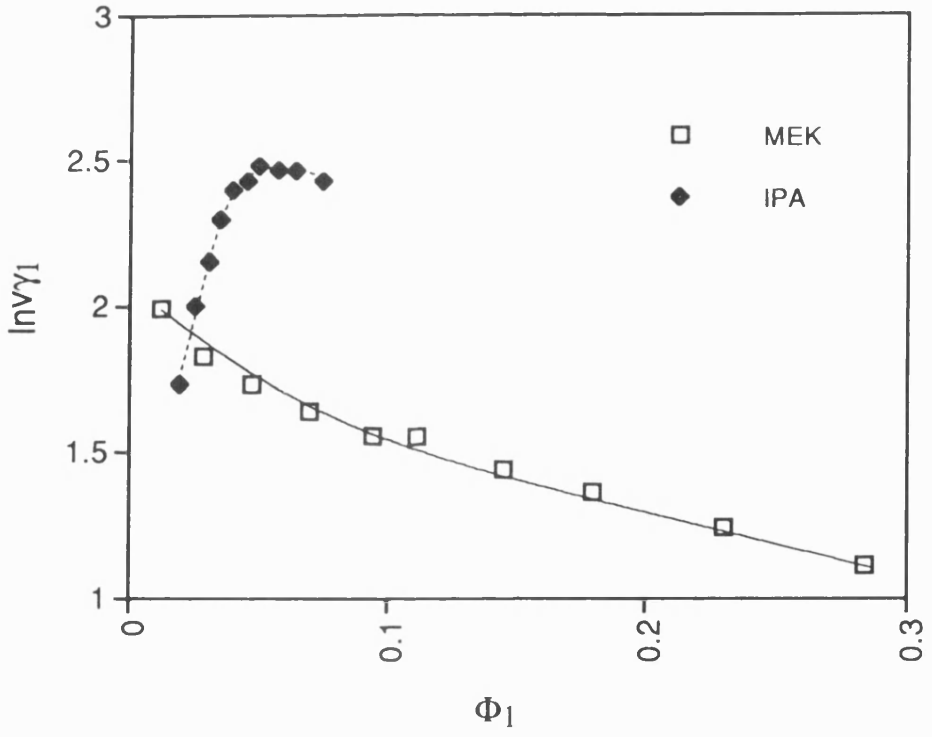

Figure 43: Sorption of MEK and IPA on Polystyrene at 30°C

Activity Coefficient

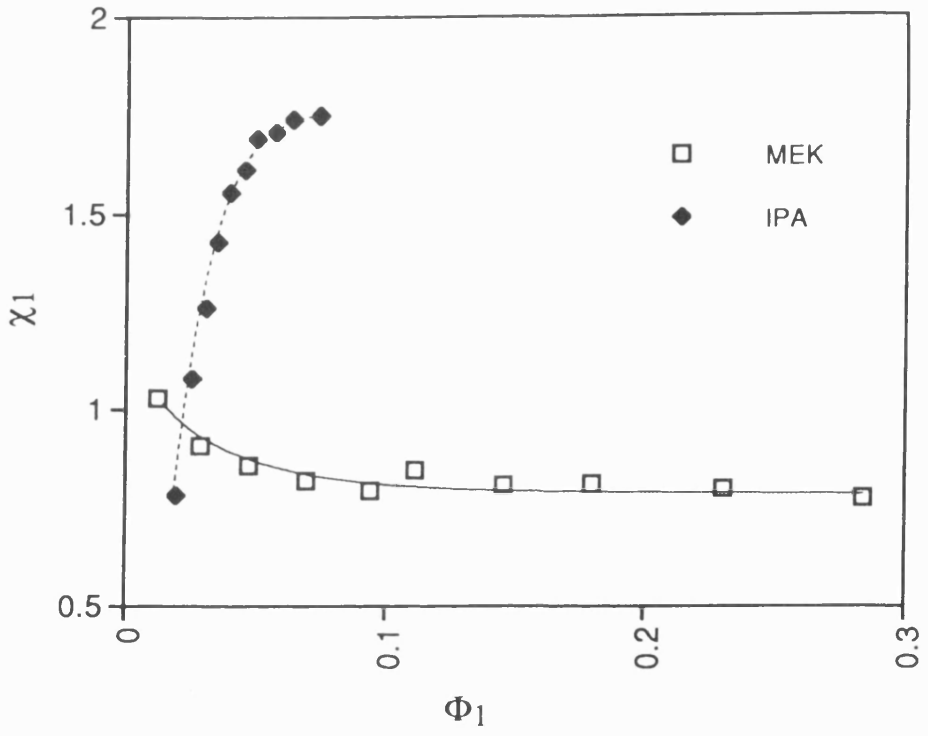

Figure 44: Sorption of MEK and IPA on Polystyrene at 30°C

Interaction Parameter

The results for the polystyrene/solvent systems clearly show that our technique is a suitable method for the determination of the activity coefficient and interaction parameter for polymer/solvent systems. The use of the piezoelectric sorption apparatus in the determination of the thermodynamics of polymer solutions has been further continued to include the study of other resist/solvent systems.

4.3 Solvent Interactions with Poly(4-chlorostyrene)

As stated in Section 1.1.2.1, recent developments in styrene-based resists have shown that the inclusion of chlorine into the benzene ring enhances the sensitivity of the resist. The addition of this chlorine atom will affect the polarity of the polymer and hence, the observed thermodynamic behaviour of poly(4-chlorostyrene) would be expected to differ from polystyrene.

4.3.1 Sorption of Benzene on Poly(4-chlorostyrene)

The activity coefficients and interaction parameters for the sorption of benzene on poly(4-chlorostyrene) at 30°C are shown in Figures 45 and 46. For comparison, the results for the polystyrene/benzene system (Section 4.2.1) have been included. After an initial rise at low solvent concentrations, the activity coefficient decreases with increasing solvent volume fraction. At the lower solvent concentrations, the activity coefficient for the sorption of benzene on poly(4-chlorostyrene) is lower than that for polystyrene with a different slope of the line. Due to the differences in polarity, a difference in activity of the two polymers would be expected. Solvent molecules surrounding a polar sub-unit of a polymer chain will tend to orient in the field of the dipole, and this effect will be greatest for poly(4-chlorostyrene). Because of these orientation effects, there are changes in the entropy and heat of dilution which do not occur in the case of the non-polar polymer. It seems that the polar contribution for poly(4-chlorostyrene) is not constant but reaches a maximum in the activity coefficient around a solvent concentration of 0.1.

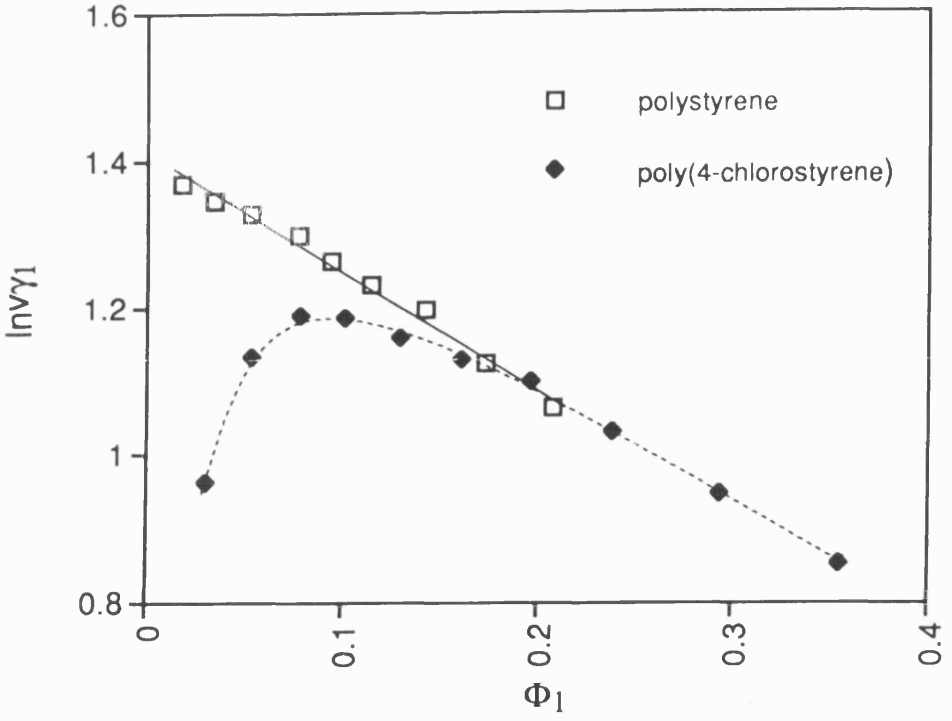

Figure 45: Sorption of Benzene on Poly(4-chlorostyrene) and Polystyrene at 30°C - Activity Coefficient

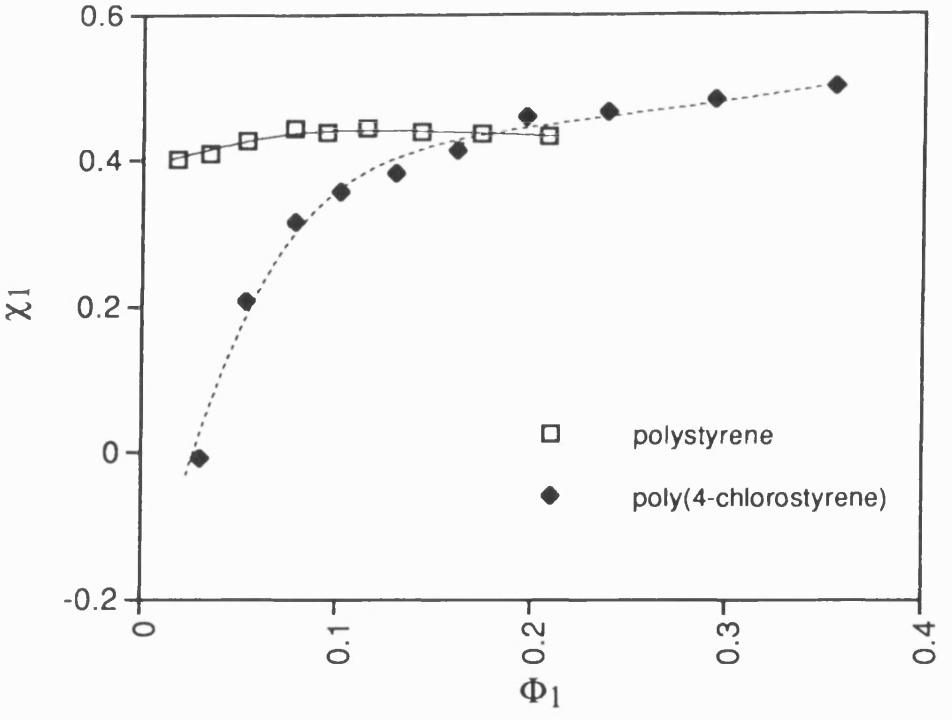

Figure 46: Sorption of Benzene on Poly(4-chlorostyrene) and Polystyrene at 30°C - Interaction Parameter

At very low solvent concentrations, the interaction parameter for the poly(4-chlorostyrene)/benzene system is negative and initially increases rapidly with solvent fraction. Above a solvent fraction of 0.1, this increase in interaction parameter becomes more gradual and the values lie closer to those of polystyrene.

The deviation from linearity for the poly(4-chlorostyrene)/benzene system at low concentrations, may be attributed to the difference between the van der Waals forces assumed in the Flory-Huggins theory and the actual intermolecular potential between the polymer segment and the solvent molecule. It is possible that a polar interaction exists between the benzene ring and the chlorine atom in the polymer. The very low value of χ indicates a very strong interaction between the solvent and polymer. At higher solvent concentrations, where there is less variation in the value of χ, the polymer becomes saturated with the solvent and hence the polar contribution becomes less significant. As discussed in Section 3.2.2, at low concentrations of solvent, there is greater experimental error associated with the interaction parameter (such as the correct attainment of the equilibrium position) and this may contribute towards the scatter of experimental data.

4.3.2 Sorption of Cyclohexane on Poly(4-chlorostyrene)

The activity coefficients and interaction parameters for the sorption of cyclohexane on poly(4-chlorostyrene) and polystyrene at 30°C are displayed in Figures 47 and 48 respectively. Both the activity coefficient and interaction parameter decrease with increasing solvent concentration, with higher values than the corresponding polystyrene/cyclohexane system. As observed in Section 4.3.1, the difference in activity coefficients between the two polymers may be accounted for by consideration of differences in polymer polarity. At solvent volume fractions greater than 0.05, the slopes of the lines in Figure 47 are similar, indicating a constant polar contribution. Figure 48 shows that the interaction parameter for poly(4-chlorostyrene) in cyclohexane has a linear dependence upon solvent concentration.

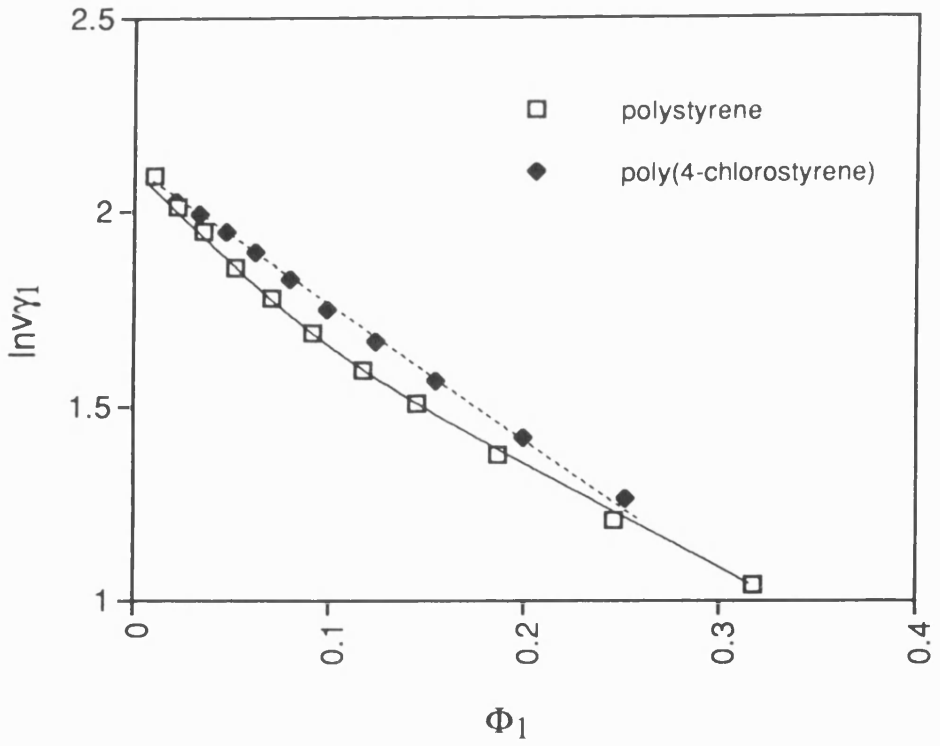

Figure 47: Sorption of Cyclohexane on Poly(4-chlorostyrene) and Polystyrene at 30°C - Activity Coefficient

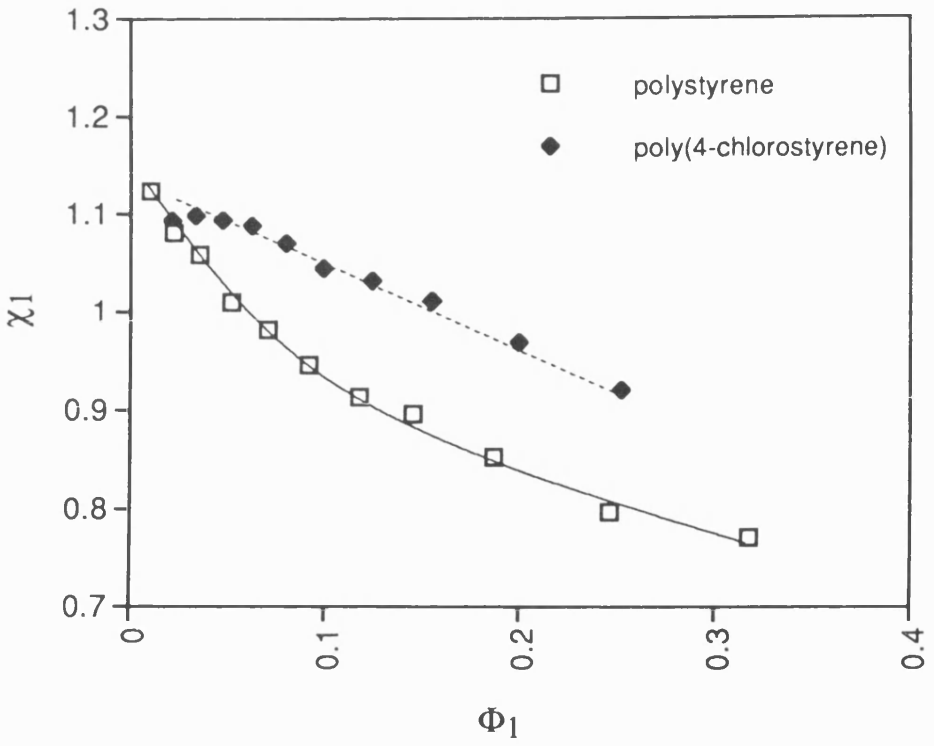

Figure 48: Sorption of Cyclohexane on Poly(4-chlorostyrene) and Polystyrene at 30°C - Interaction Parameter

An indication of the effect of the polar contribution of poly(4-chlorostyrene) to the interaction parameter can be obtained by consideration of the differences in slope of the lines in Figure 48, and by assuming that polystyrene does not have a measurable polar contribution. The overall higher value of χ for poly(4-chlorostyrene) indicates lower interaction of the solvent with the polymer (ignoring molecular weight effects) compared with polystyrene.

Using more traditional vapour sorption methods, Corneliussen and co-workers[176] have also found that the interaction parameter of poly(4-chlorostyrene) was higher than that of polystyrene in their study of toluene sorption at 20°C.

4.3.3 Sorption of Hexane on Poly(4-chlorostyrene)

The results for the sorption of hexane on poly(4-chlorostyrene) at 30°C are shown in Figures 49 and 50. There are no literature results for direct comparison with this system however at high concentrations of solvent, good reproducibility for this polymer/solvent system was obtained. At low solvent fractions, both γ and χ are strongly dependent upon solvent concentration. Above a solvent volume fraction of 0.08, γ decreases with increasing solvent concentration whilst χ remains independent of solvent concentration.

For comparison, the data for the sorption of hexane on polystyrene (Section 4.2.4) has been added to the Figures. The polar contribution of poly(4-chlorostyrene) again seems to be the predominant factor, with the thermodynamic data at low solvent volume fractions showing a great difference in activity between the two polymers. At high solvent volume fractions, comparison of the slopes of the lines for the two polymers show good agreement (i.e. parallel) with slightly higher values for the activity coefficient and interaction parameter found for the more polar polymer. For the polystyrene/hexane system, the activity coefficient increases on approaching zero solvent concentration which is contrary to the poly(4-chlorostyrene) system where γ decreases on approaching lower solvent concentrations. This is indicative of a very strong polymer/solvent interaction between poly(4-chlorostyrene) and hexane.

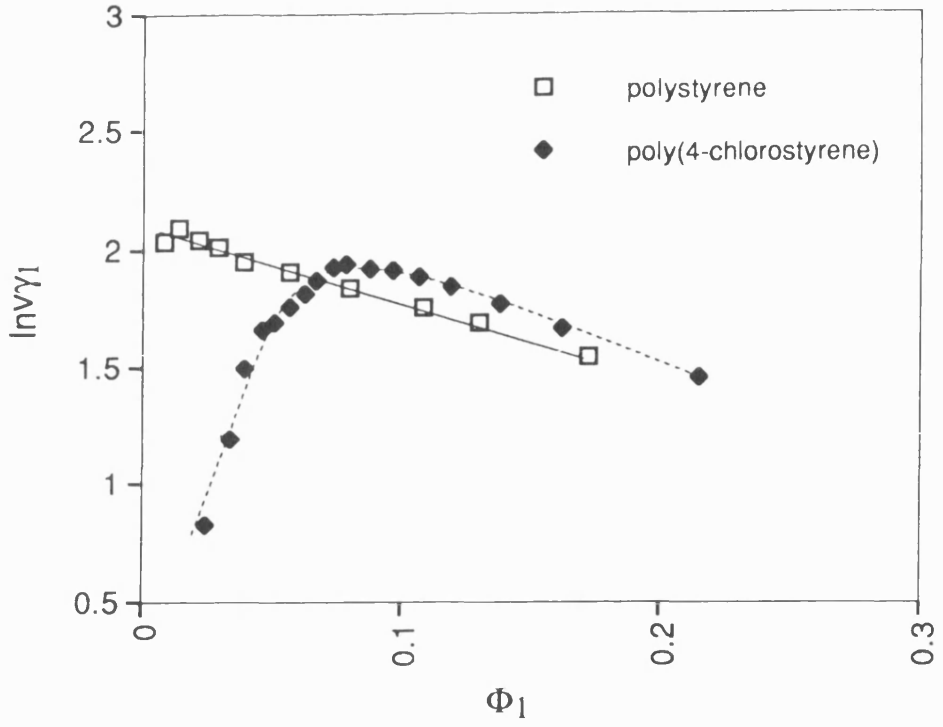

Figure 49: Sorption of Hexane on Poly(4-chlorostyrene) and Polystyrene at 30°C - Activity Coefficient

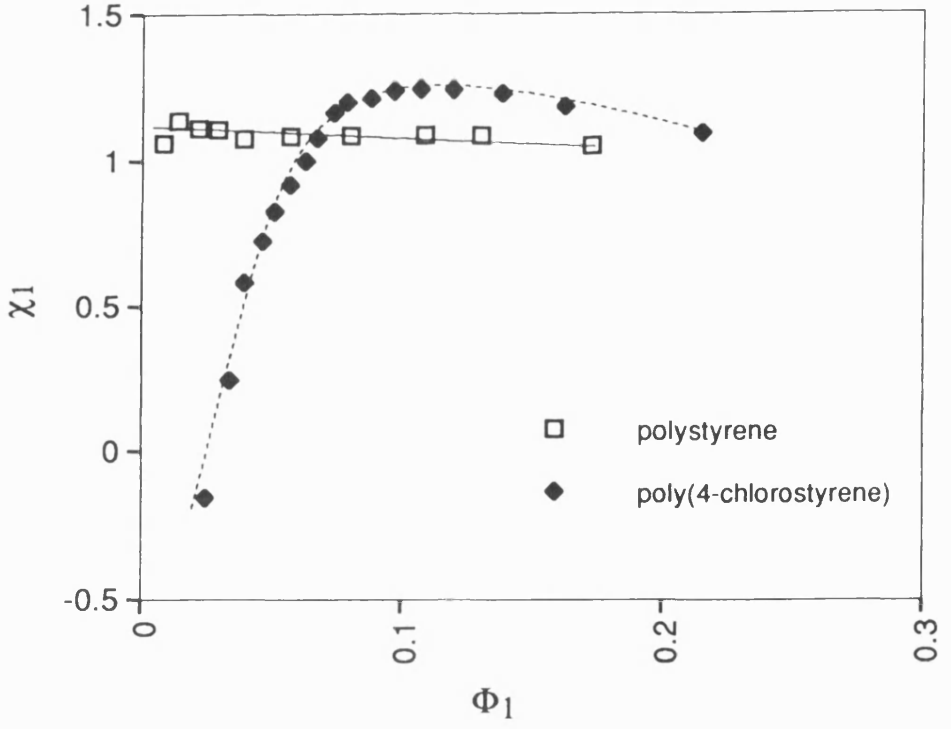

Figure 50: Sorption of Hexane on Poly(4-chlorostyrene) and Polystyrene at 30°C - Interaction Parameter

In the previous sections, we have observed some differences in thermodynamic behaviour between polystyrene and poly(4-chlorostyrene) for a series of solvents used in our PDMS studies. We have continued our study by considering the poly(4-chlorostyrene)/solvent behaviour for systems that we have used in our dissolution studies.

4.3.4 Sorption of MEK on Poly(4-chlorostyrene)

For the sorption of MEK on poly(4-chlorostyrene) at 30°C, the activity coefficient decreases whilst the interaction parameter increases linearly with increasing solvent concentration (Figures 51 and 52). Again there is good reproducibility between experimental runs, and comparison with the data for the sorption of MEK on polystyrene (Section 4.2.5) shows that both the interaction parameter and activity coefficient for poly(4-chlorostyrene) are lower than the corresponding values for polystyrene, which is the opposite to the trend previously observed in this thesis. The large difference in the interaction of MEK between the two polymers is again probably due to the strong polar interaction which exists between the dipole moment created by the chlorine atom and MEK, giving an overall lower χ value for poly(4-chlorostyrene) than for polystyrene.

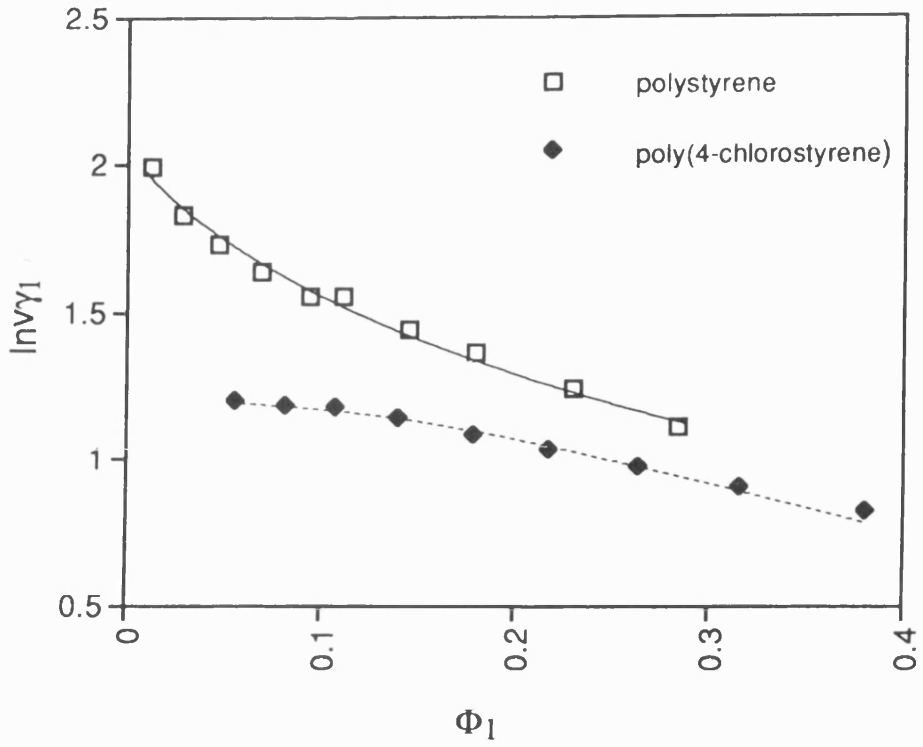

Figure 51: Sorption of MEK on Poly(4-chlorostyrene) and Polystyrene at 30°C - Activity Coefficient

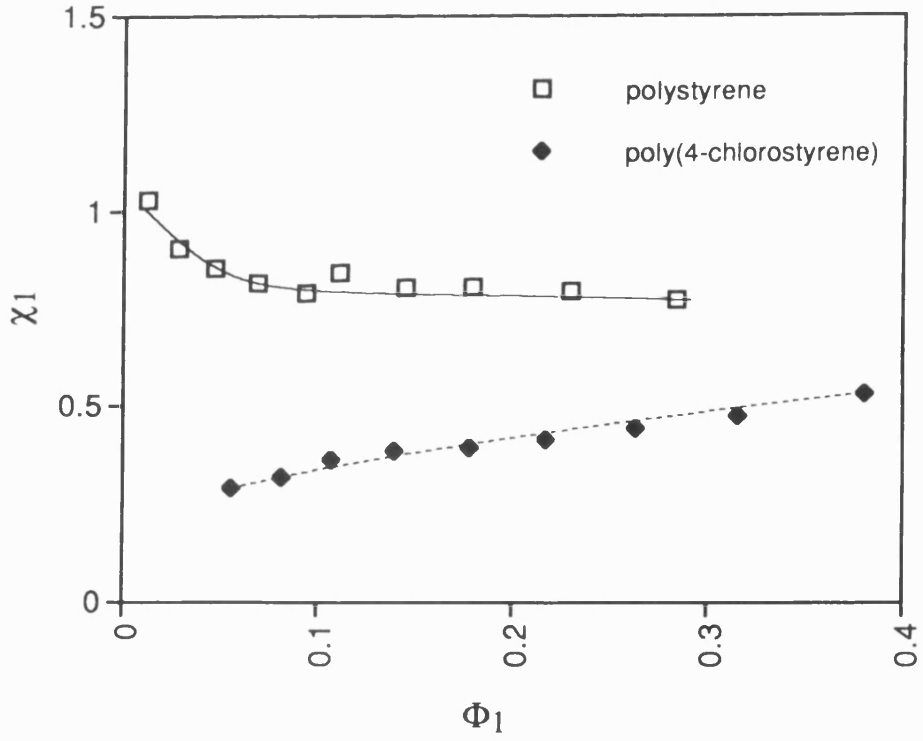

Figure 52: Sorption of MEK on Poly(4-chlorostyrene) and Polystyrene at 30°C - Interaction Parameter

4.3.5 Sorption of IPA on Poly(4-chlorostyrene)

The interaction of IPA with poly(4-chlorostyrene) has been measured at 30°C and the activity coefficients and interaction parameters are given in Figures 53 and 54 respectively. The activity coefficient decreases linearly with increasing solvent concentration, with the values much higher than those obtained for the corresponding polystyrene/IPA system (Section 4.2.6). The interaction parameter is independent of solvent concentration, with an average value of 1.9 indicating the poor interaction between solvent and polymer. This contrasts well with the thermodynamic behaviour observed for MEK in poly(4-chlorostyrene) (Figures 55 and 56). This value of interaction parameter is higher than that observed for the polystyrene/IPA system.

The greatest deviation in the values of Υ and χ for MEK sorption on polystyrene and poly(4-chlorostyrene) can be seen at low solvent concentrations (experimental error will be a partial contributing factor). This large deviation is not observed for the polymer/IPA systems because IPA is such a poor solvent for the polymers that the influence of polar interactions upon Υ and χ will be negligible and hence, should not be greatly influenced by solvent concentration. As the χ values indicate, IPA is a better "solvent" for polystyrene than poly(4-chlorostyrene)

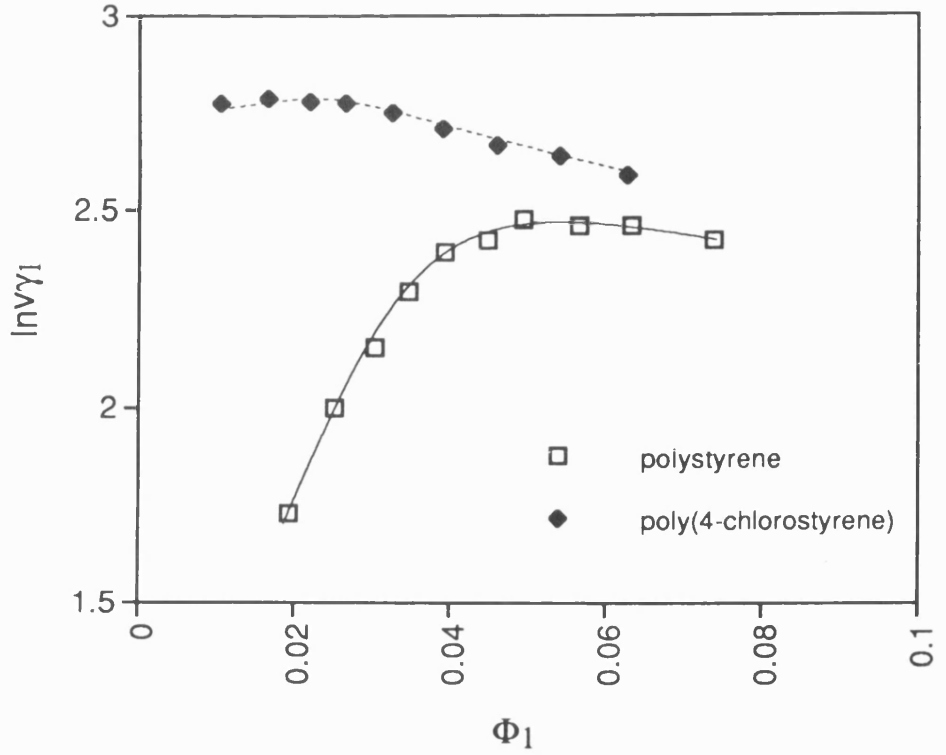

Figure 53: Sorption of IPA on Poly(4-chlorostyrene) and Polystyrene at 30°C - Activity Coefficient

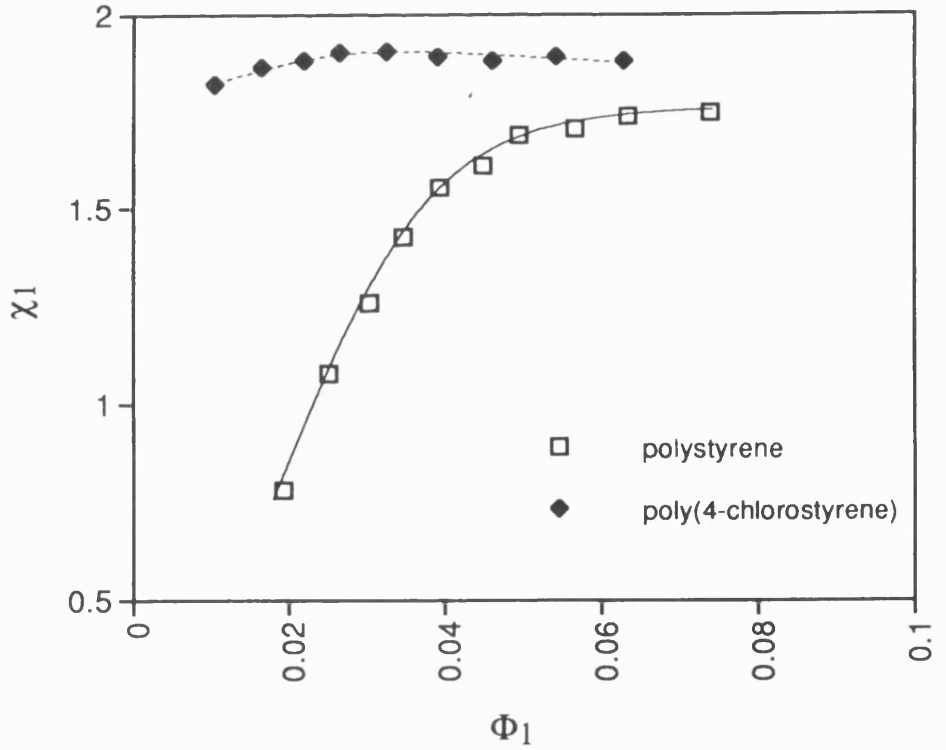

Figure 54: Sorption of IPA on Poly(4-chlorostyrene) and Polystyrene at 30°C - Interaction Parameter

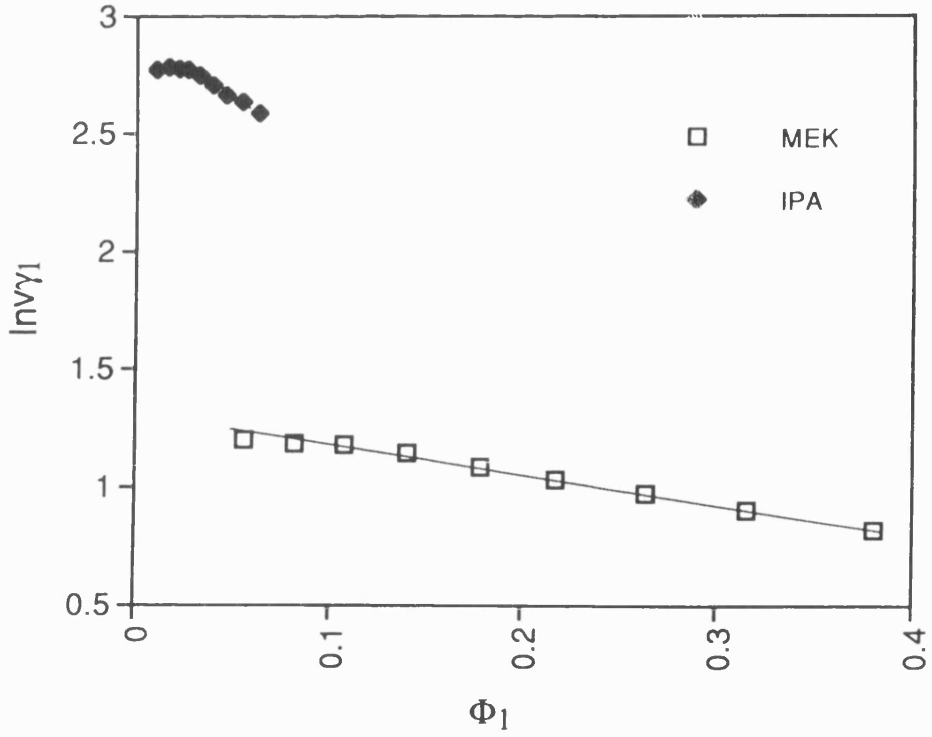

Figure 55: Sorption of MEK and IPA on Poly(4-chlorostyrene) at 30°C - Activity Coefficient

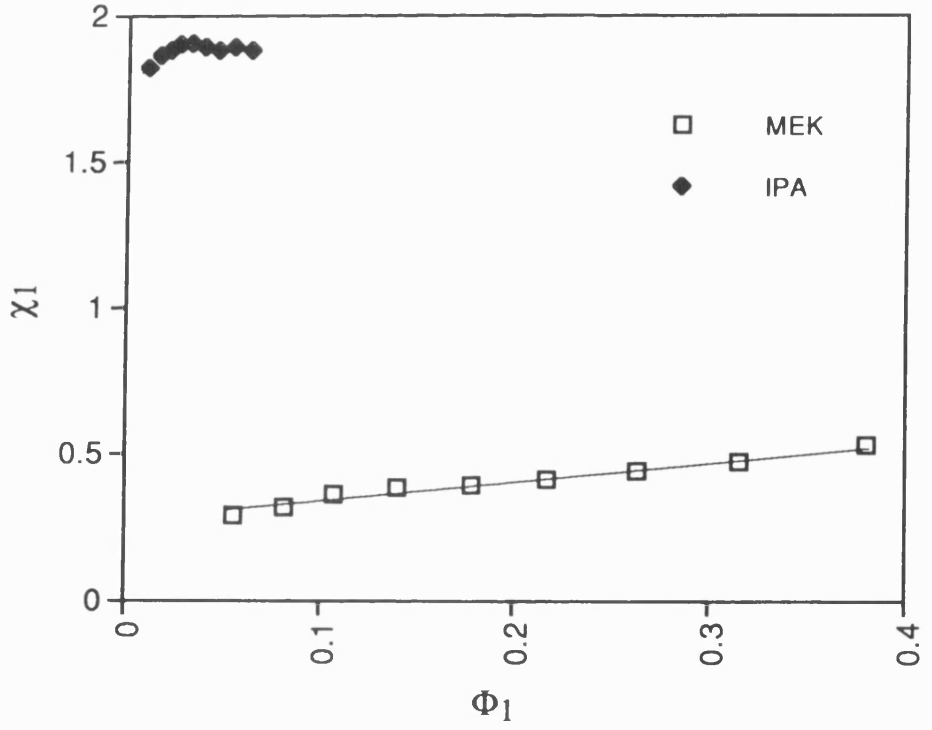

Figure 56: Sorption of MEK and IPA on Poly(4-chlorostyrene) at 30°C - Interaction Parameter

4.4 Solvent Interaction with PMMA

There is very little data in the literature for the interaction of PMMA with most common solvents and to give us an indication of the compatibility of PMMA with the solvents used in the dissolution studies, both volume fraction activity coefficients and Flory-Huggins interaction parameters have been measured for a series of PMMA/solvent systems.

To establish the validity of our method for the measurement of PMMA/solvent systems, we have initially studied the sorption of some of the solvents used in the previous sections.

4.4.1 Solvent and Temperature Effect on γ and χ

4.4.1.1 Sorption of Benzene on PMMA

The volume fraction activity coefficients and interaction parameters for the sorption of benzene on PMMA at 30 and 40°C are shown in Figures 57 and 58 respectively. For each temperature, two sets of experimental data have been shown to give an indication of the reproducibility of the data. At both temperatures, the values of activity coefficient and interaction parameter decreases linearly with increasing concentration with the slopes of the lines parallel. For the sorption of benzene at 40°C, there is deviation from linearity at lower solvent concentrations ($\Phi_1 < 0.12$). The values of interaction parameter indicate good interaction between the polymer and solvent, and that this interaction is enhanced at lower sorption temperatures. The deviation from linearity at 30°C, may be caused by the longerequilibrium times required at the lower temperature (i.e. increased experimental error).

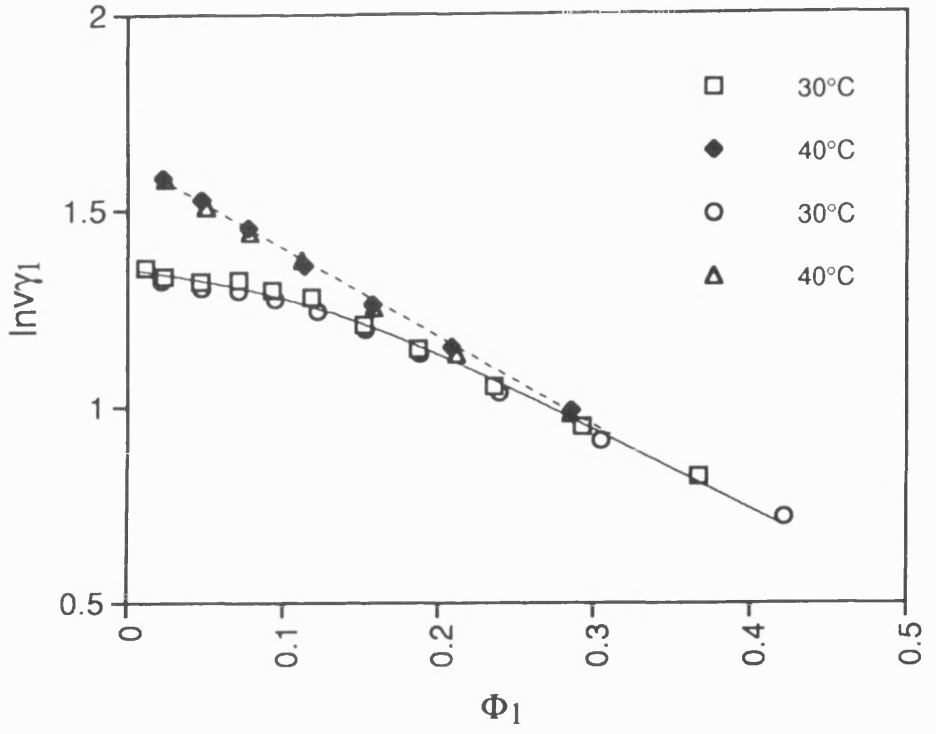

Figure 57: Effect of Temperature on the Sorption of Benzene on PMMA - Activity Coefficient

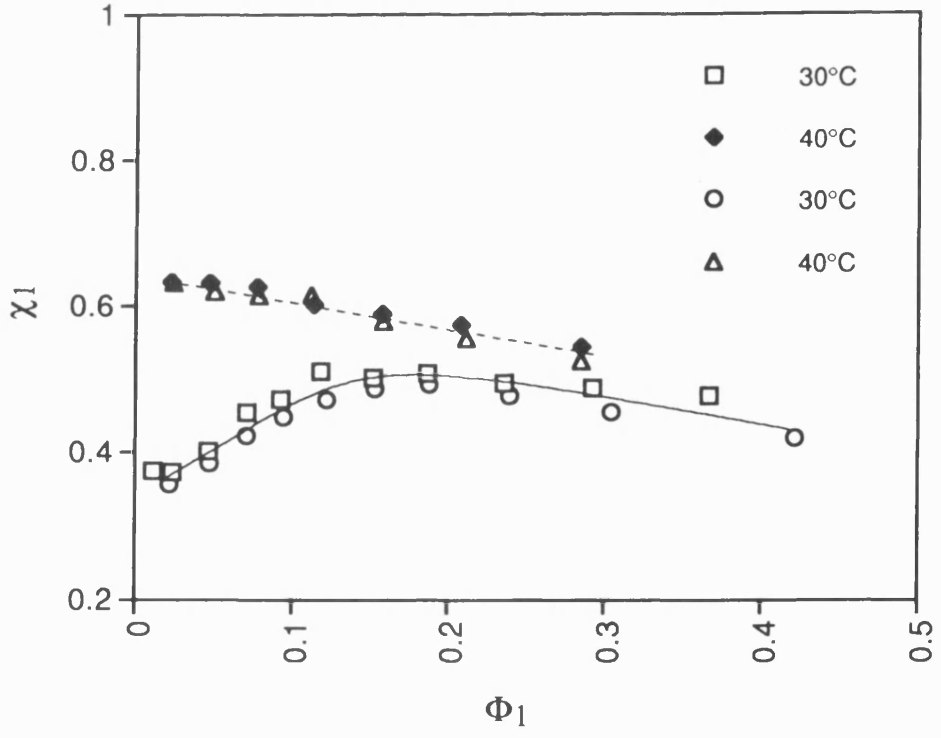

Figure 58: Effect of Temperature on the Sorption of Benzene on PMMA - Interaction Parameter

4.4.1.2 Sorption of Hexane on PMMA

The results for the sorption of hexane on PMMA at 30 and 40°C are shown in Figures 59 and 60. For both sorption temperatures, good reproducibility of experimental data was found, with γ and χ independent of temperature. The activity coefficient decreases linearly with solvent concentration, whilst at lower solvent concentrations, the interaction parameter remains independent of both concentration and temperature with an average χ value of 1.3. Above a solvent fraction of 0.08, χ decreases slightly with increasing solvent concentration. As the high value of χ indicates, hexane interacts poorly with PMMA, and the polymer/solvent interaction would therefore not be expected to change dramatically with temperature or solvent concentration.

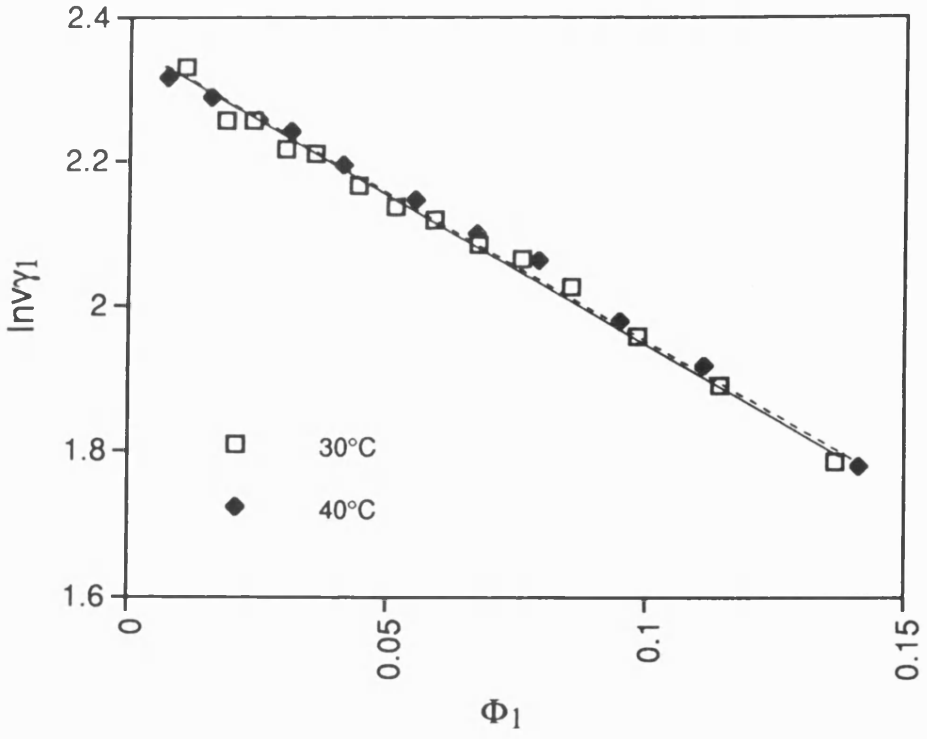

Figure 59: Effect of Temperature on the Sorption of Hexane on PMMA - Activity Coefficient

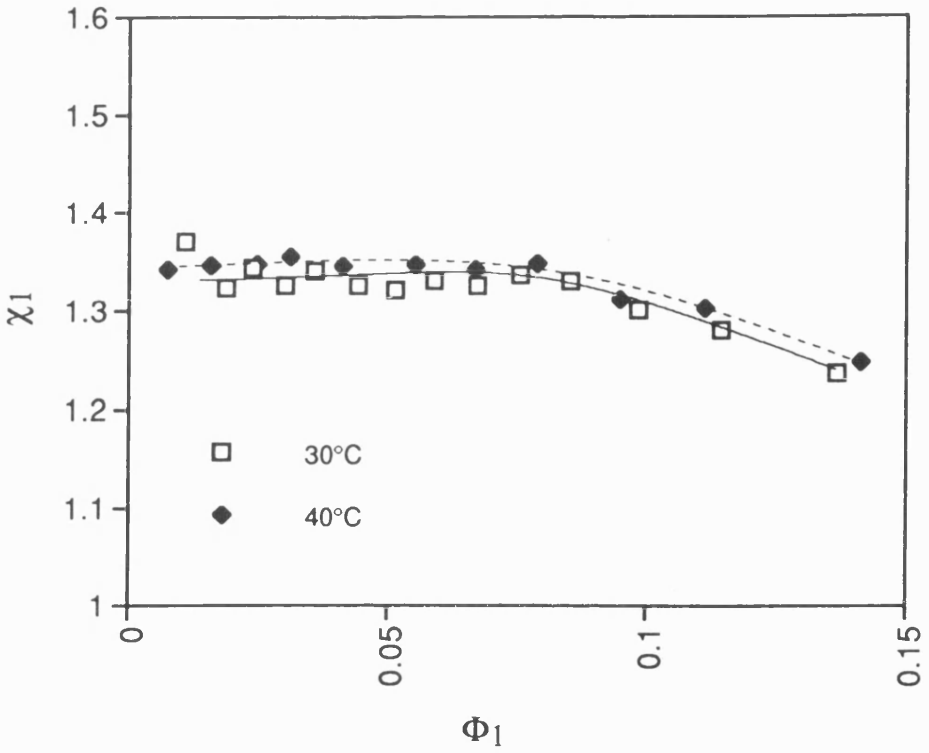

Figure 60: Effect of Temperature on the Sorption of Hexane on PMMA - Interaction Parameter

4.4.1.3 Sorption of MEK on PMMA

The volume fraction activity coefficients and interaction parameters for the sorption on MEK by PMMA at 30 and 40°C are shown in Figures 61 and 62. As with the previous systems, good reproducibility of data was achieved. At both sorption temperatures, the activity coefficient initially increases until a solvent volume fraction of 0.1 is reached, upon which it decreases with subsequent increases in solvent concentration. After an initial increase in χ, the interaction parameter at both temperatures is found to be independent of solvent concentration with the slopes of the lines lying parallel.

The temperature effect on Υ and χ only becomes apparent above solvent concentrations of 0.04. For both the values of activity coefficients and interaction parameters, the majority of the points at 40°C tend to lie at higher values than those at 30°C. However at low solvent concentrations, the lines of Υ and χ cross over with the values becoming independent of temperature. The low value of χ indicates very good polymer/solvent interaction, with the interaction becoming weaker (i.e. subsequent molecules have a weaker interaction with the polymer) as the solvent concentration is increased. Better polymer/solvent interaction is observed at the lower sorption temperature.

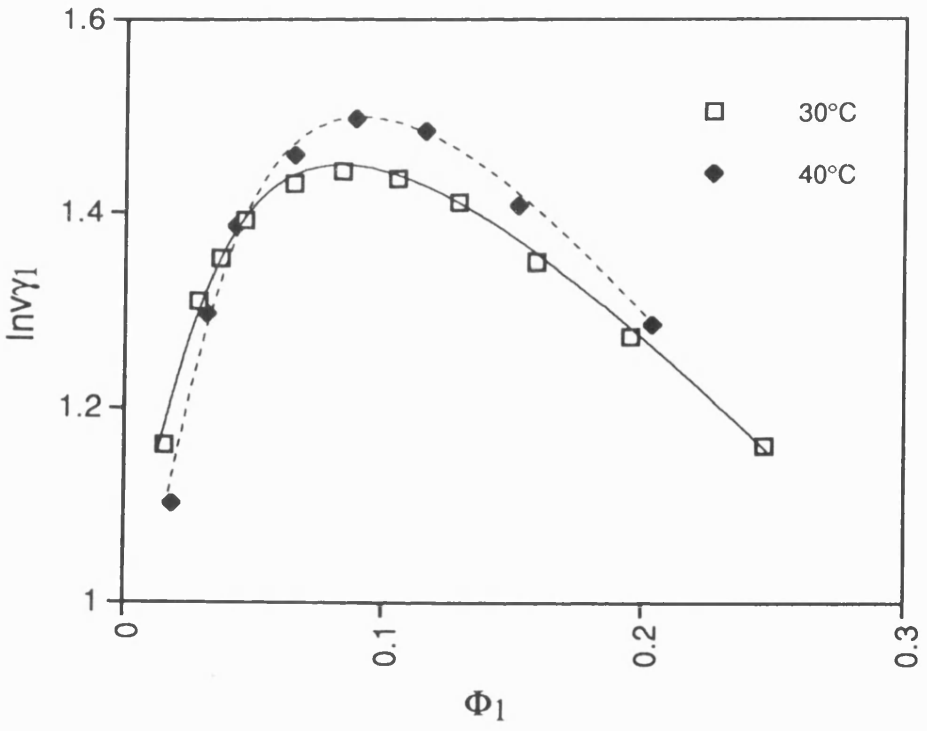

Figure 61: Effect of Temperature on the Sorption of MEK on PMMA - Activity Coefficient

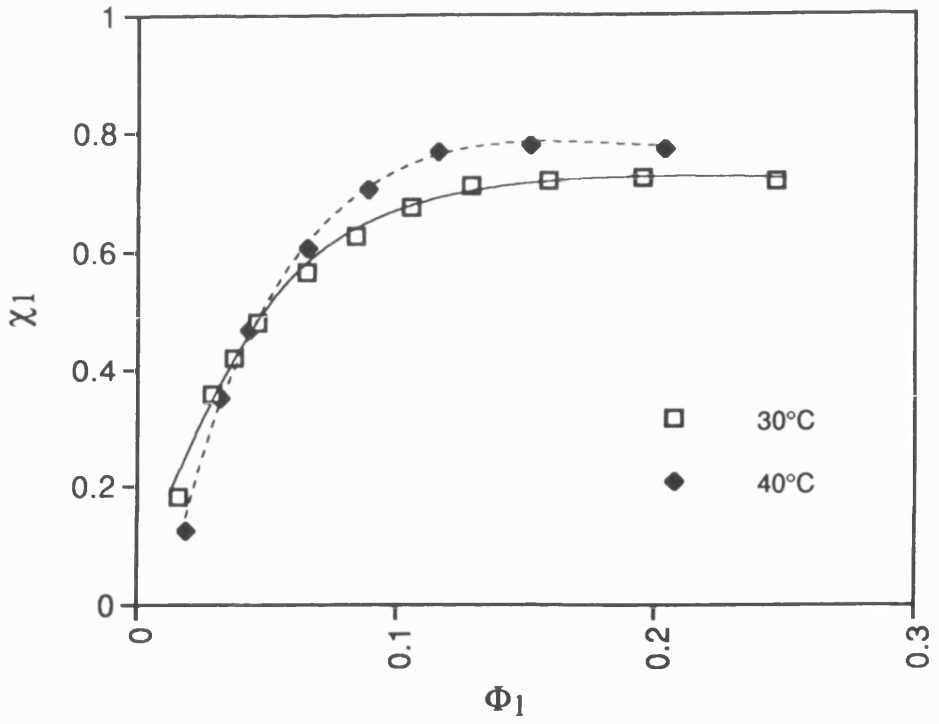

Figure 62: Effect of Temperature on the Sorption of MEK on PMMA - Interaction Parameter

4.4.1.4 Sorption of IPA on PMMA

The data for the sorption of IPA on PMMA at 30 and 40°C is shown in Figures 63 and 64. At 30°C, both the values of γ and χ lie above the respective values for the sorption at the higher temperature. This is in contrast with the temperature effect observed for the sorption of MEK in PMMA where higher γ and χ values were observed at 40°C.

At 40°C and solvent fractions less than 0.05, an initial increase in activity coefficient with increasing volume fraction is observed. Upon which the activity coefficient at 30 and 40°C is shown to be independent of solvent concentration with the slope of the lines found to be parallel. The interaction

parameter increases linearly with solvent concentration with a sharper increase observed at 30°C. The high value of interaction parameter, at both sorption temperatures, is consistent with the poor polymer/solvent interactions that would be expected for IPA.

Figures 65 and 66 show the activity coefficients for the sorption of MEK and IPA on PMMA at 30 and 40°C respectively. At both temperatures, the activity coefficient for IPA in PMMA lies at a much higher value than the corresponding value for MEK, however a similar trend in the slope of the activity coefficient line is observed for both solvents. Comparison of the interaction parameters for PMMA in MEK and IPA at 30 and 40°C (Figures 67 and 68) shows a striking difference in polymer/solvent interaction. Although the same general trend in interaction parameter with respect to solvent concentration is observed for both solvents, the values of χ for IPA are much higher than those for MEK. The high values for IPA indicating that it is a non-solvent for PMMA. It would therefore be predicted that mixtures of MEK and IPA should form a developing solvent for PMMA which is an intermediate between a good solvent and a non-solvent.

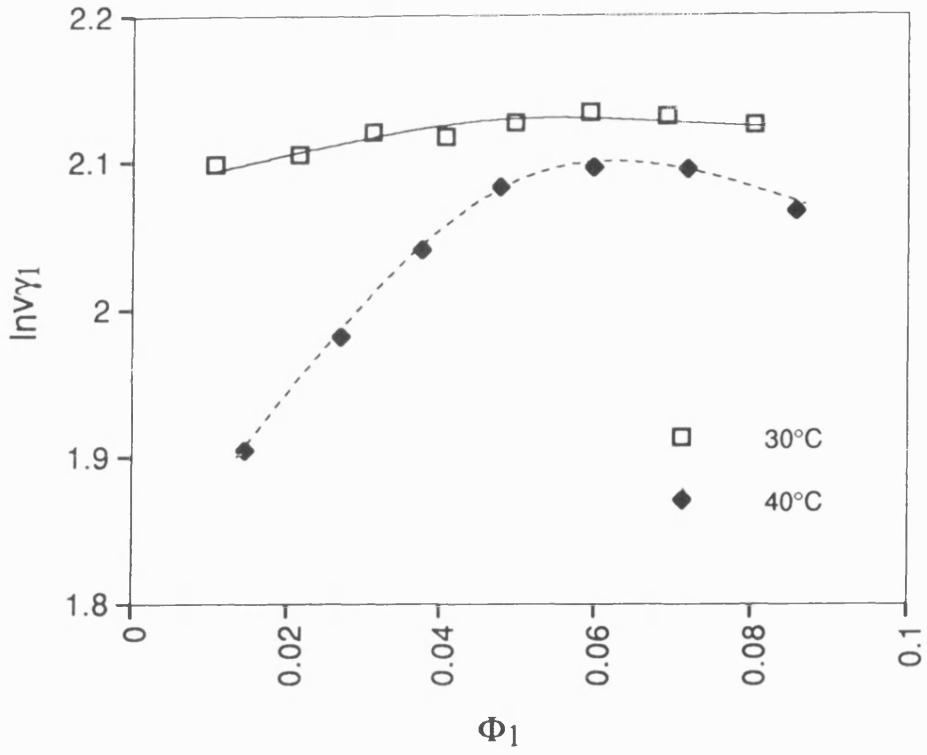

Figure 63: Effect of Temperature on the Sorption of IPA on PMMA - Activity Coefficient

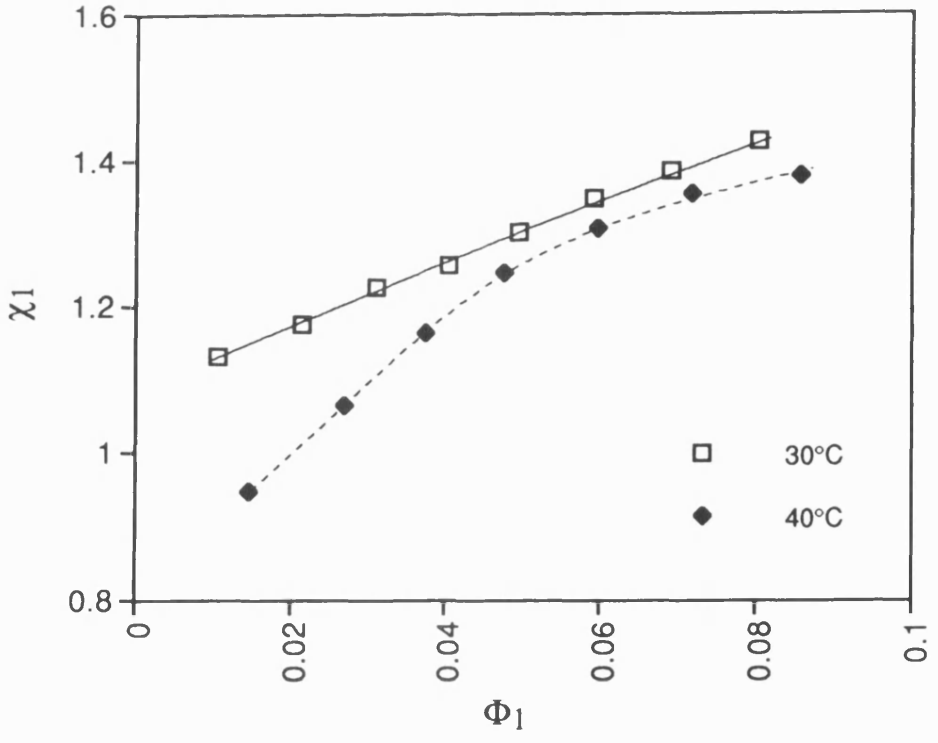

Figure 64: Effect of Temperature on the Sorption of IPA on PMMA - Interaction Parameter

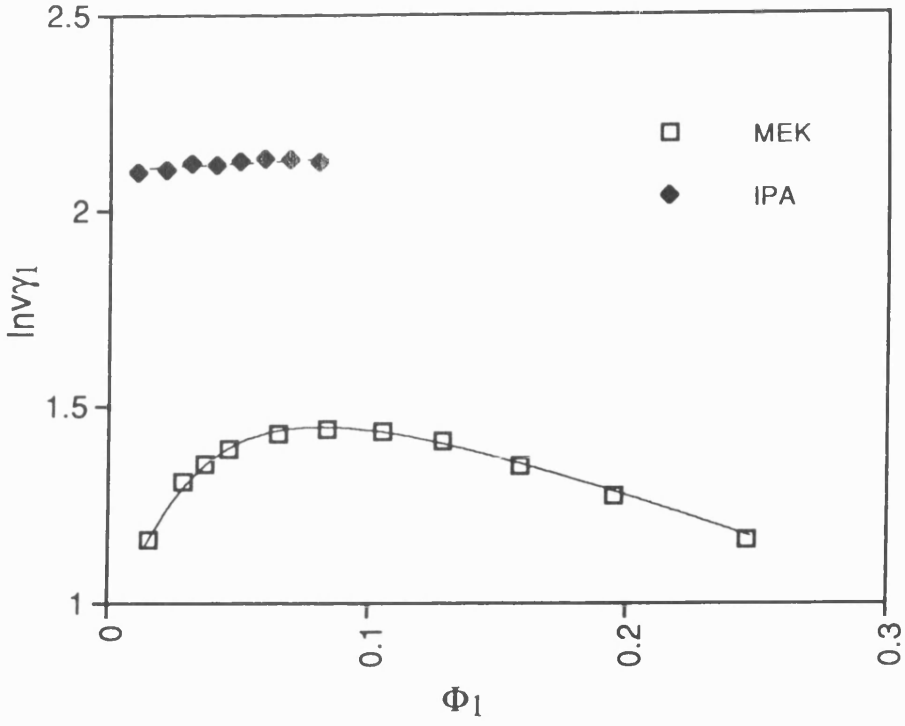

Figure 65: Sorption of MEK and IPA on PMMA at 30°C

Activity Coefficient

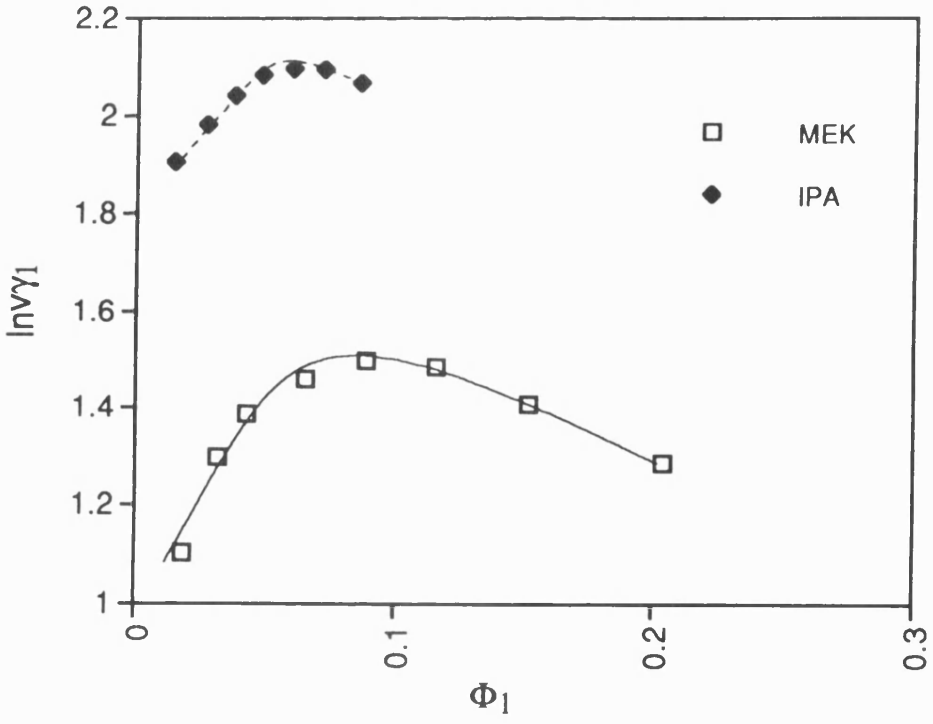

Figure 66: Sorption of MEK and IPA on PMMA at 40°C

Activity Coefficient

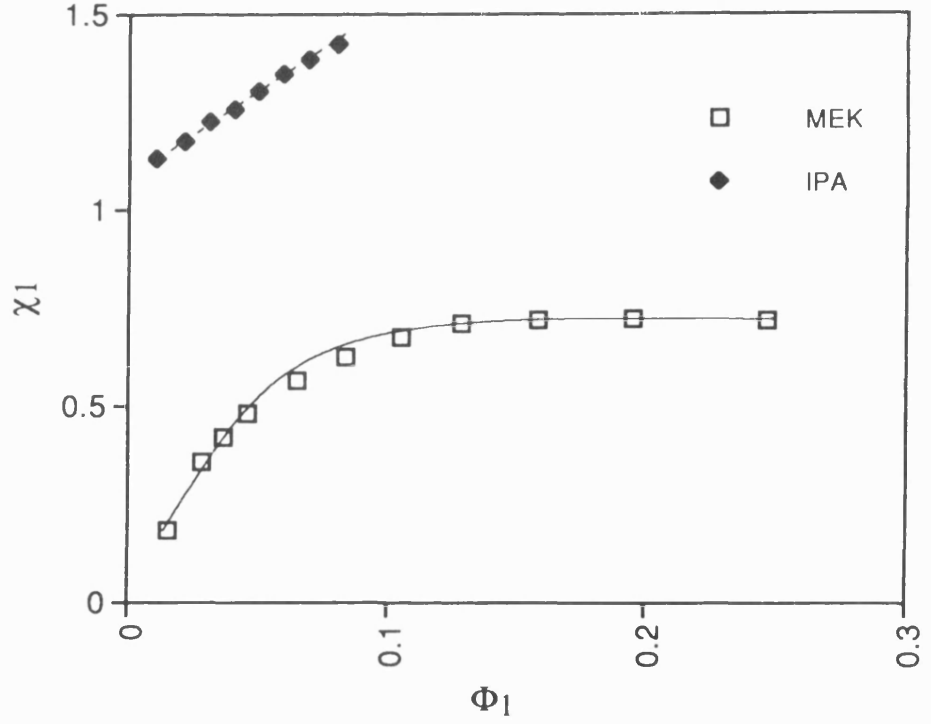

Figure 67: Sorption of MEK and IPA on PMMA at 30°C

Interaction Parameter

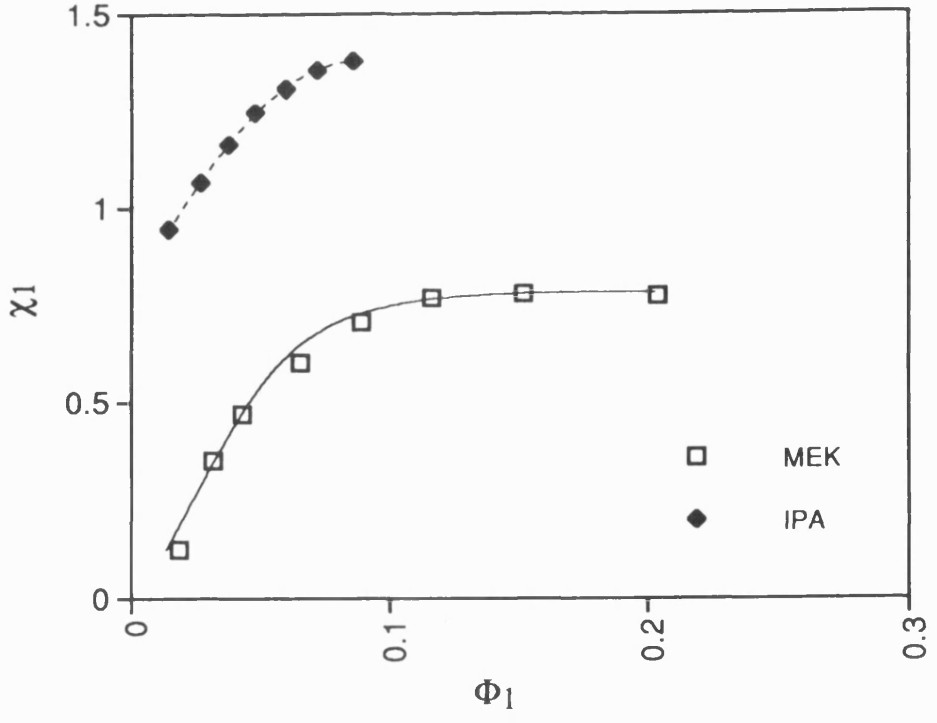

Figure 68: Sorption of MEK and IPA on PMMA at 40°C

Interaction Parameter

4.4.2 Solvent Size Effect on the Activity Coefficient and Flory-Huggins Interaction Parameter

The effect of solvent size upon the polymer/solvent interactions for PMMA/solvent systems has been studied for both an alcohol and alkyl acetate solvent series. The observed thermodynamic behaviour will aid in the interpretation of the corresponding dissolution studies.

4.4.2.1 Sorption of Methanol and Ethanol on PMMA

Figures 69 and 70 show the plots of the activity coefficients and interaction parameters against volume fraction of solvent for the PMMA/methanol and PMMA/ethanol systems. For comparison, the results from Section 4.4.1.4 for the sorption of IPA on PMMA have also been shown.

As we have previously observed, the interaction parameter for the sorption of IPA on PMMA increases linearly with solvent concentration, whilst the activity coefficient is found to be independent of the solvent volume fraction. This is in marked contrast with the thermodynamic behaviour demonstrated for the methanol and ethanol systems. At low solvent concentrations ($\Phi_1 < 0.05$ and 0.07 for methanol and ethanol respectively), an initial increase in activity coefficient is observed, with the activity coefficient decreasing linearly with further increases of solvent concentration. The deviations in linearity may be partially attributed to the higher experimental error observed at lower solvent concentrations but this does not account for the whole effect.

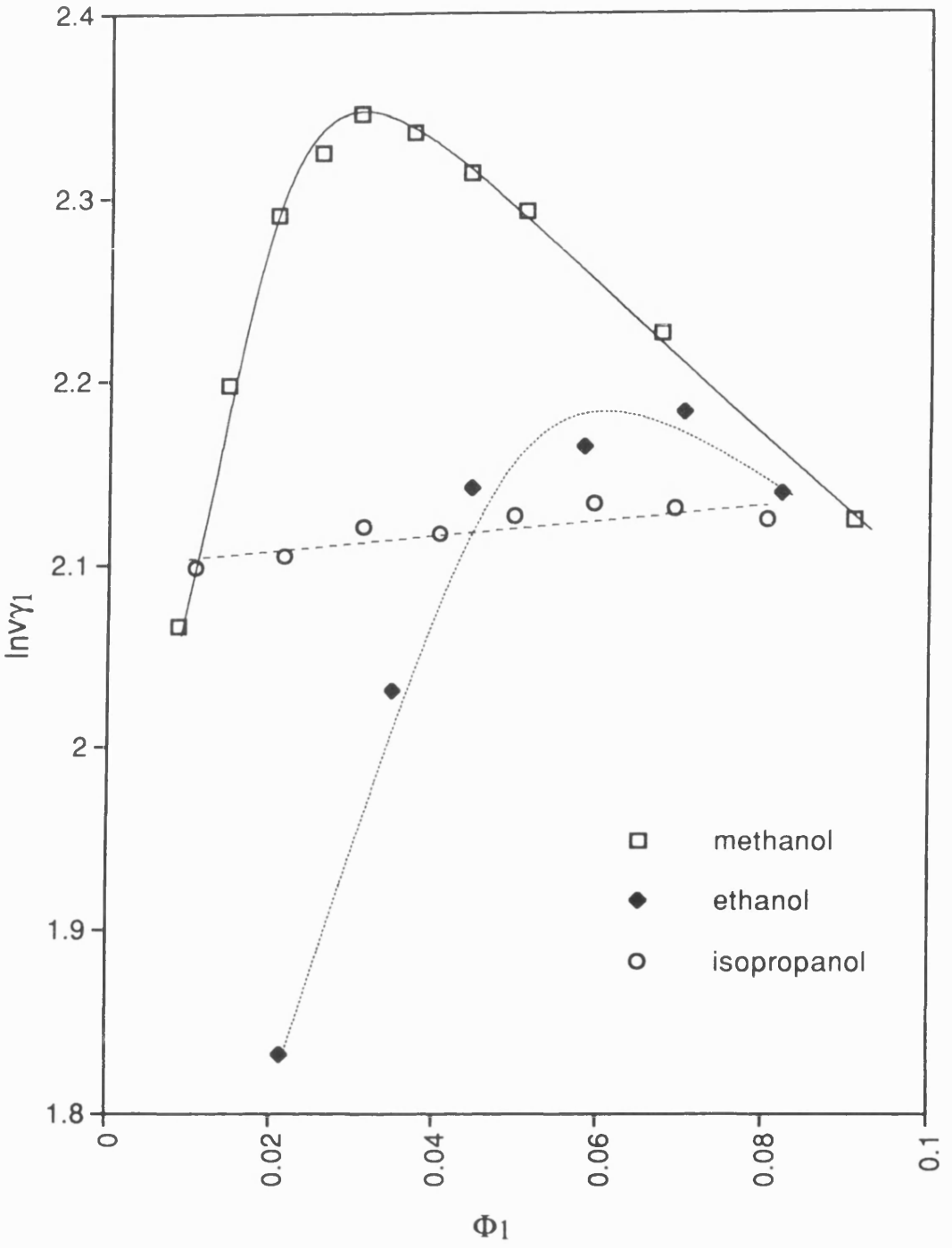

Figure 69: Sorption of Alcohols on PMMA at 30°C

Activity Coefficient

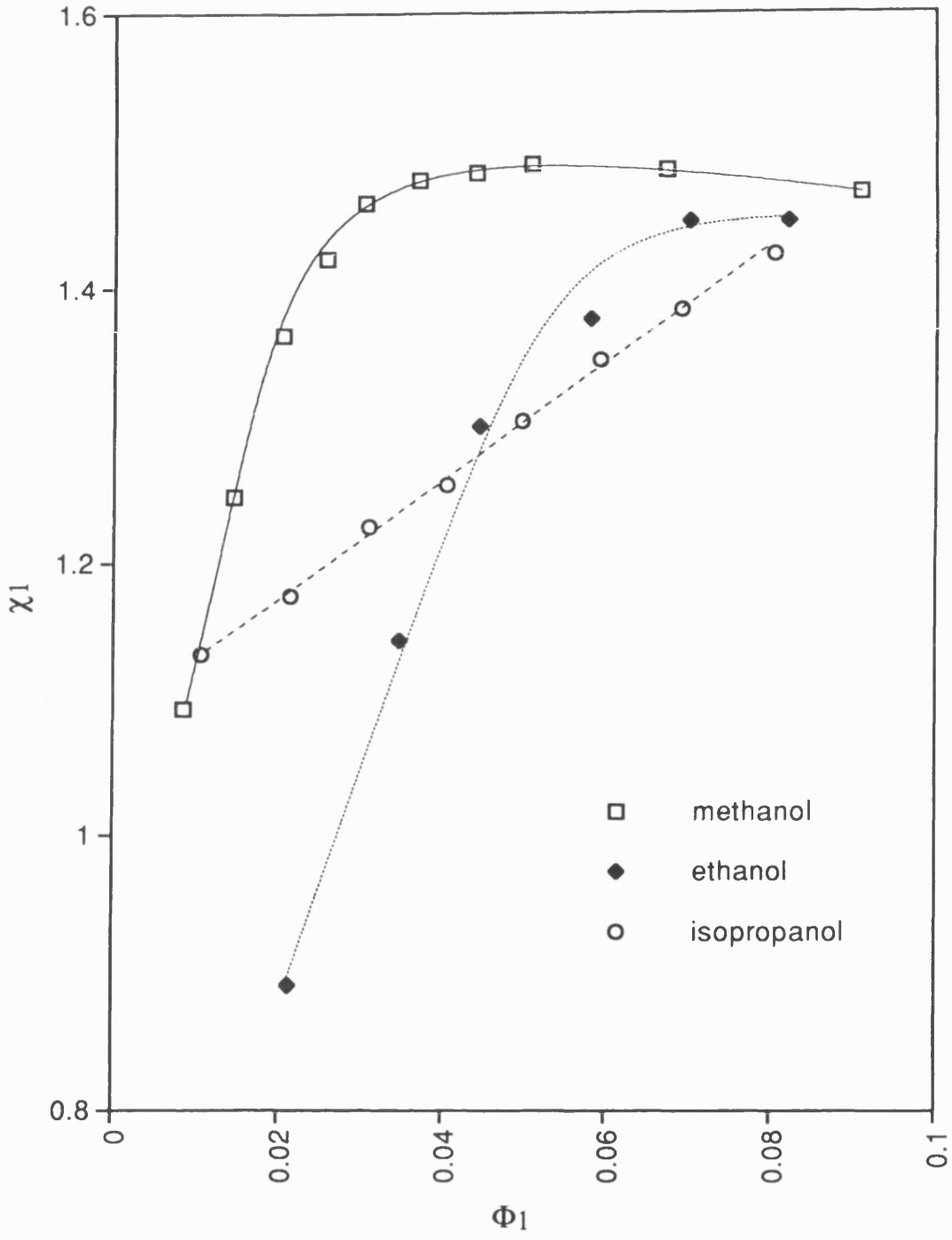

Figure 70: Sorption of Alcohols on PMMA at 30°C

Interaction Parameter

An increase in the value of interaction parameter is also observed at low solvent concentration, upon which the interaction parameter is found to be independent of concentration. Greatest deviation between the value of χ for the sorption of the alcohols on PMMA is observed at low solvent concentrations whilst at higher solvent concentrations ($\Phi_1 > 0.08$), the value of interaction parameter becomes independent of the type of alcohol. By consideration of the interaction parameters for the two polymer/solvent systems, it can be concluded that ethanol has the greatest interaction with PMMA at low solvent concentrations. The high values of χ indicate that alcohols are poor solvents for PMMA. The Flory-Huggins parameter primarily accounts for enthalpic interactions (χ_H). However, also a non-combinatorial entropy contribution (χ_S) will play a part with more polar molecules such as these making exact interpretation more difficult.

As we have stated in Chapter 1, the interaction parameter is a measurement of solvent interaction with the polymer structure. By consideration of the values of interaction parameter, the observed deviation in interaction parameter at low solvent concentrations may be attributed to differences in solvent molar volume. The smaller alcohol molecules can enter further into the polymer film (i.e. free volume) allowing more solvent to be absorbed into the polymer architecture and this is indicated by the lower values of interaction parameter.

At high solvent fractions, the polymer becomes saturated with solvent and the sorption characteristics for methanol and ethanol are then found to vary less with solvent concentration. A sharper increase in χ is seen for the smaller alcohol molecules but unexpectedly the more bulky ethanol molecule (compared with methanol) gives the lowest value of χ (i.e. highest

polymer/solvent interaction). The size of the IPA molecule will be closer to the critical molecular size required for the entry of the solvent molecule into the polymer structure and this plasticisation effect will be less obvious. For the solvent concentration range measured, only a small change is observed in polymer/solvent interaction (i.e. χ), as the majority of the IPA interacts with the polymer surface. The methanol and ethanol molecules are able to penetrate the polymer surface more easily than IPA due to their small molar volume, particularly at low solvent fractions. It would be predicted that the higher alcohols would also indicate less variation in interaction parameter due to their larger molecular size.

Linn and co-workers[180] in their study of methanol-induced opacity in PMMA, such as that used in the manufacture of contact lenses, have shown that over the temperature range 40 - 60°C the hole nuclei created by the diffusion of methanol into the PMMA film is proportional to the amount of methanol. The growth of the hole can only occur if the sample is above the glass transition temperature. According to Bueches' theory[181,182], the glass transition of PMMA increases with increasing methanol content.

At 30°C, we have observed decreased polymer/solvent interactions as the methanol concentration is increased, however above a solvent fraction of 0.05, enhanced interactions are observed as the solvent concentration is increased. By consideration of Bueches' theory and the observations of Linn and co-workers, it could be envisaged that at a solvent volume fraction of 0.05, the methanol content is great enough to reach the glass transition of the PMMA sample. As Linn has shown that, above the glass transition, the number of hole nuclei in a glassy polymer is proportional to solvent concentration, it would be expected that as the

concentration of solvent is increased above this solvent concentration, enhanced polymer/solvent interactions (i.e. lower χ values) would be observed.

In Section 4.4.1.4, we measured χ values for the IPA/PMMA system at 30 and 40°C. At 30°C, we found a linear decrease in the polymer/solvent interactions with increasing solvent concentration. However at 40°C, a tailing off of the decrease was observed indicating enhanced interaction of the solvent with the polymer. The sorption temperature is close to that of the glass transition of unexposed PMMA and hence with increasing solvent concentration, the glass transition temperature may be sufficiently lowered to allow the growth of the hole nuclei formed by the diffusion of IPA into the polymer structure hence enhancing the polymer/solvent interaction.

In our dissolution studies Chapters 5 - 9, we will present some data that will show unexpected enhanced dissolution rates for the development of PMMA in some alcohol/MEK mixtures. The thermodynamic data obtained in this section, in conjunction with the dissolution data, will help in the understanding of this phenomenon.

4.4.2.2 Sorption of n-Alkyl Acetates on PMMA

The study of the effect of solvent size on the interaction of solvents with polymers has been extended to the sorption of an alkyl acetate series on PMMA.

The volume fraction activity coefficients and Flory-Huggins interaction parameter of PMMA in a series of n-alkyl acetate solvents (methyl to butyl) at

30°C have been determined by our piezoelectric sorption detector method. (Figure 71 and 72). Good reproducibility was found between experimental runs.

Sorption of the lower n-alkyl acetates (up to propyl) shows little variation in the corresponding values of activity coefficients and interaction parameters. For all the alkyl acetate solvents measured, an increase in both γ and χ with increasing solvent concentration ($\Phi_1 < 0.1$) is observed. Above this solvent concentration, a decrease in γ is observed whilst χ is independent of solvent volume fraction (with the exception of the sorption of butyl acetate).

Methyl acetate has an overall higher value of χ than both ethyl and propyl acetate indicating lower polymer/solvent interactions. This is a surprising result as the smaller mobile solvent molecules should be able to permeate further into the polymer structure than the other bulkier solvent molecules, as observed in Section 4.4.2.1 for methanol sorption on PMMA. The results for butyl acetate sorption indicate a much lower polymer/solvent interaction. The solvent molecules are too bulky to enter the polymer structure with great ease, hence reduced polymer/solvent interactions are observed. These observations will be used to aid in the understanding of the dissolution kinetics of PMMA in alkyl acetate solvents described in Sections 5.2, 6.3 and 7.2. As the error bars indicate, the observed differences in thermodynamic behaviour between ethyl, propyl and butyl acetate may be due to experimental error and hence must be taken into account when interpreting the data.

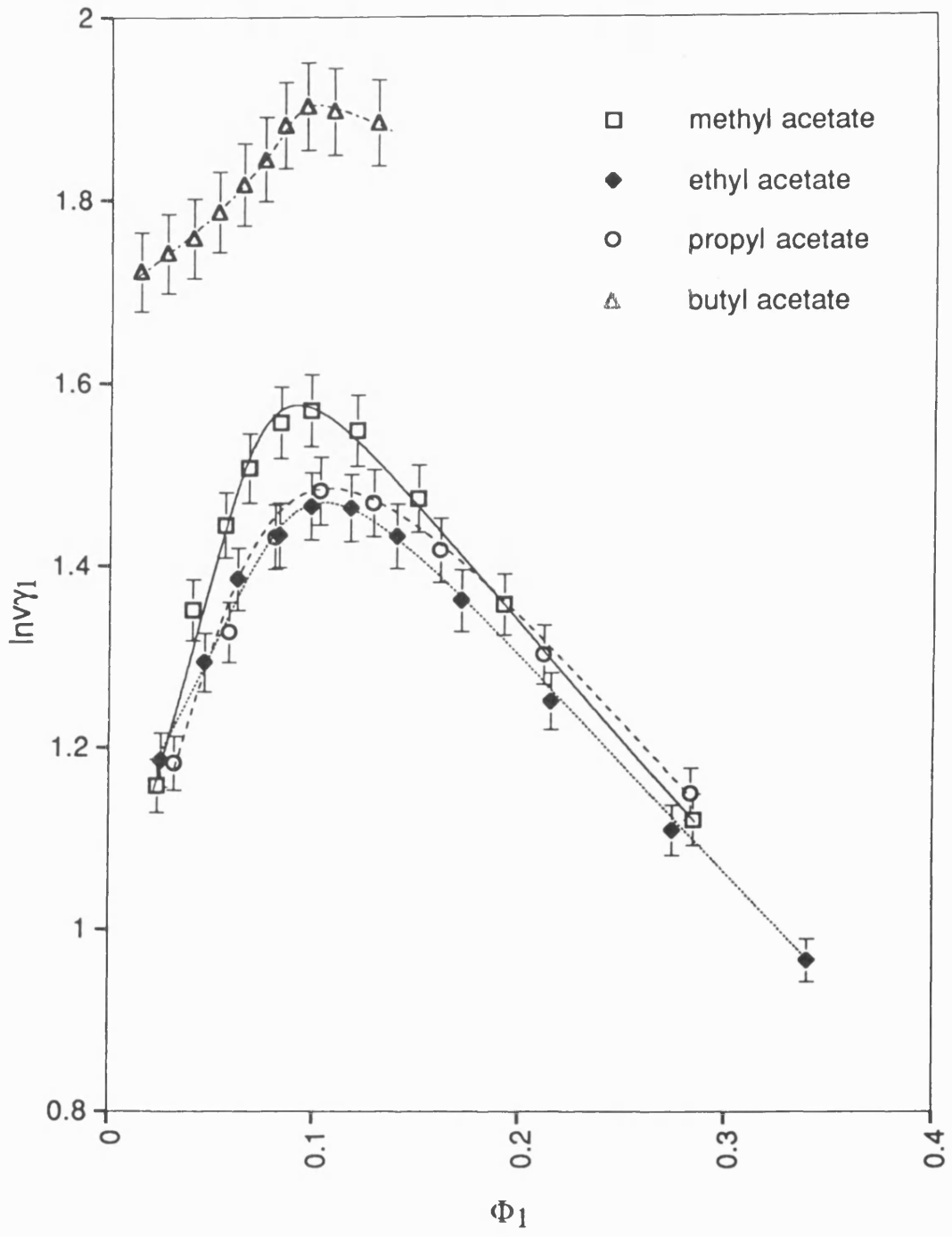

Figure 71: Sorption of n-Alkyl Acetates on PMMA at 30°C

Activity Coefficient

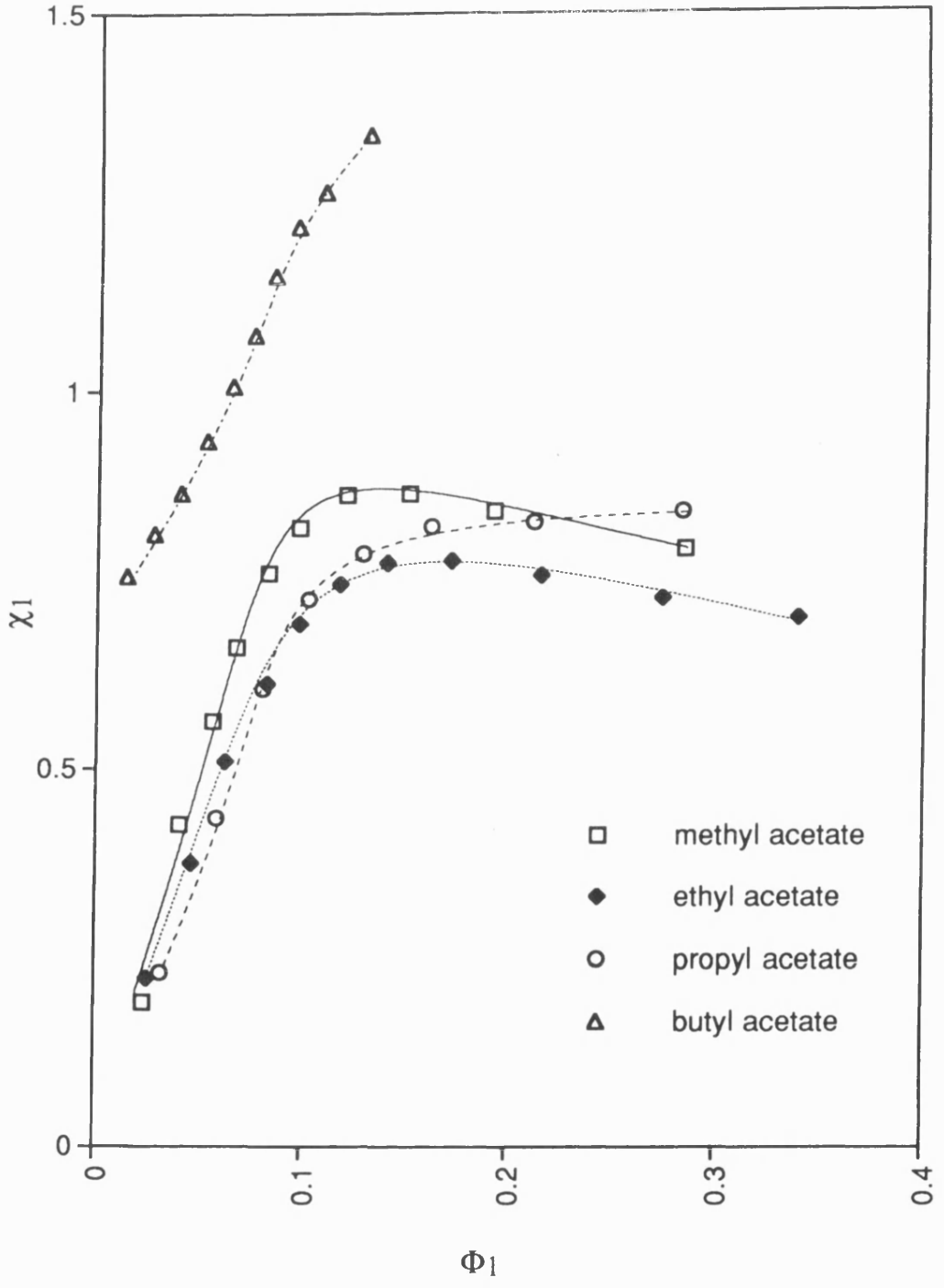

Figure 72: Sorption of n-Alkyl Acetates on PMMA at 30°C

Interaction Parameter

4.5 Conclusion

We have shown in our thermodynamic studies, that the piezoelectric sorption technique is a viable method for the determination of the activity coefficient and Flory-Huggins interaction parameter. We have obtained data closer to that from conventional methods than those presented by Saeki and co-workers. We have presented some new data for polystyrene and PMMA/solvent systems which will help in the interpretation of the phenomenon observed in our dissolution kinetics studies described in the following Chapters.

Chapter Five

5.0 Effect of Molecular Weight on PMMA Dissolution

One of the main factors that affects polymer solubility and dissolution, and one that is crucial to a resist process is the molecular weight. The dependence of dissolution rate on polymer molecular weight and the distribution could be attributable to the rate of penetration of the solvent, disentanglement of the polymer chains, or transport of disentangled chains into the bulk solvent (external mass transfer) or a combination of these.

Using our QCM dissolution apparatus, the effect of polymer molecular weight and distribution on the dissolution rate has been studied for PMMA. From this study, the changes in solubility have been correlated with polymer molecular weight and its distribution to give an insight into the main parameters affecting the dissolution kinetics and hence, the ultimate resolution of the resist.

PMMA is a positive resist and it relies on a reduction in molecular weight due to chain scission[27] to enhance the solubility of exposed regions of polymer (see Section 1.1.2.2). Therefore, the ability to correlate changes in polymer solubility as a function of molecular weight will enable the prediction of the change in swelling and dissolution kinetics of the PMMA film upon irradiation.

5.1 Dissolution Kinetics of PMMA (M_n 6100 - 1400000) in MEK

Figure 73 shows the effect of polymer molecular weight on the solubility of narrow polydispersity PMMA standards between number average molecular weights (M_n) 6100 and 1400000 (γ = 1.04 - 1.11) at 25°C in MEK. Complete dissolution was observed for all the samples studied and clearly, polymers having lower molecular weights dissolve at a considerably faster rate than those with higher values. Another significant point is that the polymers with molecular weights over 100000 show swelling prior to dissolution and the extent increases with increasing molecular weight.

An important property of most polymers is that both the solubility and dissolution rate decrease with an increase in molecular weight[183]. As the polymer chain length increases, the randomly coiled chains are entangled to such an extent that more time is required for the polymer chains to separate from one another and dissolve in the solvent. The sensitivity of resists can be enhanced by the use of high molecular weight fractions but as our results show, swelling may occur with increases in molecular weight which could cause distortion of the resist image. While swelling of the polymer complicates dissolution and limits the resolution of the image, it is useful in inhibiting the dissolution of the unexposed resist.

Further measurements of the dissolution rate of the PMMA standards in MEK have been made over the temperature range 16 - 40°C and the dissolution curves can be found in Figures 74 to 78. It can be clearly seen that the swelling characteristics change over the measured temperature range. The dissolution curves for the molecular weight range at 16°C show that only the very low molecular weight samples (M_n < 22200) indicate no

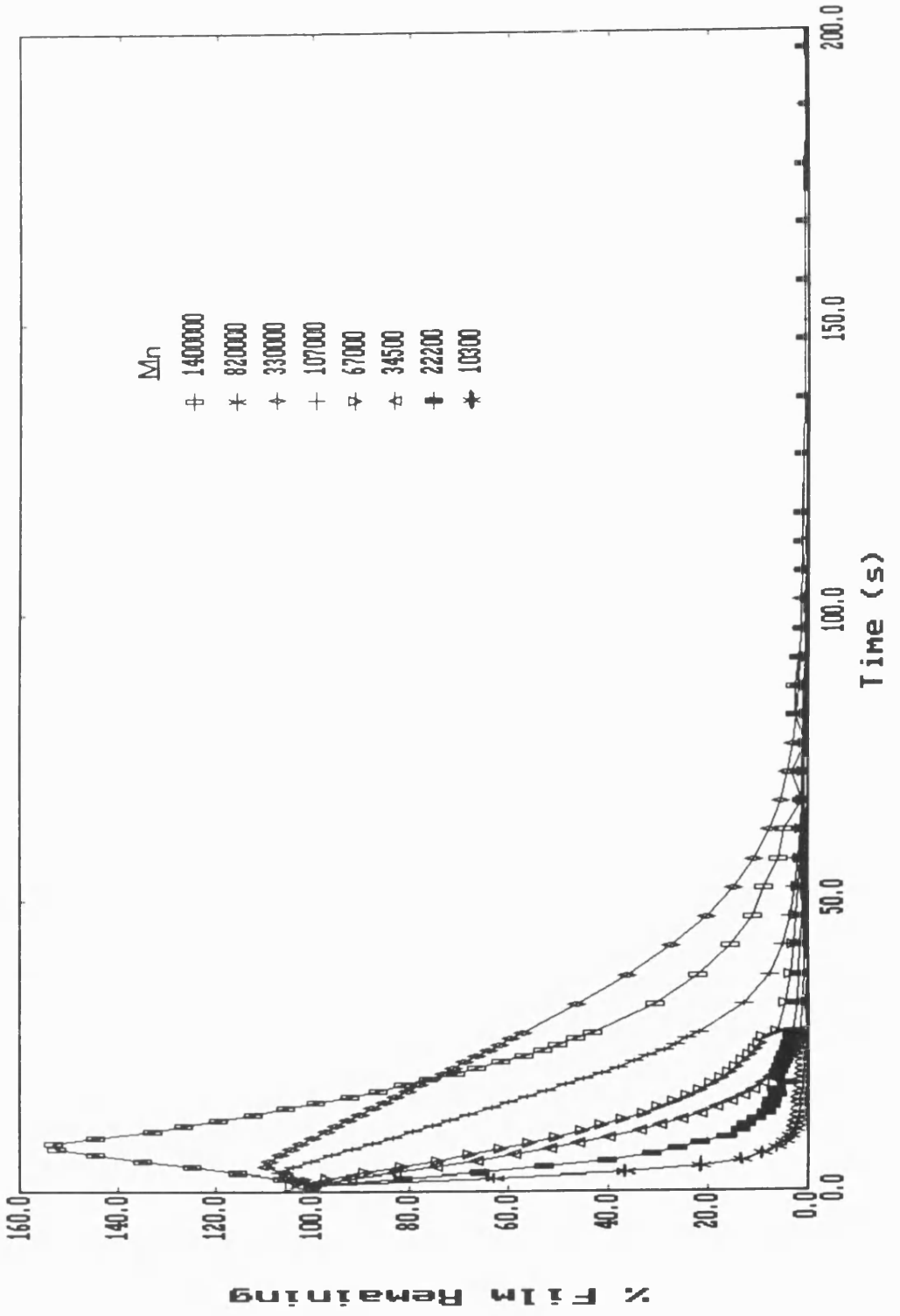

Figure 73: Dissolution of PMMA in MEK at 25°C

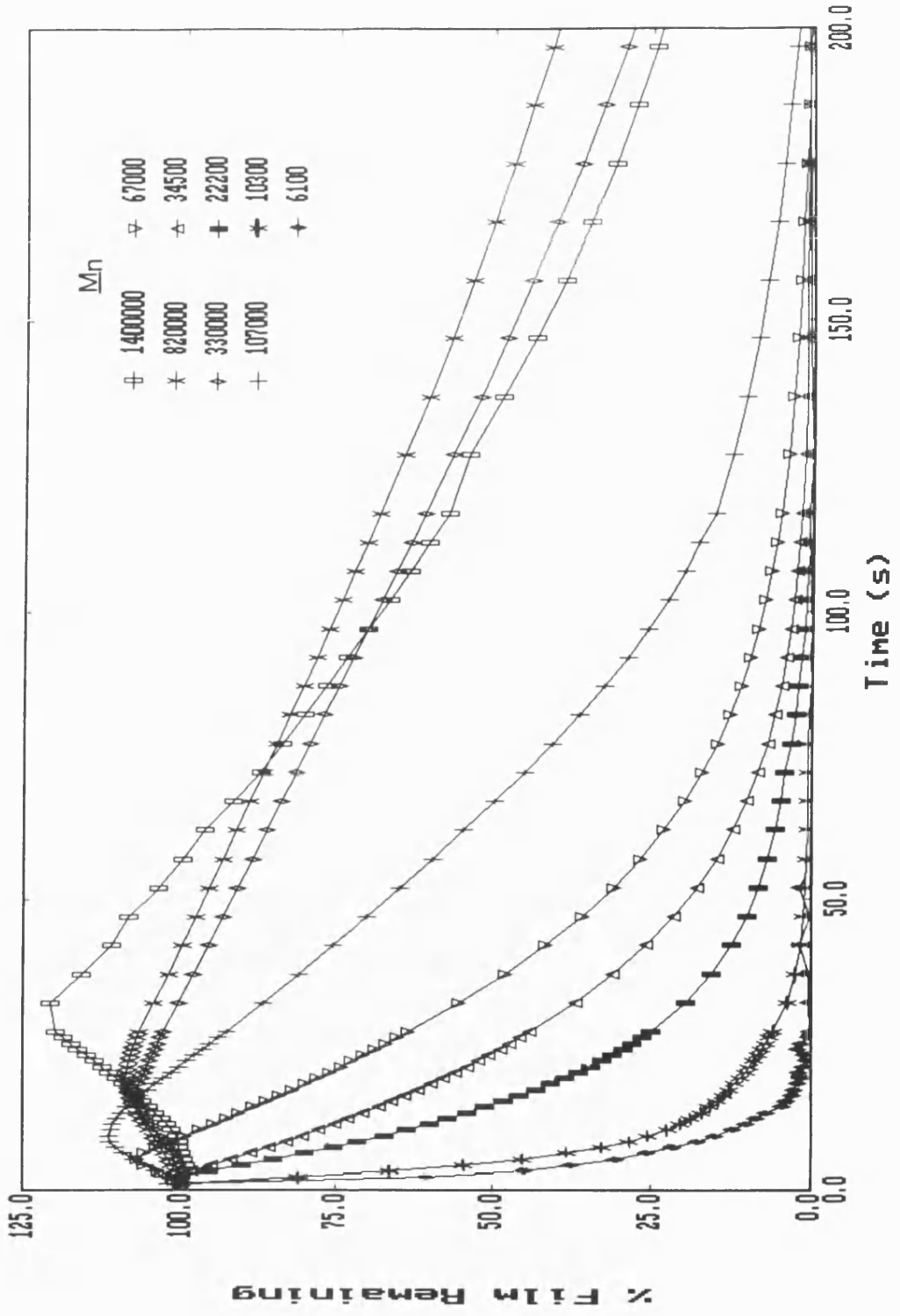

Figure 74: Dissolution of PMMA in MEK at 16°C

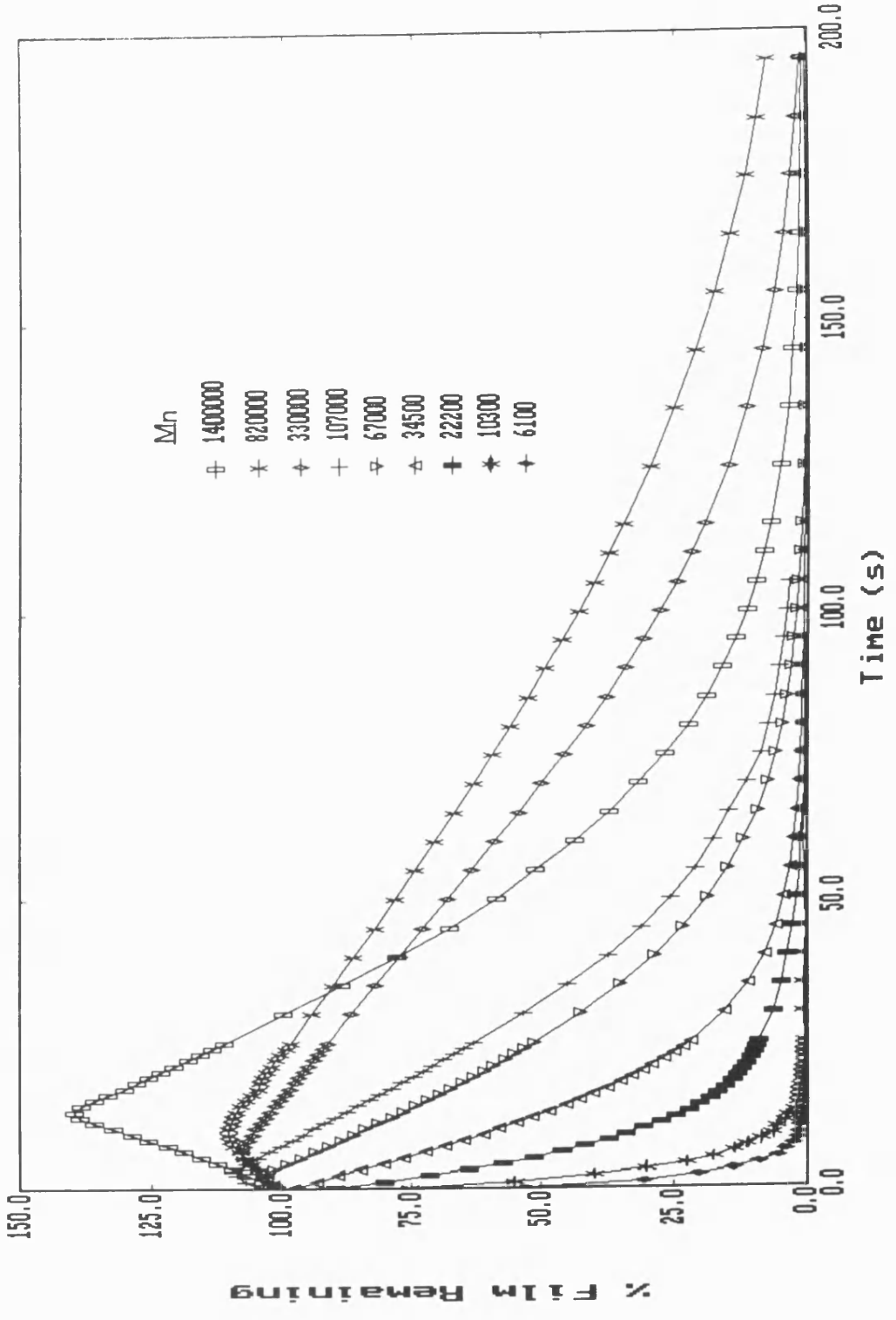

Figure 75: Dissolution of PMMA in MEK at 20°C

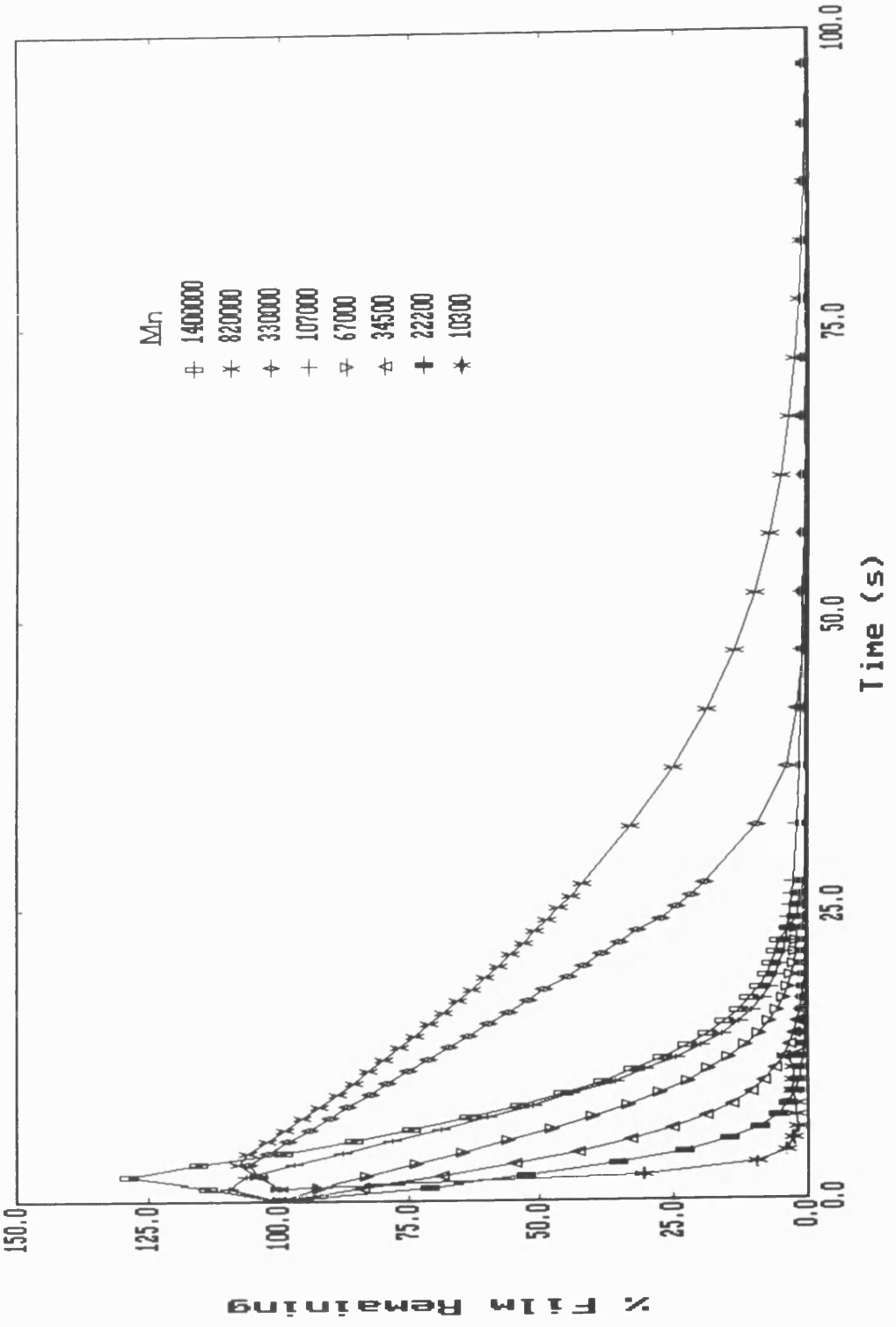

Figure 76: Dissolution of PMMA in MEK at 30°C

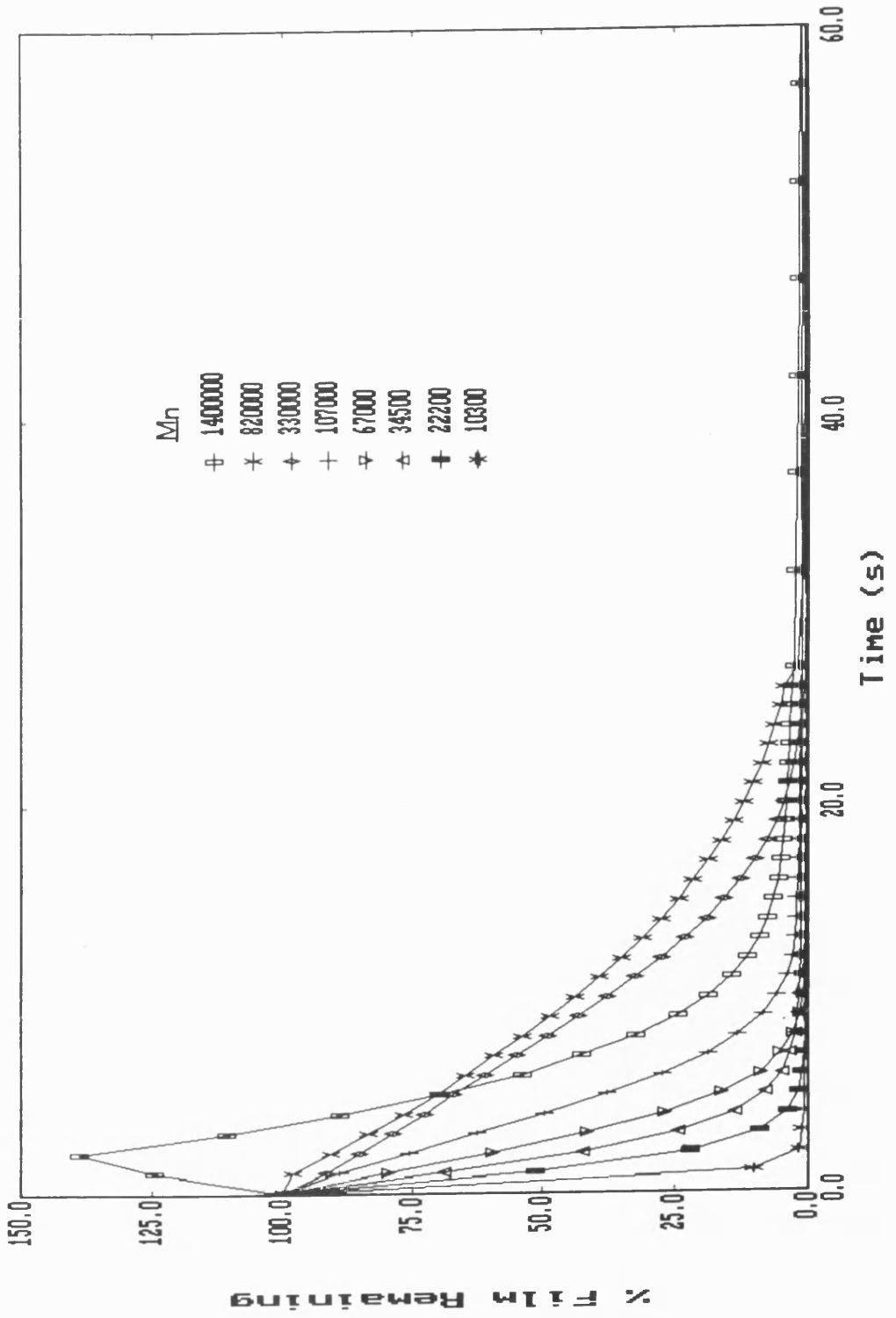

Figure 77: Dissolution of PMMA in MEK at 35°C

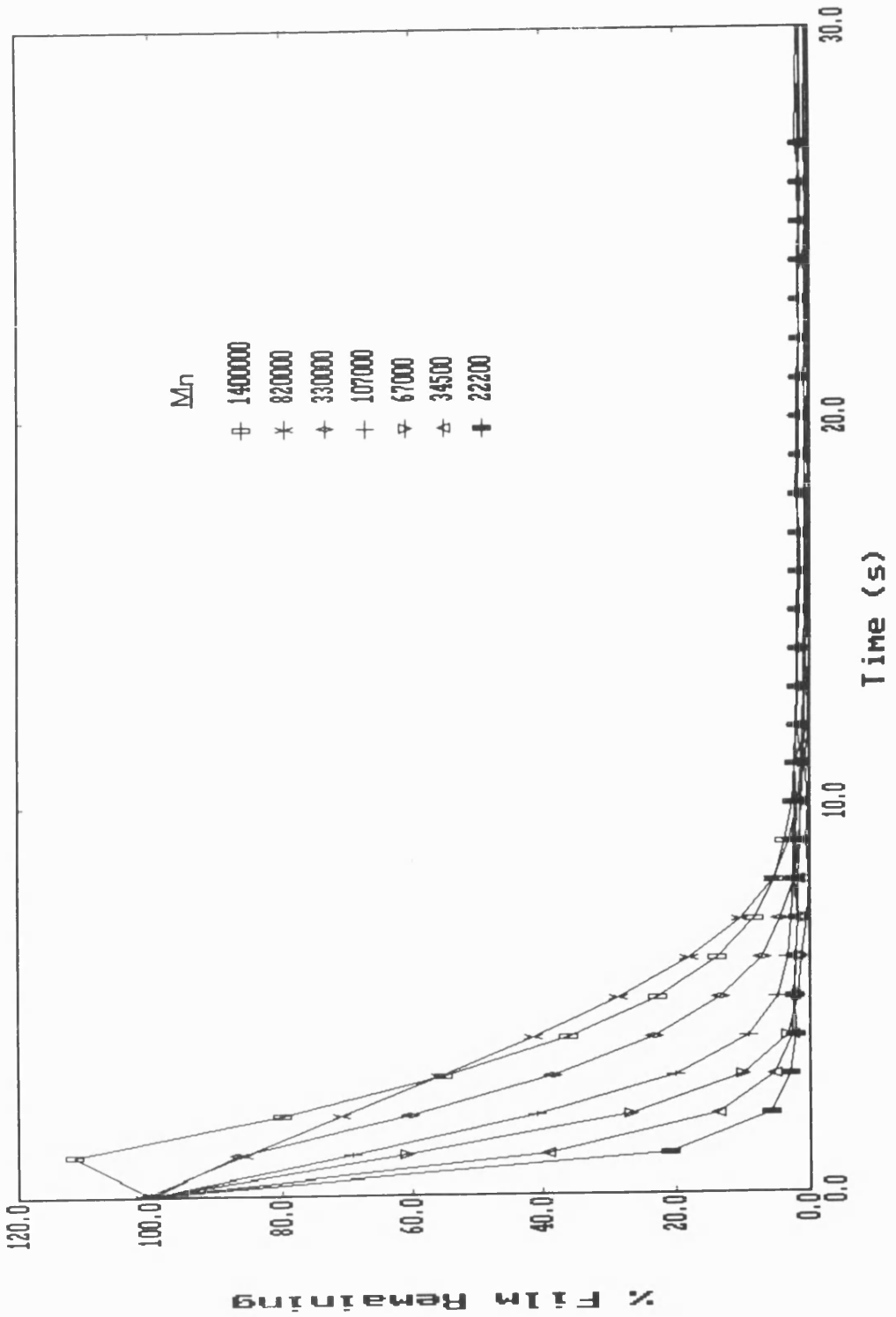

Figure 78: Dissolution of PMMA in MEK at 40°C

initial swelling. Below M_n 22200, some swelling may be taking place but the rapid overall dissolution curve obscures any initial swelling, while at 40°C, no initial swelling and complete dissolution was observed throughout the molecular weight range.

By consideration of the mean diameter of a macromolecular coil, Asmussen and Ueberreiter[63], in their study of polystyrene dissolution in toluene, concluded that the molecular weight influence is related to the increase of thickness of the transition layer as defined in Section 1.2. They found that above a molecular weight (M_w) of 150000, an enormous increase of the surface thickness occurs which considerably slows down the dissolution process. This phenomenon can be explained by consideration of Bueches' theory for the entanglement of macromolecules, where a break in the curve of the melt viscosity can be observed with increasing molecular weight[184]. As Shultz and co-workers have shown that concentrated polymer solutions are comparable to melts[185], it would not be unreasonable to expect to observe similar effects in our systems.

Krasicky and co-workers[72,186], using laser interferometry, have shown that a transition layer is detectable for PMMA samples of M_n greater than 30000 whilst the polymer is dissolving in MEK at 22.5°C. The transition layer (or offset) was found to increase with increasing molecular weight, with the lower limit of the layer again close to the "entanglement" or "critical" molecular weight found in viscous flow. The dependence of melt viscosity on molecular weight changes from an exponential value of unity to about 3.5 at a chain length of 208 atoms corresponding to a M_n of 10000. This value is increased to 30000 when the polymer is in a 30 per cent solution of non-volatile solvent. Manjkow and co-workers[187] have found a similar effect

with the dissolution of polystyrene in a series of solvents, with the dissolution rate dropping off sharply at a molecular weight of 350000.

This increase in the required thickness of the swollen layer of the polymer with increasing molecular weight before dissolution can be explained by considering the penetration depth of the solvent. The penetration depth of the solvent can be related to the thickness of the swollen surface layer and must be adequate to free the polymer chains which are anchored deeper in the polymer structure and, consequently, the thickness of the swollen layer must be large enough to release them.

Ueberreiter and Asmussen[51,188] have shown that the diffusion coefficients of solvents in polymers are independent of the chain length of the macromolecules unless the molecular weight is so low that effects of the chain ends become appreciable. As the diffusion process of the solvent is a "jump" of the solvent molecule from one chain unit to another, it should not be affected by the length of the entire chain. This indicates that the occurrence of a transition layer depends on the inability of polymers to disentangle themselves rapidly from the surface of the glassy, unswollen polymer film.

The variation of dissolution rate with molecular weight has been studied previously, although over restricted ranges and with different solvents. In his study of the factors affecting the dissolution rate of PMMA, Ouano[40] developed a series of unexposed and electron beam exposed PMMA samples of varying molecular weights in MIBK at 25°C. The dissolution rates were calculated by allowing dissolution from 30 to 70% film and dividing by the time elapsed, however, no detailed analysis of the dissolution curves was given. He combined his work with that of

Greeneich[58] for the dissolution of PMMA in the same solvent at 22.8 and 35.6°C.

Ouano suggested the following relationship between dissolution rate (DR) and polymer molecular weight (M)[40]:

$$DR = aM^b$$

where a and b are constants for a particular polymer/solvent system. Systems with high b values will exhibit a large distinction between an unexposed (high molecular weight) and exposed (lower molecular weight) area in a positive resist such as PMMA.

Over a narrow range of molecular weight, both Ouano and Greeneich found the log-log plot of dissolution rate versus molecular weight gave a linear relationship with the slopes of the lines almost identical. Over the complete range of molecular weights studied, the system could be represented by two linear regions with a sharp change in slope at M_n 20000 from 1.5 in the low molecular weight (highly exposed) region to 0.4 in the high molecular weight (unexposed and low dosage) region. Ouano suggested that this break in slopes could be attributed to the effects of irradiation such as gaseous by-products increasing the free volume of the polymer.

In their studies of the dissolution of polystyrene in MIBK, Manjkow and co-workers[187] found for narrow molecular weight distribution PMMA samples, a linear dependence existing in the log-log plot of dissolution rate versus molecular weight consistent with the behaviour predicted by Ouano. Flack and co-workers[73] found the log-log plot of dissolution of PMMA (M_n

27000 - 180000) in MIBK gave a linear relationship. However, other workers[71,189] have obtained a non-linear log-log dependence on molecular weight when a larger molecular weight range was studied. Krasicky and Cooper[71] also found curved relationships between dissolution rate and molecular weight. Their different molecular weight samples were produced by photo-degrading a high molecular weight polymer and hence had varying polydispersities which will greatly affect the dissolution rate.

In their study of dissolution of thin PMMA films in ketones and hydroxyketones, Papanu and co-workers[190] observed a similar effect of molecular weight on the dissolution of narrow molecular weight distribution samples in MIBK at 24.8°C. The dissolution rate behaviour was consistent with that predicted by the equation proposed by Ouano up to a M_n of 100000 where levelling of dissolution rate is observed. For the lower molecular weight region[56], the value of the molecular weight exponent, a, was found to be 0.98 for the dissolution of both wide and narrow polydispersity PMMA samples in MIBK at 24.8°C. At a given M_n or M_w, the dissolution rate of a wide molecular weight distribution was higher than that of a narrow distribution sample.

Manjkow found that the enhancement of dissolution rate of wide polydispersity samples could be due to their wide distribution of chain lengths, as the shorter chains dissolve at a faster rate than longer chains, and after their removal, allow easier penetration of the polymer by solvent which improves the mobility of the longer chains, hence enhancing the overall dissolution rate. As discussed previously, higher molecular weight chains are anchored deeper into the polymer and require a thicker swollen layer to release them.

To illustrate that differences in the polydispersity of polymers (with the same M_n or M_w) can affect the observed dissolution kinetics, the dissolution of a wide polydispersity PMMA (M_n 56000, γ 2.0) in MEK at 25°C has been compared with that of a molecular weight series of PMMA standards (M_n 67000, 34500 and 22000). As Figure 79 indicates, the rate of dissolution decreases with increasing molecular weight for the polymer standards. However, the dissolution curve of the wide polydispersity sample lies over that of the 34500 sample and not in the expected position (if considering the M_n of the polymer). This confirms the observations reported by previous workers that at a given M_n or M_w, the dissolution rate is higher for wide polydispersity samples than for the corresponding narrow polydispersity polymer.

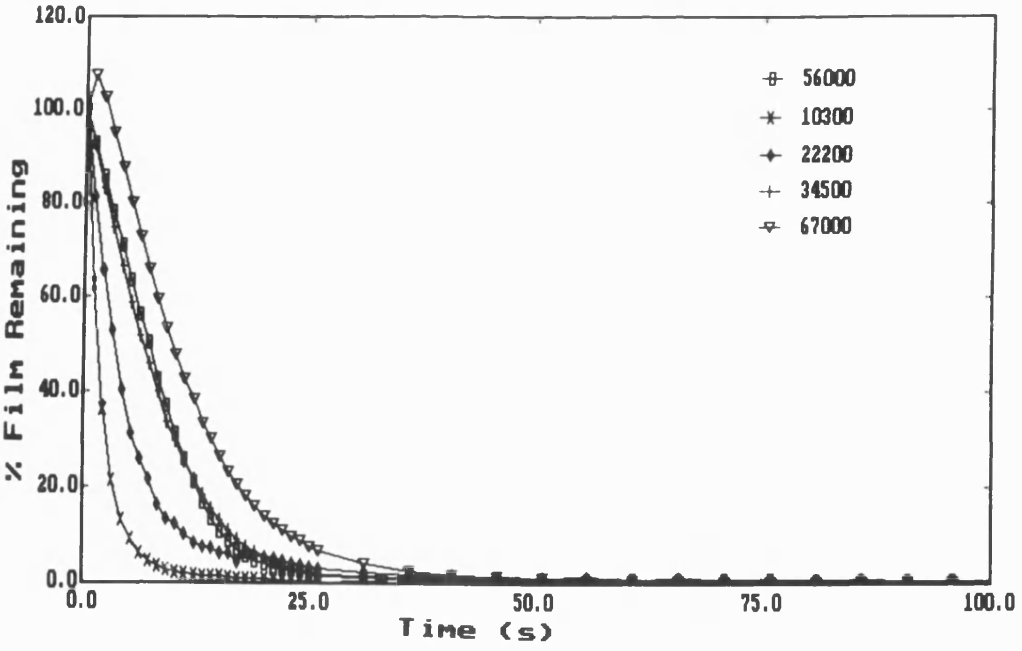

Figure 79: Effect of Polydispersity upon PMMA Dissolution

It can be seen that there is some disagreement concerning the log-log relationship of dissolution rate with molecular weight. Our results for the dissolution rate of the PMMA standards in MEK over the temperature range 16 - 40°C have been plotted in the log-log format and are shown in Figure 80. Clearly there is not a linear relation over the complete range of molecular weights studied. Each system can be represented by two linear regions. For the developing temperature range studied, the break in the lines occurs at the same molecular weight of approximately 100000. In the lower molecular weight region, the slope varies from 0.58 - 0.95 whilst above 100000, from 0.09 to 0.17 (see Table 3). Generally, higher development temperatures produced lower values. This indicates that, if swelling is not a large contributing factor, greater definition between exposed and unexposed regions can be made at lower temperatures. At low polymer molecular weights, the values of the linear correlation coefficient are very close to 1.000, whilst in the high molecular weight region, there is some deviation in the values particularly at low temperatures. This deviation may be caused by swelling obscuring the dissolution curves.

Our values of slope compare well with the results of Papanu[190] for PMMA in MIBK, who found a levelling of dissolution rate at M_n 100000 and a slope of 0.98 at the lower molecular weight region. Ouano has again found a similar trend with values of comparable magnitude, it can therefore be surmised that where swelling is not a predominant factor, the log-log relationship is linear over a narrow molecular weight range but upon the occurrence of swelling a break in linearity will occur. Clearly, Ouano's explanation of the increase in free volume of the polymer (due to irradiation) increasing the dissolution rate can be discounted as irradiation has not been a factor in our experiments.

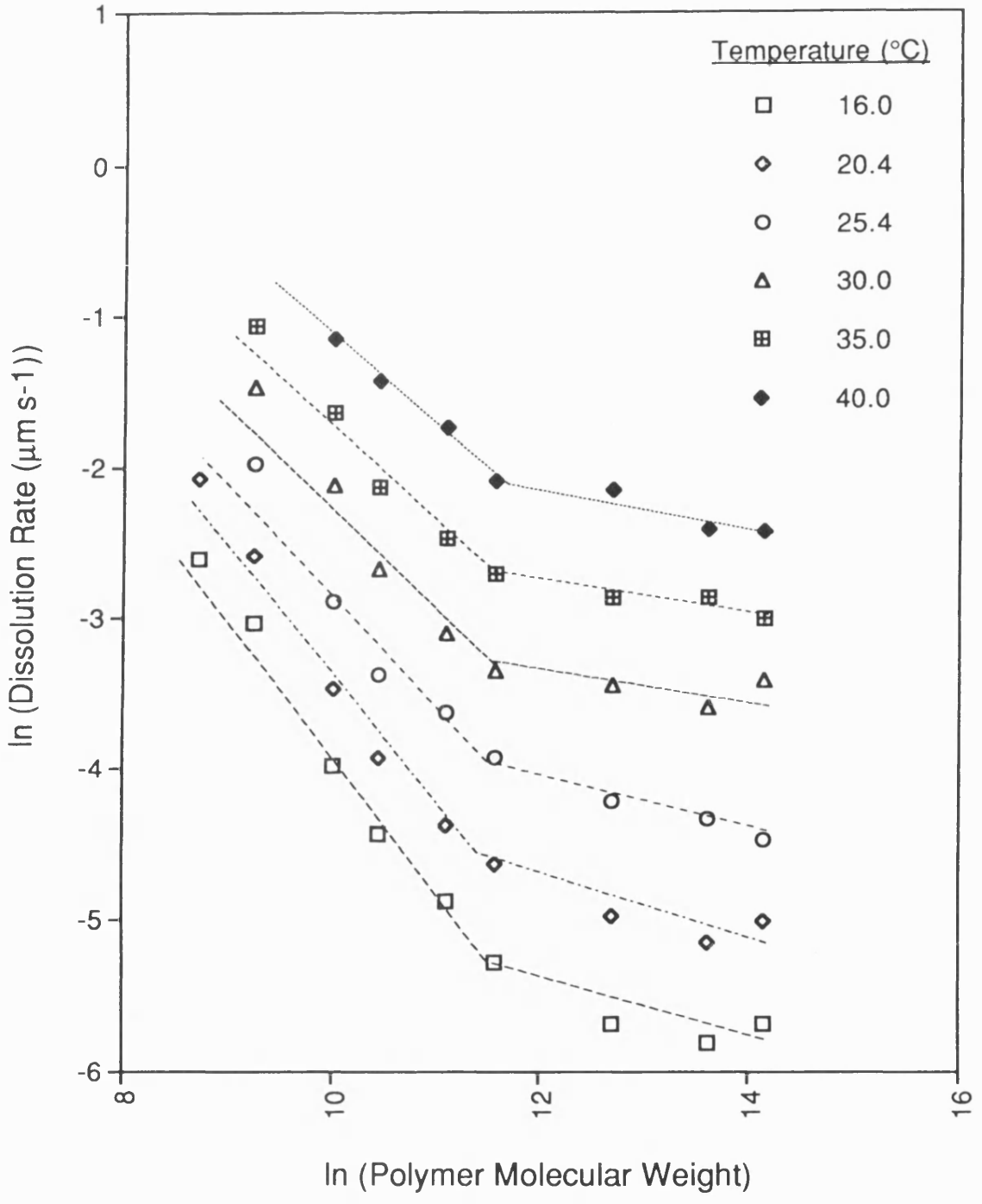

Figure 80: **Effect of Polymer Molecular Weight on the Dissolution of PMMA in MEK**

Temperature (°C)	Equation (y = mx + c)	Linear Correlation Coefficient
Low Molecular Weight Region		
16.0	-0.953x + 5.673	0.995
20.4	-0.920x + 5.857	0.992
25.4	-0.811x + 5.336	0.973
30.0	-0.824x + 6.088	0.991
35.0	-0.711x + 5.456	0.990
40.0	-0.575x + 4.610	0.995
High Molecular Weight Region		
16.0	-0.172x - 3.369	0.841
20.4	-0.165x - 2.790	0.856
25.4	-0.171x - 2.041	0.979
30.0	-0.116x - 2.002	0.983
35.0	-0.099x - 1.559	0.932
40.0	-0.145x - 0.377	0.948

Table 3: **The Gradient and Linear Correlation Coefficients for the Log-Log Plot of Dissolution Rate versus Polymer Molecular Weight for the Dissolution of PMMA in MEK**

Papanu and co-workers have suggested that in the lower molecular weight region, stress cracking occurs during the dissolution of PMMA in MIBK (as observed for the dissolution of PMMA in dimethylphthalate below 80°C[39]), indicating a strong dependence on molecular weight. The swelling of the outer region of the polymer exerts a stress on the remaining glassy core, conversely the core applies a restraint on the swelling of the outer core. The stresses developed as a result of differential swelling are often sufficiently large in magnitude to cause cracking and crazing of the polymer[47]. At higher molecular weights, the infiltration process of the solvent is immediately followed by substantial swelling which is so great that an elastic swollen layer is formed which fills in the cracks, hence the difference in dependence of dissolution rate on polymer molecular weight.

5.2 Dissolution of PMMA in Alkyl Acetate Solvents

During the investigation of the effect of solvent molar volume on the dissolution rate of PMMA (see Section 7.2), a series of quartz crystals coated with the molecular weight series of PMMA standards (M_n 22200 - 330000) were developed in a homologous series of n-alkyl acetates and the dissolution characteristics were measured over the temperature range 15 - 40°C.

Throughout the alkyl acetate solvent series and temperature range studied, the dissolution rate decreased with increasing polymer molecular weight as observed in Section 5.1 for the dissolution of PMMA in MEK. Figures 81 to 86 show the dissolution curves for PMMA in the alkyl acetate solvents at a developing temperature of 20°C.

In methyl acetate, it can be observed that rapid and complete dissolution is observed for all the polymer molecular weights studied and with the exception of the M_n 330000 standard, no swelling of the film was measured. Figure 82 shows the dissolution of the PMMA standards in ethyl acetate, the dissolution rates are much lower and the time required for complete dissolution of the M_n 330000 standard was greater than 400 s compared with 60 s in methyl acetate. Swelling of the polymer was observed above M_n 34500 and increases with polymer molecular weight. At M_n 67000, the dissolution curve has a sigmoidal shape which is not observed with the other samples throughout the solvent series.

All the polymer standards initially swell in both n-propyl and isopropyl acetate and again, the highest percentage of polymer swelling is observed

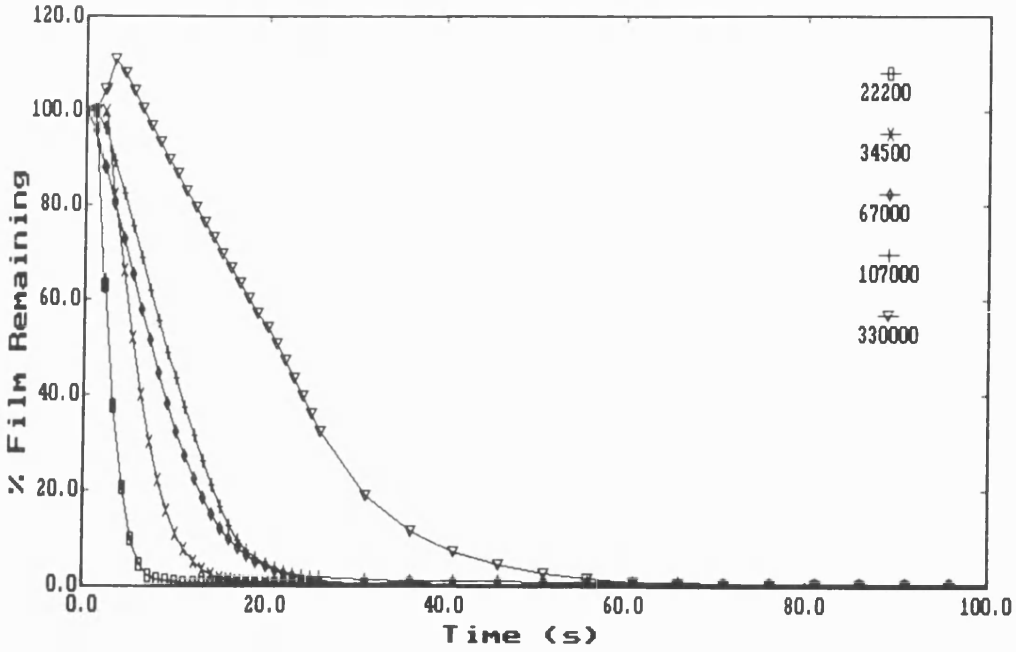

Figure 81: Dissolution of PMMA in Methyl Acetate at 20°C

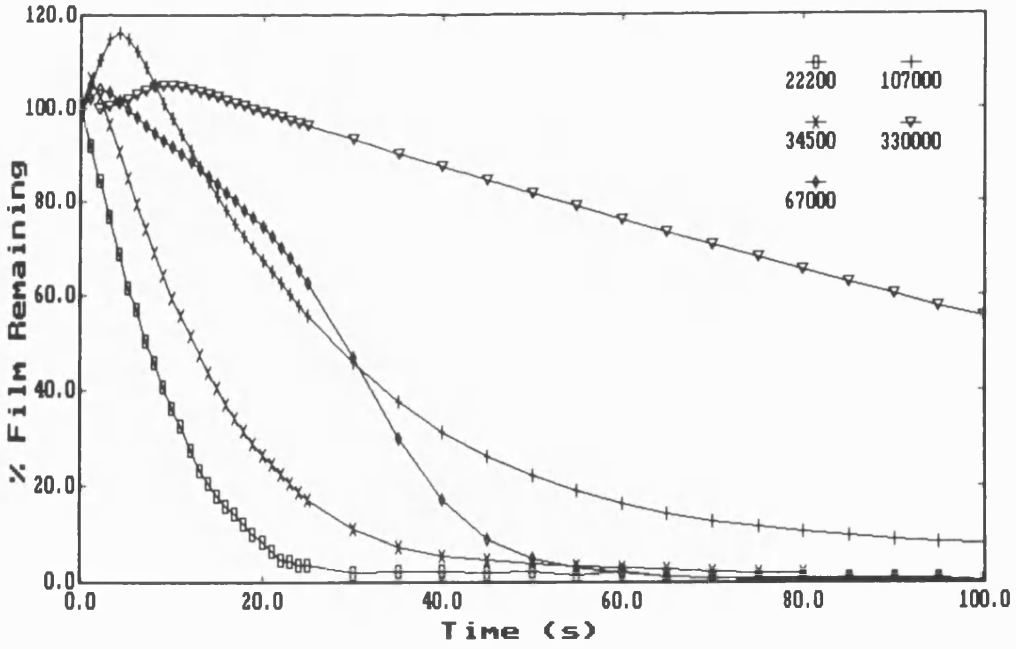

Figure 82: Dissolution of PMMA in Ethyl Acetate at 20°C

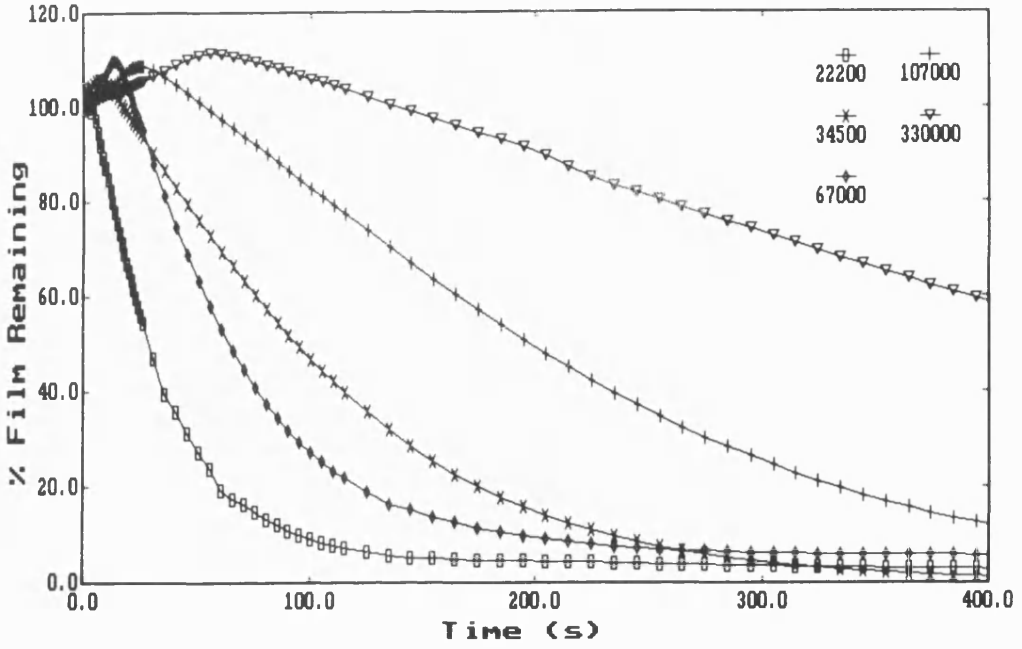

Figure 83: Dissolution of PMMA in n-Propyl Acetate at 20°C

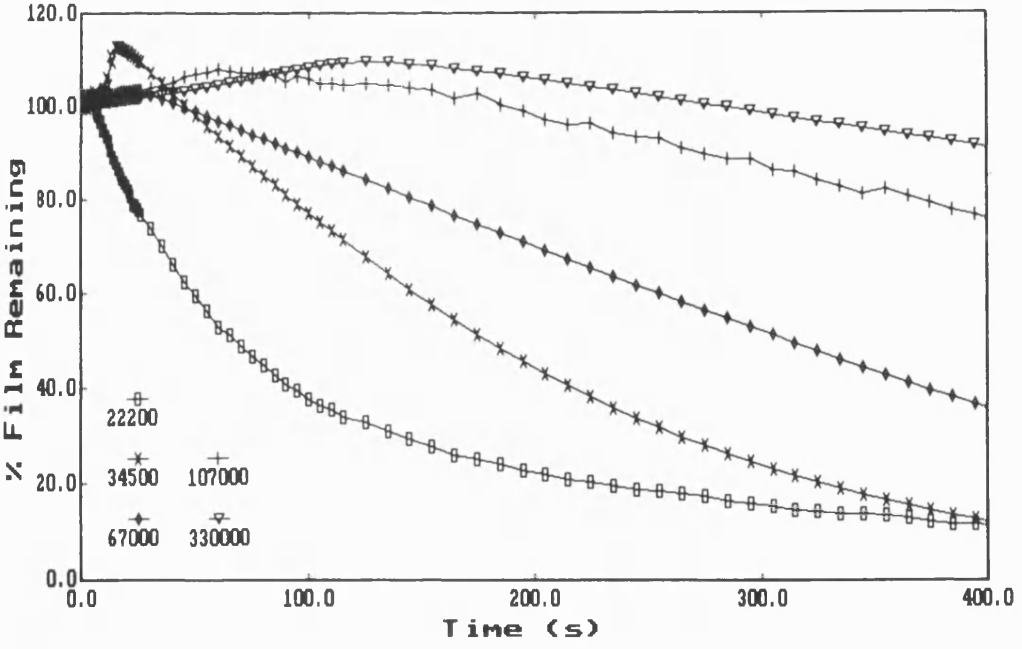

Figure 84: Dissolution of PMMA in Isopropyl Acetate at 20°C

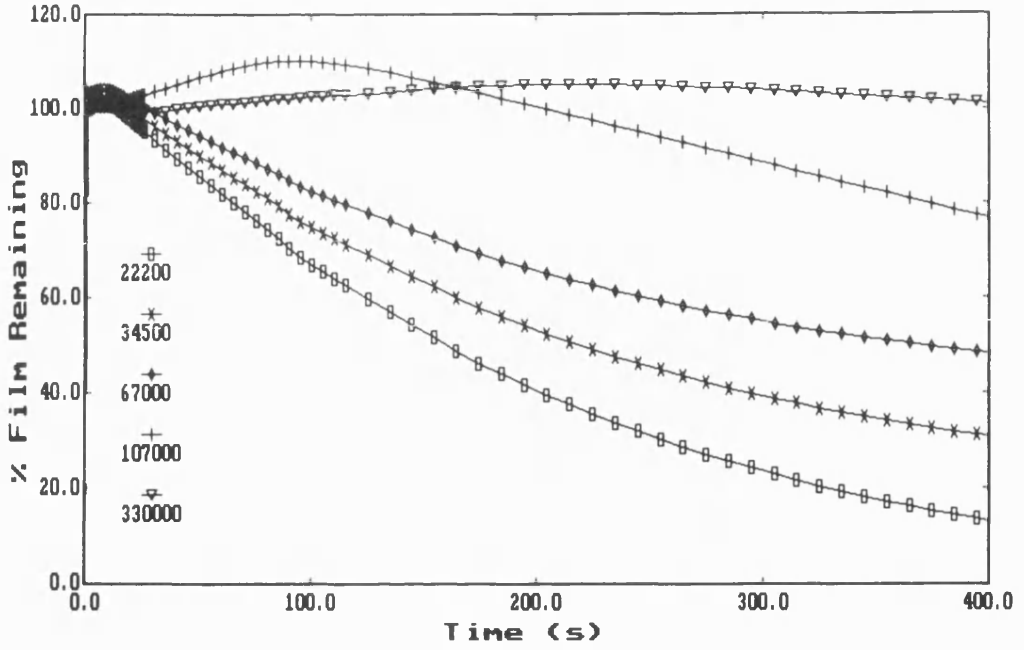

Figure 85: Dissolution of PMMA in n-Butyl Acetate at 20°C

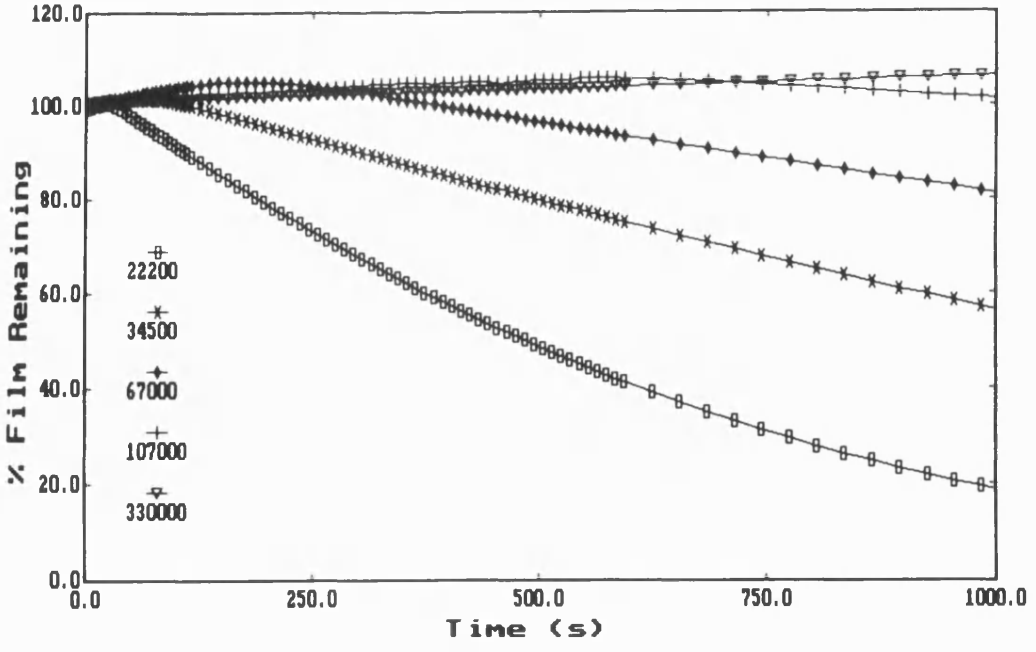

Figure 86: Dissolution of PMMA in n-Pentyl Acetate at 20°C

at the highest molecular weight. However, the dissolution rates are slower for isopropyl acetate than those for n-propyl acetate as indicated by Table 4.

PMMA M_n	Dissolution Rate ($\mu m\ s^{-1} \times 10^3$)	
	n-Propyl Acetate	Isopropyl Acetate
22200	6.0	4.0
34500	3.0	1.3
67000	2.7	1.0
107000	1.4	0.5
330000	1.1	0.4

Table 4: Dissolution Rates for PMMA in n-Propyl and Isopropyl Acetate at 20°C

Comparison of Figures 83 and 84 shows that the dissolution curves are much broader for the dissolution of PMMA in isopropyl acetate compared with those measured in n-propyl acetate. This broadening of the dissolution curves is not unexpected as the cross-section (in one direction) of the isopropyl group is much larger than for the n-propyl moiety and hence, greater disruption of the polymer structure during the diffusion of the solvent molecule will be required, causing greater swelling and slower dissolution rates of the polymer.

Throughout the range of molecular weights studied, the higher homologues of the alkyl acetates, show initial swelling of the polymer film, broadening of the dissolution curves and incomplete dissolution. As previously mentioned, further studies have been made over the temperature range 15 - 40°C and the results will be discussed further in Chapter 6.

The log-log plots of dissolution rate versus molecular weight for the dissolution of the PMMA standards over the temperature range 15 - 35°C (Figure 87 to 91) gave a linear relationship for all the alkyl acetates studied. As Table 5 indicates, the slopes of the graphs are found to be dependent on the type of alkyl acetate used with the slope increasing as the alkyl chain length increased. The difference in the slope of the lines was found to be greater at the lower temperatures. Throughout the solvent series and temperature range studied, high values of the linear correlation coefficient were achieved.

Solvent	Equation (y = mx + c) *(Linear Correlation Coefficient)*		
	15°C	25°C	35°C
Methyl Acetate	-0.492x + 1.648 *(0.973)*	-0.462x + 2.702 *(1.000)*	–
Ethyl Acetate	-0.470x + 0.026 *(0.874)*	-0.498x + 1.772 *(0.988)*	-0.358x + 1.310 *(0.766)*
n-Propyl Acetate	-0.690x + 0.738 *(0.943)*	-0.645x + 1.844 *(0.978)*	-0.572x + 2.510 *(0.963)*
Isopropyl Acetate	-0.767x + 0.662 *(0.964)*	-0.651x + 1.215 *(0.953)*	-0.566x + 1.616 *(0.977)*
n-Butyl Acetate	-0.749x + 0.077 *(0.960)*	-0.728x + 1.359 *(0.979)*	-0.658x + 2.213 *(0.936)*
n-Pentyl Acetate	-1.581x + 7.311 *(0.976)*	-0.932x + 2.289 *(0.966)*	-0.849x + 3.080 *(0.957)*

Table 5: Effect of Temperature on the Gradient of the Log-Log Plot of Dissolution Rate versus Molecular Weight for the Dissolution of PMMA in Alkyl Acetate Solvents

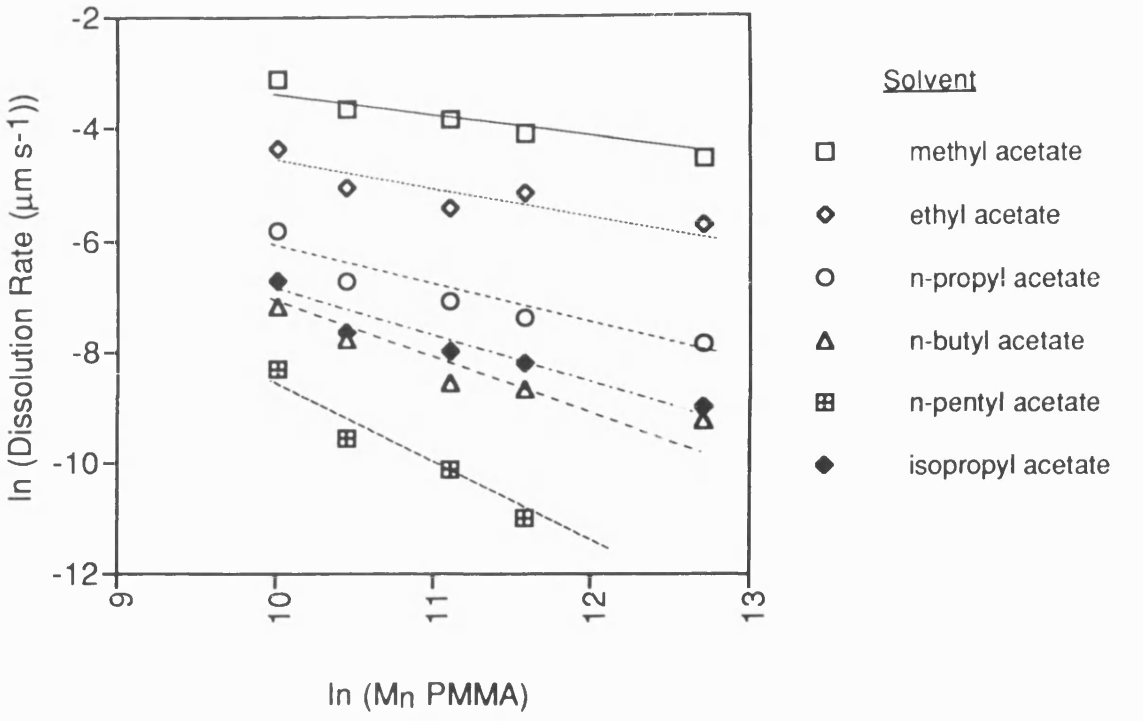

Figure 87: Dissolution of PMMA in Alkyl Acetates at 15°C

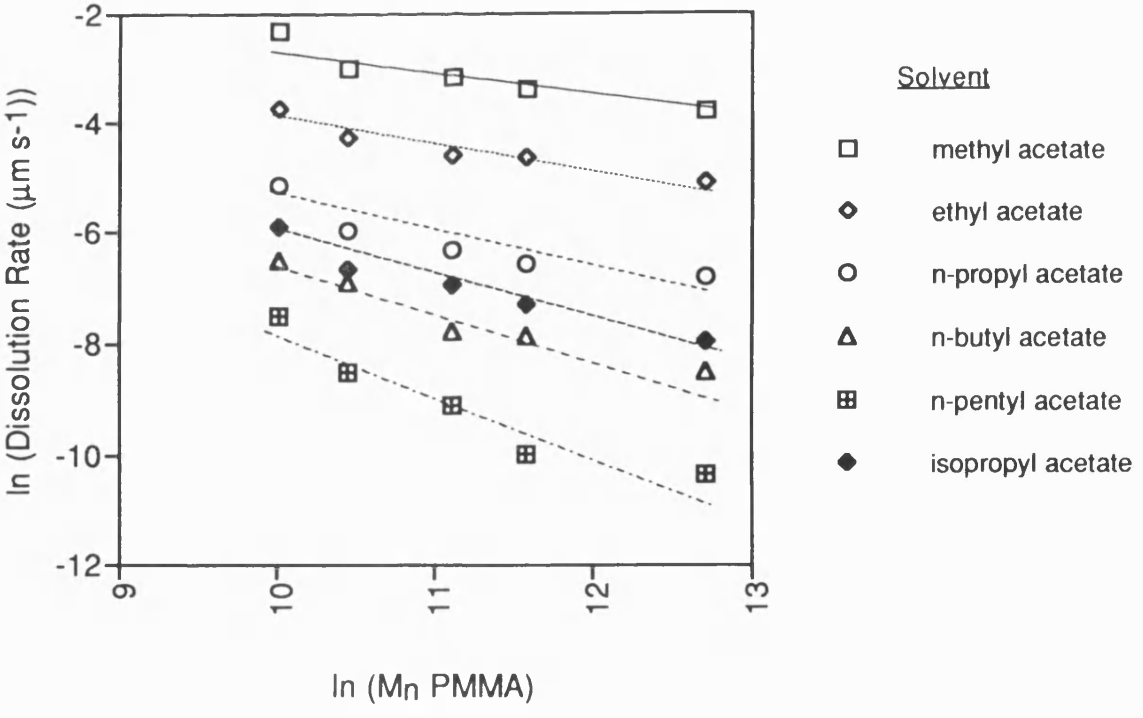

Figure 88: Dissolution of PMMA in Alkyl Acetates at 20°C

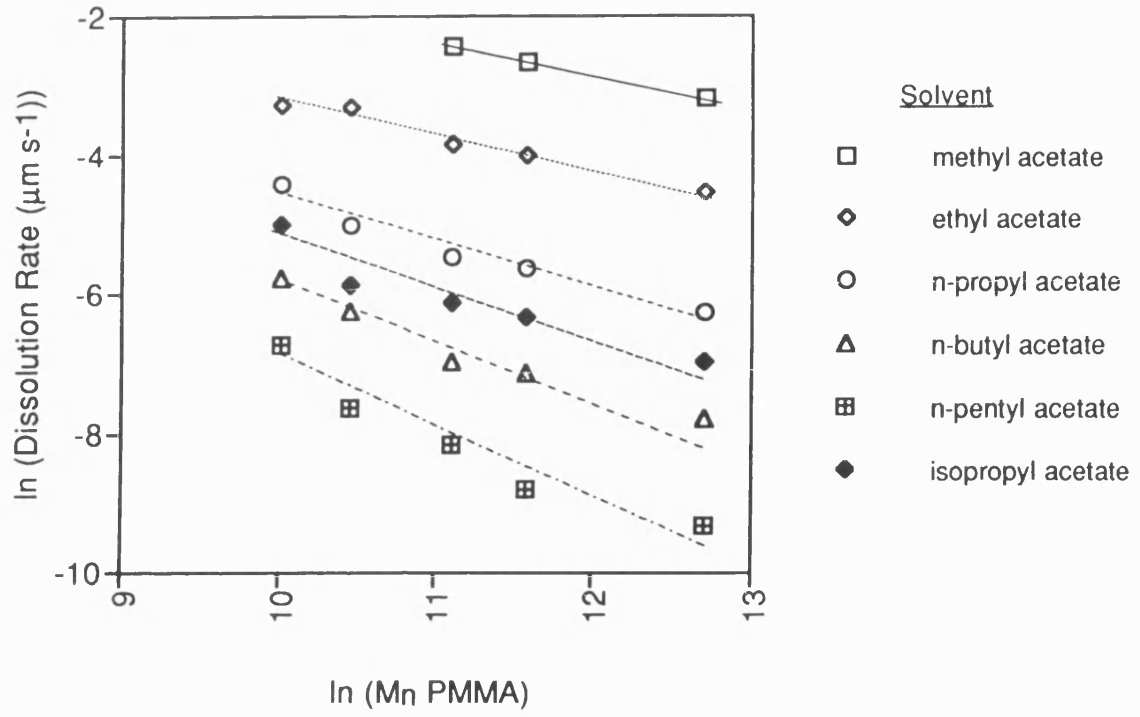

Figure 89: Dissolution of PMMA in Alkyl Acetates at 25°C

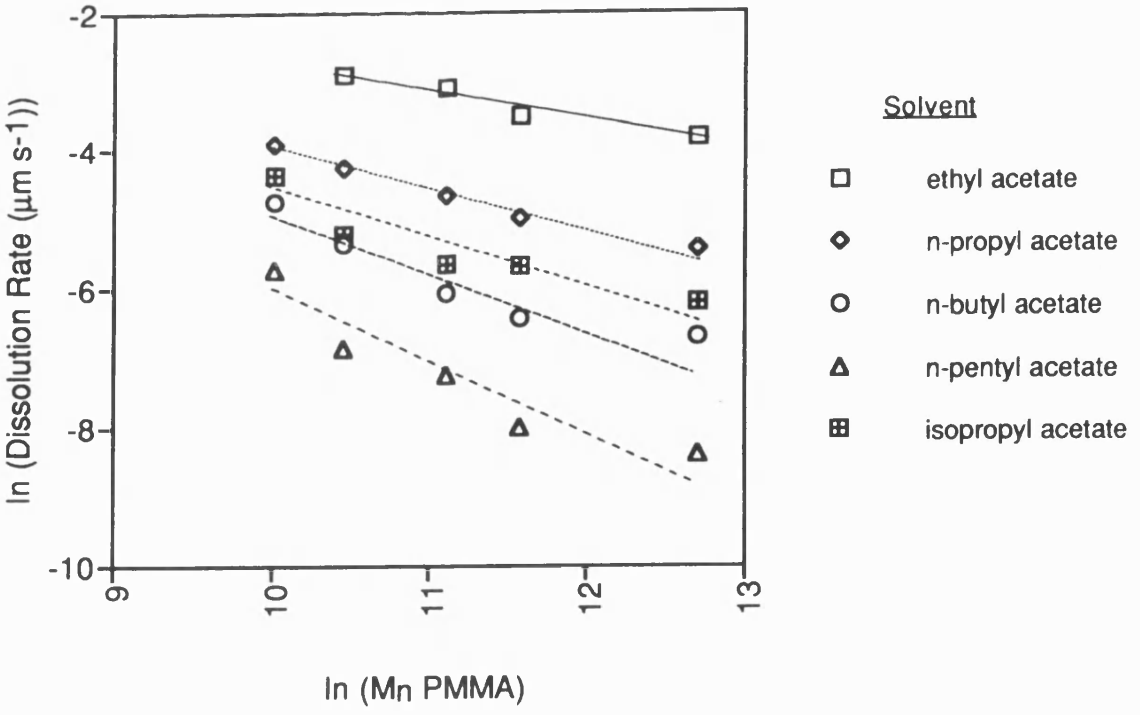

Figure 90: Dissolution of PMMA in Alkyl Acetates at 30°C

a) Linear Relationship

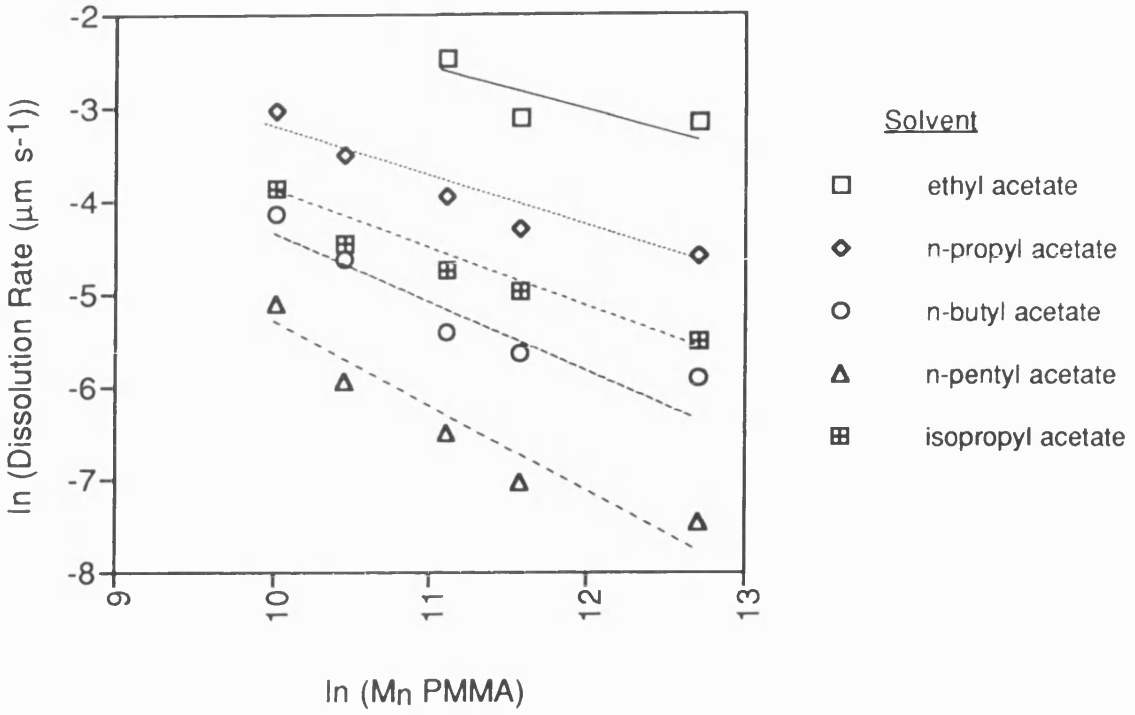

b) Break in Linearity

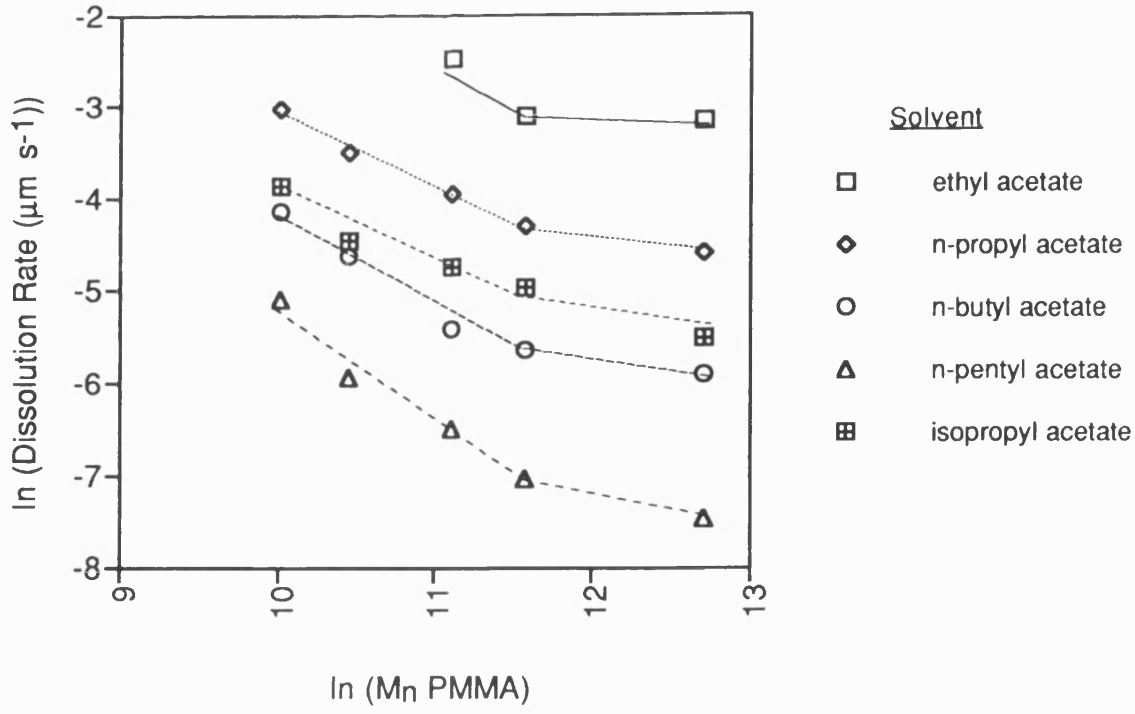

Figure 91: Dissolution of PMMA in Alkyl Acetates at 35°C

In the study of the effect of polymer molecular weight on the dissolution of PMMA in MEK (Section 5.1), a break in linearity was observed at a M_n of approximately 100000. Closer observation of Figure 91a for the dissolution of PMMA in the alkyl acetate solvent series at 35°C indicates that a break in linearity of the log-log plot may also occur, and Figure 91b shows the results with the lines redrawn to indicate the possible break in linearity. The change in slope occurs at approximately M_n 100000 for all the alkyl acetate solvents studied which corresponds to the same molecular weight observed for the dissolution in MEK. Therefore, although the change in linearity is not as obvious, a similar explanation for this difference in dependence of dissolution rate on polymer molecular weight can be used.

As the break in linearity occurs at the same polymer molecular weight throughout the solvent series, it is unlikely that this change in dissolution rate is due to swelling of the polymer film overshadowing the dissolution curve (as swelling tends to increase with increasing solvent molar volume), and hence preventing an accurate determination of the dissolution rate. Further investigation is required to determine the extent of this effect.

The dissolution rate of PMMA in isopropyl acetate lies between that of n-propyl and n-butyl acetate throughout the temperature range. However, the slopes of the lines shown in Table 5 show a correlation between isopropyl acetate and n-butyl acetate at 15°C, but at 25 and 35°C, the slopes for isopropyl acetate are close to that observed for the dissolution of n-propyl acetate. This reversal of order may be explained by consideration of the solvent diffusion mechanism. At lower temperatures (i.e. below 25°C), the diffusion of the bulkier isopropyl acetate molecules (compared with those of n-propyl acetate) is more hindered, particularly into the high molecular weight polymer chains and this is substantiated by a steeper

gradient. As the temperature of the developing solvent is increased, the diffusion of the molecules throughout the alkyl acetate series becomes less dependent on steric effects and polymer molecular weight becomes a less dominant factor and hence the gradient becomes less steep.

During his investigations on the effect of solvent molecular size on the dissolution rates of PMMA in a homologous series of acetates, Ouano[191] measured the dissolution rate of a series of molecular weights of 1 μm PMMA films (in the three tactic forms) at 25°C in n-pentyl acetate. He found a linear relationship for the log-log plot of dissolution rate versus polymer molecular weight (M_W 39000 to 316000). Gipstein and co-workers[57] have also considered the effect of polymer molecular weight on the dissolution rate for the series of alkyl acetate solvents. Three polymer molecular weights (M_W) of 39000, 94000 and 476000 were considered. Over the molecular weight range studied, the log-log plot gave a series of lines of increasing slope and followed the relationship found by Ouano. Our results are in agreement with those found by Gipstein and additionally with our experimental technique, we have been able to gain some insight into the effect of polymer molecular weight on the swelling of the polymer film.

5.3 Conclusion

In a series of solvents, we have demonstrated that the dissolution of PMMA decreases whilst swelling of the film increases with increasing polymer molecular weight. Wider polydispersity resists are found to dissolve at a faster rate with less swelling than the corresponding narrow molecular weight distribution resists. The appearance of substantial swelling of the polymer film is found to change the dependence of the dissolution rate on polymer molecular weight. If swelling is not a large contributing factor, greater definition between exposed and unexposed regions of the resist can be made at lower temperatures. The molecular weight and its distribution is therefore found to have a great effect on the ultimate resolution of the resist.

The log-log relationship of dissolution rate with polymer molecular weight for the dissolution of PMMA in MEK has shown a break in linearity at M_n 100000 for all the developing temperatures studied. This break can be related to the ability of polymers to disentangle themselves. We have resolved the disagreement amongst other workers concerning this log-log relationship. On first consideration, the log-log plot for the dissolution of PMMA in alkyl acetates is found to be linear throughout the molecular weight series. However, closer examination of the Figures has shown that a change in slope may also occur at approximately M_n 100000 for all the alkyl acetates studied, though the effect is less marked than with the other solvents.

Further studies of the effect of molecular weight upon dissolution of other polymers are given in Chapter 9.

Chapter Six

6.0 Effect of Temperature on PMMA Dissolution

The developing temperature of a polymer/solvent system can greatly affect the resolution of the resist, particularly in solvent/non-solvent systems. A change in diffusion mechanism may occur when a large enough change in temperature is considered. The activation energy of the dissolution process gives some indication of the penetration mechanism involved which can help in the prediction of the dissolution behaviour for a polymer/solvent system.

A series of polymers have been developed at various temperatures and the activation energies have been measured to gain an insight into the diffusion mechanisms involved.

6.1 Dissolution of PMMA in MEK

As part of our study into the effect of developing temperature on the solubility of polymers, a series of PMMA (M_n 107000, γ 1.03) coated crystals were developed in MEK over the temperature range 16 - 40°C. Figure 92 indicates the importance of solvent temperature to the dissolution process. Dissolution rates for PMMA are found to increase with temperature. All the samples went to complete dissolution, and above a temperature of 30°C, there was negligible swelling. Below this temperature, initial swelling (i.e. induction period) of the polymer was observed which also appears to be temperature dependent.

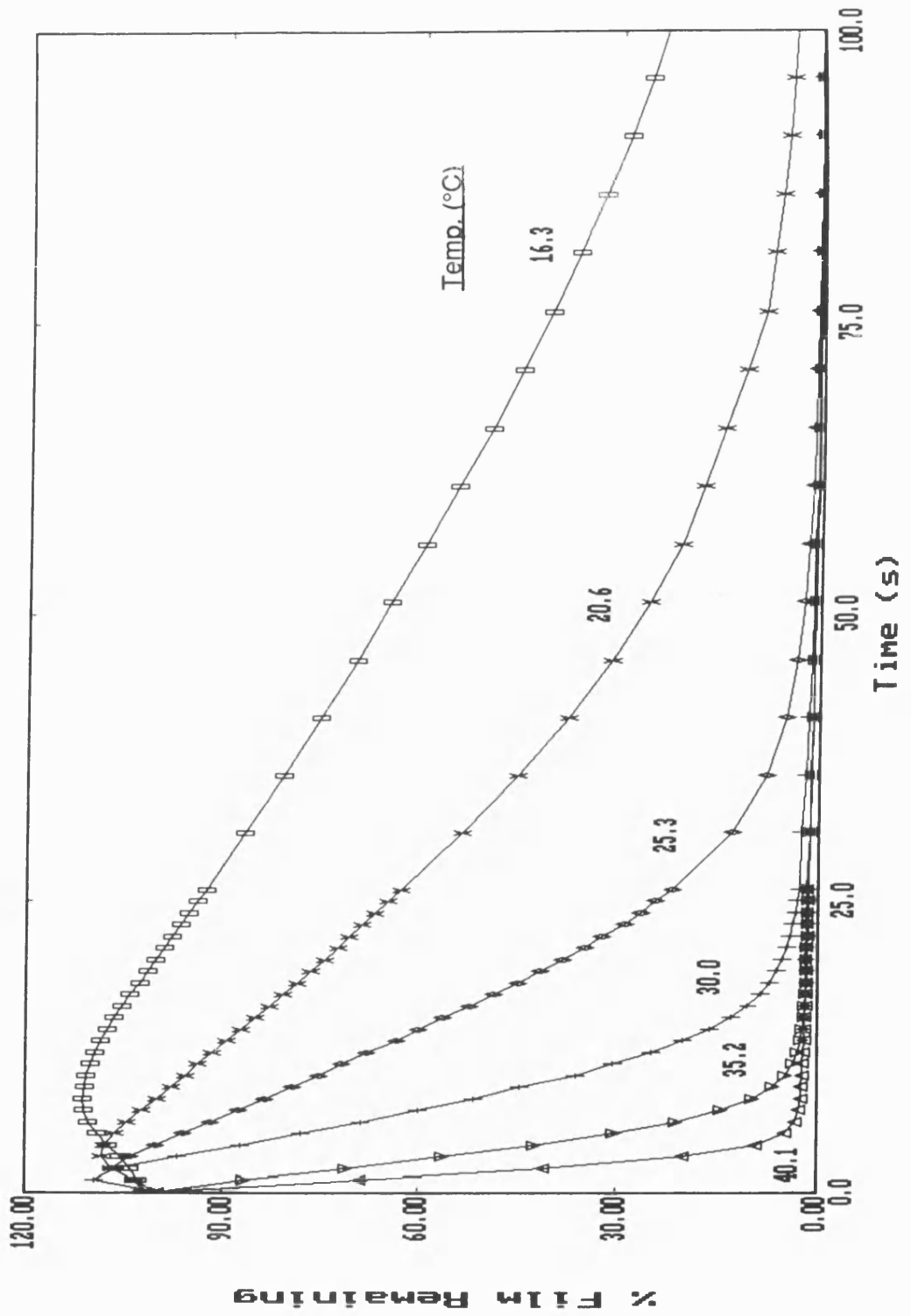

Figure 92: Effect of Temperature on Dissolution of PMMA (M_n 107000) in MEK

In rubbery polymers, solvent diffusion is generally described by Fick's laws of diffusion, but with glassy polymers, "non-Fickian" diffusion kinetics (i.e. Case II) may be observed because of the time-dependent response of the polymer as it rearranges its structure to accommodate the incoming molecules. Fickian diffusion is observed when the penetrant mobility is much less than segmental relaxation rates, whilst Case II diffusion occurs when the penetrant mobility is much greater than segmental relaxation rates[47]. With Case II diffusion, solvent transport in the swollen region of the polymer is still preceded by Fickian diffusion but a sharp front is observed between the unpenetrated and swollen region[48,192].

The appearance of the induction period in the dissolution of PMMA in MEK indicates that the diffusion process is Case II and the activation energy of the process should give an indication of the controlling diffusion process. The dissolution process should vary with temperature in accordance with an Arrhenius type equation:

$$DR = k \exp^{-E_a / RT}$$

where DR is the dissolution rate, T is the absolute temperature, E_a is the activation energy of dissolution, R is the gas constant and k is a constant. As Figure 93 shows, the dissolution of PMMA in MEK obeys this relationship with an activation energy of 101.1 ±1.0 kJ mol^{-1} (linear correlation coefficient = 1.000) for the dissolution process.

The study has been extended to the dissolution of a molecular weight range of PMMA standards in 100% MEK (as detailed in Section 5.1) over the temperature range 16 - 40°C. The Arrhenius plots for the molecular weight

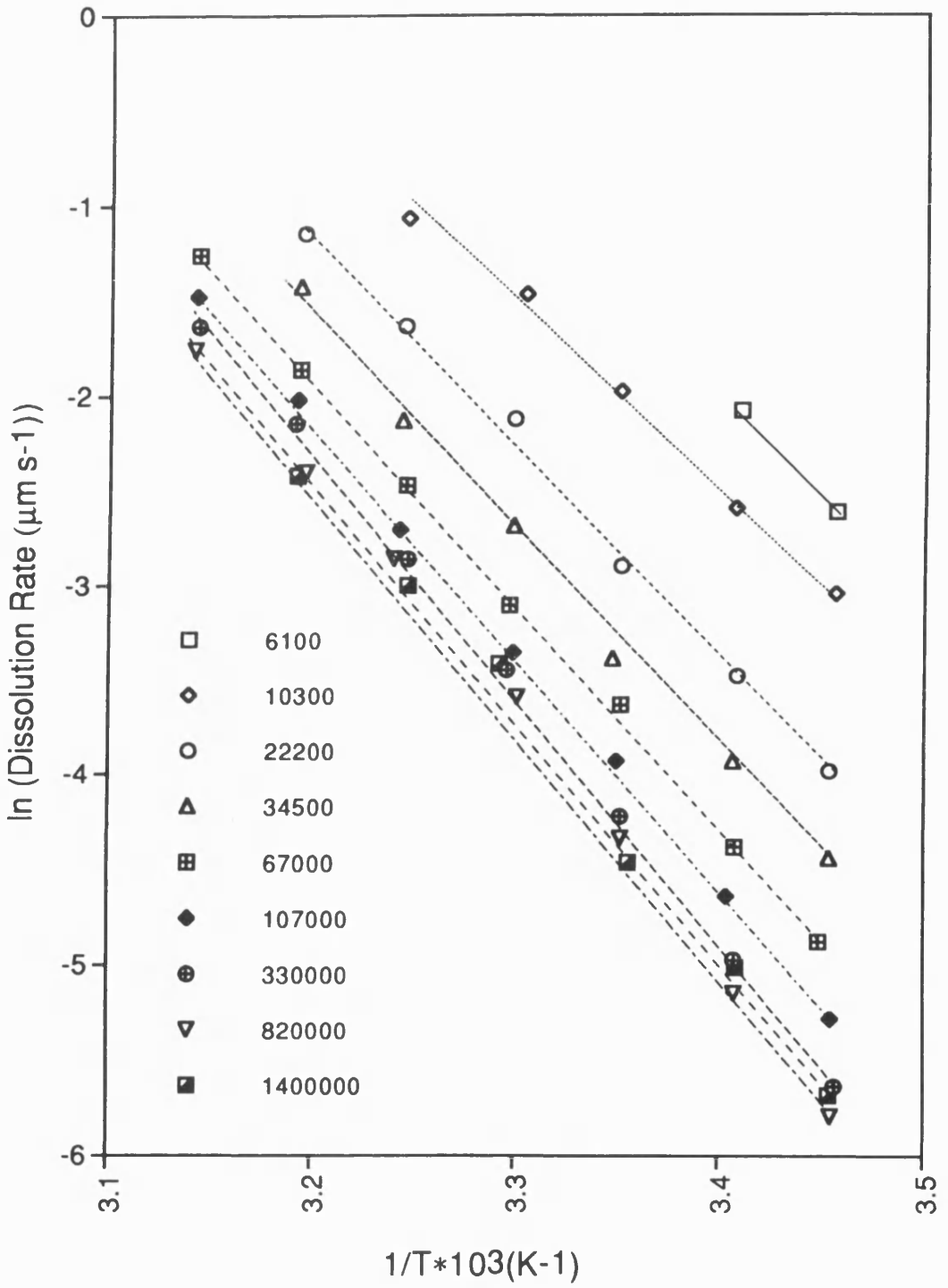

Figure 93: Arrhenius Plots for the Dissolution of PMMA in MEK

Effect of Polymer Molecular Weight

series give the expected linear relationships (Figure 93) and an average activation energy for dissolution of approximately 99 kJ mol^{-1} with a range of 85.8 - 107.4 ±1.1 kJ mol^{-1} (see Table 6). At high molecular weights (above M_n 107000), the activation energy is essentially independent of molecular weight. However, there is a slight deviation in activation energy for the low molecular weight polymers which may be due to the fewer experimental points and faster dissolution rates making the calculation of activation energy less accurate. In Chapter 5, we observed a break in linearity, at approximately M_n 100000, for the log-log plot of dissolution rate versus polymer molecular weight (for a range of developing temperatures). It therefore appears that for the dissolution of PMMA in MEK, the activation energy is susceptible to polymer molecular weight until a limiting molecular weight of 107000 is reached. Further analysis is required to fully understand this phenomenon but changes in the extent of chain entanglement is a possible explanation.

Polymer M_n	E_a (kJ mol^{-1})	Linear Correlation Coefficient
10300	85.8	0.999
22200	92.5	0.998
34500	95.4	0.998
67000	97.4	1.000
107000	101.1	1.000
330000	106.9	0.999
820000	107.4	0.998
1400000	105.0	0.997

Table 6: Activation Energies and Linear Correlation Coefficients for Dissolution of PMMA in MEK

A range of swelling and dissolution kinetics were observed throughout the molecular weight series. For the temperature range studied, no initial swelling was observed for the polymer molecular weight of 10300 (Figure 94), and swelling was not observed until temperatures below 25.4°C at a molecular weight of 67000 (Figure 95). At M_n 820000 (Figure 96), swelling was observed throughout the temperature range and the amount of swelling increased with decreasing temperature.

The increase in temperature provides energy for a general increase in segmental motion hence an increase in diffusion kinetics is observed. The activation energy is an indication of the energy required to uncoil the polymer chains and to overcome the intramolecular and intermolecular forces binding the polymer together. The movement of the solvent molecules takes place through "holes" which are produced as a result of polymer segment mobility. Therefore movement of the molecules is controlled by the motions of the polymer molecules and hence molecular weight dependent. As the Arrhenius plots indicate, the dissolution rate slows down with increasing molecular weight.

Table 7 shows the literature results for the temperature dependence of the diffusion of ethyl acetate in polymethylacrylate[193]. It can be clearly demonstrated that the diffusion coefficient increases with temperature indicating an increase in diffusion kinetics (with an activation energy of 156.5 kJ mol^{-1} for diffusion).

The swelling of PMMA at lower temperatures has also been observed by Manjkow and co-workers[65] during the study of dissolution of PMMA (M_n180000, γ 2.8) in 50:50 v/v MEK/IPA over the temperature range 18.4 - 24.8°C. At 24.8°C, the PMMA completely dissolved whilst at 18.4°C,

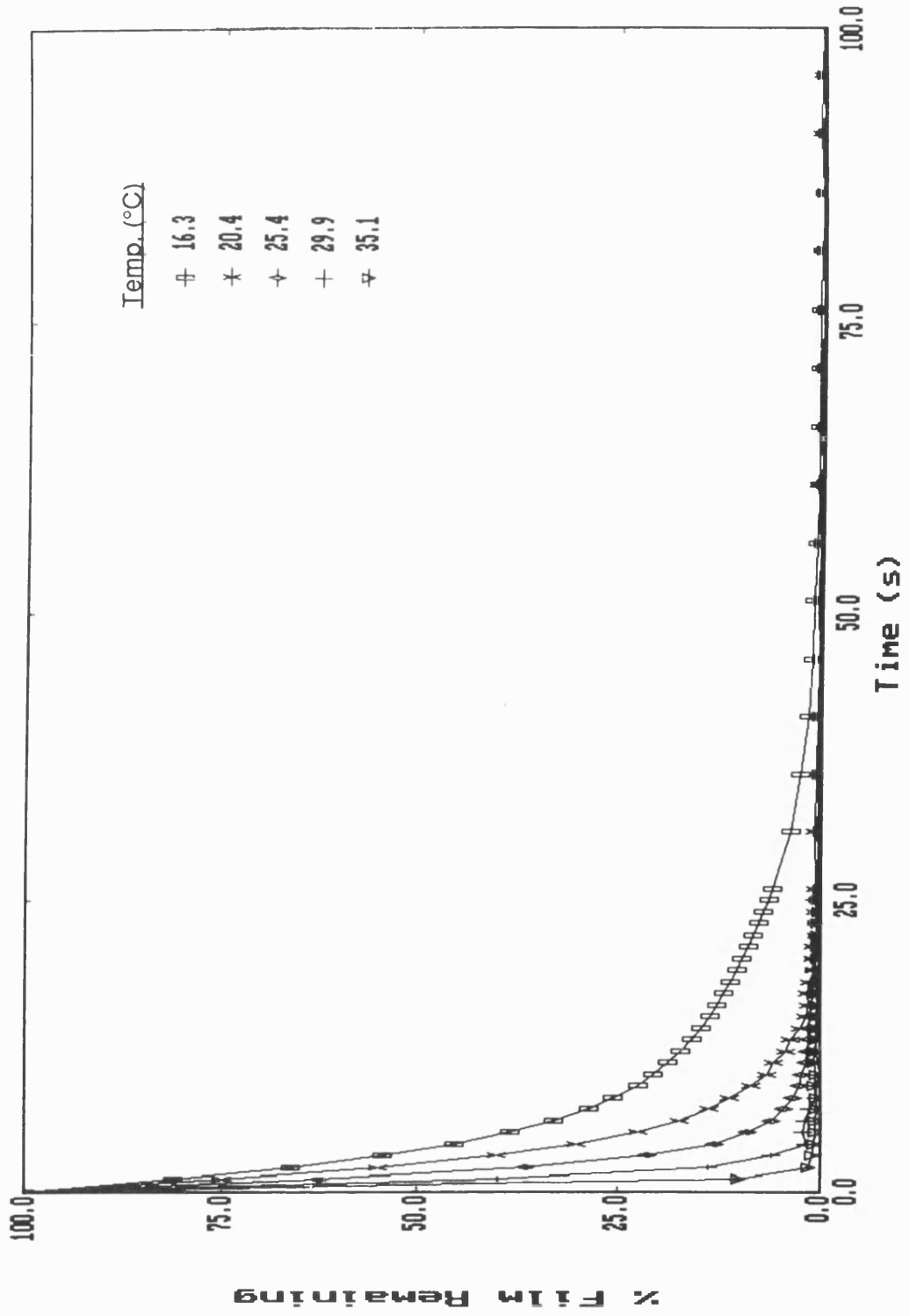

Figure 94: Effect of Temperature on Dissolution of PMMA (M_n 10300) in MEK

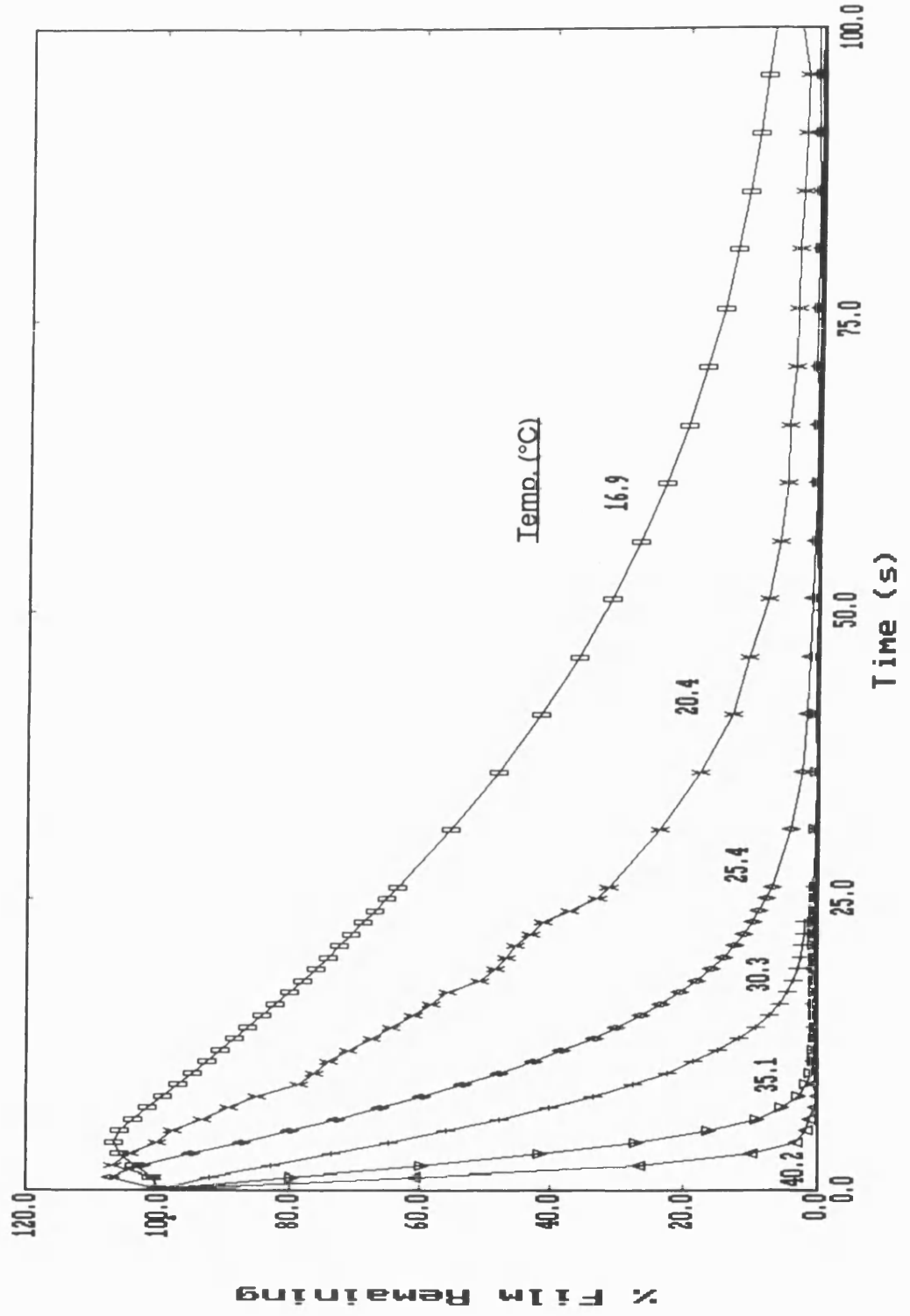

Figure 95: Effect of Temperature on Dissolution of PMMA (M_n 67000) in MEK

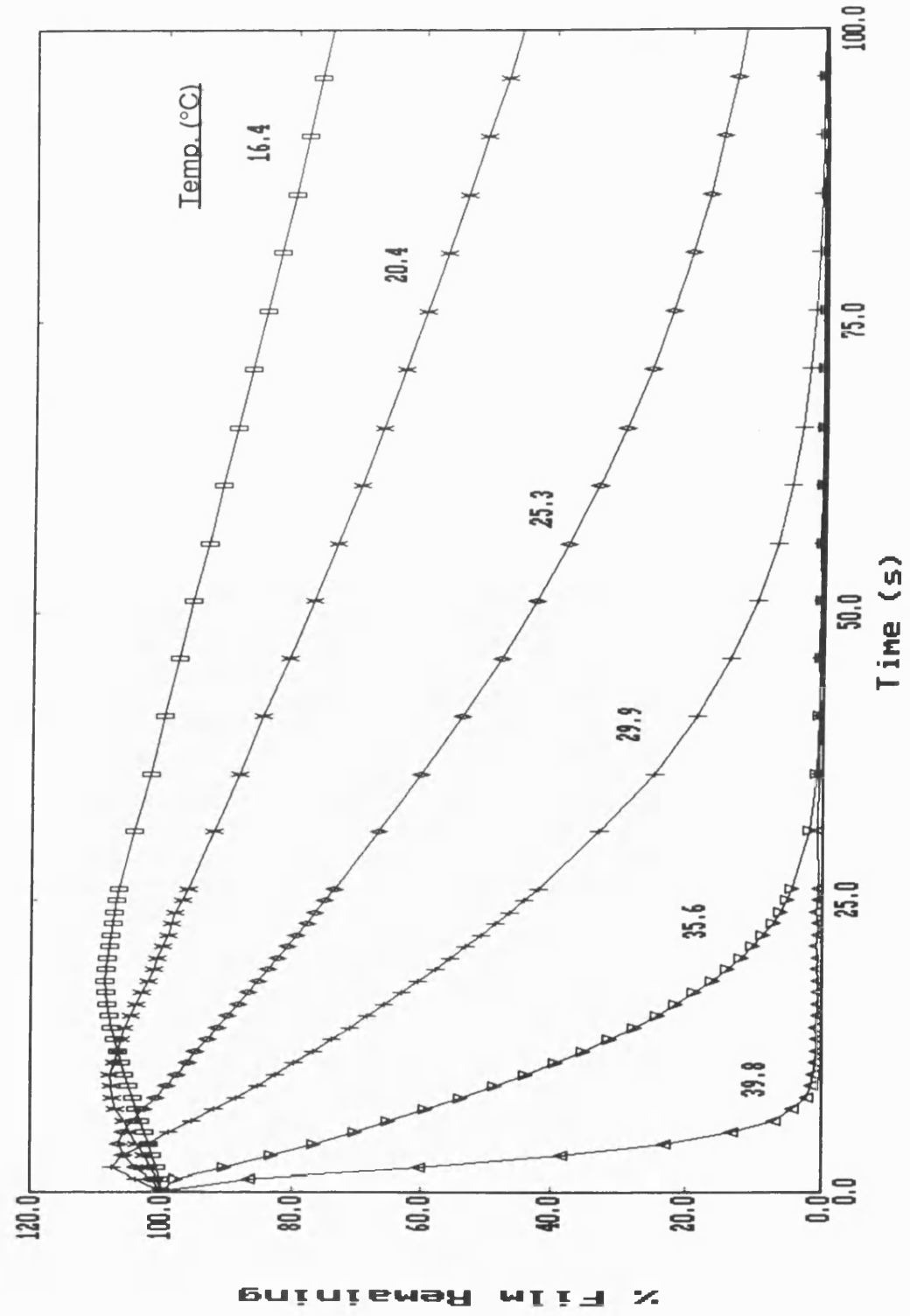

Figure 96: Effect of Temperature on Dissolution of PMMA (M_n 820000) in MEK

65% of the PMMA film remained with swelling observed at the lower temperature. The diffusion of the lower molecular weight polymer chains in the wide polydispersity sample is hindered by the presence of the high molecular weight polymer chains so, at the initial stages the swelling of the polymer predominates the process. As the PMMA sample swells further, the free volume of the polymer increases and the release of polymer is less hindered and hence the dissolution of the polymer molecules is the predominant process. This behaviour is typical of Case II diffusion which is characterised by an independence of activation energy with diffusivity where as diffusion-controlled processes (Case I) tend to vary with the diffusivity of the solvent molecule. This linear dependence of the Arrhenius plot was first observed by Greeneich for the dissolution of PMMA (M_W 39000 and 25000) however no swelling data was reported[58].

Temperature (°C)	Diffusion Coefficient ($cm^2\ s^{-1}$)
65	$5.7 * 10^{-7}$
55	$1.8 * 10^{-7}$
45	$6.3 * 10^{-8}$
35	$7.0 * 10^{-9}$
25	$6.0 * 10^{-10}$
15	$4.0 * 10^{-11}$

Table 7: Value of Diffusion Coefficient for Ethyl Acetate in Polymethylacrylate[193]

The independence of activation energy for dissolution with or without swelling concurs with the results obtained by Cooper and co-workers for the dissolution of PMMA[66] in MEK and MEK/ethylene glycol mixtures and gives excellent agreement with their value of 103 kJ mol^{-1}. Papanu and co-workers in their study of the effect of temperature on the dissolution of narrow polydispersity PMMA (M_n 66700 and 129000, γ 1.11) in MIBK[56] found no difference in activation energy and the high value (110 kJ mol^{-1}) was indicative of Case II sorption. Comparison of activation energy for the dissolution of wide polydispersity (M_n 180000, γ 2.8) and narrow polydispersity PMMA sample (M_n 129000, γ 1.11) shows an increase in activation energy from 103 to 152 kJ mol^{-1} as the sample becomes more polydisperse.

In his study of the effect of temperature on the dissolution of polydisperse PMMA for different prebake cooling rates, Papanu found faster dissolution rates for the samples with the fastest cooling rates. This enhancement in the rate of dissolution can be related to the proportion of free volume present in the polymer sample. The removal of solvent from the sample during the prebaking process opens up the polymer structure i.e. enhances the free volume. After prebaking, this is frozen into the polymer structure if the sample is quenched to room temperature. However, as the cooling rate is decreased, the polymer is able to reorganise hence closing up the increased free volume. Therefore Manjkow was observing faster dissolution rates for the PMMA samples with the greatest proportion of free volume. This dependence of dissolution rate on free volume further confirms our findings that the Case II diffusion process is operating i.e. above M_n 107000, the activation energy is independent of molecular weight but dependent upon polydispersity.

6.2 Transport of Methanol in PMMA

The resolution and sensitivity of a resist/developer system is strongly influenced by solvent transport in the polymer. During the development of resist images, the retained regions of polymer will swell due to solvent penetration. The amount of swelling observed is dependent upon the developer system but will affect the quality of the developed image. Hence a study into the effect of temperature upon swelling of resists (with no dissolution) would provide a better understanding into the diffusion process involved in resist development.

We have studied the effect of temperature on the swelling of PMMA thin films in methanol. PMMA was coated onto a series of quartz crystals and "developed" in pure methanol over the temperature range 15 - 40°C and the swelling curves for this system can be seen in Figure 97.

It can immediately be seen that the amount of swelling of the polymer increases with increasing temperature i.e. the final swollen thickness increases with temperature when no dissolution is observed. The swelling rate of the polymer increases with temperature and Figure 98 shows the Arrhenius plot for the swelling of the PMMA film. The plot shows a break in linearity at 30°C, which may be indicative of a change in the kinetics for the transport of methanol into the polymer. At the lower developing temperatures, an activation energy of 110.7 kJ mol-1 was obtained compared with a value of 57.2 kJ mol-1 for temperatures above 30°C.

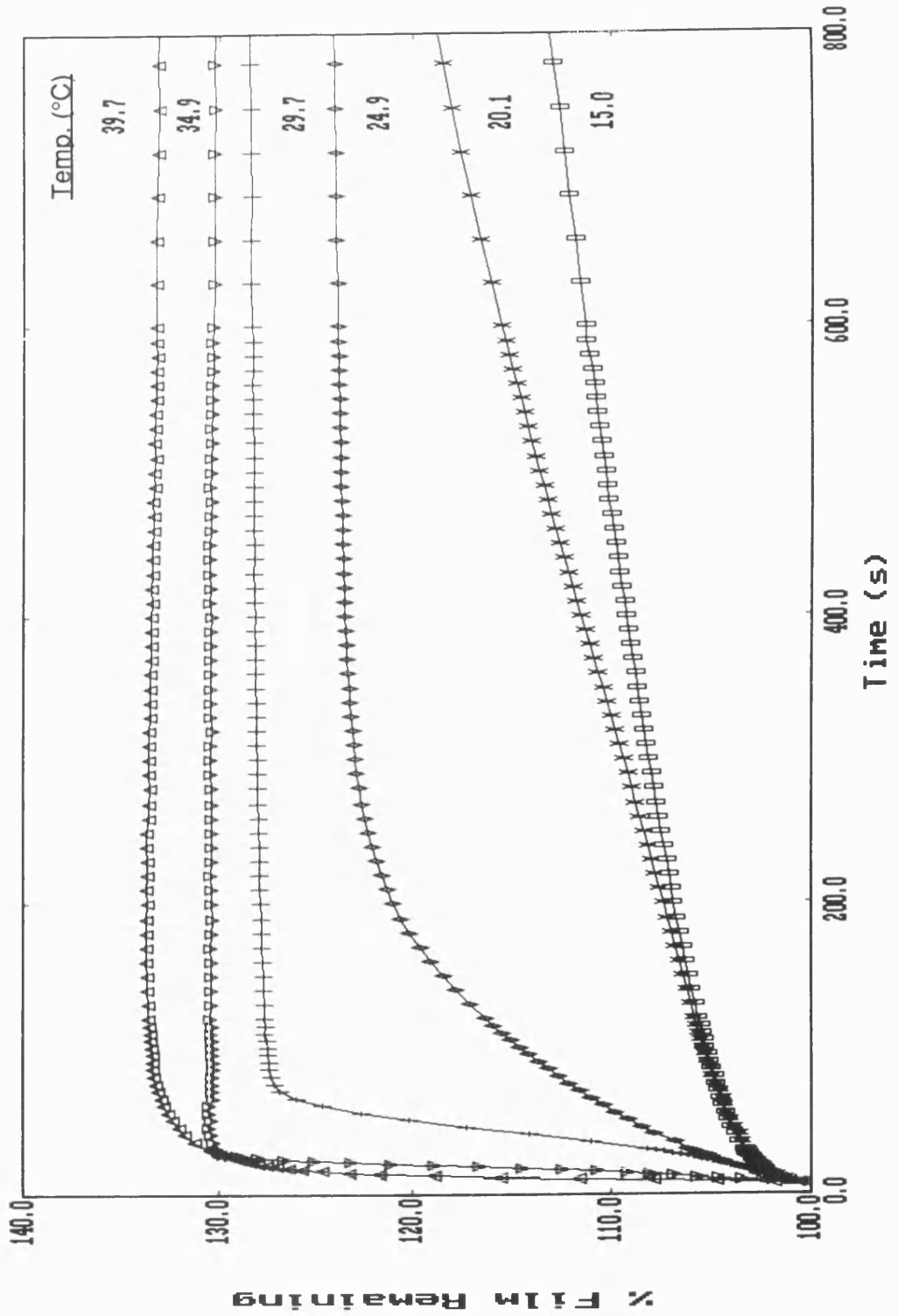

Figure 97: Effect of Temperature on the Swelling of PMMA in Methanol

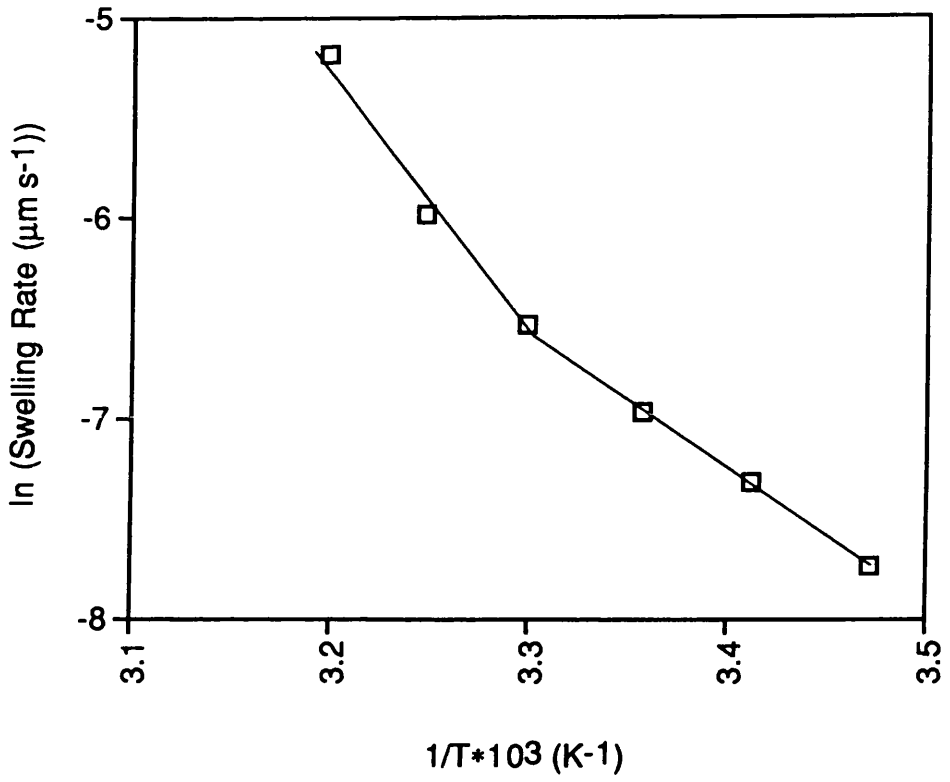

Figure 98: Effect of Temperature on the Swelling of PMMA in Methanol

The transport kinetics of the solvent into the polymer is controlled by both the diffusion of solvent molecules into the polymer and the local relaxation of the polymer segments. The type of diffusional transport observed will be determined by the relative times for diffusion and relaxation. At low temperatures, Case II relaxation controlled transport dominates the overall observed kinetics whilst as the temperature is increased, the diffusion of the penetrant into the relaxing boundary contributes increasingly to the observed swelling kinetics. As the temperature is raised, the completion of sorption lags significantly behind the penetration of the relaxation boundary of the polymer film.

Thomas and Windle[48] observed a change in diffusion kinetics with temperature in their study of the transport kinetics of liquid methanol in 1 - 3 mm thick PMMA sheets over the temperature range 23 - 63°C. At ambient temperature, the absorption of methanol followed Case II kinetics with the methanol penetrating the polymer behind a sharp front which moves at a constant velocity. At higher temperatures, the absorption of methanol increasingly deviated from Case II kinetics with the concentration of methanol at the front and the front velocity decreasing with increasing penetration. The mass absorption kinetics in which the exponent of time is unity for Case II sorption, approaches 0.5 which is indicative of Fickian diffusion. Other workers[194,195] have reported swelling data for sheet PMMA in a series of alcohols. The analysis of the swelling of PMMA in methanol, ethanol, isopropanol and n-propanol at 20 and 45°C corresponded to Case II diffusion[194]. However, the swelling data for PMMA in ethanol and n-propanol between 50 and 95°C showed Case II diffusion near 50°C, but a movement towards Fickian penetration at higher temperatures[195].

Papanu and co-workers[196] have studied the swelling of 1μm PMMA (M_n 180000, γ 2.8) thin films in pure alcohols using ellipsometry. The penetration rate was calculated by dividing the initial film thickness by the time required for the film to swell completely. By comparing the experimental curves with the theoretical curves generated for Fickian and Case II transport models, they predicted that the swelling of wide polydispersity PMMA in methanol at 19°C followed the Fickian model. Based on Thomas and Windle's studies, Case II behaviour would have been expected for this temperature.

Papanu suggested that the difference could be due to a thin film effect, with the observed Fickian behaviour being due to the initial uptake of methanol. With sheet samples, observations are not usually made until the solvent has penetrated the first 1000 nm of the film, so that only the sharp front characteristic of Case II diffusion is observed. With thin films, the initial Fickian uptake could be a major fraction of the overall swelling, and the sharp front would not be established. This thin film effect has been observed with n-alkane swelling of polystyrene[50]. In thin films, the diffusional resistance of the swollen polymer is negligible, and swelling tends to be controlled by solvent penetration at the front. Whilst in thick films, the diffusional resistance of the swollen region increases as the film swells, and Fickian diffusion of solvent between the polymer/solvent interface and the penetrating front may control the swelling kinetics and an apparent shift to Fickian transport can occur[48]. The small molecular size of the penetrant i.e. methanol may also have contributed to this observed Fickian behaviour, as the molecules would have been able to penetrate ahead of the Case II front which would produce a diffuse interface indicative of Fickian diffusion. Peterlin[197] has suggested that in Case II diffusion, a Fickian precursor precedes the penetrating front. Papanu found that as the molecular size of the penetrant increased the diffusion mechanism progressed from Fickian to Case II, as the contribution of the diffusive interface diminished.

Case II penetration was observed for the swelling of PMMA in isopropanol at 50.1°C, and Case II diffusion with overtones of Fickian diffusion was observed for ethanol penetration at 40.8°C. As the temperature was increased from 19.0 to 25.8°C for methanol penetration, a certain degree of Case II diffusion was observed in later stages of the experiment. Therefore a progression from Fickian to Case II swelling was observed with increasing molecular size (and temperature).

In the current work, we have observed a change in diffusion mechanism from Case II to Fickian with increased temperature for the penetration of methanol in PMMA with both the swelling curves and Arrhenius plot indicating a change in mechanism at approximately 30°C. A plot of the final percentage of swelling thickness versus the initial swelling rate also shows a break in linearity at 30°C (Figure 99). In the lower temperature range, the final swelling thickness changes to a much larger extent than the swelling rate, whilst at temperatures above 30°C, the change in swelling thickness begins to parallel the increase in swelling rate. From this analysis, it appears that the solvent penetration is much quicker than the relaxation of the polymer segments in the low temperature region, indicating that polymer relaxation is the rate determining factor (Case II). As the temperature increases, the diffusion mechanism moves towards Fickian with the solvent penetration equalling the rate of polymer relaxation and becoming the rate determining factor.

At higher temperatures, the observed decrease of activation energy for the methanol penetration is indicative of a change of diffusion mechanism. It would be expected that the activation energy would increase as the Case II mechanism became predominant, as the relaxation processes become rate-determining. Our observations and calculated activation energies contradict the predictions made by Papanu and co-workers[196].

Papanu and co-workers suggested that the difference between their experimental results and those of Thomas and Windle could be due to the difference in polymer film thicknesses. However, our experimental technique uses film thicknesses similar to those of Papanu's and yet our results are similar to those observed by Thomas and Windle. Papanu and co-workers used the average swelling rate which does not take into account

any changes in swelling rate during the time scale of the experiment, whilst our method allows us to observe any changes in swelling rate and to measure the initial swelling rate.

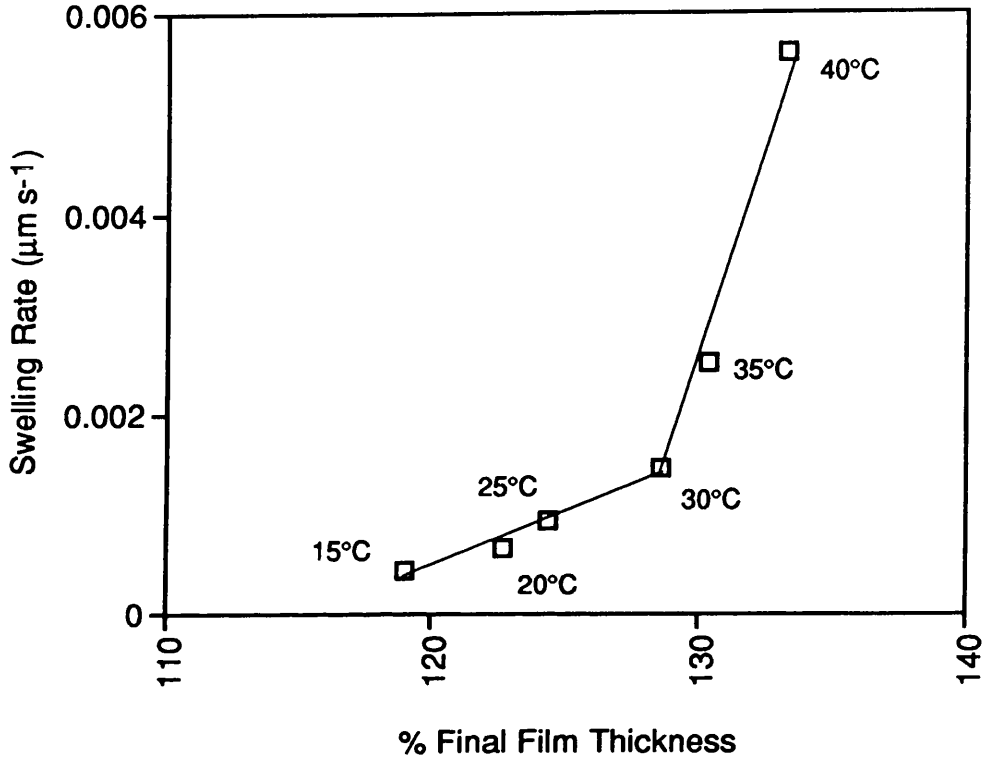

Figure 99: Effect of Temperature on the Film Thickness of PMMA in Methanol

6.3 Dissolution of PMMA in Alkyl Acetate Solvents

A series of quartz crystals were coated with the PMMA standards (M_n 22200 - 330000) and developed in a homologous series of alkyl acetates over the range 15 - 40°C. For each polymer/solvent system studied, the dissolution rates were calculated for each developing temperature and can be found in Appendix 2. Throughout the polymer molecular weight range and alkyl acetate solvent series, the dissolution rate increased with increasing developing temperature. To study the effect of polydispersity on the dissolution of PMMA, the dissolution rates of the wide polydispersity PMMA sample (M_n 56000) in the solvent series has also been measured.

As an illustration of the effects observed with increasing temperature when the solvent size is increased, the dissolution/swelling curves for PMMA (M_n 330000) in the alkyl acetate series are shown in Figures 100 to 105. In methyl acetate, the dissolution of the polymer is very rapid and results in complete removal of the polymer film. The dissolution curves could only be measured at the lower end of the temperature range as at the higher temperature the polymer dissolution was too rapid for accurate determination.

Throughout the solvent series, initial swelling of the polymer is observed and, as expected, the amount of swelling increases with solvent size. Comparison of the curves for n-propyl and isopropyl acetate (Figures 102 and 3 respectively) indicates much faster swelling for the molecule with the smaller cross-section (i.e. n-propyl) with a broad distribution of dissolution rates for the bulkier molecule. For the development time studied, no dissolution of the polymer was observed at the lower development temperatures in n-pentyl acetate.

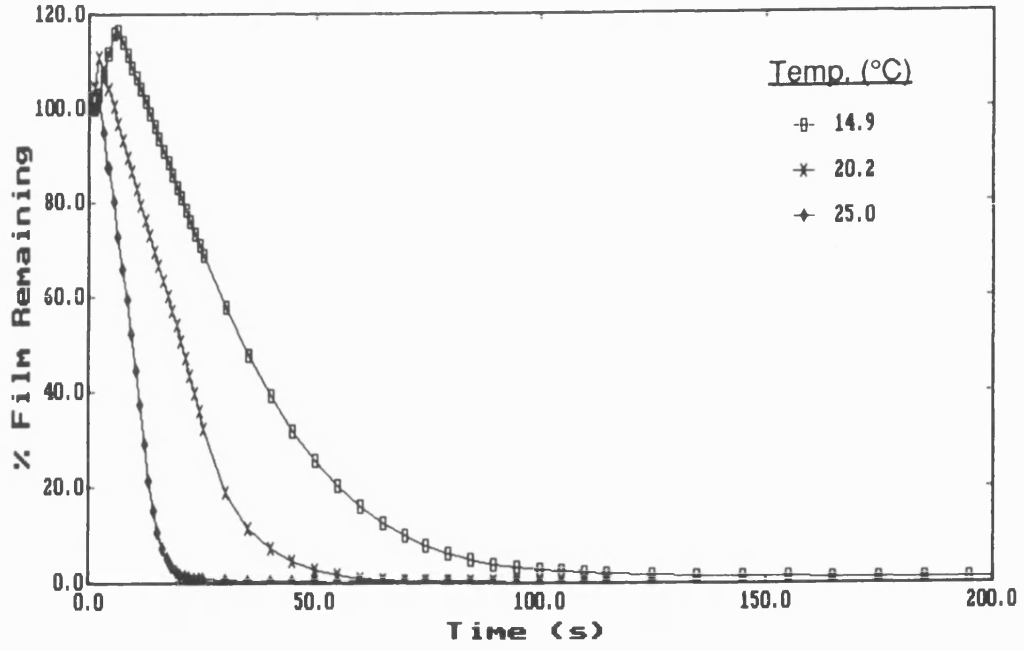

Figure 100: Dissolution of PMMA (M_n 330000) in Methyl Acetate

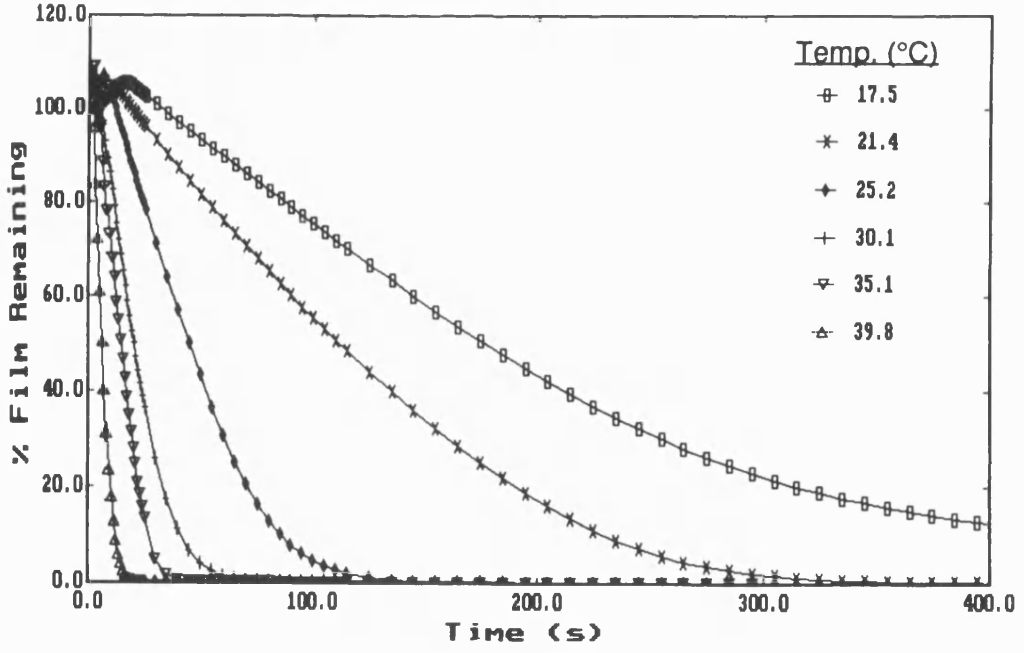

Figure 101: Dissolution of PMMA (M_n 330000) in Ethyl Acetate

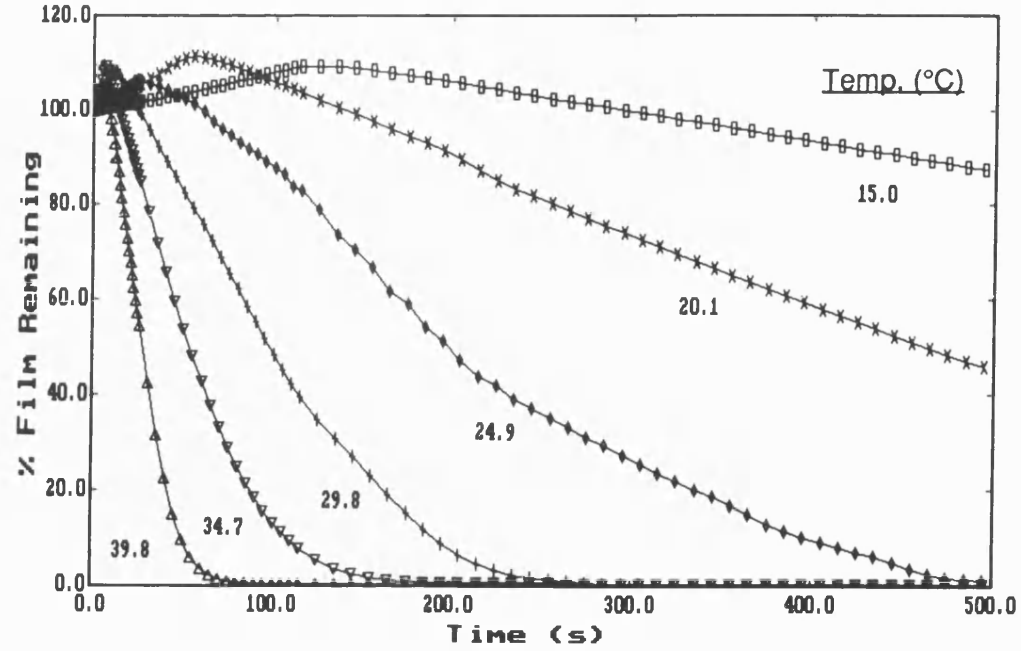

Figure 102: Dissolution of PMMA (M_n 330000) in n-Propyl Acetate

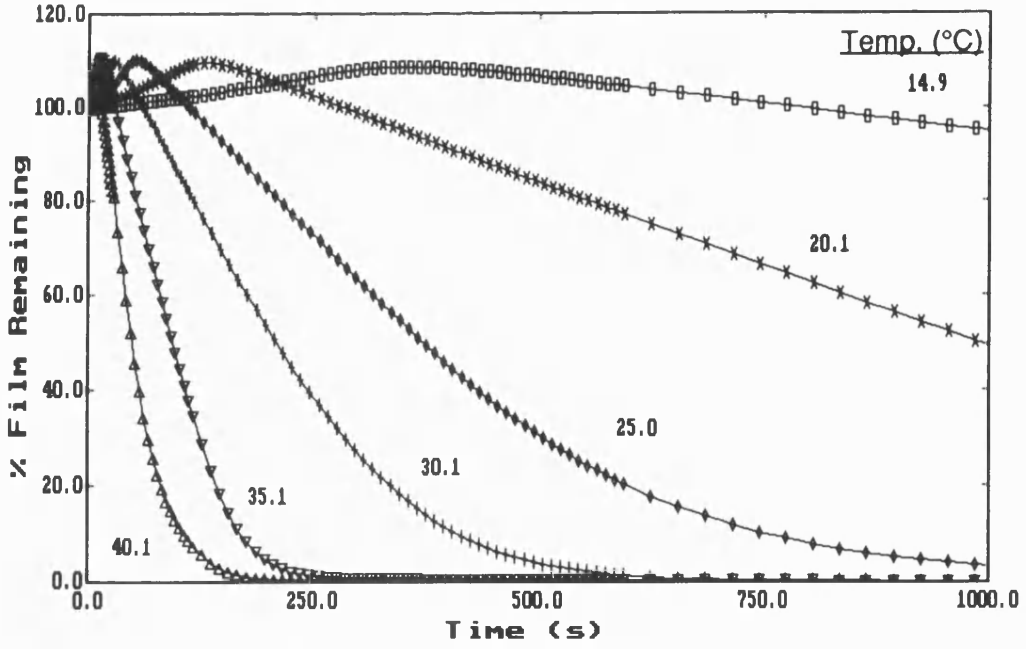

Figure 103: Dissolution of PMMA (M_n 330000) in Isopropyl Acetate

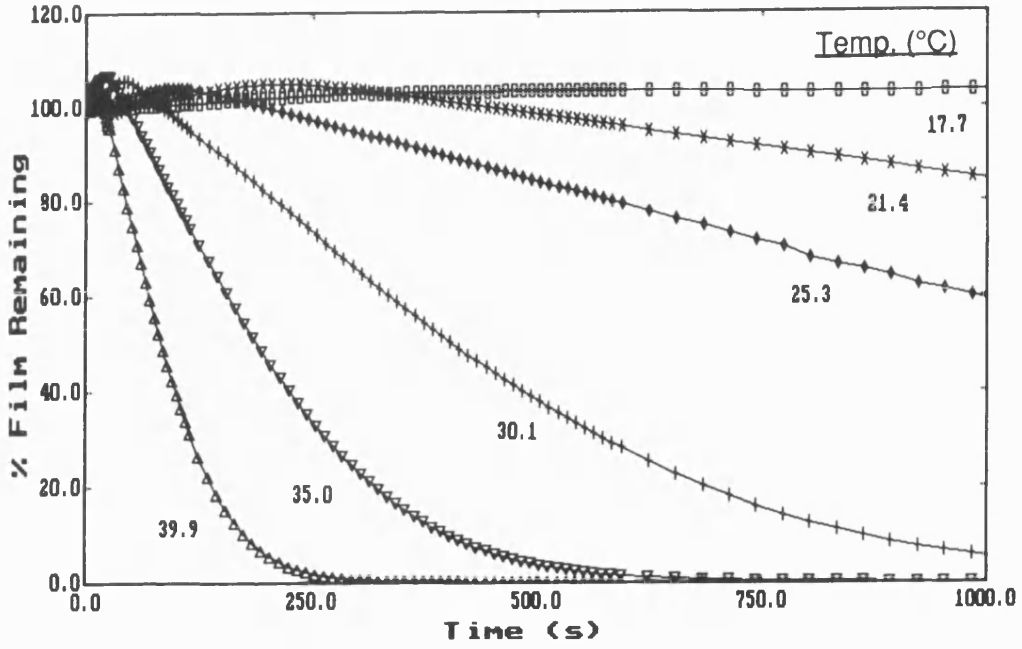

Figure 104: Dissolution of PMMA (M_n 330000) in n-Butyl Acetate

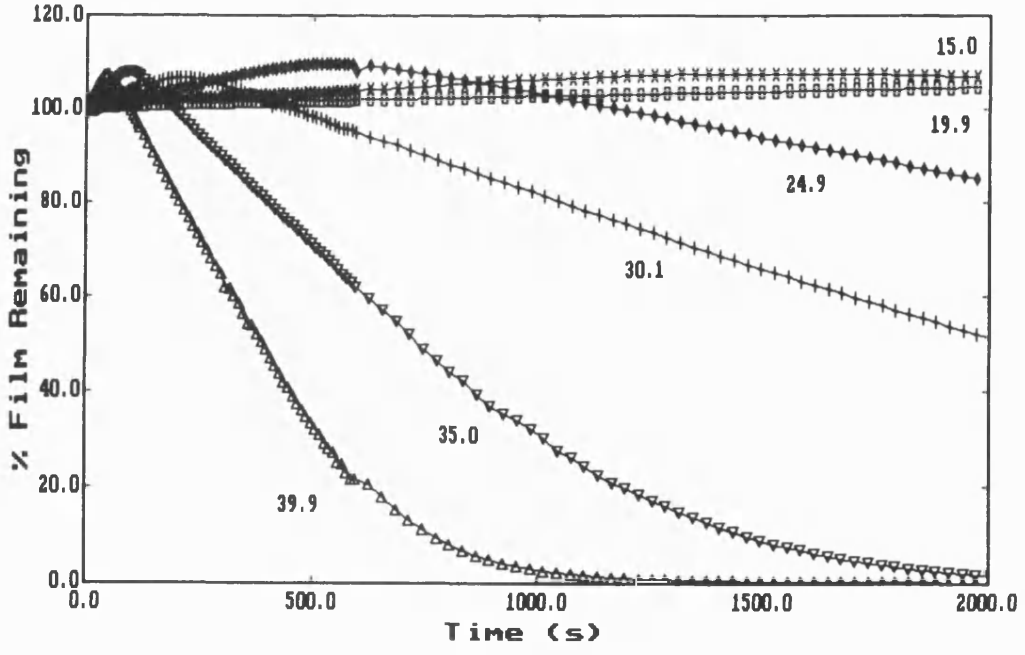

Figure 105: Dissolution of PMMA (M_n 330000) in n-Pentyl acetate

To illustrate the effect of temperature with changing the polymer molecular weight upon the dissolution of PMMA, Figures 103 and 106 to 109 show the dissolution curves for the molecular weight series of PMMA in isopropyl acetate over the temperature range 15 - 40°C. It is clearly shown that the rate of dissolution increases and swelling decreases with increasing temperature throughout the molecular weight series. The dissolution curves for the wide polydispersity PMMA (M_n 56000) are also shown (Figure 110) and it can be clearly seen the percentage of swelling is lower than the corresponding narrow polydispersity sample. As we have observed in the Chapter 5, the lower molecular weight chains in the wide polydispersity sample are initially removed which increase the free volume of the polymer film hence minimising the percentage of swelling observed.

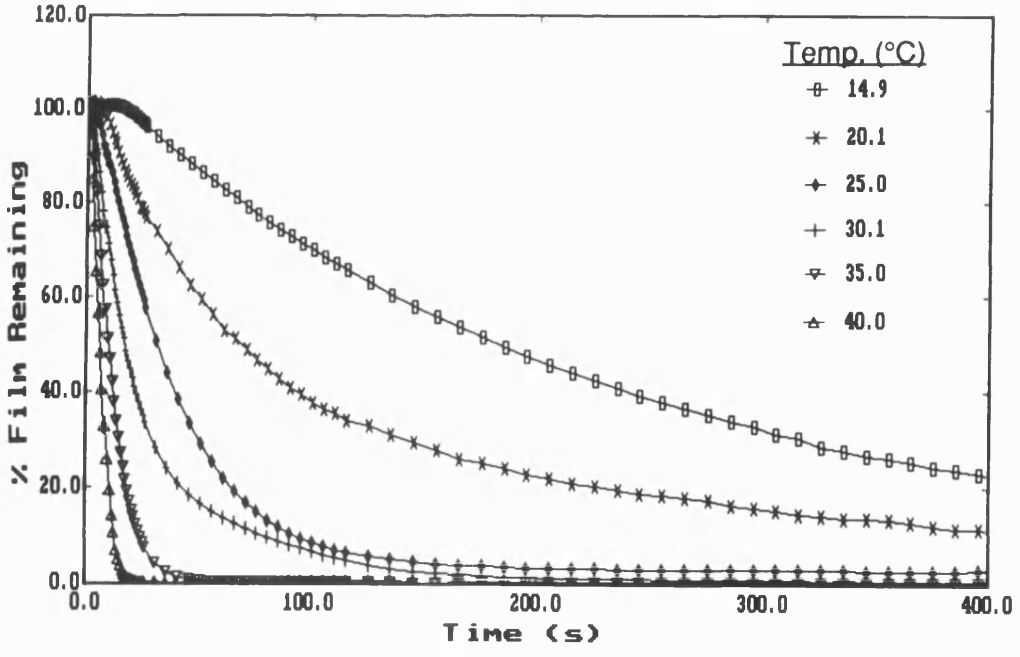

Figure 106: Dissolution of PMMA (M_n 22200) in Isopropyl Acetate

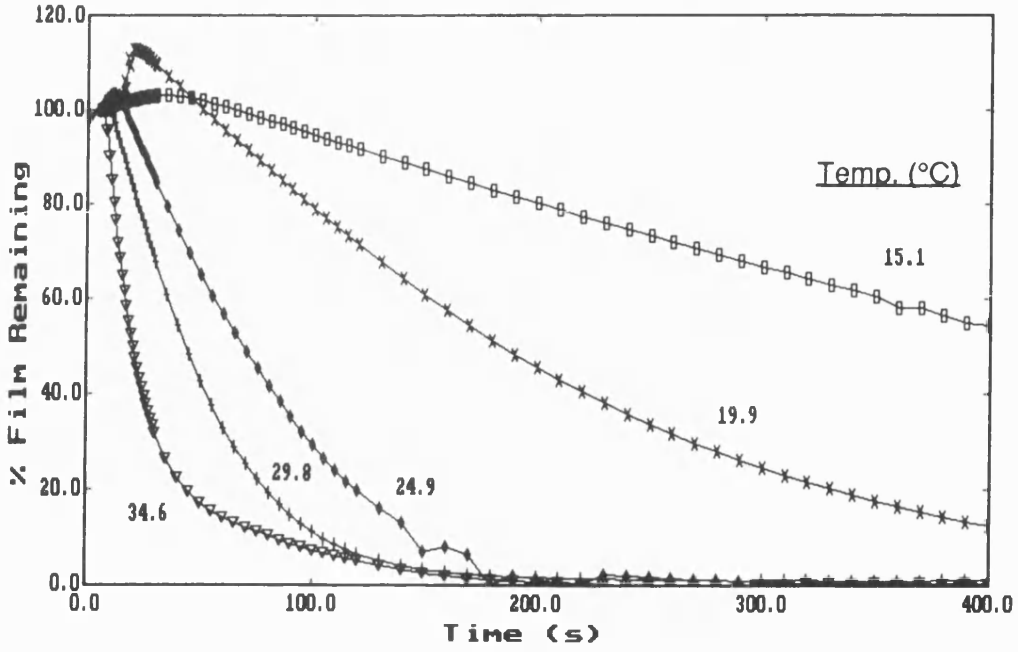

Figure 107: Dissolution of PMMA (M_n 34500) in Isopropyl Acetate

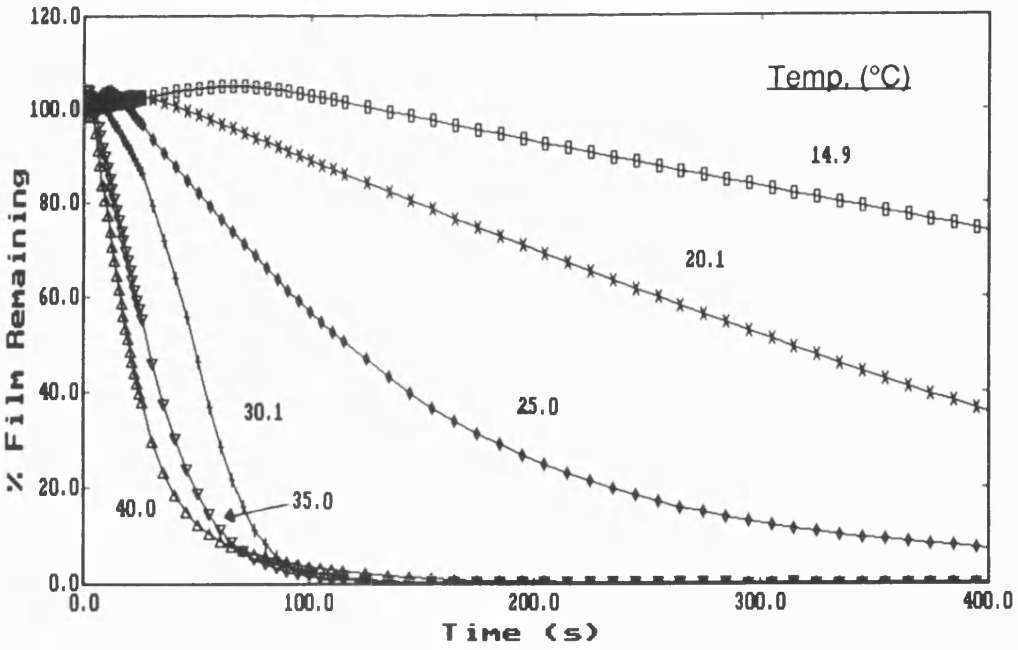

Figure 108: Dissolution of PMMA (M_n 67000) in Isopropyl Acetate

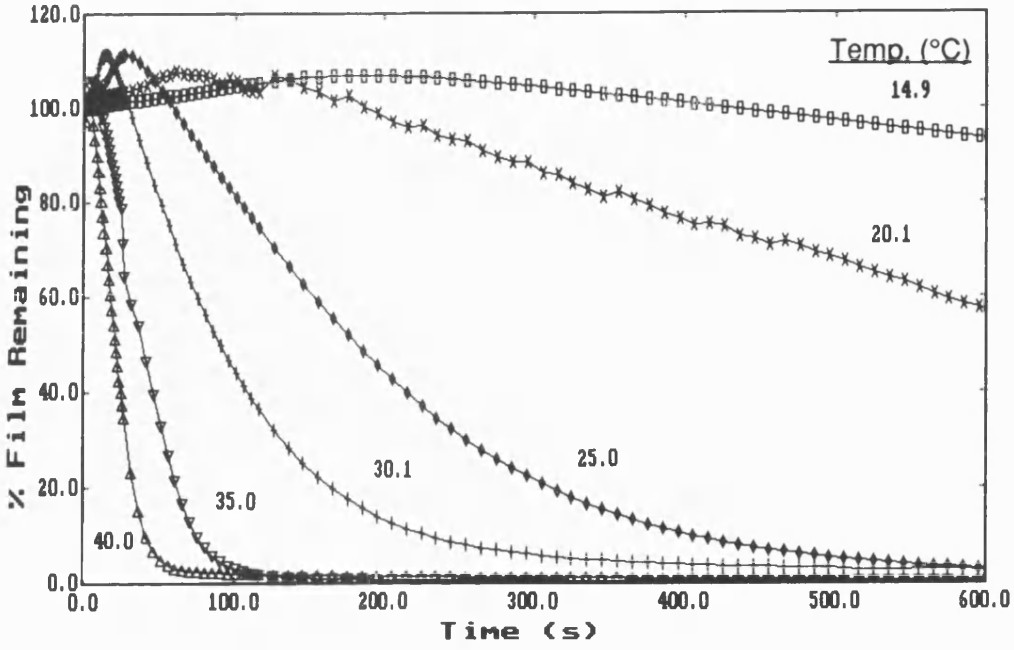

Figure 109: Dissolution of PMMA (M_n 107000) in Isopropyl Acetate

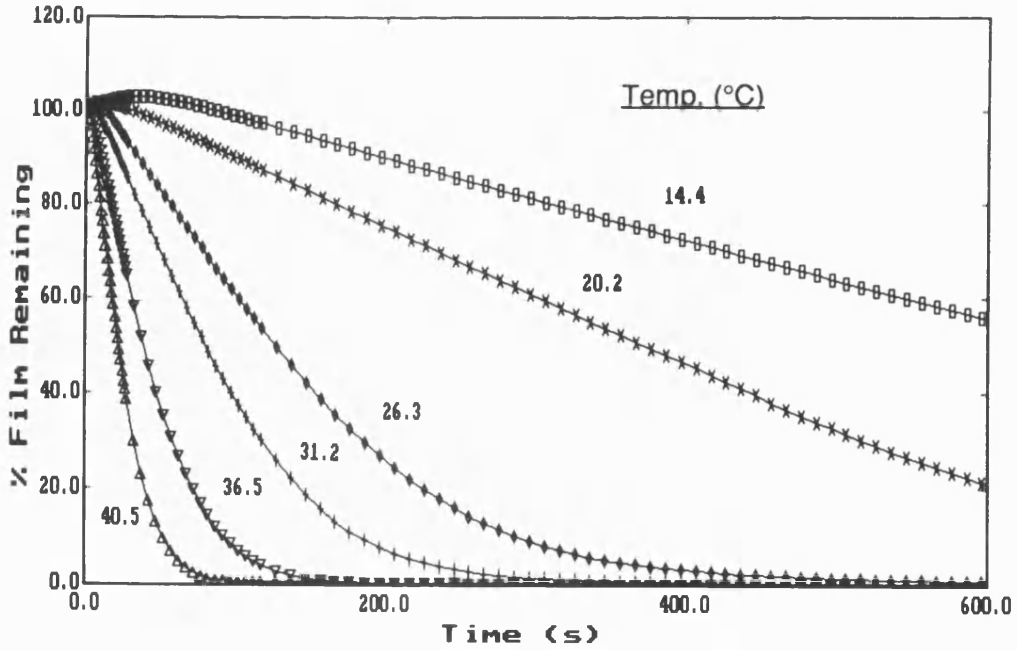

Figure 110: Dissolution of PMMA (M_n 56000) in Isopropyl Acetate

Throughout the range of polymer molecular weight studied, the Arrhenius plots for the dissolution of PMMA in the alkyl acetate series (Figures 111 - 116) show the same linear relationships and a general independence of the slopes with solvent size and molecular weight. Table 8 shows the range of activation energies calculated for the polymer molecular weights studied. The results for dissolution in pentyl acetate indicates the greatest variation in activation energy (121.5 - 148.7 ±1.5 kJ mol^{-1}) increasing with polymer molecular weight and these values have been quoted separately in Table 8. The range of activation energy values observed for the wide distribution PMMA does not differ greatly from that of the standards. The values of activation energy are indicative of a Case II diffusion process.

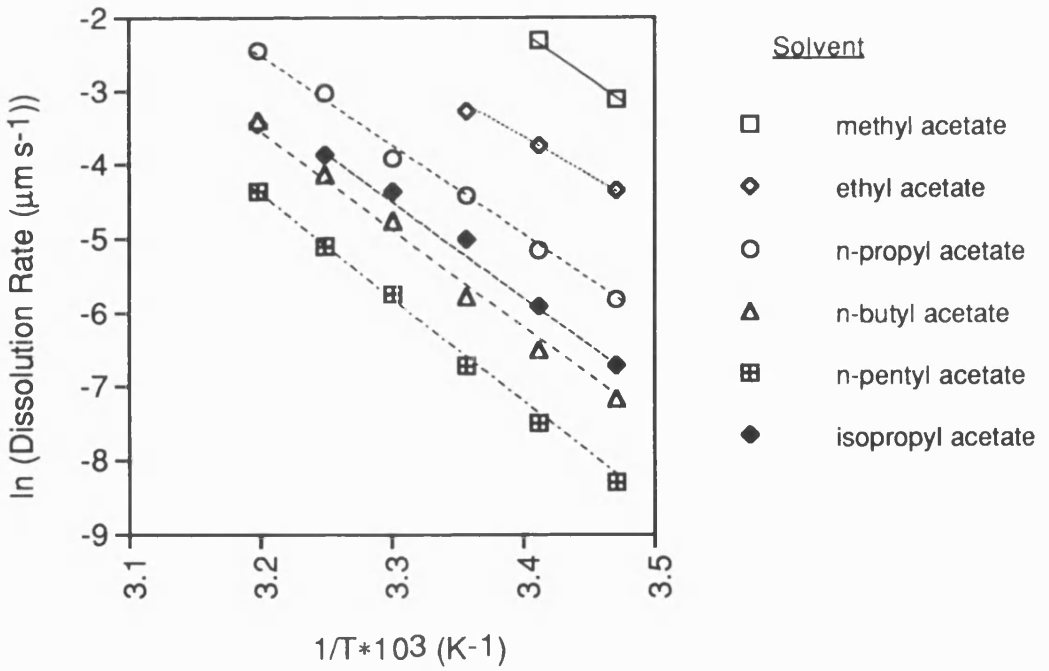

Figure 111: Arrhenius Plots for the Dissolution of PMMA (M_n 22200) in the Alkyl Acetate Series

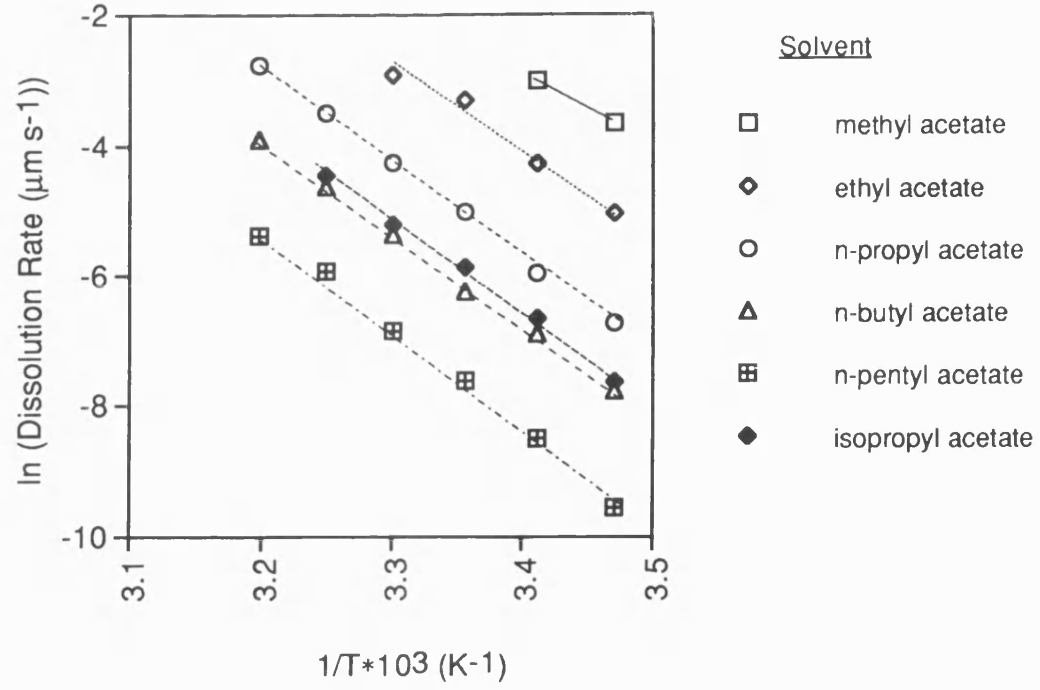

Figure 112: Arrhenius Plots for the Dissolution of PMMA (M_n 34500) in the Alkyl Acetate Series

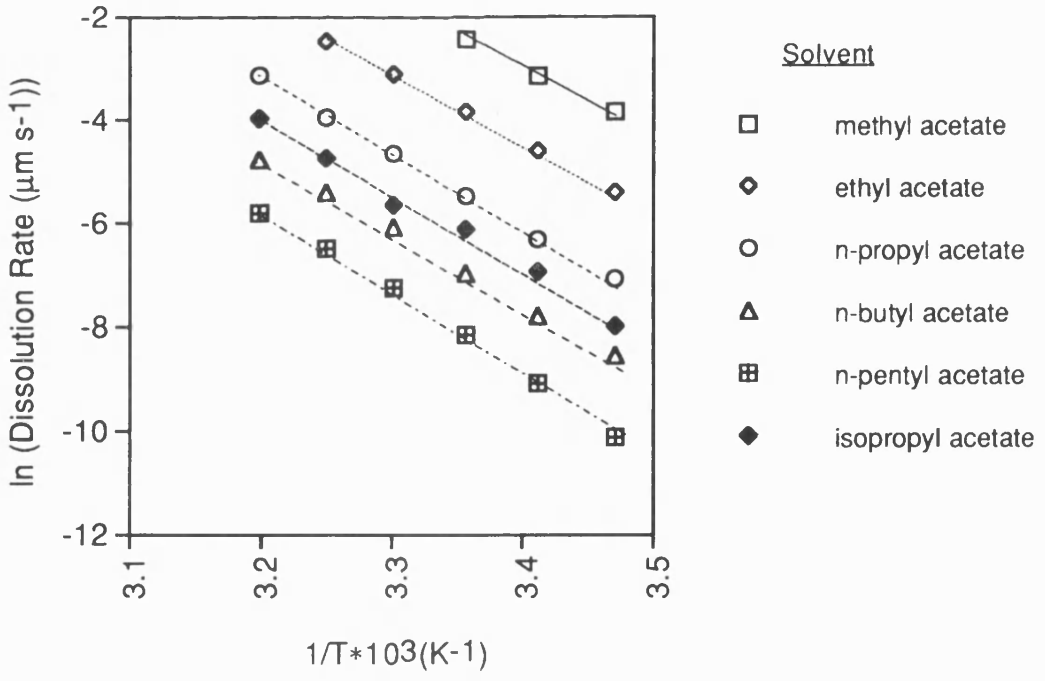

Figure 113: Arrhenius Plots for the Dissolution of PMMA (M_n 67000) in the Alkyl Acetate Series

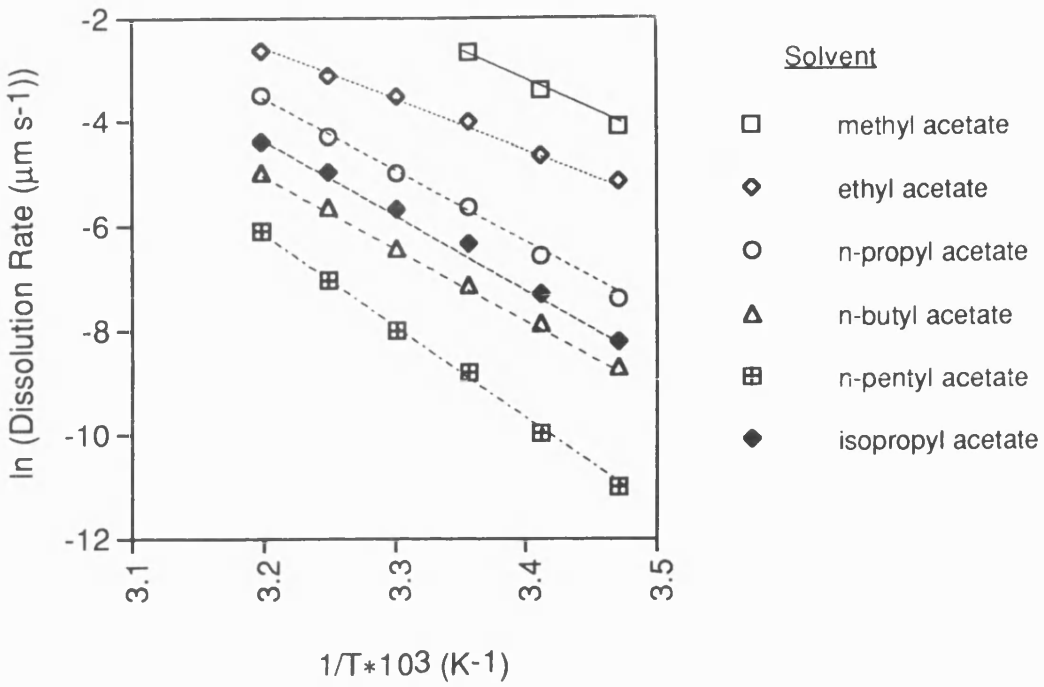

Figure 114: Arrhenius Plots for the Dissolution of PMMA (M_n 107000) in the Alkyl Acetate Series

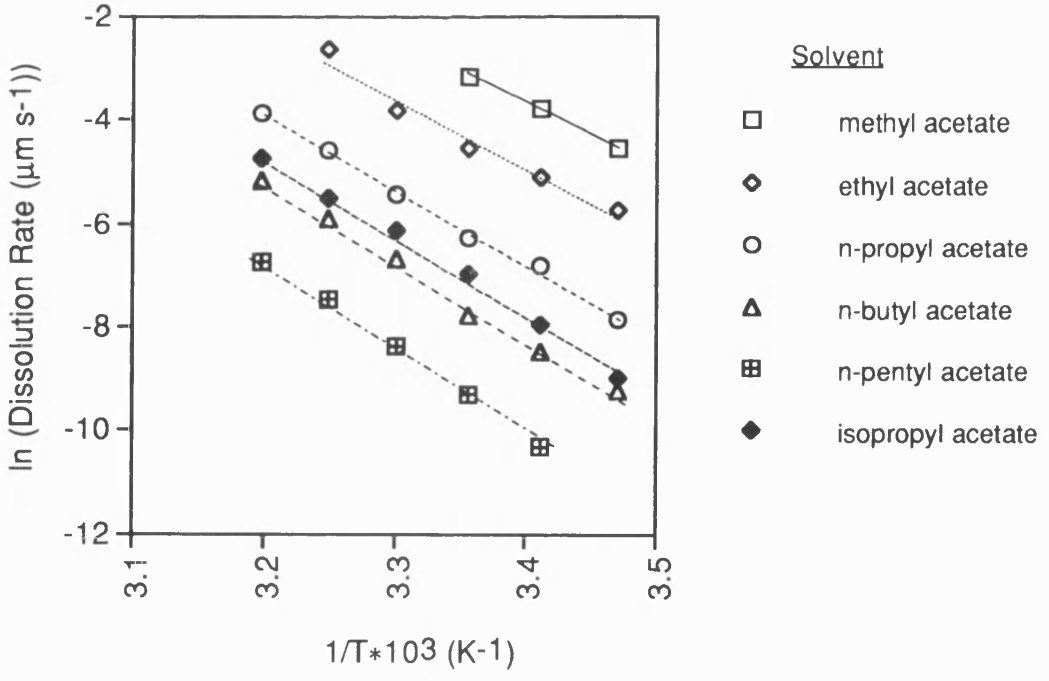

Figure 115: Arrhenius Plots for the Dissolution of PMMA (M_n 330000) in the Alkyl Acetate Series

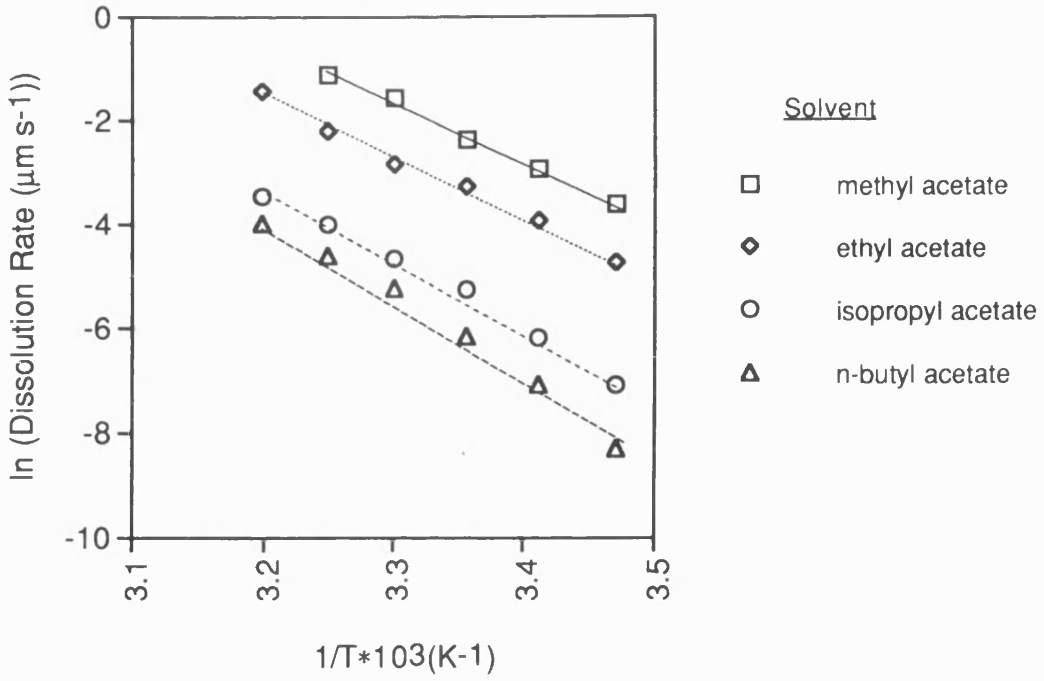

Figure 116: Arrhenius Plots for the Dissolution of PMMA (M_n 56000) in the Alkyl Acetate Series

Polymer M_n	E_a (kJ mol^{-1})	
	Methyl - Propyl	Pentyl
22200	103.1 - 117.3	121.5
34500	108.1 - 117.8	127.9
67000	110.4 - 117.2	131.7
107000	105.2 - 117.1	148.7
330000	111.3 - 127.2	140.3
56000	96.4 - 130.3	

Table 8: Activation Energies Calculated from Figures 111 - 116

The observed increases in the value of activation energy for pentyl acetate could be partly due to experimental error and to the greater percentage of swelling observed at the higher solvent molar volumes.

In their studies of PMMA/alkyl acetate solvent systems, Ouano[40,191,198] and Gipstein[57] found a break in the solubility rate/solvent molar volume relationship between butyl and propyl acetate for the PMMA molecular weights (M_W) of 94000 and 476000. They attributed this break in linearity to a change in diffusion mechanism, however, the experimental method used ("Dip and Dry") does not enable the measurement of the swelling of the polymer film which we have shown to occur at the higher solvent molar volumes. In Chapter 7, a more thorough comparison between our experimental and literature results and the thermodynamic data obtained in Chapter 4, has been made.

6.4 Conclusion

The solvent temperature has been found to be of great importance to the dissolution process with generally faster dissolution observed at higher temperatures. A range of swelling and dissolution kinetics have been observed for a series of PMMA/solvent systems.

By the measurement of the dissolution of PMMA in MEK, it has been shown that the diffusion process is controlled by the relaxation of the polymer (Case II). The activation energy has been shown to be susceptible to polymer molecular weight until a limiting molecular weight of 107000 is reached. Throughout a range of polymer molecular weight and alkyl acetate solvent series, the dissolution rate of PMMA has been shown to increase with increasing developing temperature.

By the monitoring of the swelling curves and Arrhenius plot for the swelling of PMMA in methanol, a change in diffusion kinetics with temperature has been observed. Below 30°C, the Case II diffusion process dominates the swelling kinetics whilst at higher temperatures, the Fickian process predominates.

It has been clearly shown that the developing temperature will greatly determine the possible resolution of a resist. In Chapter 9, these studies have been continued to other resist systems.

Chapter Seven

7.0 Effect of Solvent Composition on PMMA Dissolution

The role of the solvent composition during resist development must be considered as the developer can have a great effect on the swelling and dissolution kinetics of the polymer film, and subsequently the overall resolution of the resist. At present, developers tend to be chosen empirically on the basis of molecular size, polarity, surface tension or surface reactivity but our aim was to make a more quantitative assessment of the factors involved in order to assist developer selection.

During the development process, solvent penetration and resist dissolution are controlled by both kinetic and thermodynamic polymer/solvent interactions. The kinetic polymer/solvent interaction tends to be influenced by the solvent molecular size, whereas the strength of the interactions between the structural groups of the polymer and solvent molecules primarily influence the thermodynamic compatibility[63]. Thermodynamic effects can be inferred from equilibrium behaviour, by the degree of swelling and polymer/solvent solubility (see Chapter 4). Kinetic effects can be determined by dissolution and penetration rate measurements.

To gain an understanding of the various roles of solvent quality in solvent composition during the development of resist systems, the dissolution rate of PMMA in solvent/non-solvent mixtures has been measured. These studies have been further extended to include the effect of solvent molar volume on the dissolution kinetics of the polymer.

7.1 Effect of Alcohols on the Dissolution of PMMA in MEK

Most photoresist processing is not carried out in pure solvents but in a mixture of a good solvent with a moderating non-solvent, and PMMA is typically developed in ketone/alcohol mixtures[13]. Ketones are good solvents whilst alcohols tend to be poor solvents for PMMA usually swelling the polymer. Therefore, the alcohol moderates the dissolution rate and inhibits dissolution of the unexposed regions, allowing better process control which enhances the contrast of the resist.

7.1.1 Dissolution of PMMA in MEK/IPA Mixtures

The effect of added alcohol to MEK on the dissolution characteristics of PMMA in MEK can clearly be seen in Figure 117. This shows results at 25°C for the development of wide polydispersity PMMA in pure MEK, pure IPA and six mixtures of varied composition. The pure solvent (i.e. MEK) gives rapid and complete dissolution of PMMA within 50 s, whilst development in pure non-solvent (i.e. IPA) shows no dissolution and slight swelling of the polymer film. The solvent/non-solvent mixtures give dissolution rates intermediate between those of the single components. Figure 118 shows a plot of dissolution rate versus composition for the dissolution of the wide polydispersity sample and for a PMMA standard (M_n 107000, γ 1.10). The decrease in dissolution rate is proportional to the amount of non-solvent added until only swelling of the film is observed. Our thermodynamic studies in Chapter 4 for the IPA/PMMA system have shown that the value of the Flory-Huggins interaction parameter increases with solvent fraction indicating the reduced polymer/solvent interaction.

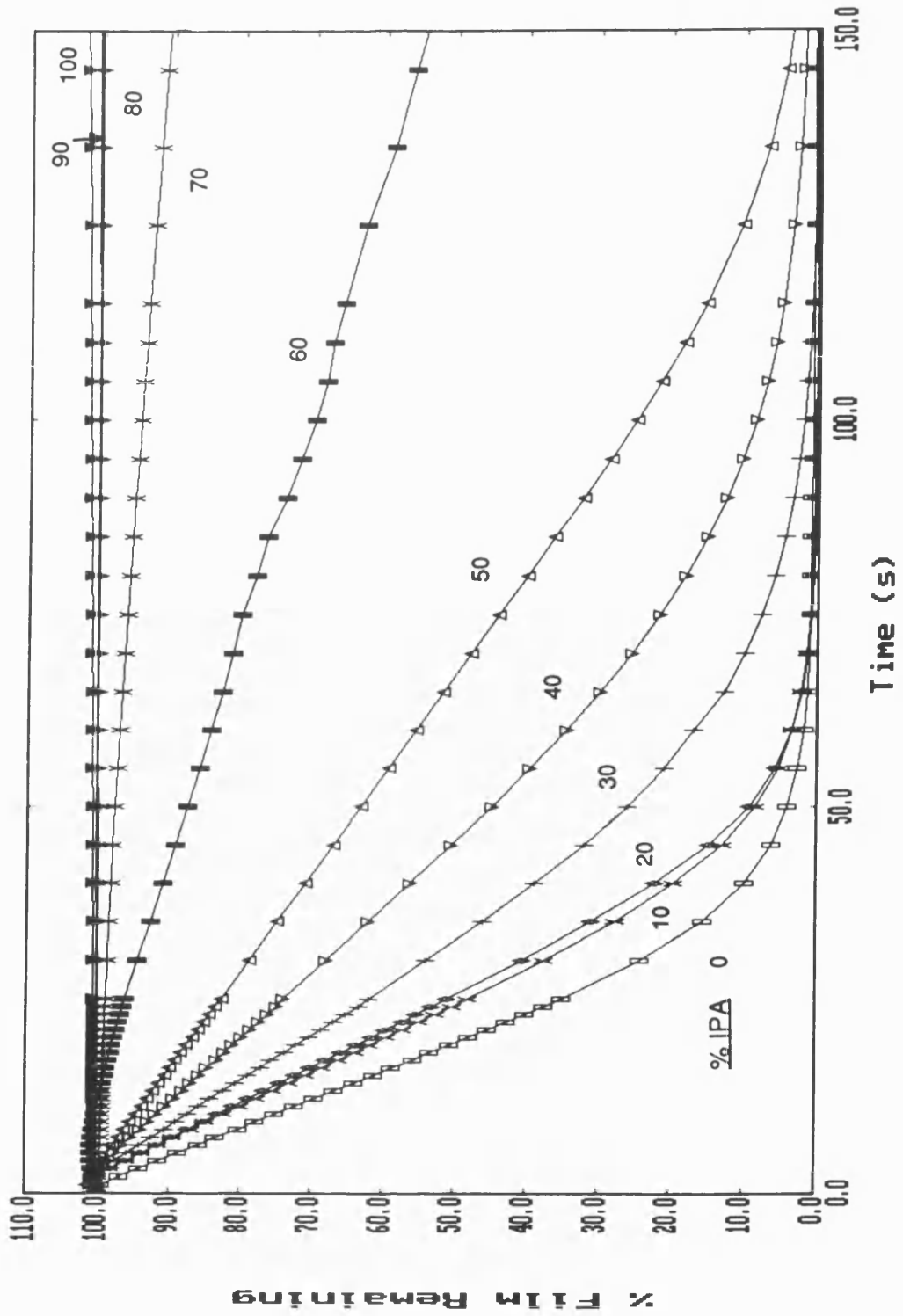

Figure 117: Effect of Isopropanol on the Dissolution of PMMA in MEK at 25°C

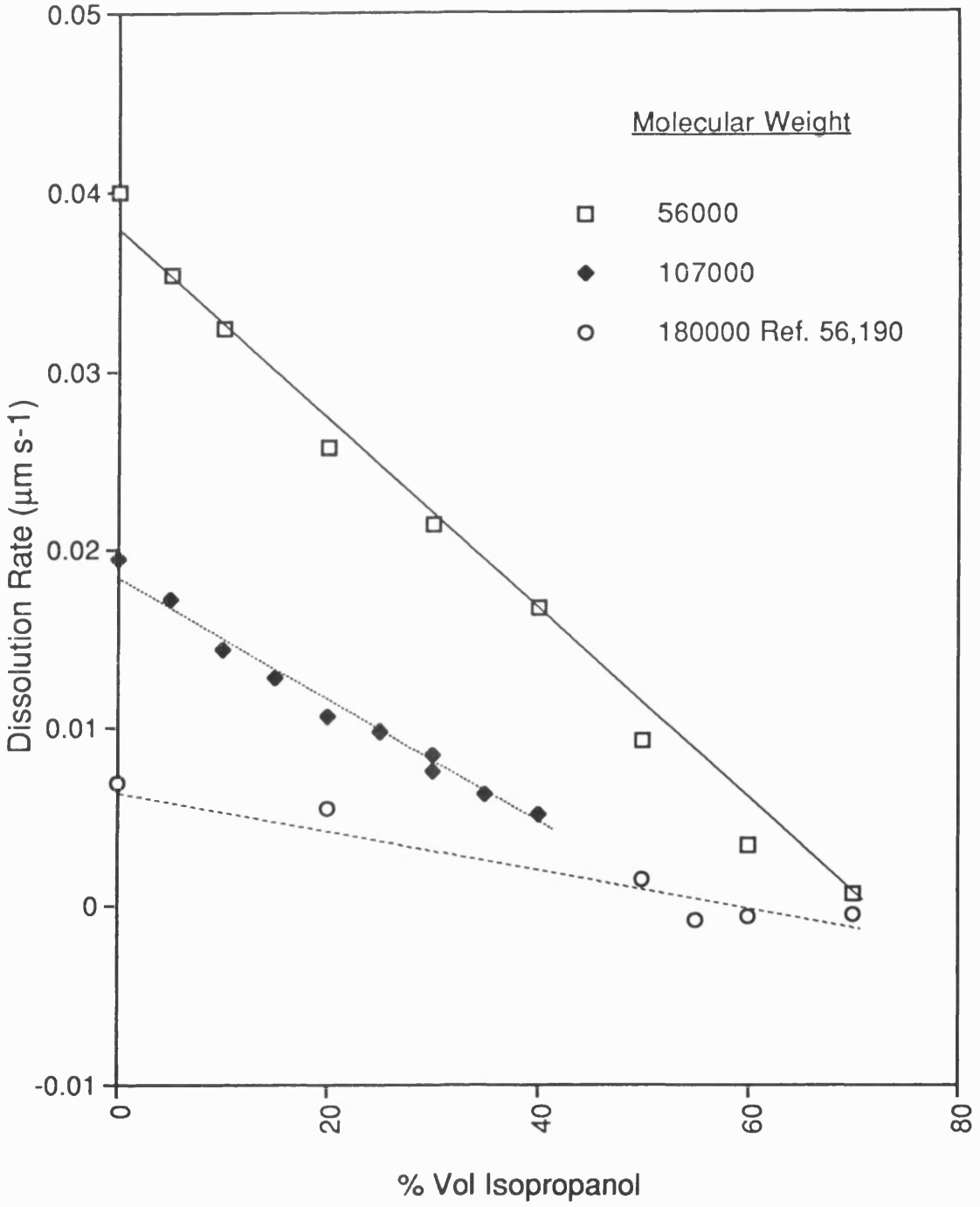

Figure 118: Effect of Isopropanol on the Dissolution of PMMA in MEK at 25°C

Papanu and co-workers[56,190] have studied the swelling and dissolution of thin PMMA films in MEK/IPA mixture using *in situ* ellipsometry. They found that for a 1.2 μm PMMA film (M_W 180000, γ 2.8) developed in 40:60 v/v MEK/IPA at 24.8°C, less than 2% of the polymer dissolved, whilst in 80:20 v/v MEK/IPA, the sample dissolved in about 4 minutes with negligible swelling. They suggested that a narrow transition range (NTR) between dissolution and penetration occurred from 45:55 to 50:50 v/v MEK/IPA. We have observed the initial occurrence of swelling (i.e. increased weight) of the PMMA (M_n 56000, γ 2.0) film between 30:70 and 20:80 v/v MEK/IPA corresponding to the NTR observed by Papanu. The appearance of the swelling in our systems is observed at a higher concentration of non-solvent, which is probably due to the lower molecular weight of our sample.

We have previously shown that the rate of polymer dissolution increases with decreasing molecular weight (see Chapter 5), and Lai and Shepherd[53] have also shown that the width and position of the NTR would be expected to be functions of both temperature and polymer molecular weight. The results of Papanu have been plotted in Figure 118, and the decrease in dissolution rate is also found to be proportional to the amount of isopropanol present. The gradients of the lines increase with decreasing molecular weight (i.e. dissolution rate decreases in similar proportions irrespective of molecular weight.)

Manjkow and co-workers[65] showed by comparison of predicted with experimental dissolution data, that the diffusion of the solvent/non-solvent (i.e. MEK/IPA) into the polymer is characteristic of Case II diffusion (i.e. the diffusion is characterised by a front of constant penetrant composition that

enters the polymer at a constant rate). For non-solvent penetration, concentration in the solvent swollen layer remains constant and the mass uptake is linear with time[46]. In strong solvents, the gel layer dissolves into the solvent and its thickness is not detectable which gives rise to a constant dissolution rate[67]. Manjkow has suggested that no dissolution of PMMA occurs until the NTR is reached, where the dissolution rises rapidly to equal the penetration rate.

With our experimental technique, we have been able to demonstrate that both initial swelling and overall dissolution of the polymer film can be detected at intermediate MEK/IPA concentrations.

7.1.2 Effect of Alcohol Molar Volume on the Dissolution of PMMA

Many workers have assumed that the properties of mixed solvent systems would be the average of those of the single components, however, this is not always the case. Alcohols are non-solvents for PMMA and when added to a solvent they would be expected to decelerate the dissolution of the polymer. This has been shown in Section 7.1.1, where the addition of IPA (2-propanol) to the solvent, MEK, decelerates the rate of dissolution. However, it has been found that the addition of some of the lower alcohols to MEK actually accelerates the dissolution of PMMA.

Figure 119 shows the results for the dissolution of the wide polydispersity PMMA (M_n 56000, γ 2.0) in a series of MEK/alcohol mixtures at 25°C.

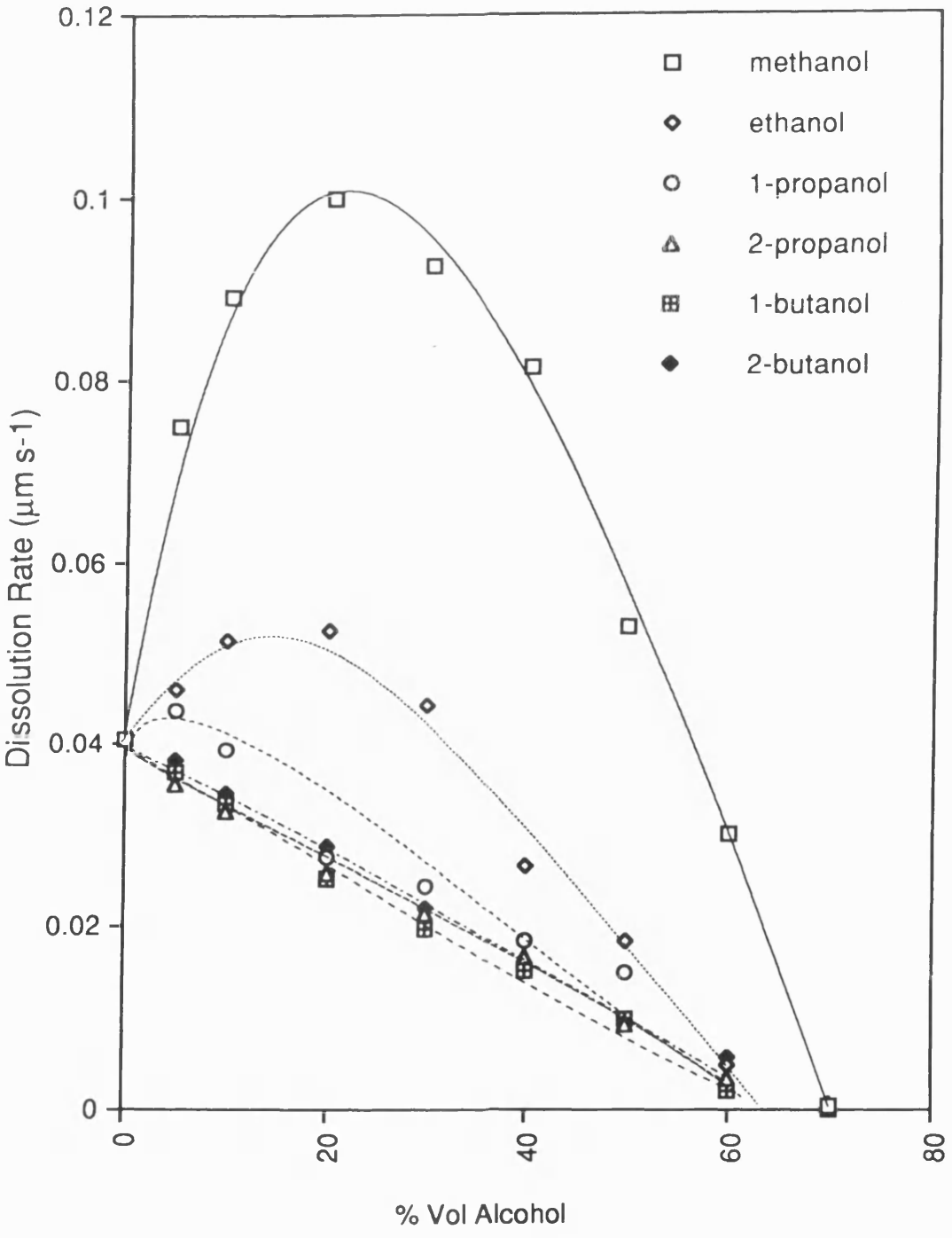

Figure 119: Effect of Alcohol on the Dissolution of PMMA in MEK at 25°C

The addition of the higher alcohols (2-propanol, 1-butanol and 2-butanol) to MEK showed the expected decrease in dissolution rate with little difference in dissolution rates as indicated by the similar slopes. However, the addition of ethanol showed an increase in dissolution rate, whilst methanol showed the greatest enhancement with 150% increase in dissolution rate at a concentration of 20%.

Cooper and co-workers[66] also demonstrated this phenomenon for methanol and ethanol with PMMA (M_n 320000, γ 1.6) at 27.5°C. They observed a doubling of the dissolution rate by the presence of 20% methanol in the MEK, wheras ethanol showed a maximum increase in dissolution rate of only about 12%. We therefore found a greater enhancement in dissolution rate for our PMMA sample. This difference could be due to the molecular weights of the PMMA samples (M_n 56000 and 320000, respectively) and their polydispersities.

The effect of added alcohol on the dissolution of narrow polydispersity PMMA samples at M_n 67000, 107000 and 330000 has been studied, and the dissolution rates and the maximum enhancement of these rates are shown in Figure 120 and Table 9 respectively.

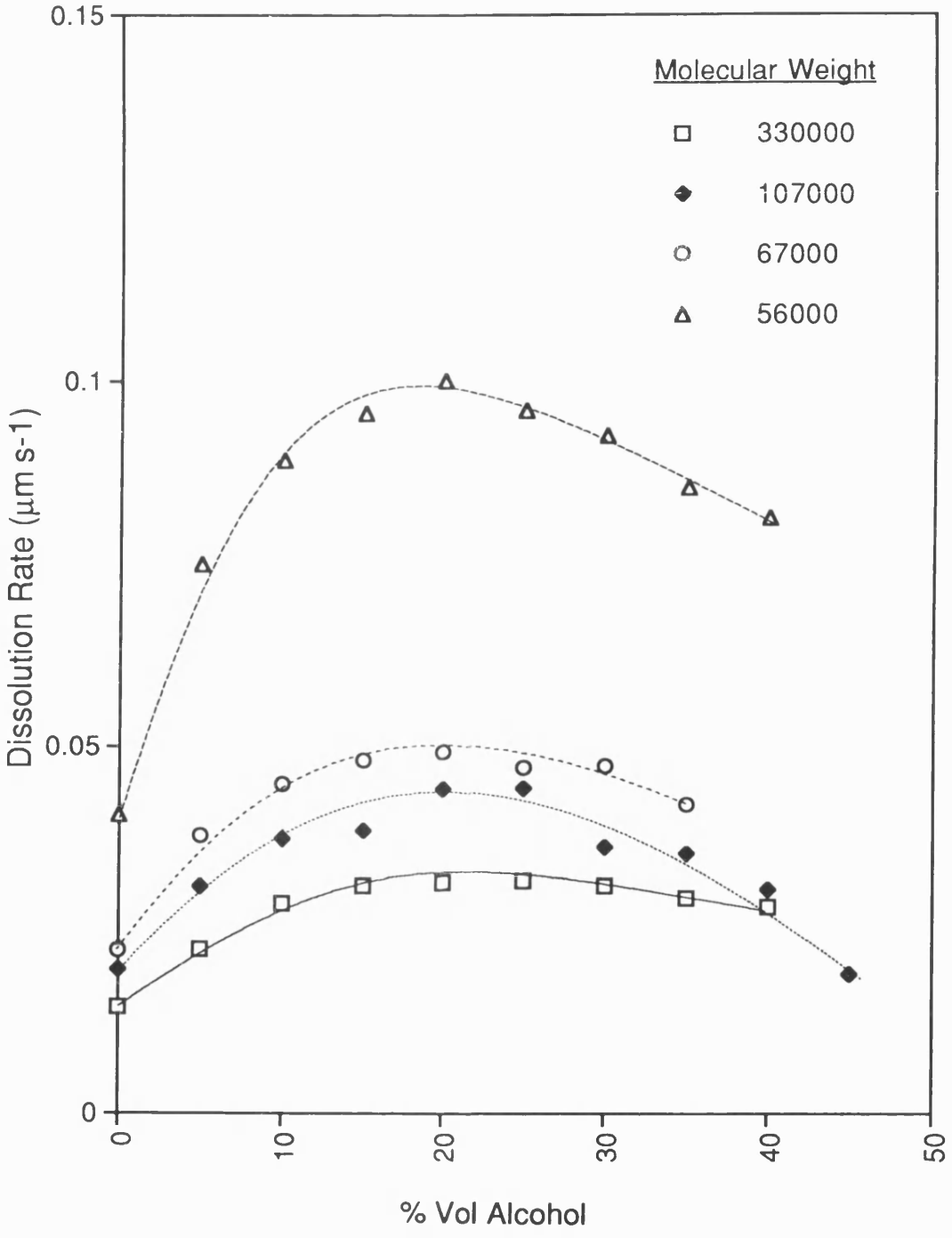

Figure 120: Effect of Methanol on the Dissolution of PMMA (M_n 56000 - 330000) in MEK at 25°C

Throughout the molecular weight range studied, the maximum enhancement was observed at 20% methanol. As expected an overall increase in the dissolution of the polymer was observed with decreasing molecular weight. It can be seen from Figure 120, that for the narrow polydispersity samples there is no significant difference in the maximum enhancement of the dissolution rate. However, there is a notable difference in the dissolution characteristics between the wide and narrow polydispersity PMMA samples.

Polymer M_n	γ	Maximum % Enhancement	% Alcohol
Addition of Methanol			
56000	2.0	147	20
67000	1.04	124	20
107000	1.10	127	20/25
330000	1.11	118	20/25
Addition of Ethanol			
56000	2.0	30	20
107000	1.10	18	10

Table 9: Effect of Alcohol on the Dissolution of PMMA in MEK at 25°C

The dissolution rate for PMMA (M_n 56000, γ 2.0) in MEK is double that obtained for the higher molecular weight PMMA (M_n 67000, γ 1.04) sample, and this is a greater difference in dissolution rate than would be expected when the molecular weight of the samples is considered. As indicated by Table 9, a much greater enhancement in dissolution rate upon

addition is observed for the wide polydispersity sample. This can again be seen when comparing the dissolution data of the wide polydispersity sample with that of M_n 107000 for the ethanol and 2-propanol addition (see Figure 121).

A maximum dissolution rate enhancement of 18% for the addition of ethanol was observed for the narrow polydispersity sample compared to a 30% enhancement for PMMA (M_n 56000, γ 2.0). No enhancement was observed for the addition of 2-propanol on the dissolution rate of PMMA (M_n 107000, γ 1.11).

Papanu and co-workers[56] have studied the effect of adding methanol to MIBK on the dissolution rate of PMMA at 24.8°C. They found for PMMA (M_n 180000, γ 2.8) that the penetration rate of methanol into the polymer is appreciable. The dissolution and penetration rates reached a maximum at about 75% MIBK (synergistic effect), with pure solvent actually yielding the slowest penetration rate.

Rodriguez and Greole[67] have also observed the enhancement of penetration rates due to the presence of kinetically mobile species. Water and methanol having an analogous effect on polystyrene dissolving in MIBK but to a lesser extent than with PMMA.

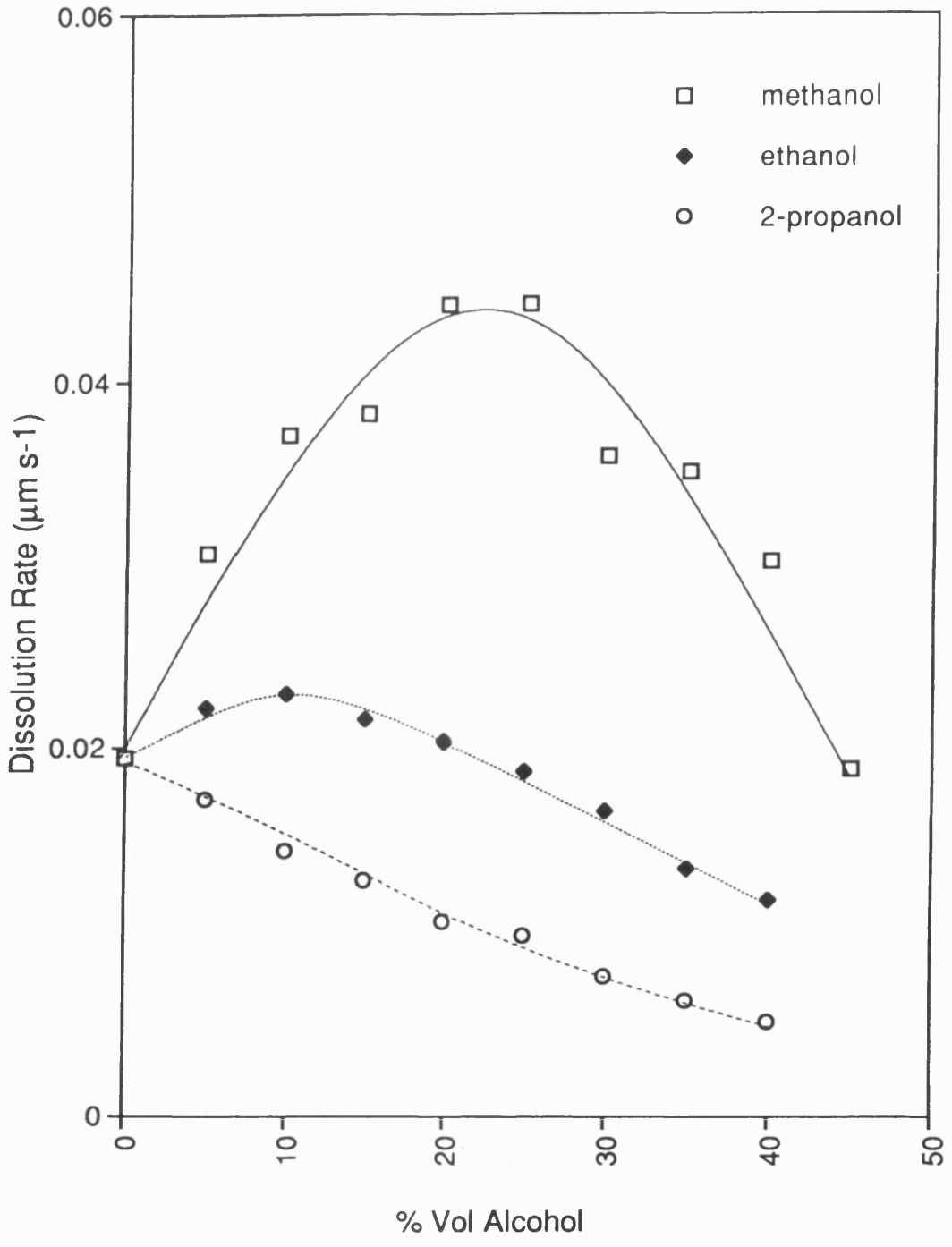

Figure 121: Effect of Alcohol on the Dissolution of PMMA (M_n 107000) in MEK at 25°C

In Chapter 4, we have measured the Flory-Huggins interaction parameters for the methanol, ethanol and isopropanol/PMMA systems at 30°C (Section 4.4.2.1). For isopropanol, the value of χ was found to increase linearly with the solvent fraction whilst the methanol system showed different thermodynamic behaviour with a steep increase in χ (i.e. reduced polymer/solvent interactions) at very low solvent fraction values (< 0.02) followed by a decrease in χ values (i.e. enhanced polymer/solvent interactions) with further increases in solvent volume fraction. The ethanol system showed thermodynamic behaviour intermediate of that of methanol and isopropanol. For all three solvents, the high value of χ indicates that they are poor solvents.

This thermodynamic behaviour correlates well with the observed dissolution kinetics. The addition of isopropanol to MEK has been shown to decrease the dissolution of PMMA and as Figure 70 indicates, the interaction between IPA and PMMA decreases with increasing solvent fraction throughout the solvent concentration range measured. The addition of methanol has enhanced the dissolution rates and this enhancement has been ascribed to the ease of diffusivity of the small molecular size of methanol. Observation of Figure 70 shows that the thermodynamic parameter for methanol/PMMA is seen to decrease with solvent fraction (i.e. enhanced interaction) between solvent and polymer, and it is therefore apparent that both diffusional (i.e. solvent size) and thermodynamic interactions are influencing the dissolution kinetics observed. As we have shown in Figure 70 , a higher value of solvent fraction is reached before ethanol shows an increase in polymer/solvent interaction and hence although the size of ethanol is sufficiently small to easily enter the PMMA

structure, the thermodynamic interaction will not be as great a contributory factor as in the case of methanol.

Cooper and co-workers[66] have tried to rationalise this dissolution behaviour by considering the contrasting dependence of thermodynamic interaction and diffusion on various molecular parameters. The overall solubility parameter of the components can be used to study the thermodynamic interactions of the components. The solubility parameters of a selection of solvents can be seen in Table 10.

Solvent	Molar Volume[199] ($cm^3\ mol^{-1}$)	Solubility Parameter[64] ($[MPa]^{1/2}$)
MEK	90.1	19.0
MIBK	125.8	17.0
Methanol	40.7	29.7
Ethanol	58.5	26.1
1-Propanol	77.5	24.9
2-Propanol	79.4	23.4
1-Butanol	91.8	28.7
2-Butanol	92.2	22.7
Water	18.0	47.8

Table 10: Molar Volumes and Solubility Parameters of a Series of Solvents at 25°C

It can be seen that there is a large difference in the value of solubility parameter between MEK and the alcohols and water. The addition of each alcohol to MEK should raise the solubility parameter of the solvent and it

would be expected that the addition of a small amount of methanol should be as effective as a larger amount of propanol due to the higher value of solubility parameter for methanol. However, the observed dissolution rates show that a small amount of propanol slows the dissolution rate of PMMA whereas the same amount of methanol dissolves the polymer at a faster rate. It becomes apparent that the enhancement of dissolution rate upon the addition of methanol can not be explained by the thermodynamic interactions alone, but must involve some diffusional property. 2-Propanol, 1-butanol and 2-butanol show no enhancement of dissolution rate and hence above a value of molar volume of approximately 77 cm^3 mol^{-1} the effects can be explained by thermodynamic interactions.

The diffusion coefficient is usually used to describe the diffusional characteristics of a molecule. The Wilke-Chang correlation[200] states that the dependence of the solvent diffusion coefficient should be inversely proportional to the cube root of its molar volume. The enhancement observed for the addition of methanol and water could therefore be ascribed to the small, mobile molecules diffusing rapidly into the polymer and opening up the structure (i.e. plasticisation) so as to allow the solvent (i.e. MEK) into the polymer at a faster rate, and hence enhancing the dissolution, i.e. the effective diffusion coefficient of MEK is increased.

This plasticisation effect has been observed by Long and Thompson when the addition of water vapour to acetone or carbon tetrachloride vapours increased the swelling rate of poly(vinyl acetate)[201]. If the enhancement of the dissolution rate is due to this plasticisation effect, it would be expected that the enhancement would diminish as the size and

subsequent mobility of the non-solvent increases. This has been observed in this work, and that of Cooper for the addition of ethanol where a smaller enhancement in dissolution rate was observed (compared to methanol) as the larger molecule diffuses at a slower rate into the polymer. As the size of alcohol molecule is further increased, a further reduction in the enhancement of the dissolution rate would be expected until the rate of diffusion of the solvent into the polymer structure will be greater than that of the alcohol, and a decrease in dissolution rate would be observed due to the alcohols' non-solvent effect.

Sfirakis and Rogers[202] have also observed this phenomenon for the sorption of alcohol vapours by PMMA compression moulded films. They observed that the amount of penetrant sorbed by the polymer decreased linearly with increasing molecular size for methanol, ethanol and propanol followed by a large decrease in solubility for 2-propanol and 1-butanol. Ueberreiter[39] has stated that some thermodynamically poor solvents may penetrate a polymer matrix at a much faster rate than thermodynamically good ones.

Cooper observed that the addition of 2-propanol gave an enhancement whilst 1-propanol did not. However, we have observed the opposite, with the addition of 1-propanol giving an enhancement of dissolution rate. By considering the effective cross-section of 1-propanol and 2-propanol, it would be expected that the addition of the former would give the greater enhancement as it has the smaller cross-section. The 1-propanol molecules could align such that the longer backbone does not hinder diffusion.

It can therefore be concluded that the rate of diffusion of the non-solvent molecules into the polymer is the predominant factor for the lower alcohols, with the polymer/solvent interactions (i.e. thermodynamics) becoming increasingly important as the solvent molecular size is increased. Both Cooper's work and this work observed the transition between domination by kinetic effects and by thermodynamic effects between ethanol and the propanols. It has been shown that the polydispersity of the polymer will effect the enhancement of dissolution rates and that differences in polydispersity have a greater effect on the enhancement of dissolution rate than differences in molecular weight.

7.1.3 Effect of Water on Dissolution of PMMA in MEK

The effect of adding water to MEK up to the solubility limit of 10% v/v on the dissolution rate of PMMA (M_n 56000, γ 2.0) at 16.0 and 25.3°C in MEK is shown in Figure 122.

Water is a non-solvent for PMMA, and it would therefore be expected that the addition of the non-solvent would lead to a drop in the dissolution rate of PMMA as the water content is increased. However, we have again observed an acceleration in dissolution rate upon the addition of the non-solvent (see Section 7.1.2). Our results show that up to a concentration of 6% and 4% v/v water/MEK at 25.3 and 16.0°C respectively, there is an increase in the dissolution rate of PMMA. A doubling of the dissolution rate was observed compared to that of MEK alone. A slow tail off of the increase in dissolution rate was then observed. The maximum enhancement of dissolution rate at 16.0°C was 105% of the polymer film whilst at 25.3°C it was 113%.

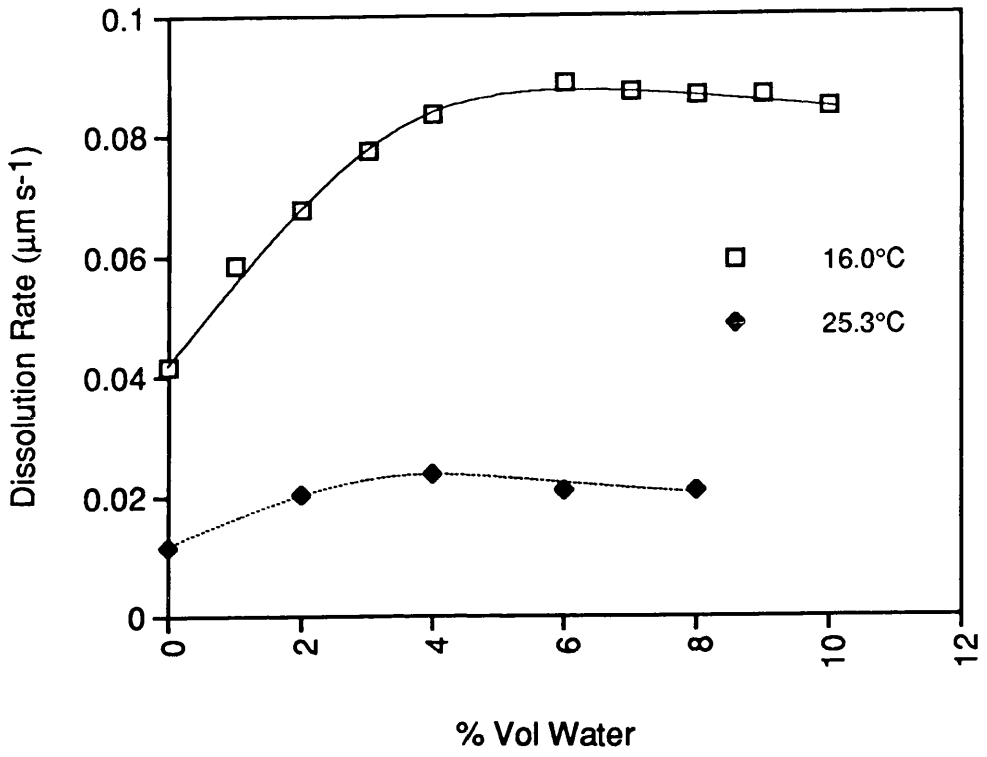

Figure 122: Effect of Water on the Dissolution of PMMA in MEK

Cooper and co-workers[66] have observed this enhancement of the dissolution rate of PMMA when adding water to MEK. PMMA samples (M_n 36000, γ 1.5 and M_n 320000, γ 1.6) were developed at 27.5°C and the dissolution rates for these samples can be seen in Figure 123. They also observed an increased enhancement effect with increasing temperature. It must be noted that we again observed higher dissolution rates and a greater enhancement of dissolution rate than Cooper. Initially this is surprising as it would be expected that our results would lie between those of the two samples. However, if the polydispersity of the samples is considered, it can be seen that the PMMA (M_n 56000, γ 2.0) sample has a higher polydispersity than the other samples. As shown in Chapter 5, polymers with the same molecular weight but varying polydispersities will dissolve at different rates in the same solvent. The polymer with the highest

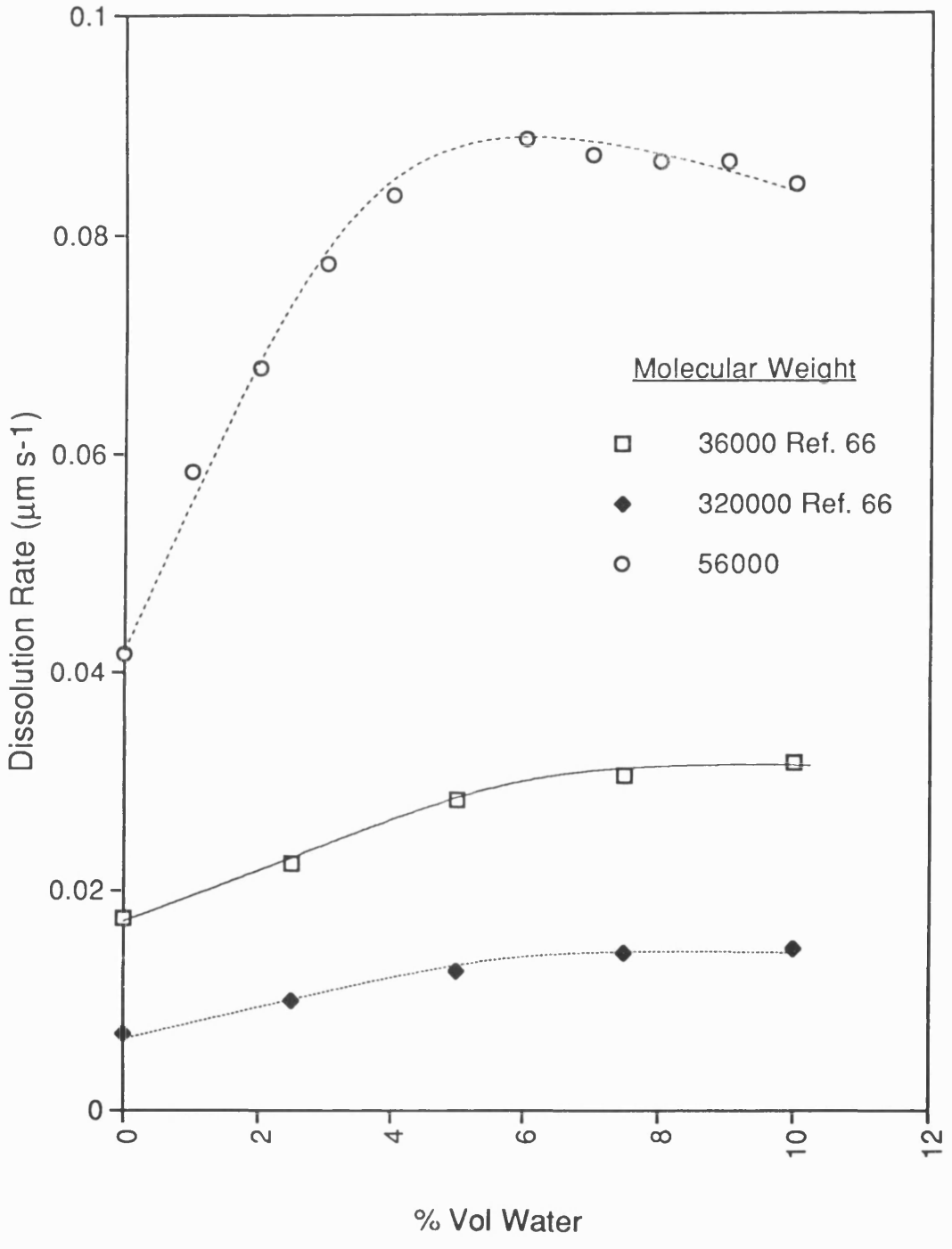

Figure 123: Effect of Water on the Dissolution of PMMA (M_n 56000 - 320000) in MEK

polydispersity will generally have a higher initial dissolution rate. It is therefore not surprising that we see a variation between our results and that of the work of Cooper.

7.2 Dissolution of PMMA in Alkyl Acetate Solvents

The investigation of the effect of the size of the solvent molecule on the dissolution rate of wide polydispersity PMMA (M_n 56000, γ 2.0) has been continued by using acetate solvents ranging from C_1 to C_5 at 25°C. As we have demonstrated in Section 7.1, it is expected that the solubility of the polymer will be greatly affected by the solvent molar volume, as the mobility of a solvent is strongly affected by the relative size of the free volume between the polymer chains and that of the solvent molecule. The results shown in Table 11 and Figure 124 indicate that the dissolution rate of PMMA decreases with increasing size of the acetate molecule, and for acetate solvents larger than ethyl, swelling is observed prior to dissolution.

Solvent	Solvent Molar Volume $(cm^3\ mol^{-1})$203	Dissolution Rate $(\mu m\ s^{-1} * 10^3)$
Methyl acetate	62.6	95.4
Ethyl acetate	80.2	38.3
Propyl acetate	97.6	5.2
Butyl acetate	115.2	2.2
Pentyl acetate	131.6	0.2

Table 11: Dissolution of PMMA (M_n 56000, γ 2.0) in Alkyl Acetate Solvents at 25°C

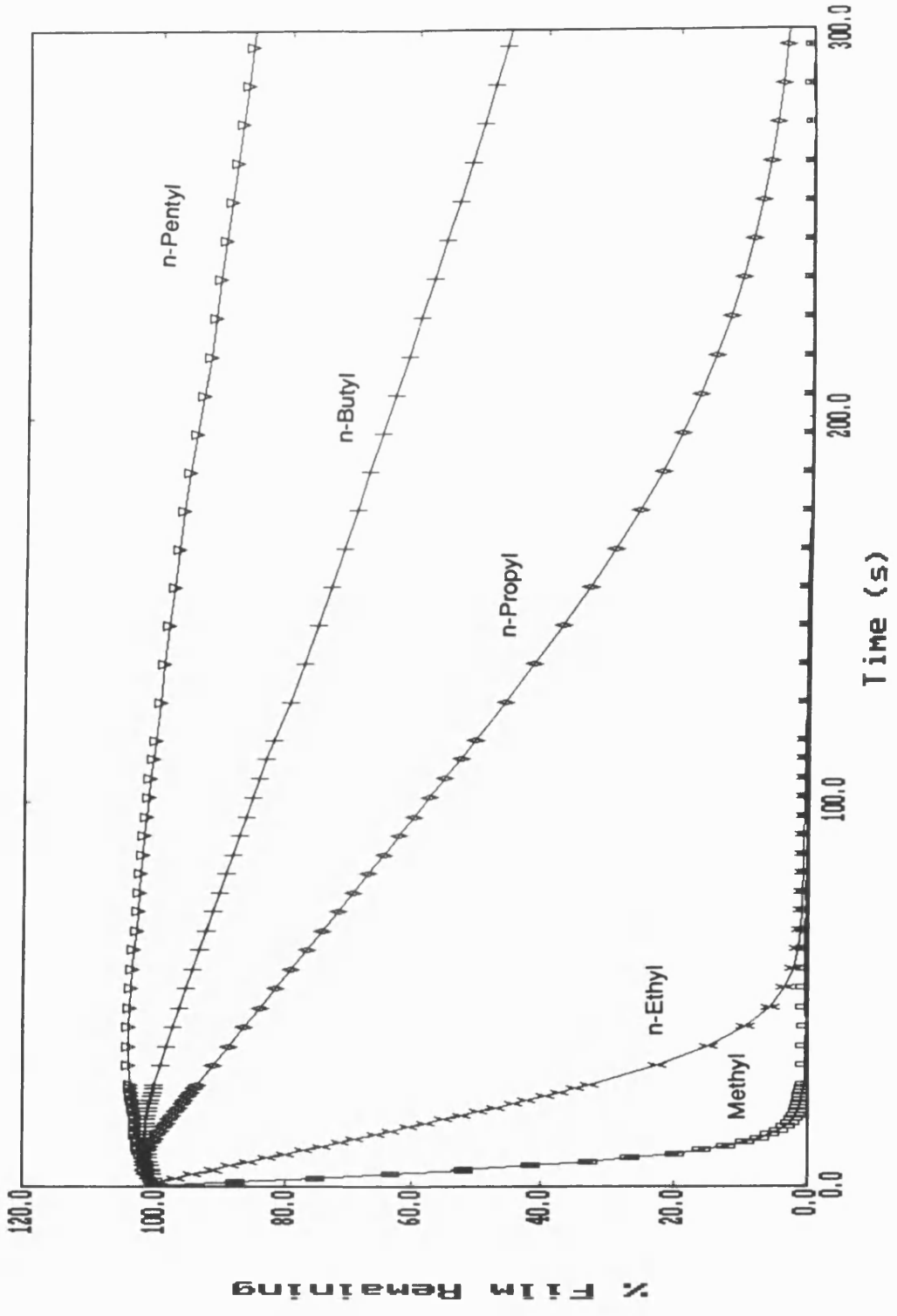

Figure 124: Dissolution of PMMA (M_n 56000, γ 2.0) in Alkyl Acetate Solvents at 25°C

The same trend of dissolution rate for these solvents was found by Ouano for the development of PMMA (M_W 476000) in the acetate solvents[40,57,191,198].

The dissolution of PMMA in the alkyl acetate solvents has been studied in a series of PMMA standards (M_n 22200 - 330000) over a temperature range 15 - 40°C. The effect of molecular weight and temperature has been discussed in Chapters 5 and 6 respectively. A similar trend in dissolution curves has been observed with the standards compared with the wide polydispersity sample. Throughout the molecular weight range, the proportion of initial swelling of the PMMA film observed is found to increase with increasing solvent molar volume.

The log-log plots of dissolution rate versus solvent molar volume for the molecular weight and temperature range show the dependence of dissolution rate on solvent molar volume (Figures 125 to 130). Generally a linear dependence of polymer solubility on the solvent molar volume has been shown with good linear correlation, and the slopes are independent of developing temperature as shown in Table 12. A wider range of values of slope is observed at 40°C which could be due to a greater experimental error at the higher developing temperatures. Throughout the temperature range, the results for PMMA (M_n 56000) lie close to those obtained for M_n 34500. The slopes of the lines for M_n 56000 are similar to those observed for the PMMA standards, hence the polydispersity of the polymer is not greatly affecting this log-log relationship.

a) Linear

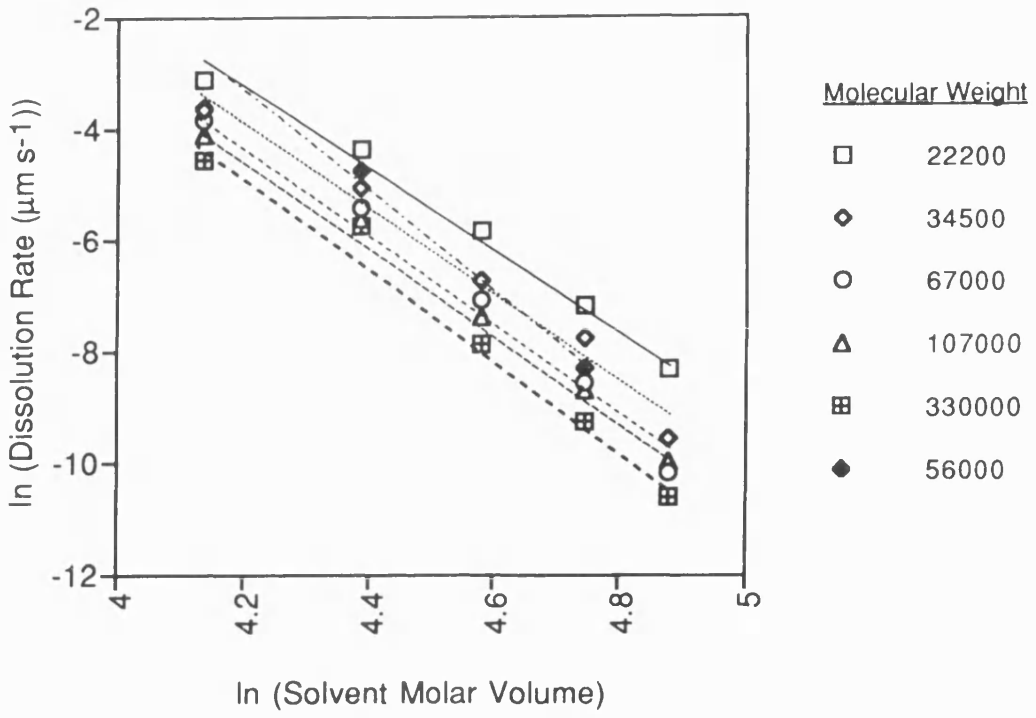

b) Break in linearity

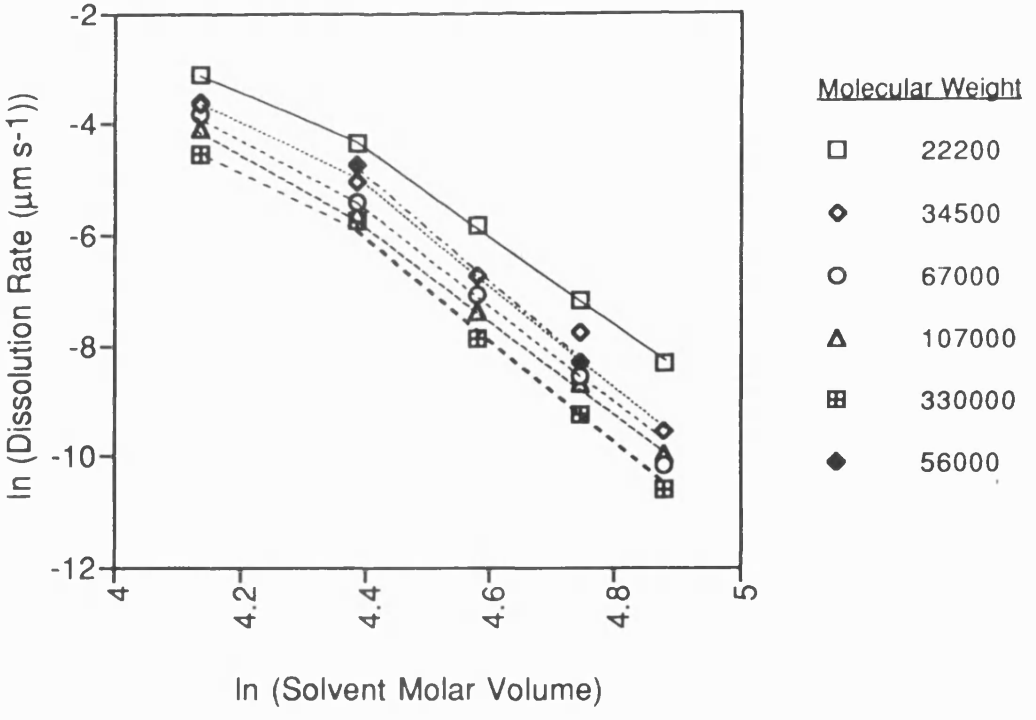

Figure 125: **Dissolution of PMMA in Alkyl Acetates at 15°C**

a) Linear

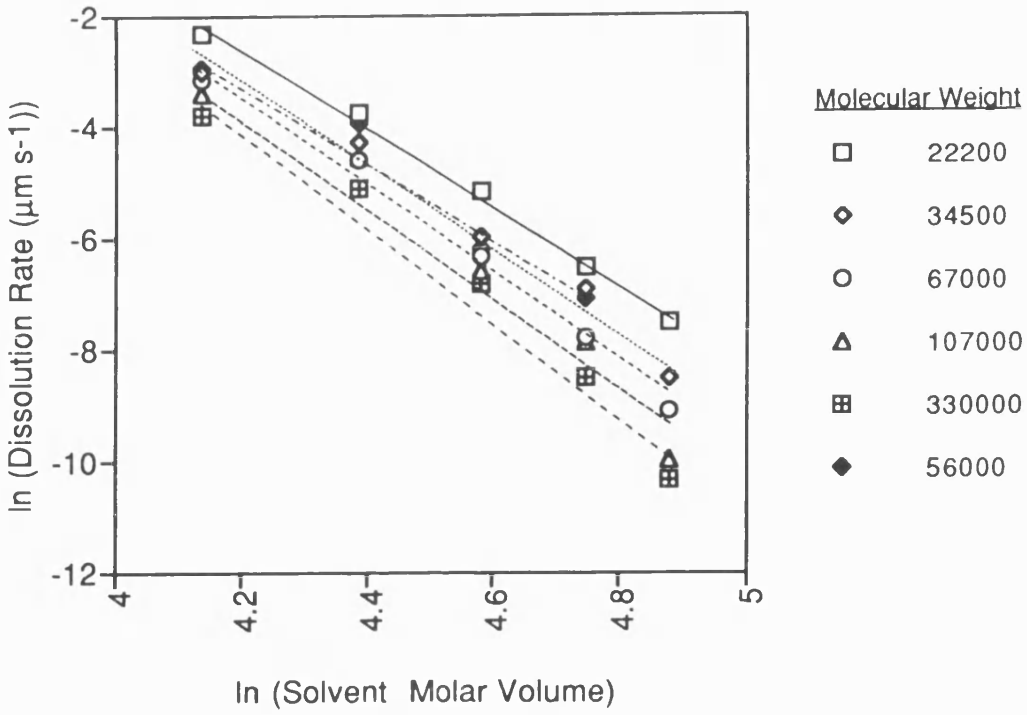

b) Break in linearity

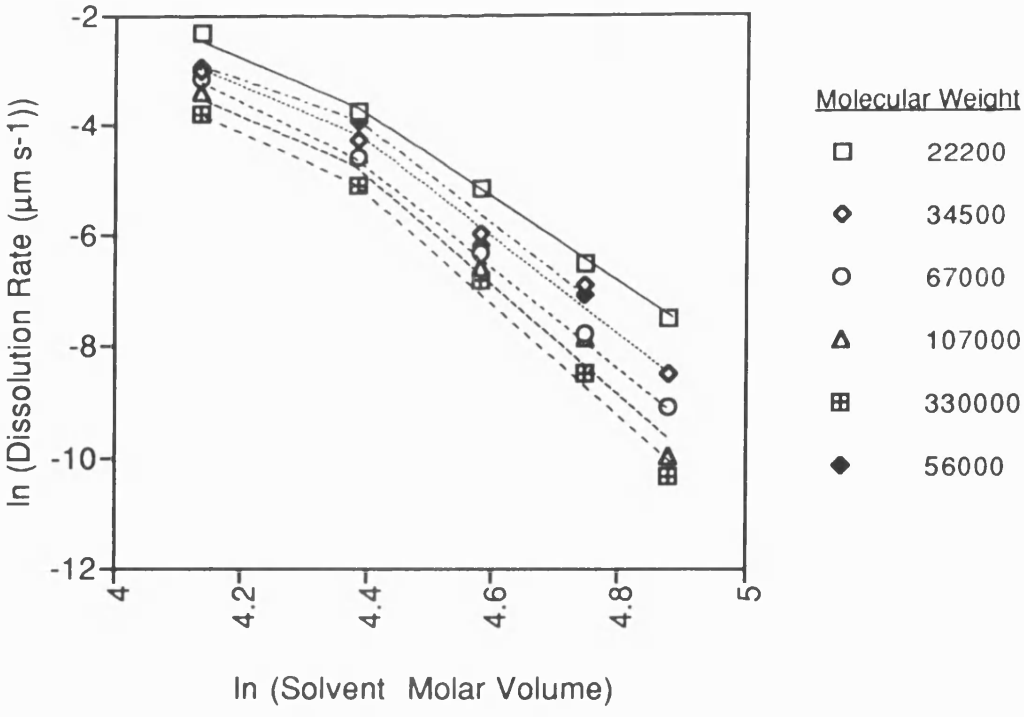

Figure 126: Dissolution of PMMA in Alkyl Acetates at 20°C

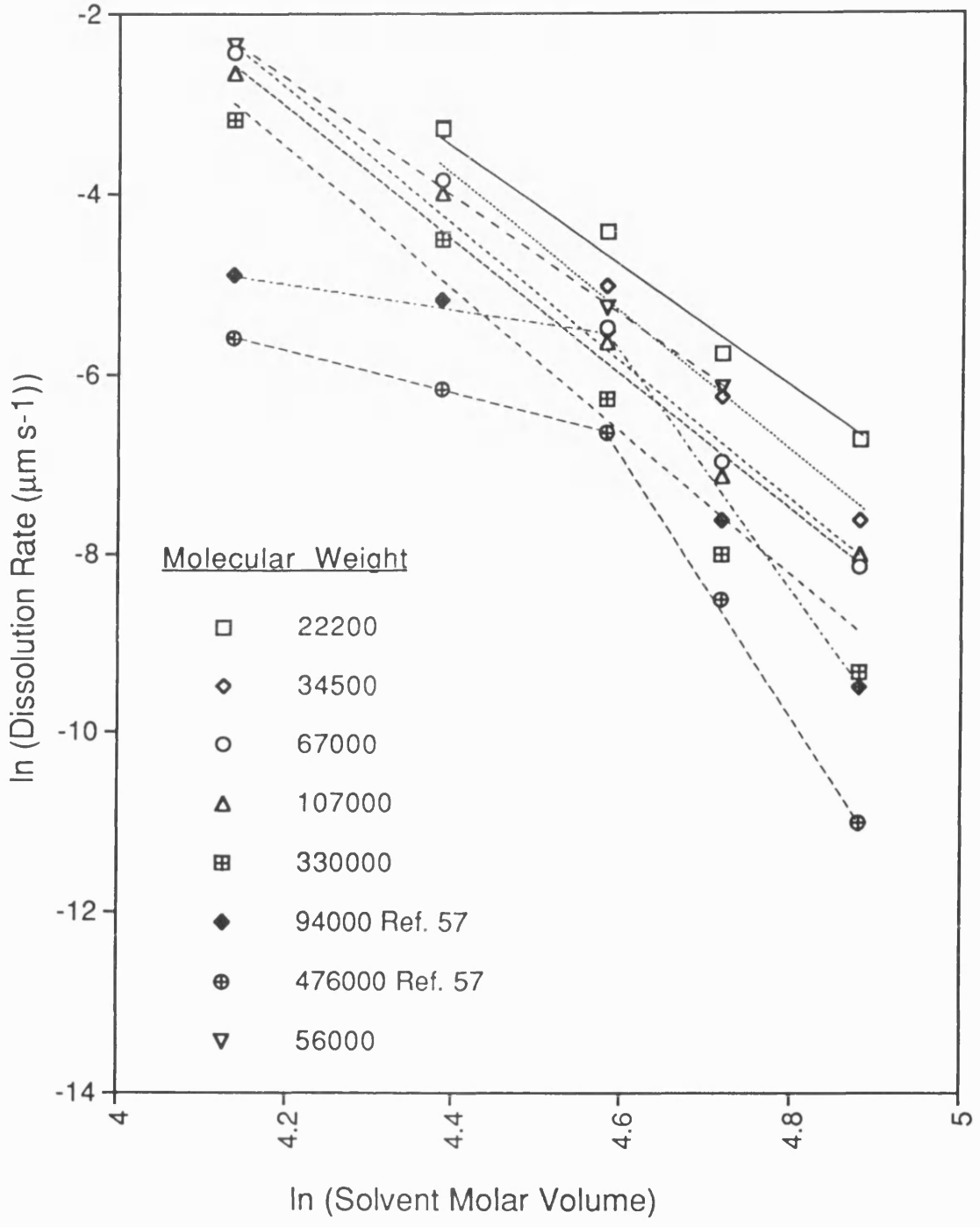

Figure 127: Dissolution of PMMA in Alkyl Acetates at 25°C

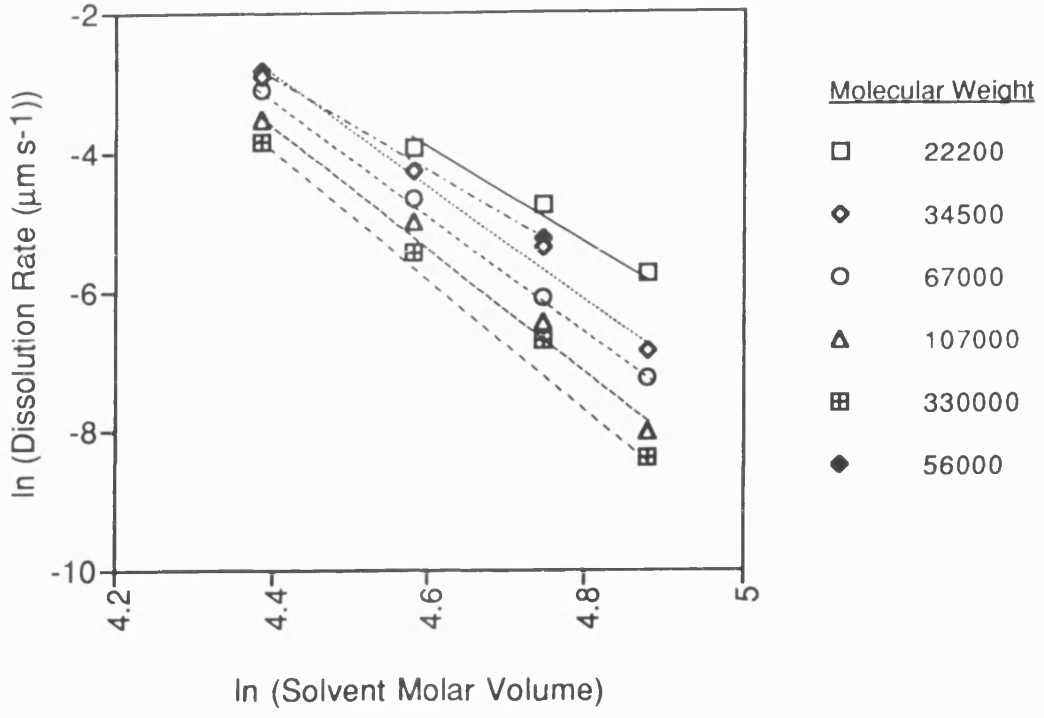

Figure 128: Dissolution of PMMA in Alkyl Acetates at 30°C

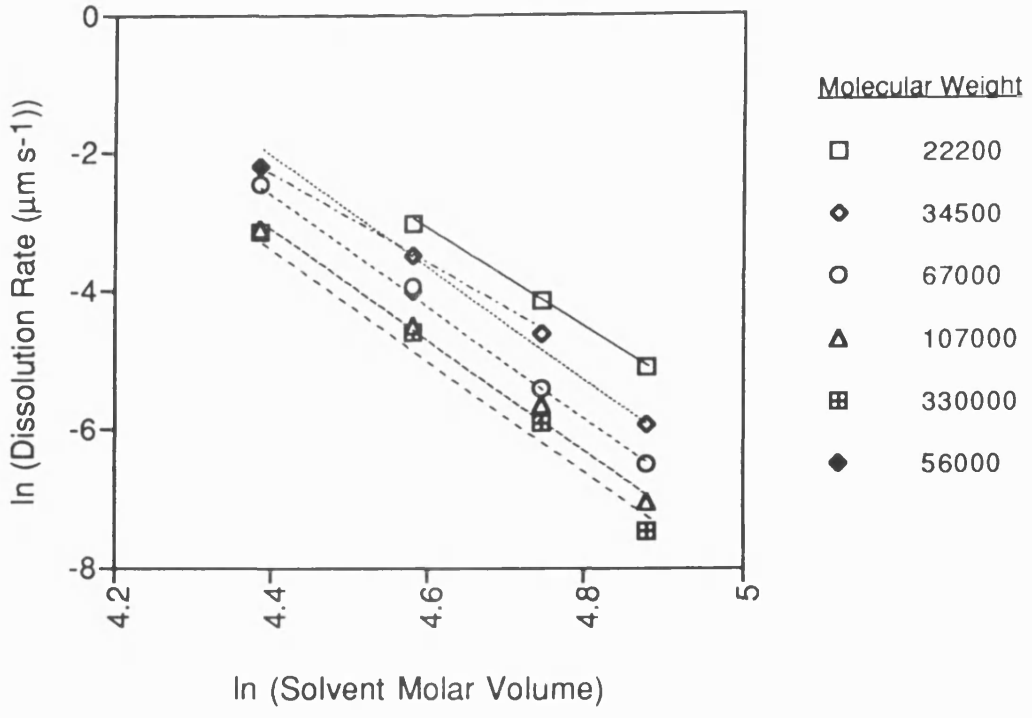

Figure 129: Dissolution of PMMA in Alkyl Acetates at 35°C

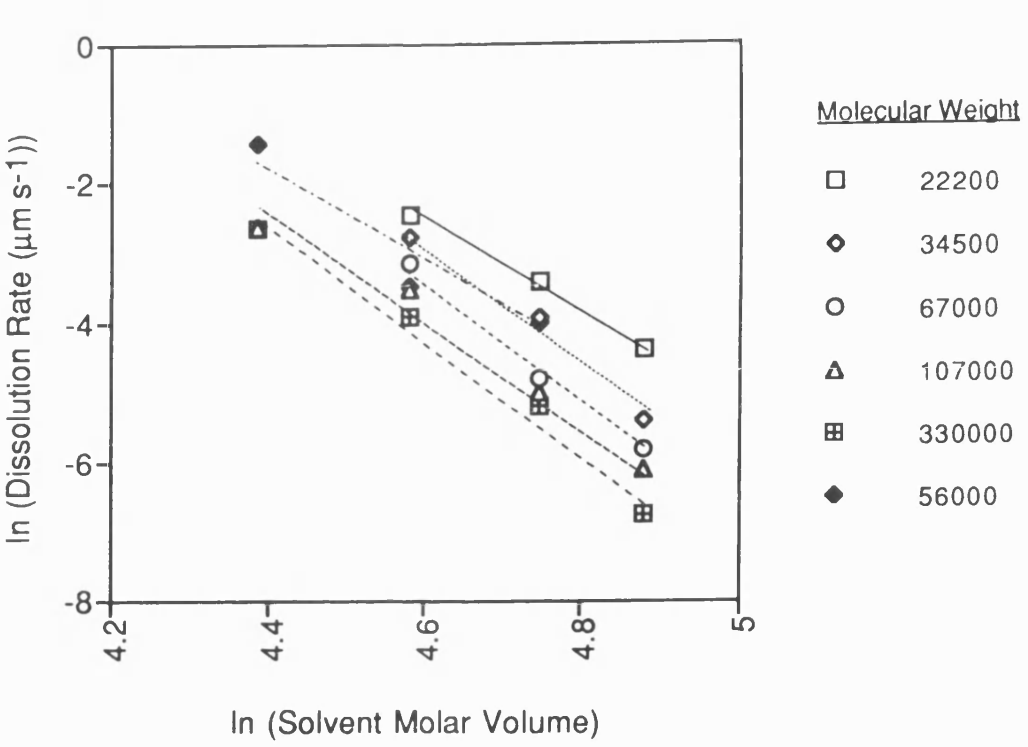

Figure 130: Dissolution of PMMA in Alkyl Acetates at 40°C

Temperature (°C)	Slope (w.r.t. M. Wt.)	Linear Correlation Coefficient
15	7.06 - 8.43	0.983 - 0.997
20	7.06 - 8.72	0.979 - 0.998
25	7.20 - 8.54	0.980 - 1.000
30	6.74 - 8.53	0.986 - 0.993
35	6.88 - 8.94	0.987 - 1.000
40	6.37 - 8.96	0.960 - 0.998

Table 12: Effect of Temperature on the Slopes of Figs. 125 to 130

The effect of polymer molecular weight upon the log-log relationship can be observed in Table 13. Although, initial observation of the respective Figures indicates an independence of slope with molecular weight, the data in Table 13 shows that there is a slight increase in the value of slope as the polymer molecular weight is increased from 22200 to 34500 (throughout the temperature range). This may be due to the swelling of the polymer film obscuring the dissolution data.

Although we have generally found a linear relationship for the log-log plot, as indicated by Figures 125 to 130, closer examination of the plots indicates that there may be a break in linearity at a solvent molar volume equivalent to ethyl acetate. Figures 125 and 126 for the dissolution of PMMA in the acetate solvents at 15 and 20 °C have been plotted to show this possible break in linearity. It can be seen that the break in linearity is very small, and may be partly due to the greater experimental error involved in measuring dissolution rates at the lower solvent molar volumes (i.e. faster rates). It therefore becomes apparent that further investigation of these dissolution characteristics is required.

In their study of the dissolution of polystyrene in a homologous series of alkyl acetates at 25°C, Asmussen and Ueberreiter[54] have shown a sharp drop in solubility rate of polystyrene between propyl and butyl acetate. This drop in solubility has also been found by Ouano and Gipstein[57] for polymer molecular weights M_W 94000 and 476000. They found that the solubility rate/solvent molecular weight relationship for each molecular weight of PMMA in the alkyl acetate series gave two straight lines with different slopes (2.4 and 13.8). The break in linearity is much greater than that observed in Figures 125 and 126b. It has been suggested that the sharp change in the

Polymer M_n	Slope	Linear Correlation Coefficient
Developing Temp. 15°C		
22200	7.06	0.994
34500	7.74	0.989
67000	8.43	0.993
107000	7.94	0.997
330000	8.35	0.991
56000	7.99	0.983
Developing Temp. 20°C		
22200	7.06	0.998
34500	7.27	0.991
67000	8.05	0.995
107000	8.72	0.981
330000	8.72	0.985
56000	7.17	0.979
Developing Temp. 35°C		
22200	6.01	0.998
34500	7.75	0.991
67000	8.35	0.998
107000	8.94	0.989
330000	8.94	0.990
56000	6.74	0.960

Table 13: Effect of Polymer Molecular Weight upon the Slopes of Figs. 125 to 130

slopes of the log-log plot could be due to a change in the diffusion mechanism. Ouano and Gipstein have used a "Dip and Dry" method in the determination of the dissolution rates, which is not able to give any information on the swelling of the polymer, and have therefore quoted the overall dissolution rate of the polymer which include any initial swelling hence reducing the dissolution rate observed. These results have been plotted in Figure 127 and the deviation between our results and the literature can be clearly observed.

Our experimental technique is able to monitor the initial swelling of the polymer and separate this from the dissolution rate. The change in linearity observed by Ouano coincides with our observation of swelling of the PMMA film. Figure 124 shows there is a noticeable break between no swelling and swelling of the PMMA film (M_n 56000) at 25°C when increasing the solvent chain length from C_2 to C_3. The results therefore clearly show that the change in slope observed by Ouano is due to the appearance of swelling of the polymer which, as shown previously, is dependent upon molecular weight and developing temperature.

Observation of the thermodynamic data for the sorption of the alkyl acetates on PMMA, shows that there is a great difference in the thermodynamic behaviour for methyl acetate compared with the other alkyl acetates. Methyl acetate has much higher values of interaction parameter throughout the concentration range studied indicating lower polymer/solvent interactions. The interaction parameter values for methyl acetate is so high, that no swelling of PMMA is observed and from our dissolution data it is apparent that the diffusional properties of the small methyl acetate molecule has a greater influence on the dissolution. With increases in the size of the

alkyl acetate molecule, the thermodynamic behaviour becomes a contributing factor and hence swelling of the polymer film is observed due to the greater polymer/solvent interactions compared with methyl acetate.

7.3 Conclusion

The direction of resist technology is towards narrower lines and greater line density which indicates the need for the careful choice of developers to enable the development of the polymer surface with geometrical integrity. In this Chapter, we have shown that interesting dissolution characteristics can be observed by the changing of solvent molar volume and that the size of the solvent molecule must be taken into account when predicting dissolution behaviour of a resist system. It has been demonstrated that the variation of the composition of solvent/non-solvent mixtures can greatly affect the observed dissolution/swelling kinetics of polymer films. Enhancement of the dissolution rate of PMMA has been demonstrated upon the addition of small alcohol molecules (non-solvents) to MEK. By the use of our piezoelectric sorption detector, we have been able to obtain thermodynamic data that has aided us in the understanding of the dissolution behaviour observed.

In Chapter 9, we will continue this study by considering the effect of solvent composition on both negative and positive resist systems.

Chapter Eight

8.0 Dissolution Studies of other Resist Systems

In the previous Chapters, we have considered the effect of various developing parameters on the dissolution of PMMA. PMMA is a well known photoresist and has been well characterised in the literature. This has given us the opportunity to compare our results with other experimental techniques and to further develop some of the observations made by previous workers whilst showing the viability of our QCM technique for the study of dissolution and swelling kinetics. In this Chapter, we have extended our studies to both positive (polystyrene, poly(4-chlorostyrene) and poly(phenylmethylsilane)) and negative (poly(vinyl cinnamate)) resist systems, which have not been as well studied, considering the effect of molecular weight, temperature and solvent composition upon the development of the resists.

8.1 Effect of Molecular Weight on Polymer Dissolution

In Chapter 5, we have demonstrated that both the molecular weight and its distribution can have a great effect on the dissolution and swelling of PMMA films. In this Chapter, we have considered the change of solubility of the above positive resists with respect to molecular weight and compared the results with trends observed for PMMA.

8.1.1 Dissolution of Polystyrene in 60:40 v/v MEK/IPA

As contrast tends to increase with decreasing molecular weight for polystyrene-based resists[13], the QCM dissolution apparatus has been used to investigate the effect of molecular weight on the dissolution of polystyrene. Figures 131 and 132 show the dissolution characteristics of polystyrene in a 60:40 v/v MEK/IPA solution over a series of temperatures. The solubility of a

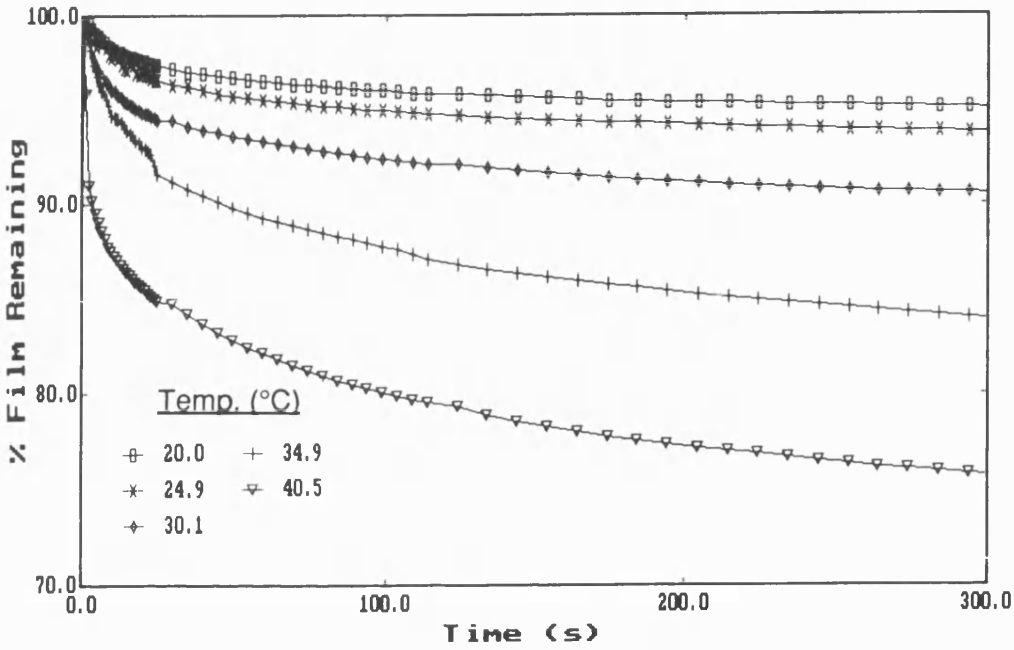

Figure 131: Dissolution of Polystyrene (M_W 430000) in 60:40 v/v MEK/IPA

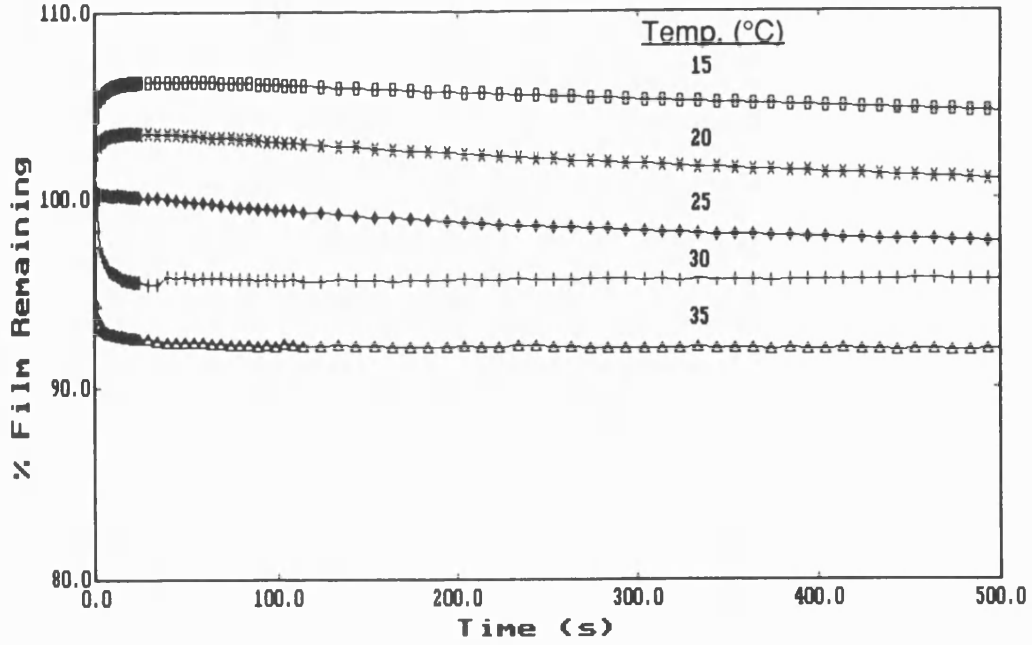

Figure 132: Dissolution of Polystyrene (M_W 675000) in 60:40 v/v MEK/IPA

wide polydispersity polystyrene sample (M_W 430000, γ 3.1) has been compared with the solubility of a low polydispersity polystyrene standard (M_W 675000, γ 1.05) to enable a correlation to be made between dissolution characteristics and molecular weight and its distribution. Initially the dissolution of polystyrene in pure MEK had been studied but the polymer film was found to dissolve almost instantaneously, and certainly too fast to be measured by our apparatus. The same situation was observed for the 80:20 v/v MEK/IPA mixture. Difficulties were encountered in obtaining a crystal oscillation for the 70:30 v/v MEK/IPA mixture and this is thought to be due to viscosity effects. However, as the non-solvent concentration was increased above the 70:30 composition, the crystal oscillation was regained.

On comparison of the dissolution/swelling curves of the two polystyrene samples, a number of striking differences can be observed. No swelling is observed over the temperature range studied for the wide distribution sample, whilst at the lower temperatures, the polystyrene standard initially swells. For both samples, there was incomplete removal of the polymer film due to the presence of the non-solvent inhibiting the dissolution. Greater film removal is observed for the wide distribution sample with dissolution occurring over a much longer time-scale. The initial dissolution rates observed at the higher temperature range for the polystyrene standard are much higher than the corresponding rates for the wide distribution sample, whilst the overall dissolution rates for the wide distribution polystyrene are faster than those for the polystyrene standard.

The striking differences between the swelling/dissolution curves of the two samples can be accounted for by the differences in molecular weight and polydispersity (as was observed for the dissolution of PMMA in MEK). On consideration of the number average molecular weights of the polystyrene

samples, the slower overall dissolution rates observed for the polystyrene standard would be expected due to the higher molecular weight (M_W 675000) of the sample. The wide distribution sample is made up of a range of molecular weights including a significant proportion above 67500 and, when the solvent mixture enters the polymer structure, the low molecular weight polymer chains dissolve away more quickly than the bulk of the polymer. The early removal of these polymer chains opens up the polymer structure enabling the solvent to enter and dissolve away the remaining higher molecular weight polymer at a faster rate. This opening up of the structure also increases the total amount of polymer removed. The initial removal of the low molecular weight material overshadows any swelling of the polymer that may occur.

The polystyrene standard has a narrow range of polymer molecular weights and there is no initial removal of low molecular weight polymer hence, more solvent must enter before any material is removed. At sufficiently low temperatures, the diffusion of the solvent before dissolution is so slow that the swelling of the polymer structure is observed. As more solvent enters, the polymer starts to dissolve and dissolution is observed. Further lowering of the temperature will increase the amount of swelling observed before the dissolution mechanism dominates.

Once dissolution occurs, the polymer chains will dissolve away from the substrate at approximately the same rate until no more polymer is removed. Therefore a fast initial dissolution rate is observed for the narrow polydispersity sample which tails off rapidly with little polymer removed, the wide polydispersity sample shows a faster overall dissolution rate with dissolution lasting longer and hence a larger percentage of polymer being removed.

In conclusion, although the molecular weight of the polystyrene resist can greatly affect the obtained contrast of a resist (i.e. contrast enhanced at lower molecular weights) it must not be considered in isolation as such factors as the polydispersity of the sample will also affect the contrast obtained.

8.1.2 Dissolution of Poly(phenylmethylsilane) (M_n 7500 - 53700) in 75:25 v/v MEK/IPA

The effect of polymer molecular weight upon the dissolution of poly(phenylmethylsilane) has been studied in a developer composition of 75:25 v/v MEK/IPA. The effect of solvent composition will be discussed in later sections. As detailed in Section 2.3.2.3, a range of molecular weights (M_n 7500 - 53700) of the poly(phenylmethylsilane) were prepared from a wide polydispersity polysilane sample by preparative GPC and fractionation precipitation. These molecular weight samples were developed in 75:25 v/v MEK/IPA over the temperature range 15 - 40°C and the dissolution curves for the respective molecular weights can be found in Figures 133 to 139. It was hoped that the presence of the non-solvent would enhance any swelling characteristics of the samples. A direct comparison of the dissolution characteristics between the molecular weight samples can not be made because of the differences in polydispersity. However, some qualitative information can be obtained, and Table 14 gives an indication of the trends in percentage of film removed and swelling of the polymer sample at 15, 25 and 40°C.

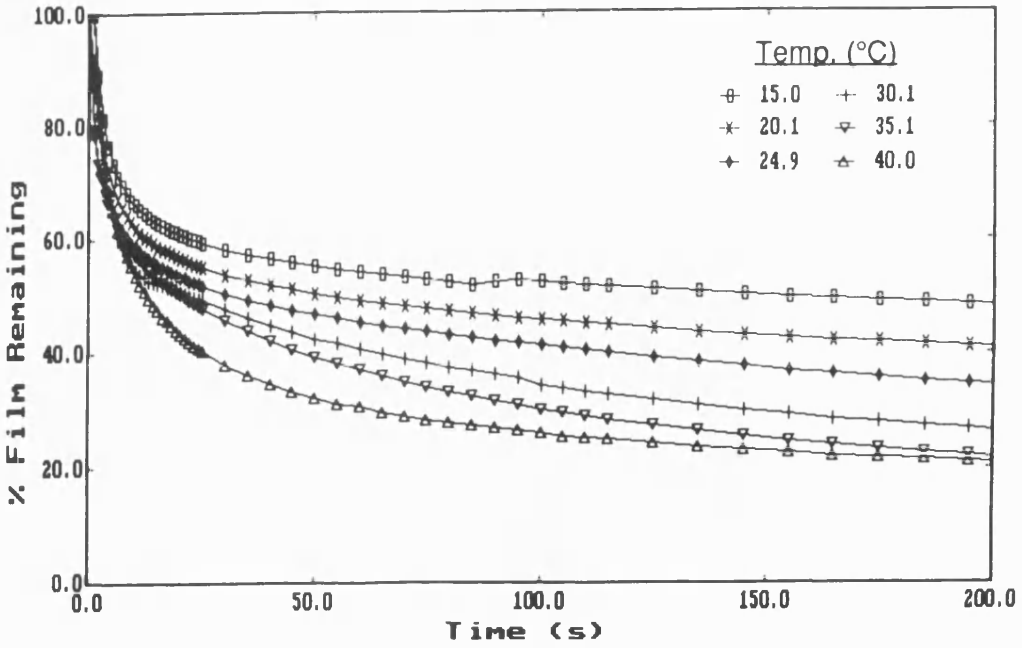

Figure 133: Dissolution of Poly(phenylmethylsilane) (M_n 7500) in 75:25 v/v MEK/IPA

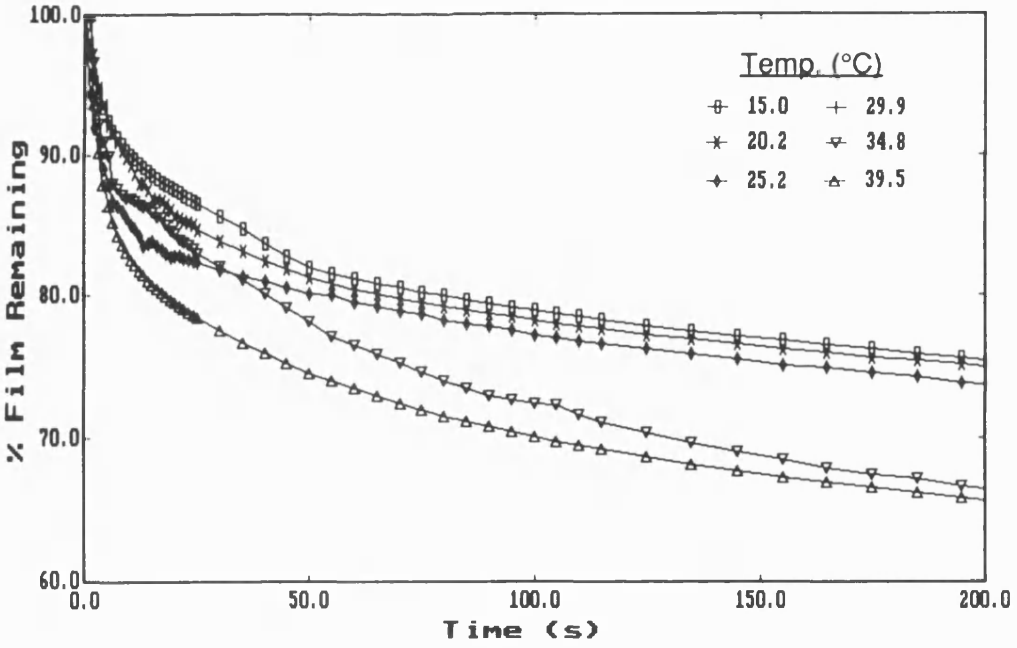

Figure 134: Dissolution of Poly(phenylmethylsilane) (M_n 9600) in 75:25 v/v MEK/IPA

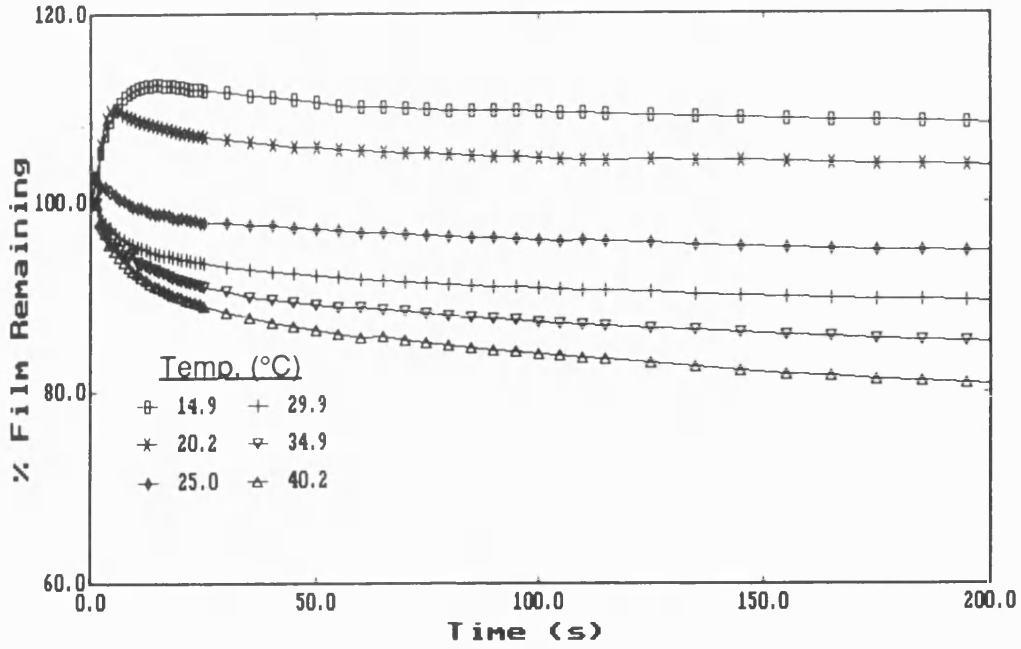

Figure 135: Dissolution of Poly(phenylmethylsilane) (M_n 14500) in 75:25 v/v MEK/IPA

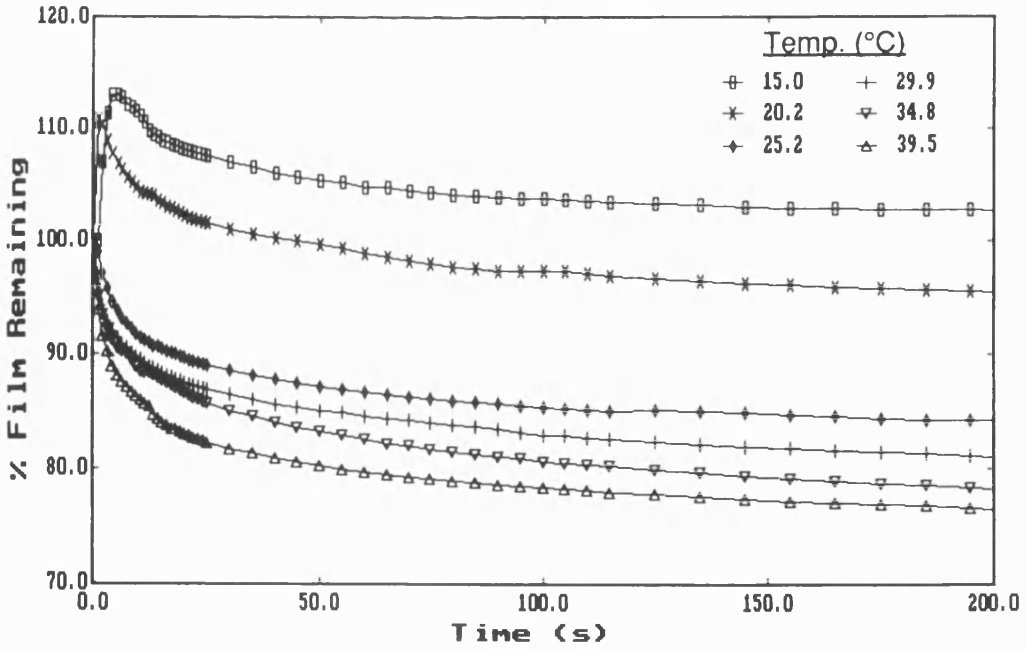

Figure 136: Dissolution of Poly(phenylmethylsilane) (M_n 18400) in 75:25 v/v MEK/IPA

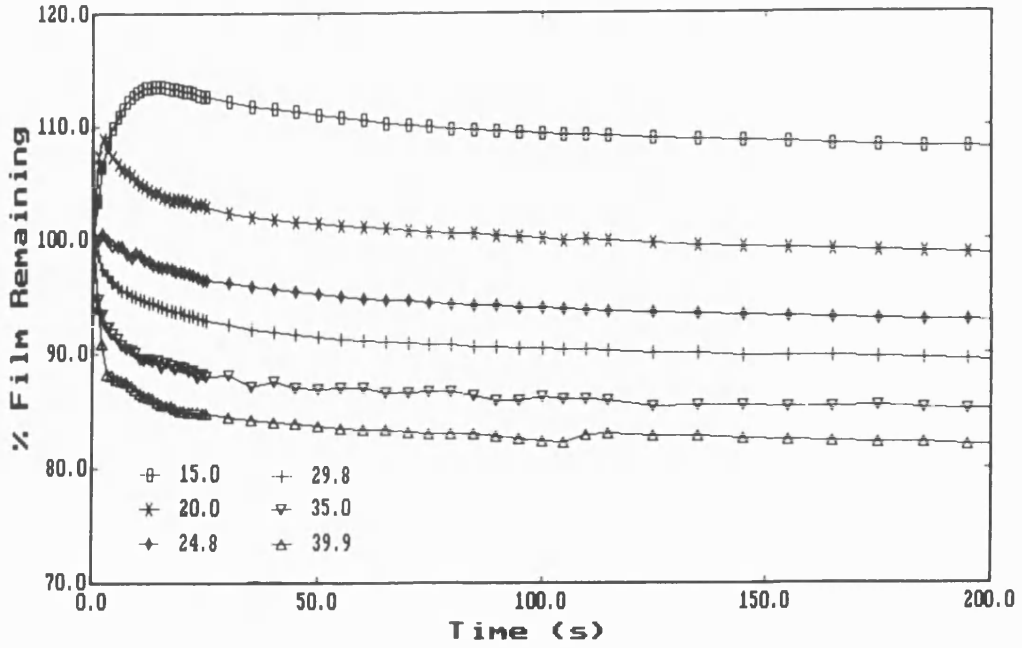

Figure 137: Dissolution of Poly(phenylmethylsilane) (M_n 29300) in 75:25 v/v MEK/IPA

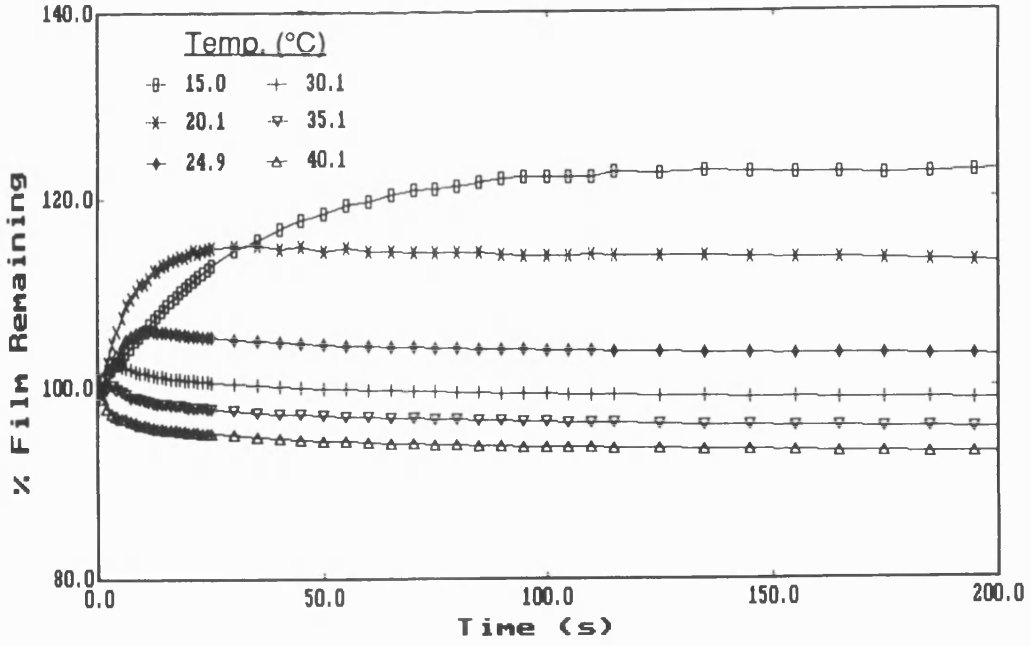

Figure 138: Dissolution of Poly(phenylmethylsilane) (M_n 36500) in 75:25 v/v MEK/IPA

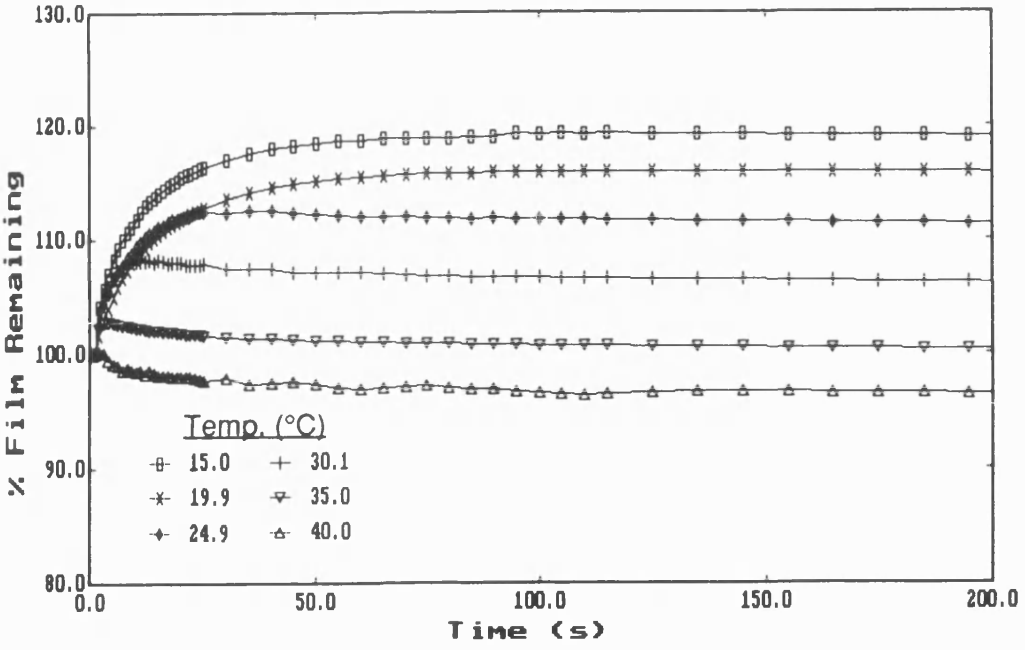

Figure 139: Dissolution of Poly(phenylmethylsilane) (M_n 53700) in 75:25 v/v MEK/IPA

At 15°C, with the exception of the low molecular weight samples (M_n 7500 and 9600) (Figures 133 to 134), initial swelling is observed throughout the molecular weight series which is followed by very slow dissolution rates. Above M_n 36500, no dissolution of the polymer film was observed for the recorded development time. Comparison of the dissolution curves of the M_n 53700 and 36500 samples (Figures 139 and 138) shows a lower percentage of swelling for the higher molecular weight sample, which is opposite to the trend observed at lower molecular weights. The polydispersities of the M_n 53700 and 36500 polysilane samples are 5.8 and 1.8 respectively, and therefore as we have observed previously, it would be expected that the sample with the wider molecular weight distribution would have shown a faster dissolution rate. The smaller polymer molecules found in the higher polydispersity sample will be more readily removed from the top layers of the

Polymer M_n	Maximum % Swelling	Final % Film Remaining
Developing Temp. 15°C		
7500	none	48
9600	none	76
14500	10	108
18400	13	103
29300	14	108
36500	23	123
53700	19	119
Developing Temp. 25°C		
7500	none	35
9600	none	74
14500	2	95
18400	none	84
29300	1	93
36500	8	103
53700	11	112
Developing Temp. 40°C		
7500	none	21
9600	none	66
14500	none	81
18400	none	76
29300	none	82
36500	none	93
53700	none	96

Table 14: Dissolution of Poly(phenylmethylsilane) in 75:25 v/v MEK/IPA

polymer film, hence increasing the free volume of the film and enabling the entry of the solvent with minimal swelling.

The swelling of the film can be suppressed by the use of a higher developing temperature and this was demonstrated at 40°C, where none of the polysilane samples swell and faster dissolution rates are recorded. The effect of polydispersity is again observed with very little difference between the percentage of film removed for the higher molecular weight samples. At 25°C, the balance between swelling and dissolution is clearly illustrated with no measurable initial swelling below a molecular weight of 29300 (Figure 137) and no dissolution at M_n 53700 (Figure 139). Surprisingly, considering the polydispersity, the dissolution curves observed for M_n 14500 and 18400 (Figures 135 and 136) are very similar. This is because swelling of the film is observed around this molecular weight region and is obscuring the actual dissolution curves. Again the effect of polydispersity can be seen for the swelling characteristics of M_n 34500 and 53700 with little difference between the two samples.

The general trend observed for all the developing temperatures studied is an increase in dissolution rate and percentage of film removed, and decrease in the proportion of swelling with an increase in molecular weight, if the polydispersity is kept constant. Throughout the temperature range, a great difference is observed between the dissolution/swelling curves for M_n 9600 and 7500. One possible explanation for this great deviation is the difference in polydispersity, but considering the comparatively small effect observed at the higher molecular weight region it is unlikely that this is the only factor operating.

The log-log plot of dissolution rate versus polymer molecular weight shows a linear relationship with an increase in the slope of the lines with an increase in temperature (Figure 140). Table 15 shows the change in slopes observed. The break in linearity with respect to molecular weight observed for the dissolution of PMMA in MEK and alkyl acetate solvents, has not been observed with the polysilane samples. This may be due to the wider polydispersity of the polysilane samples compared with the PMMA series.

Throughout the temperature range studied, there is an anomalous point at M_n 29300. The dissolution rates measured deviate greatly from the linear relationship and although differences in polydispersity can be used as one possible explanation, further analysis is required to give a fully satisfactory explanation for this deviation.

As stated in Chapter 5, the diffusion coefficient of the solvent has been found to be independent of molecular weight over a large range of chain lengths[17], but the results for the polysilane molecular weight series indicates a decrease in dissolution rate with increasing chain length. This is in agreement with the trend found for the dissolution of PMMA in MEK where the slowing of the rate of dissolution is due to an increasing entanglement of the macromolecules. The swelling thickness of the polymer has increased with the decrease in dissolution rate, therefore by keeping the diffusion coefficient constant the following equation proposed by Ueberreiter and Asmussen is still obeyed.

$$D = s\delta$$

where D is the mean diffusion coefficient, δ is the swollen surface layer and s is the dissolution rate.

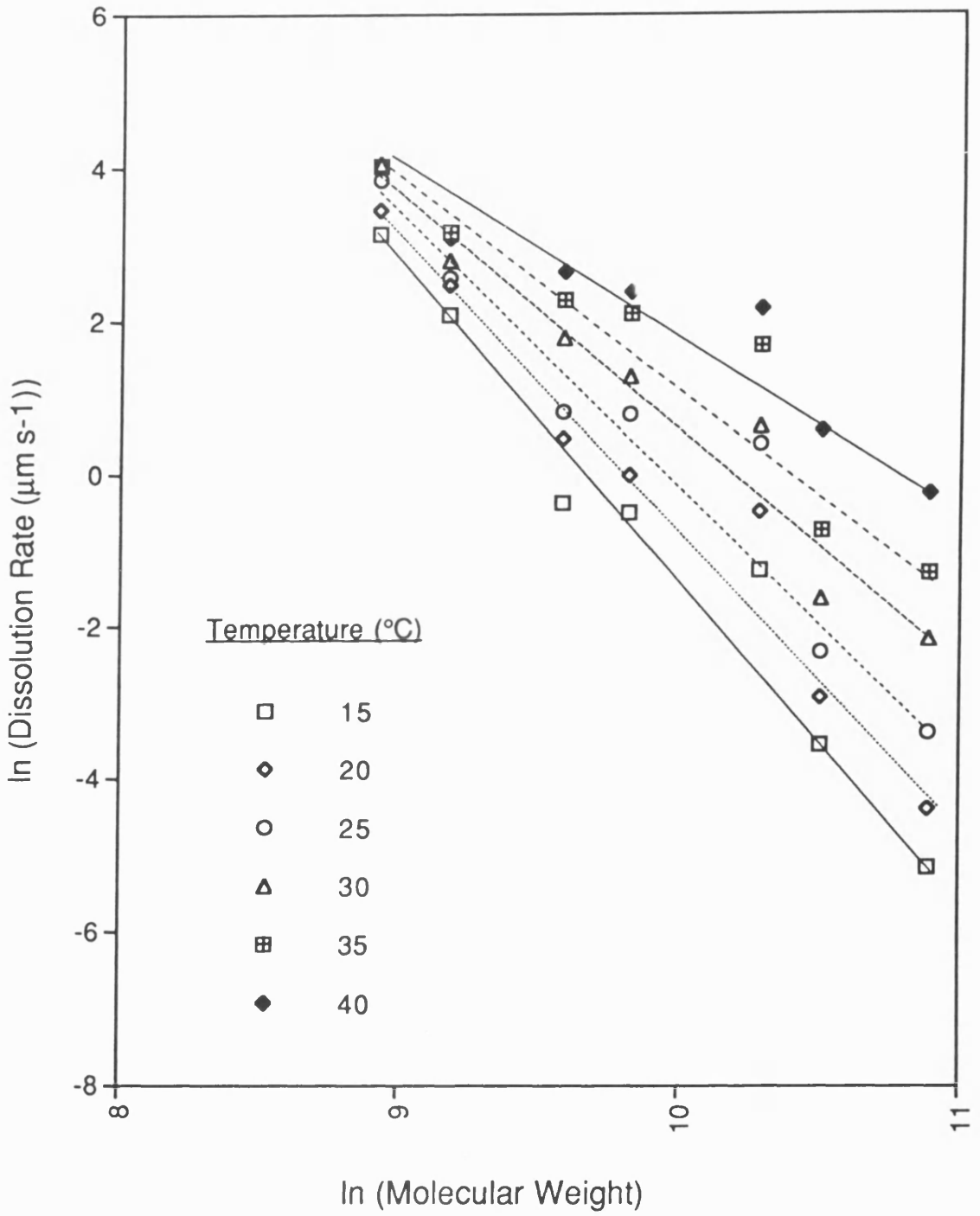

Figure 140: Dissolution of Poly(phenylmethylsilane) in 75:25 v/v MEK/IPA

Temperature (°C)	Equation (y = mx+c)
15	-3.968x + 38.410
20	-3.770x + 37.052
25	-3.400x + 33.989
30	-3.049x + 31.094
35	-2.588x + 27.179
40	-1.910x + 20.949

Table 15: Change in Gradient with Temperature for Figure 140

In all our molecular weight studies, for both positive and negative resists, we have observed an overall trend of decreased rate of dissolution and a greater degree of swelling of the polymer film with increasing molecular weight. Wide polydispersity samples tend to dissolve at a faster rate, with reduced swelling, than the corresponding standards. The swelling of the resist film can therefore be moderated by the useful selection of the polymer molecular weight and its distribution.

8.2 Effect of Temperature on Polymer Dissolution

In Chapter 6 , we have made some preliminary studies on the effect of temperature on the dissolution kinetics of PMMA and generally found that the rate of dissolution increases with temperature whilst, any swelling of the film can be suppressed or diminished by increasing the developing temperature. These studies have been continued by considering the effect of temperature on the development of styrene-based resists, poly(phenylmethylsilane) and poly(vinyl cinnamate).

8.2.1 Dissolution of Styrene-based Resists

8.2.1.1 Dissolution of Polystyrene in MEK/IPA Mixtures

The effect of changing temperature on the dissolution kinetics of polystyrene in three solvent/non-solvent concentrations of MEK/IPA has been studied. The dissolution curves for polystyrene (M_W 430000, γ 3.1) in a 60:40 v/v MEK/IPA mixture for the temperature range 20 - 40°C are shown in Figure 141. In this temperature range, no initial swelling of the polystyrene film was observed and the dissolution rate and percentage film removed increased with increasing temperature. For the development time studied, there is approximately 25% dissolution at 40°C, whereas only 5% at 20°C. Figure 142 shows the Arrhenius plot for the dissolution of polystyrene in 60:40 v/v MEK/IPA which gives an activation energy value of 88.1 kJ mol^{-1} with a linear correlation coefficient of 0.998. This value of activation energy is comparable to that observed in Section 6.1 for the dissolution of PMMA in MEK (E_a = 85.8 - 107.4 kJ mol-1) is indicative of Case II diffusion mechanism.

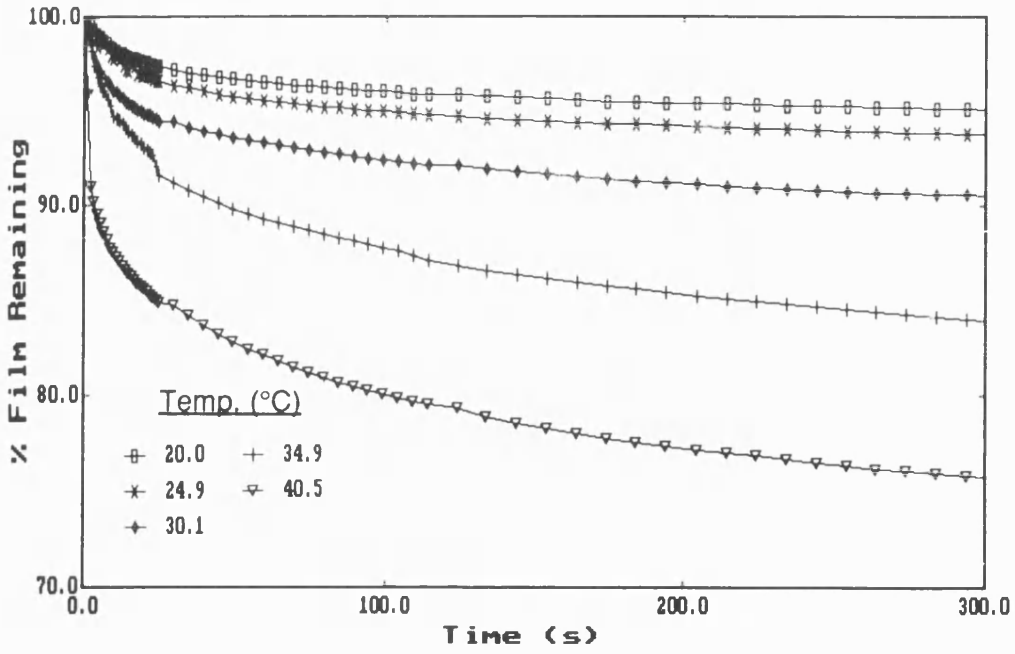

Figure 141: Effect of Temperature on the Dissolution of Polystyrene (M_W 430000) in 60:40 v/v MEK/IPA

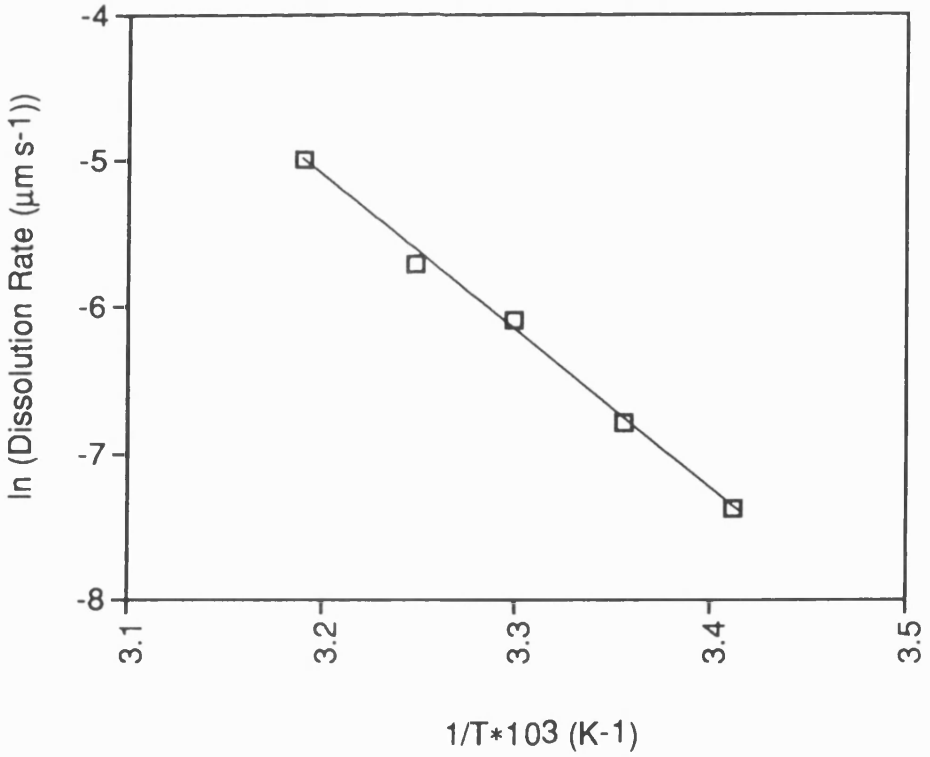

Figure 142: Arrhenius Plot for the Dissolution of Polystyrene (M_W 430000) in 60:40 v/v MEK/IPA

On increasing the concentration of non-solvent (i.e. IPA) in the solvent mixture to 50:50 v/v MEK/IPA, slower dissolution rates were observed and below 25°C, initial swelling of the polymer could be seen (Figure 143). As the dissolution curves and final film thickness were very similar throughout the temperature range, it was very difficult to obtain accurate dissolution rates, and hence no Arrhenius plot is shown for this concentration. However on examination of Figure 143, it can be seen that the final film thickness decreases and dissolution rate increases with increasing temperature. Development of polystyrene in 40:60 v/v MEK/IPA showed a larger degree of initial swelling and throughout the temperature range, the final swelling thickness increased with no dissolution of the polymer (Figure 144). An activation energy of 177.1 kJ mol^{-1} for the swelling of the polymer was obtained from the Arrhenius plot with a linear correlation coefficient of 0.998, as shown in Figure 145.

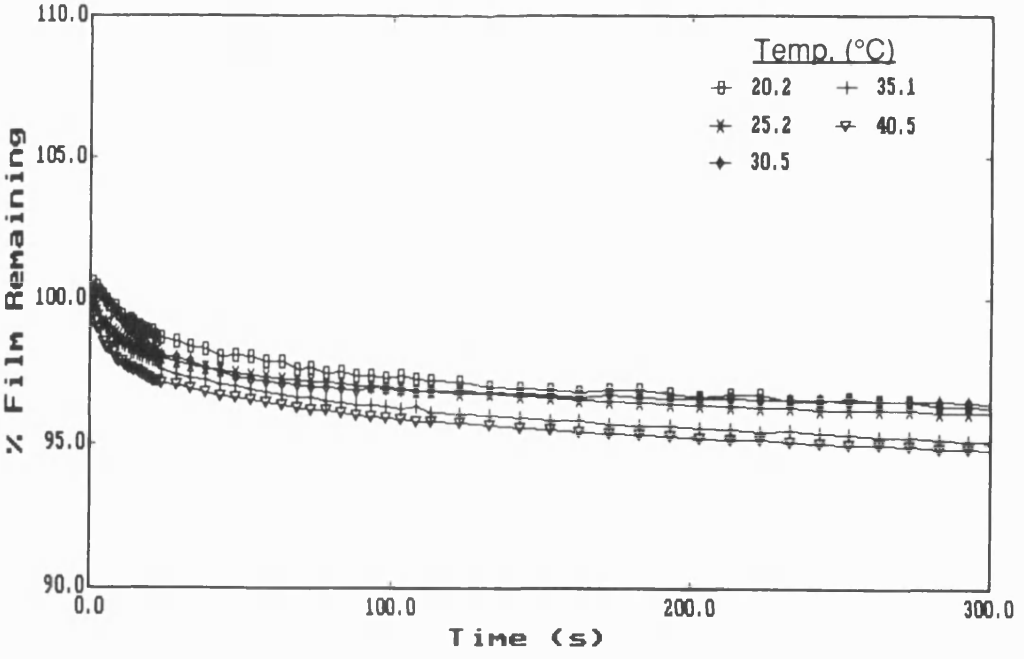

Figure 143: Effect of Temperature on the Dissolution of Polystyrene (M_W 430000) in 50:50 v/v MEK/IPA

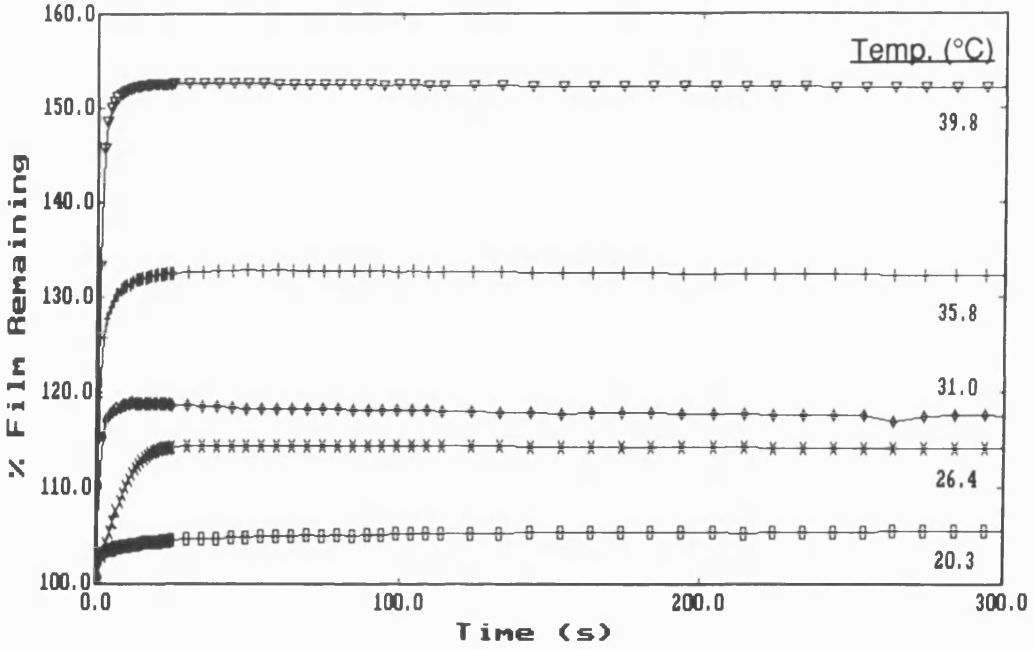

Figure 144: Effect of Temperature on the Swelling of Polystyrene (M_W 430000) in 40:60 v/v MEK/IPA

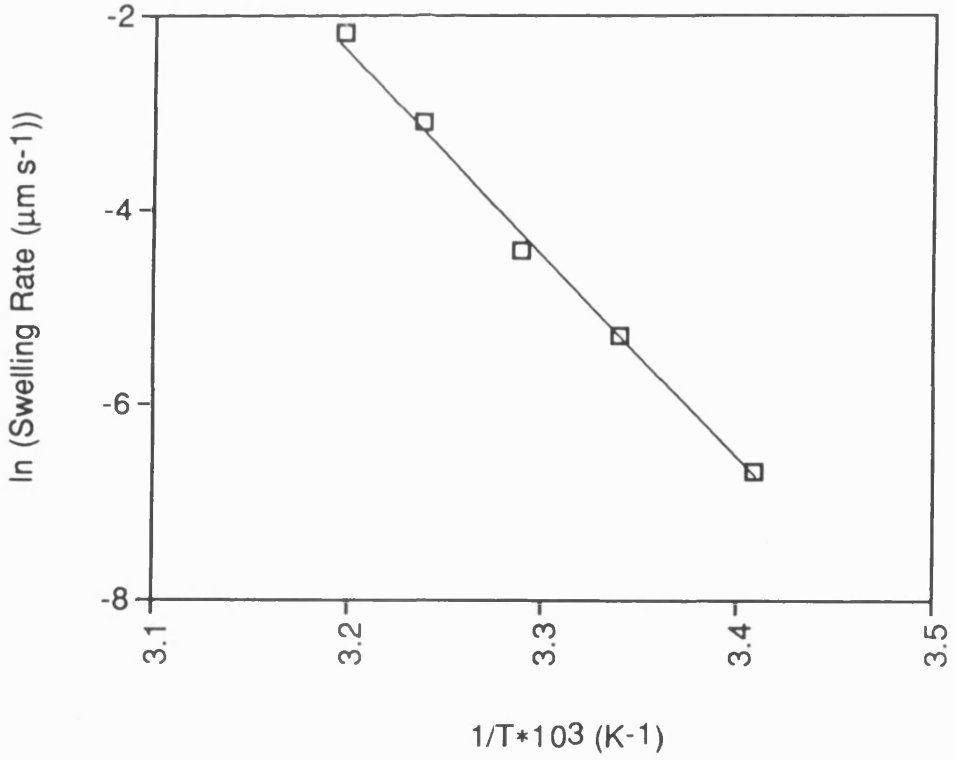

Figure 145: Arrhenius Plot for the Swelling of Polystyrene (M_W 430000) in 40:60 v/v MEK/IPA

In terms of the dissolution mechanism for polystyrene, it seems that the polymer develops a thick swollen layer between the solvent and polymer and this has also been noted by Ueberreiter[39] and Ouano[59]. At the 60:40 v/v MEK/IPA concentration, the slow formation of an initial gel layer is overshadowed by dissolution of the polymer and, even at the low temperatures only the dissolution of the polymer is observed. As the temperature is increased at this concentration, the dissolution rate increases, and the formation of the gel layer is further obscured.

When the concentration of IPA is raised to 60%, the dissolution rate of the polymer is reduced due to the lower concentration of solvent and the initial gel layer is thicker due to the increased fraction of non-solvent swelling the polymer. The swelling of the polymer predominates and hence an overall swelling (gel formation) rate is observed. As the temperature is increased, the swelling rate as opposed to the dissolution rate increases, and no dissolution is observed as there is insufficient solvent present in the system.

The difference in values of activation energy for the dissolution process reflects the need for greater swelling of the polymer film when a larger concentration of non-solvent is used (i.e. higher activation energy value indicating more energy required for movement of the polymer chains).

At the intermediate solvent/non-solvent concentration of 50:50 v/v MEK/IPA, the swelling and dissolution processes appear to be acting with the same effect, as both a small amount of initial swelling and dissolution of the polymer is observed. As the temperature is increased, the amount of swelling observed decreases and the overall dissolution increases. Therefore it can be concluded that the resist dissolution kinetics of polystyrene can be

controlled by the careful selection of both temperature and developer composition.

8.2.1.2 Dissolution of Poly(4-chlorostyrene) in 40:60 v/v MEK/IPA

The results of the development of poly(4-chlorostyrene) (M_n 60000) in 40:60 v/v MEK/IPA over the temperature range 20 - 40°C are shown in Figure 146. Over the complete temperature range, only swelling of the polymer was observed with the total amount of swelling decreasing with increasing temperature whilst, the initial swelling rate increased with an increase in temperature.

On comparison of the swelling curves of polystyrene (M_w 430000, γ 3.1) with those of poly(4-chlorostyrene) in 40:60 v/v MEK/IPA (Figures 144 and 146 respectively), a number of differences can be noted. With increasing temperature, the extent of swelling of polystyrene increase, whilst with poly(4-chlorostyrene) it decreases. Slower initial swelling rates and greater differences in the extent of swelling throughout the temperature range are observed for the development curves than those of poly(4-chlorostyrene). The thermodynamic studies in Chapter 4, indicated that for both polystyrene and poly(4-chlorostyrene) there is poor solvent/polymer interaction between IPA and the polymers. However, poly(4-chlorostyrene) has lower values of Interaction parameter for MEK, particularly at low solvent fractions, indicating that there will be some interactions between the solvent and polymer and may account for the faster initial swelling rate observed for poly(4-chlorostyrene). The extent of swelling is greater for polystyrene as the values of χ for IPA are lower for this polymer than poly(4-chlorostyrene) and hence although IPA is not a solvent for polystyrene there will be greater solvent/polymer interaction.

On consideration of the molecular weights of the two polymers, a slower swelling rate for the higher molecular weight polystyrene sample would be expected. The amount of swelling would also increase with temperature as the longer molecular weight polymer chains become more mobile. It is surprising that the percentage of swollen film for poly(4-chlorostyrene) decreases with increasing temperature. However, the concentration of the solvent/non-solvent may be such that the polymer may be partially soluble in the developer but that the swelling effect of the non-solvent overshadows any dissolution that may occur. With increasing temperature, the polymer will become more soluble and hence less swelling will be observed.

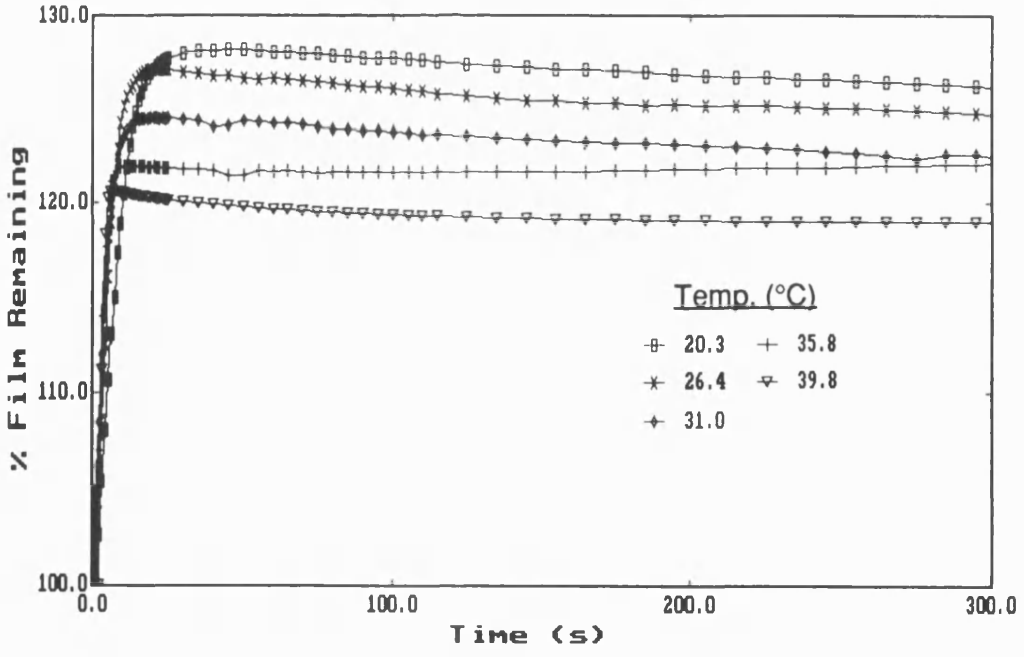

Figure 146: Effect of Temperature on the Swelling of Poly(4-chlorostyrene) in 40:60 v/v MEK/IPA

8.2.2 Dissolution of Poly(phenylmethylsilane)

8.2.2.1 Dissolution of Poly(phenylmethylsilane) in 50:50 v/v MEK/IPA

The dissolution kinetics of the wide polydispersity polysilane sample (see Section 2.3.2.3) has been measured in a 50:50 v/v MEK/IPA mixture over a temperature range of 15 - 40°C (Figure 147). Throughout this temperature range, none of the films went to complete dissolution with the maximum reduction of mass observed at the highest developing temperature (≈45% mass loss). At 15°C, initially a small amount of swelling is observed followed by slow dissolution of the polymer film. Above this developing temperature, no further swelling of the polymer is observed.

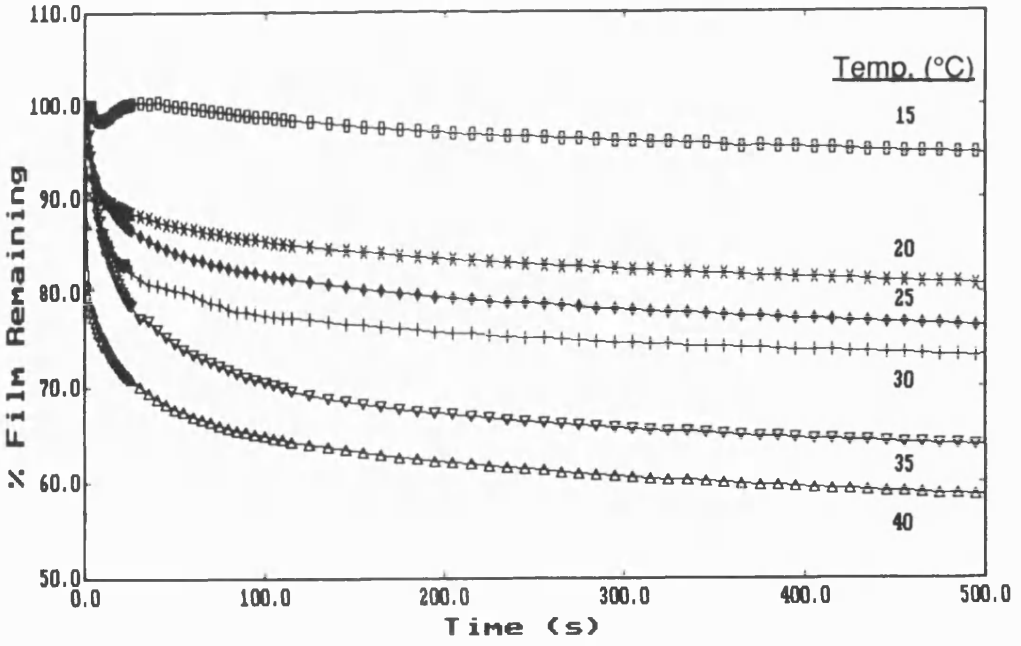

Figure 147: Effect of Temperature on the Dissolution of Poly(phenylmethylsilane) in 50:50 v/v MEK/IPA

The Arrhenius plot for this polymer/solvent system gave an activation energy of 67.7 kJ mol^{-1} (linear correlation coefficient of 0.985) for the dissolution process (Figure 148). This value of activation energy is indicative of a Case II diffusion process[47]. The wide polydispersity of the polysilane samples has helped to reduce the amount of observed initial swelling of the polymer films. By the early removal of the low molecular weight molecules from the surface, the solvent is able to penetrate the network without swelling of the polymer structure.

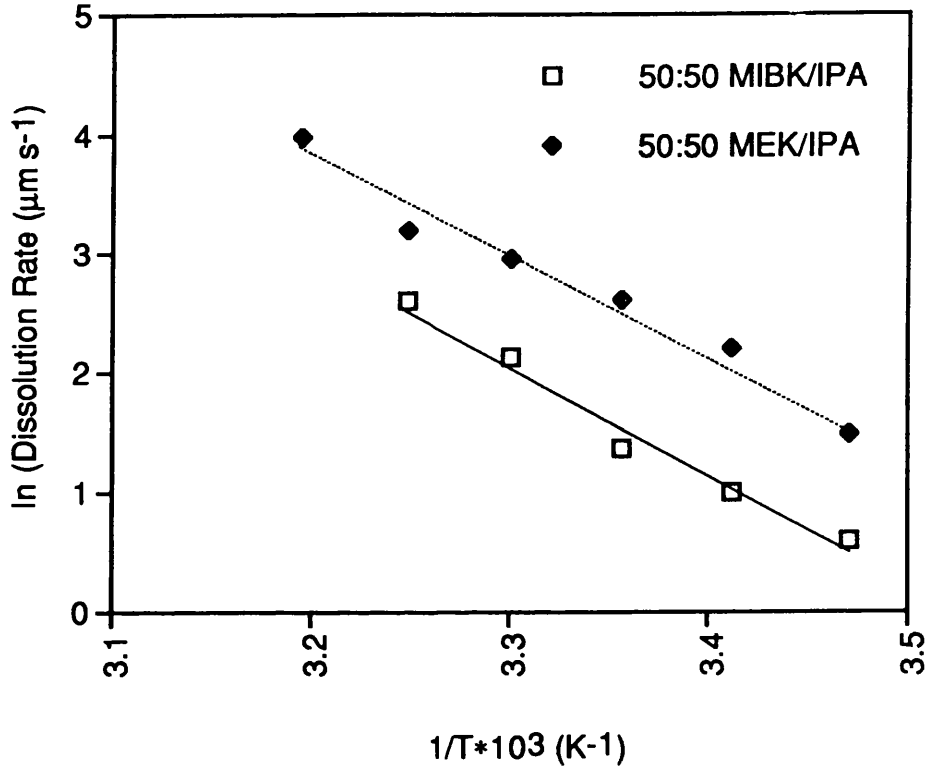

Figure 148: **Arrhenius Plot for the Dissolution of Poly(phenylmethylsilane) (M_n 9600)**

8.2.2.2 Dissolution of Poly(phenylmethylsilane) in 50:50 v/v MIBK/IPA

A series of crystals coated with wide polydispersity poly(phenylmethylsilane) were developed in 50:50 v/v MIBK/IPA over the temperature range 15 - 40°C and the dissolution curves are shown in Figure 149. The curves indicate incomplete dissolution of the films with initial swelling below 20°C. As the developing temperature is increased the degree of swelling decreases and hence the rate determining step is being controlled by a relaxation mechanism in which a sharp boundary exists between the glassy core and the solvent front.

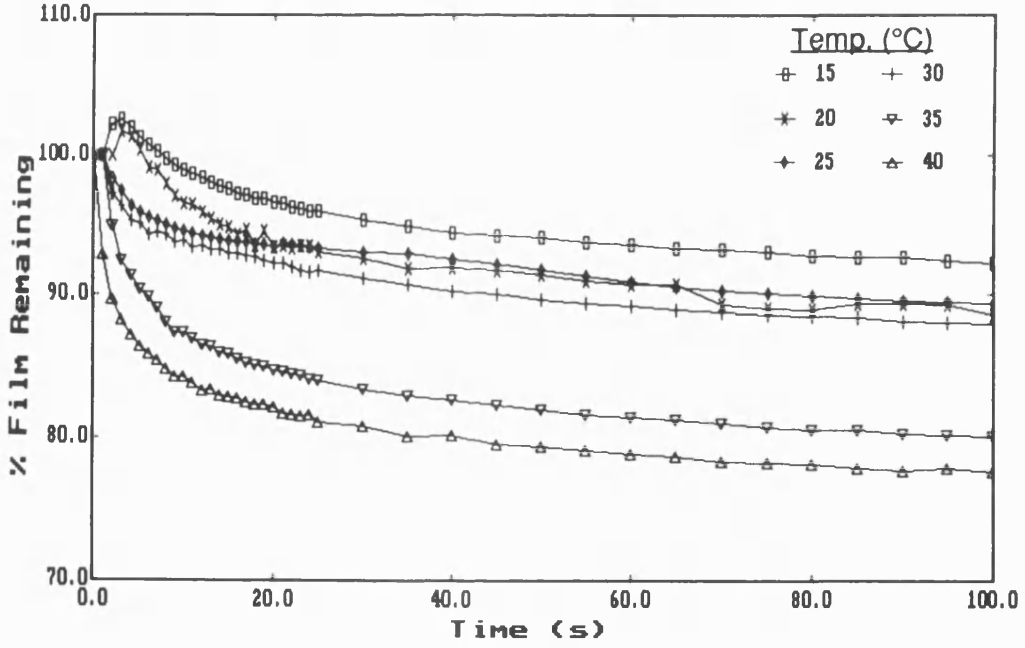

Figure 149: Effect of Temperature on the Dissolution of Poly(phenylmethylsilane) in 50:50 v/v MIBK/IPA

The Arrhenius plot gives an activation energy of 79.5 kJ mol^{-1} (linear correlation coefficient of 0.994). The Arrhenius plots for the dissolution of poly(phenylmethylsilane) in both 50:50 v/v MEK/IPA and 50:50 v/v MIBK/IPA have been combined in Figure 148. The MEK/IPA system gives faster dissolution rates throughout the temperature range studied. However, similar activation energies are observed as indicated by the slopes of the Arrhenius plots hence the same diffusion process is operating. As there is the same proportion of non-solvent present in the two systems, it can be inferred that MIBK is a poorer solvent for polysilane which may be due to the bulkier nature of the MIBK molecule (i.e. MEK is a smaller molecule and hence can diffuse more rapidly into the polymer structure).

8.2.2.3 Dissolution of Poly(phenylmethylsilane) in 75:25 v/v MEK/IPA

The effect of changing temperature on the dissolution kinetics of the molecular weight series of poly(phenylmethylsilane) in 75:25 v/v MEK/IPA has been measured. A variety of dissolution/swelling behaviour was observed throughout this molecular weight/temperature range as detailed in Section 8.1.2. Generally, an increase in temperature or decrease in molecular weight enhances the dissolution rate of the polymer and, conversely, a decrease in percentage of swelling of the film is observed. For the development time studied (1000 s), the total amount of film removed increases with temperature, however none of the polysilane films went to complete dissolution.

Figure 133 shows the dissolution curves for the M_n 7500 sample. Throughout the temperature range studied, the polymer initially dissolves without swelling with the rate and total removal of film increasing with

temperature. The M_n 9600 standard (Figure 134) dissolves at slower rates and there is less variation of rate with temperature. On consideration of the molecular weights of the two samples, it is surprising that there is such a large difference in the dissolution rates. As stated in Section 8.1.2, the deviation in dissolution behaviour may be partly accounted for by the differences in polydispersity of the samples. The temperature dependence of dissolution of poly(phenylmethylsilane) appears to be greater for higher polydispersity samples.

As the molecular weight of the polymer is increased from 14500 to 18400, swelling of the polymer is observed (Figures 135 and 136) with the percentage of swelling decreasing with temperature. With further increases in molecular weight similar dissolution patterns are observed with the rate of dissolution decreasing and percentage of swelling increasing with decreasing temperature.

As Figures 138 and 139 indicates for the dissolution of M_n 36500 and 53700, there is a similarity in dissolution curves despite the differences in molecular weight and this again can be attributed to the differences in polydispersity of the two samples (1.8 and 5.8 respectively).

The Arrhenius plots for the molecular weight series are shown in Figure 150. The Figure clearly shows that polydispersity of the polymer can affect the dissolution characteristics of the polymer. A linear relationship is observed throughout the molecular weight range and the slopes of the lines are proportional to the activation energy. Table 16 shows the gradients and linear correlation coefficients for the molecular weight series obtained from the Arrhenius plots. For the complete molecular weight range studied, there is good correlation of data.

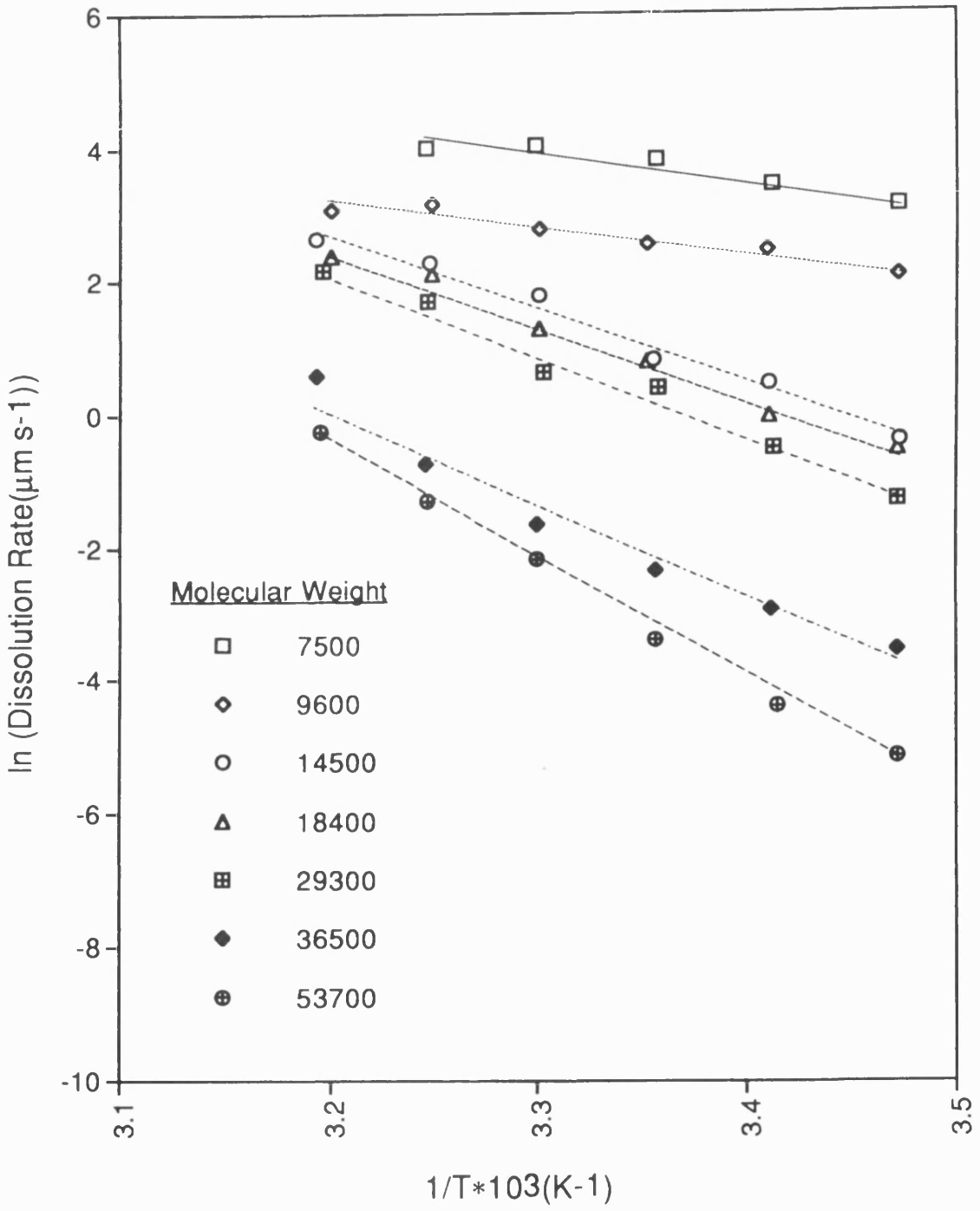

Figure 150: Dissolution of Poly(phenylmethylsilane) in 75:25 v/v MEK/IPA

Polymer M_n	Slope (y = mx + c) *(linear correlation coefficient)*
7500	-4.190x +17.766 *(0.951)*
9600	-3.870x + 15.584 *(0.969)*
14500	-11.054x + 38.089 *(0.992)*
18400	-11.201x + 38.323 *(0.995)*
29300	-12.363x + 41.716 *(0.993)*
36500	-14.267x + 45.747 *(0.984)*
53700	-18.014x + 57.235 *(0.998)*

Table 16: The Gradients and Linear Correlation Coefficients for the Arrhenius Plots in Figure 150

Generally, the activation energy for the dissolution of polysilanes in 75:25 v/v MEK/IPA increases with molecular weight. There is a large increase in activation energy (i.e. 32.2 - 91.9 kJ mol^{-1}) when the polymer is observed to swell (i.e. between M_n 9600 and 14500). This is a reflection of the increased movement of the polymer chains needed to allow the diffusion of the solvent molecules for the longer polymer chains. Above M_n 9600, the value of activation energy ranges from 91.9 to 149.8 kJ mol^{-1}. A similar increase in activation energy has been found for the dissolution of PMMA in MEK (see Section 6.1).

8.2.3 Dissolution of Poly(vinyl cinnamate)

Poly(vinyl cinnamate) (an example of a negative resist) has poor solubility in solvents such as MEK and MIBK which are conventionally used in the wet development of resists. Hence, alternative solvents which are used commercially have been used to study the effect of temperature on the dissolution of poly(vinyl cinnamate).

8.2.3.1 Dissolution of Poly(vinyl cinnamate) in a Series of Solvents

A series of poly(vinyl cinnamate) coated crystals were developed in toluene, acetone and xylene over a temperature range 15 - 35°C and the dissolution curves are shown in Figures 151, 152 and 153 respectively.

In toluene, partial dissolution with no initial swelling was observed throughout the temperature range with only 50% of the polymer film removed even at the highest developing temperature (i.e. 35°C). In acetone, initial swelling of the polymer film was observed for developing temperatures below 25°C, and the swelling increased with decreasing temperature (maximum 10% mass increase). There is a marked difference in the dissolution/swelling kinetics for the development of poly(vinyl cinnamate) in xylene (Figure 153). At temperatures below 25°C, the initial swelling of the polymer film predominated the dissolution process and only the swelling of the film could be monitored. The amount of initial swelling and swelling rate increased with increasing temperature (until 30°C where the dissolution process dominates the initial swelling). The overall dissolution rate of the polymer also increased with temperature, so the swelling curve becomes broader with decreasing temperature. Over the complete temperature range, the poly(vinyl cinnamate) films exhibited incomplete dissolution.

Figure 154 shows the Arrhenius plot for the dissolution of poly(vinyl cinnamate) in the three solvents. Table 17 gives the activation energies for the dissolution of the polymer/solvent systems and an indication of the goodness of fit of our results. The low values of activation energy for toluene and acetone indicate the narrow distribution of dissolution rates over the temperature range studied and the similarity of the values indicates that the same dissolution process is operating. The Arrhenius plot for the dissolution of poly(vinyl cinnamate) in xylene gives a much higher activation energy value.

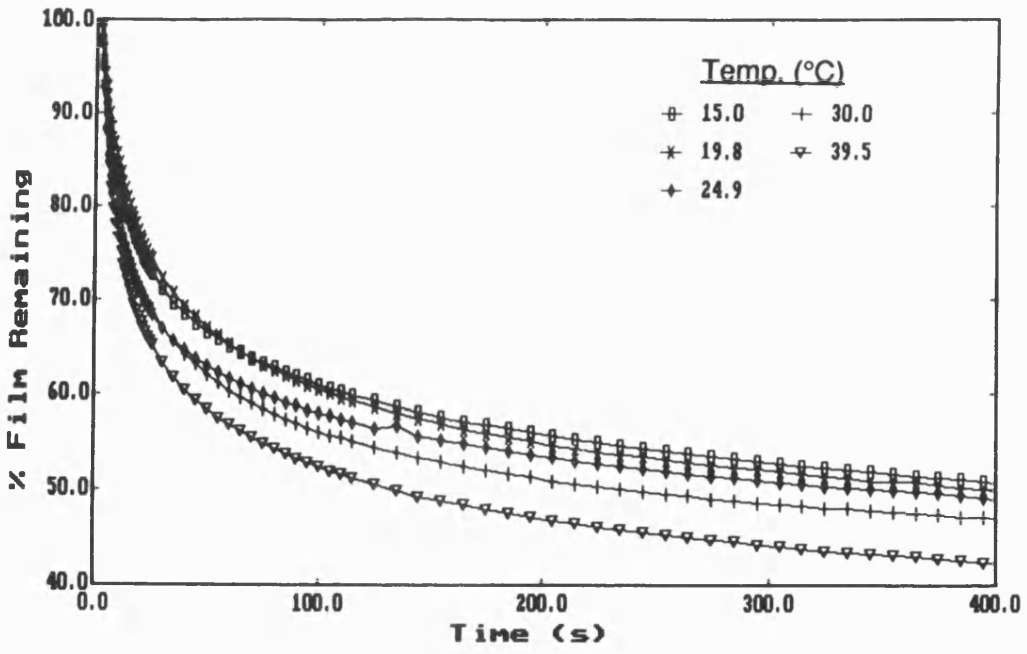

Figure 151: **Effect of Temperature on the Dissolution of Poly(vinyl cinnamate) in Toluene**

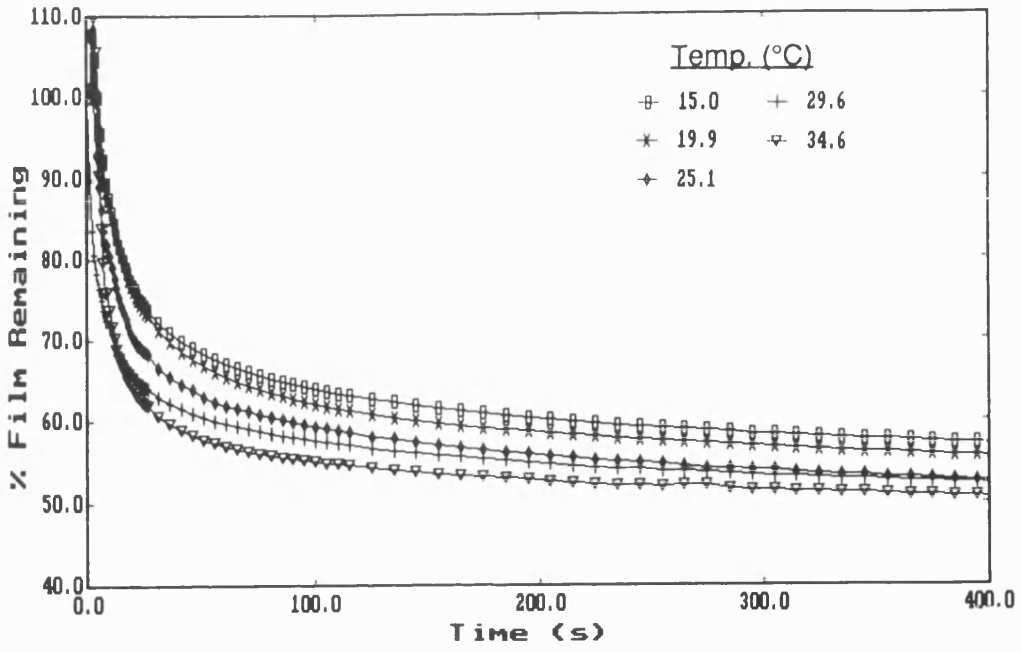

Figure 152: Effect of Temperature on the Dissolution of Poly(vinyl cinnamate) in Acetone

On comparison of the Arrhenius plots and activation energies for the dissolution of poly(vinyl cinnamate) in toluene and acetone, it is evident that changing of the developing temperature will have little effect on the dissolution characteristics of poly(vinyl cinnamate). However, a greater temperature dependence is found for xylene and this is reflected by the steeper gradient of the Arrhenius plot and hence higher activation energy. Therefore to obtain good resolution of a poly(vinyl cinnamate) resist, the choice of an appropriate developing temperature, in order to minimise the amount of swelling of the film, is more important when using xylene as a developing solvent. These observations illustrate the importance of choosing both developing temperature and type of solvent system in tandem prior to the development of a resist system.

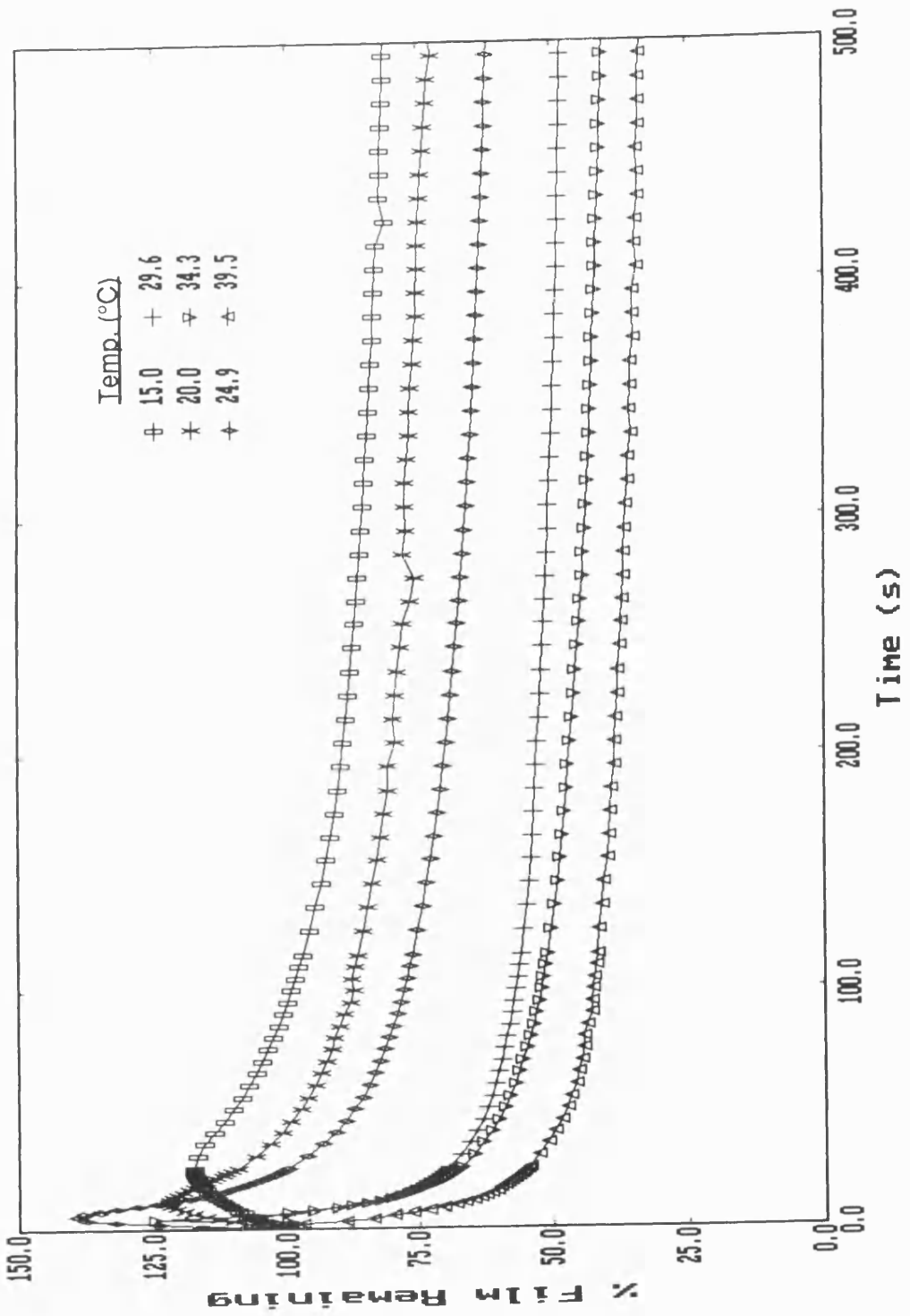

Figure 153: Effect of Temperature on the Dissolution of Poly(vinyl cinnamate) in Xylene

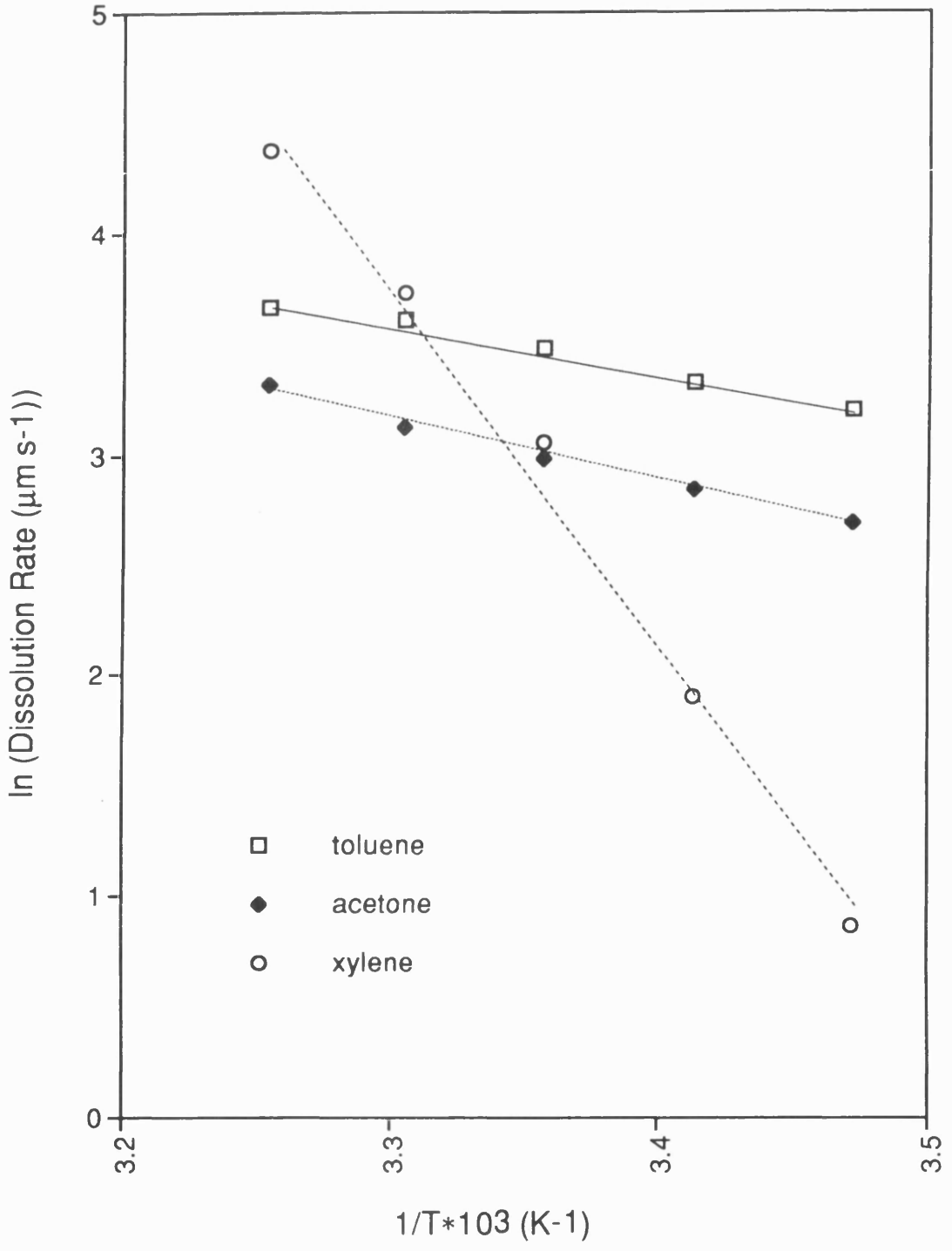

Figure 154: Arrhenius Plots for the Dissolution of Poly(vinyl cinnamate) in a Series of Solvents

Solvent	Equation (y = mx + c)	Linear Correlation Coefficient	E_a (kJ mol^{-1})
Toluene	-2.20x + 10.87	0.993	18.3
Acetone	-2.80x + 12.36	0.996	23.3
Xylene	-16.33x + 57.67	0.995	135.8

Table 17: The Gradients and Linear Correlation Coefficients for Figure 154

We have shown that changing the development temperature can be used to adjust the swelling/dissolution kinetics of polymers. Whilst swelling of the polymer at the low temperatures complicates the dissolution kinetics and can cause loss of adhesion of the resist to the substrate due to the stress force imposed, it can be useful in inhibiting the dissolution of unexposed parts of the resists.

8.3 Effect of Solvent Composition on Polymer Dissolution

As we have observed in Chapter 7, both the solvent and non-solvent concentration can have a great effect on the resolution of the resist. The dissolution kinetics of polystyrene and poly(phenylmethylsilane) in solvent/non-solvent mixtures have been measured and the effect of swelling of the polymer during development has been considered with respect to resist resolution.

8.3.1 Dissolution of Polystyrene in MEK/IPA Mixtures

Since cross-linking in negative resists produces a drastic change in solubility, a wide range of solvents could be used for development. However a common problem with cross-linked polymers is their swelling during development, and this can overcome the adhesion of the resist to produce complete delamination. In thermodynamically good solvents, styrene-based resists can be prone to swelling of images upon development[204], whilst in developers which are poor thermodynamic solvents the resist does not appreciably swell[205]. It is therefore important that a good choice of solvent is made to suppress this swelling and a knowledge of the factors affecting the swelling kinetics will aid in this choice.

The effect of changing the solvent/non-solvent composition on the development of unexposed polystyrene (M_W 430000, γ 3.1) for the developer system MEK/IPA was studied at 20 and 40°C, and the results are shown in Figures 155 and 156 respectively. MEK is a thermodynamically good solvent for polystyrene whilst IPA is a non-solvent. Our thermodynamic studies (Section 4.2.6) have shown that MEK has much lower values of χ than IPA for the sorption on polystyrene. As the concentration of IPA is increased the

value of χ increases indicating that IPA is becoming thermodynamically comparable with polystyrene.

At 40°C, some dissolution of the polymer is observed for the concentrations 60:40 and 50:50 v/v MEK/IPA with the rate of dissolution slowing down as the concentration of non-solvent is increased, but with only partial dissolution observed. As the concentration of IPA was increased further to 60%, a degree of swelling in the polystyrene films was observed with no dissolution taking place. At the lower temperature, swelling of the polystyrene was also observed at 60% IPA, and the polymer initially swelled at 50% IPA before partial dissolution. At the higher concentration of MEK (i.e. 60:40) only partial dissolution with no swelling occurred. As observed in Section 8.2.1.1, the rate of swelling and dissolution and the polymer film thickness decreased with decreasing temperature.

In their study of the dissolution dynamics of polystyrene in MEK at room temperature using critical angle illumination microscopy, Ouano and Carothers[59] found that polystyrene develops a thick swollen layer between the liquid and glassy layers. Ueberreiter[39] and Alfrey[47] have also observed this boundary although Alfrey has also observed cracking of the sample.

With the QCM method, it is difficult to completely observe this boundary layer as it becomes obscured by the overall dissolution of the polymer. However, we can observe the initial formation of the boundary and the extent of the boundary between the glassy region and the solvent is found to increase at lower concentrations, i.e. the size of gel layer increased. It seems that at a higher concentration of solvent (i.e. 60:40), dissolution of the polymer commences before the formation of a gel layer. As the temperature is increased, a higher concentration of non-solvent is required to observe the

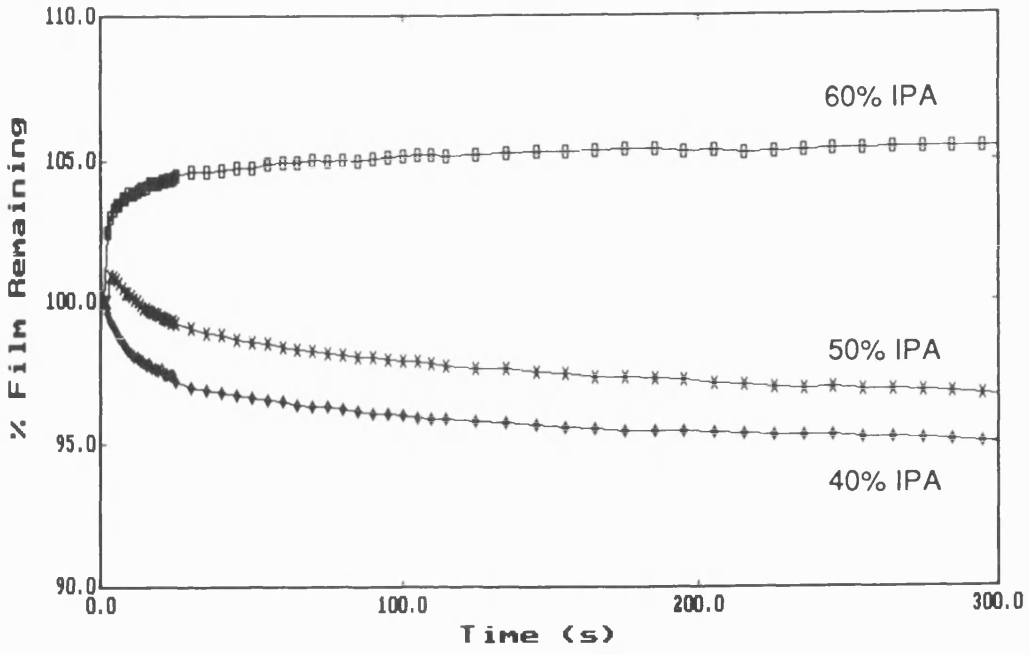

Figure 155: Dissolution of Polystyrene (M_n 430000) in MEK/IPA at 20°C

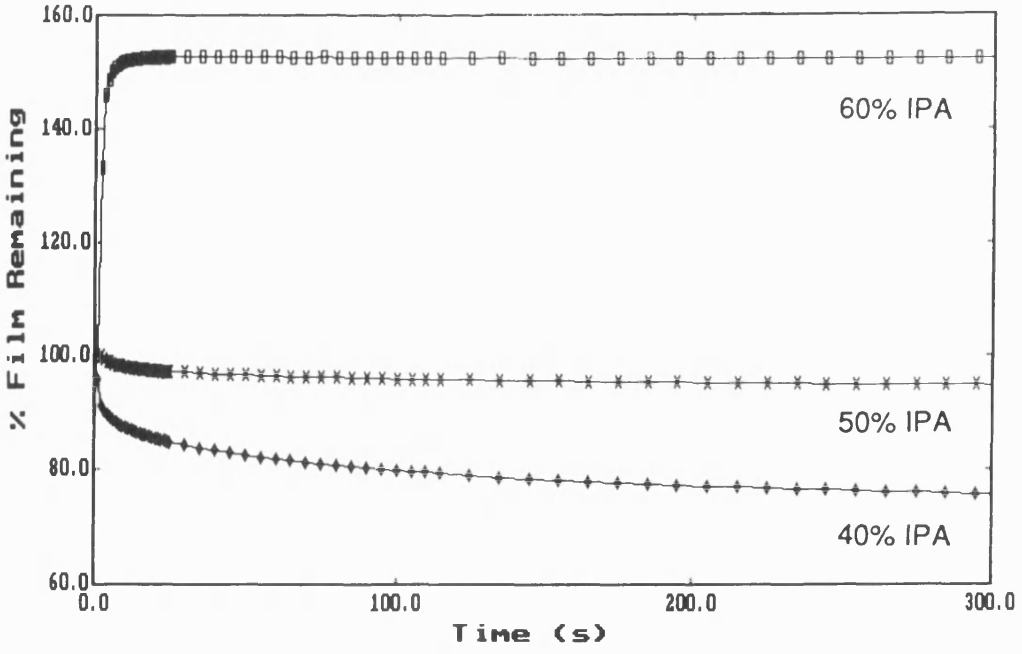

Figure 156: Dissolution of Polystyrene (M_n 430000) in MEK/IPA at 40°C

formation of the gel layer, because the dissolution rate increases and hence a larger proportion of polymer is dissolved before the gel layer is formed. At the 40:60 v/v MEK/IPA concentration, it seems that the gel layer is formed within a few seconds and the concentration of non-solvent is such that the rate of swelling of the polymer dominates its dissolution rate and an overall swelling is observed. At 50:50 v/v MEK/IPA concentration, the polymer dissolution proceeds at the same rate as polymer transition to the gel state, and hence neither effect is observed to a great extent.

Figure 157 shows the change of normalised film thickness with respect to the log of swelling rate for the swelling of polystyrene in 40:60 v/v MEK/IPA. The results show a break in linearity at the swelling rate equivalent to the swelling of polystyrene at 30°C. The corresponding plot for the dissolution of polystyrene in 60:40 v/v MEK/IPA also shows a break in linearity at 30°C (Figure 158). Steeper slopes are observed for the lower developing temperatures, indicating that there is less variation of film thickness with swelling or dissolution rate at low temperatures. At a developing temperature of 30°C, there appears to be a change in the diffusion mechanism from Case II to Fickian i.e. the system becomes less controlled by the relaxation of the polymer as the temperature is increased.

We have therefore seen from our results that the rate of dissolution and swelling of polystyrene films can be moderated by the careful selection of solvent/non-solvent mixtures and that the change in dissolution/swelling rates with temperature may deviate if a change in diffusion mechanism occurs.

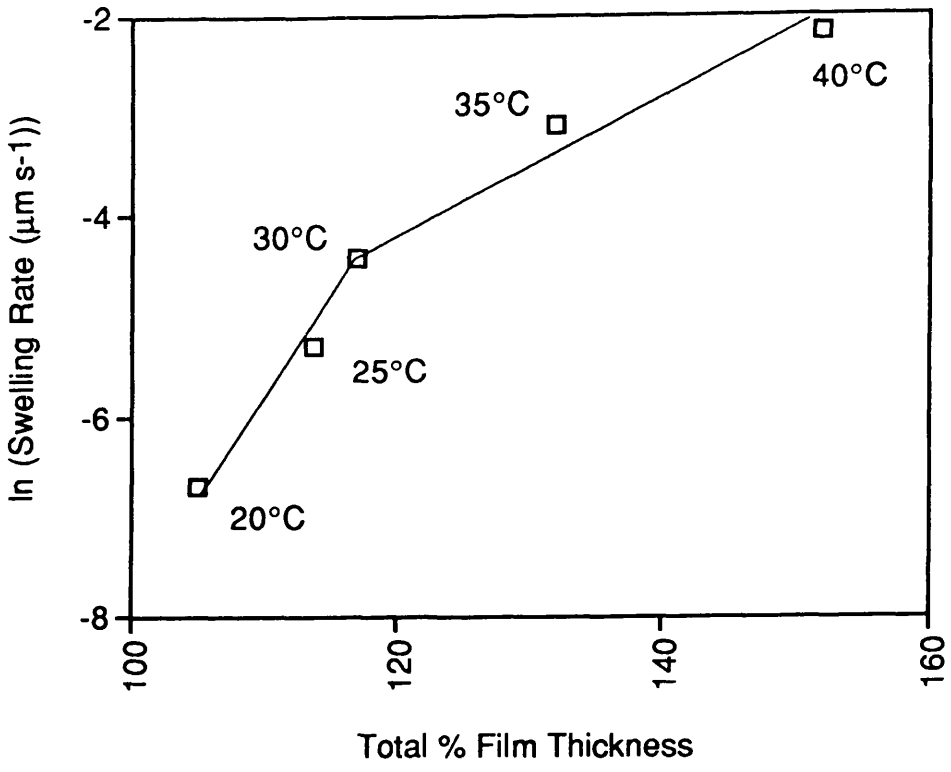

Figure 157: Swelling of Polystyrene in 40:60 v/v MEK/IPA

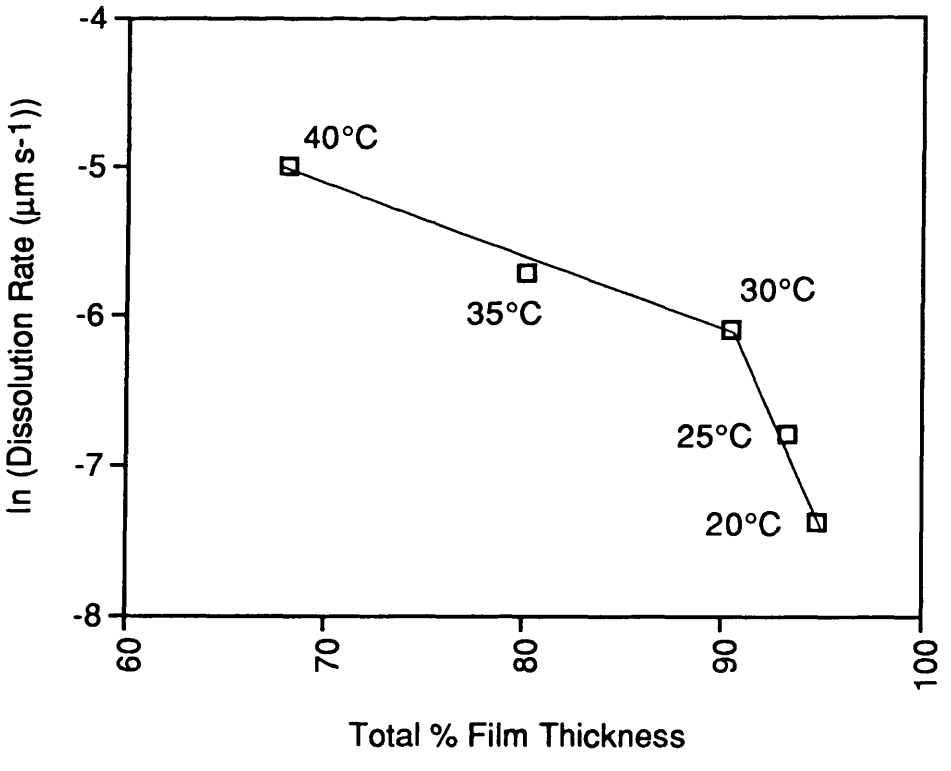

Figure 158: Dissolution of Polystyrene in 60:40 v/v MEK/IPA

8.3.2 Dissolution of Poly(phenylmethylsilane) in MIBK/IPA Mixtures

The effect of the addition of IPA to MIBK on the developing characteristics of poly(phenylmethylsilane) has been studied. A series of polysilane (M_n 9600, γ 6.2) coated quartz crystals were developed in MIBK/IPA mixtures of varied compositions at 24.7°C. IPA is a non-solvent for poly(phenylmethylsilane) and should help to moderate the dissolution kinetics.

In pure MIBK, approximately 30% of the polysilane dissolved before dissolution ceased. In a 10% v/v IPA/MIBK mixture, a slower initial dissolution rate was observed and only 20% of the film was removed before the cessation of dissolution. As the concentration of non-solvent (i.e. IPA) was increased further, the dissolution rate and the percentage of film removed decreased. At a concentration of 50% v/v IPA/MIBK, initial swelling was observed, and the percentage of initial swelling increased with the concentration of non-solvent. Beyond 80% v/v IPA/MIBK, the polysilane film became swollen and did not dissolve in the developing mixture.

The effect of changing the percentage of non-solvent on the rate of dissolution of poly(phenylmethylsilane) is shown in Figure 159 and the dissolution rate is shown to be a logarithmic function of the concentration of MEK (Figure 160). As expected the alcohol moderates the dissolution rate of the polysilane, but it also enhances the swelling of the film indicating that care must be taken in choosing the appropriate solvent/non-solvent concentrations for development of polymer systems. The log-log plot of dissolution rate versus % MIBK can be represented as two straight lines with a break in linearity at 50% MIBK.

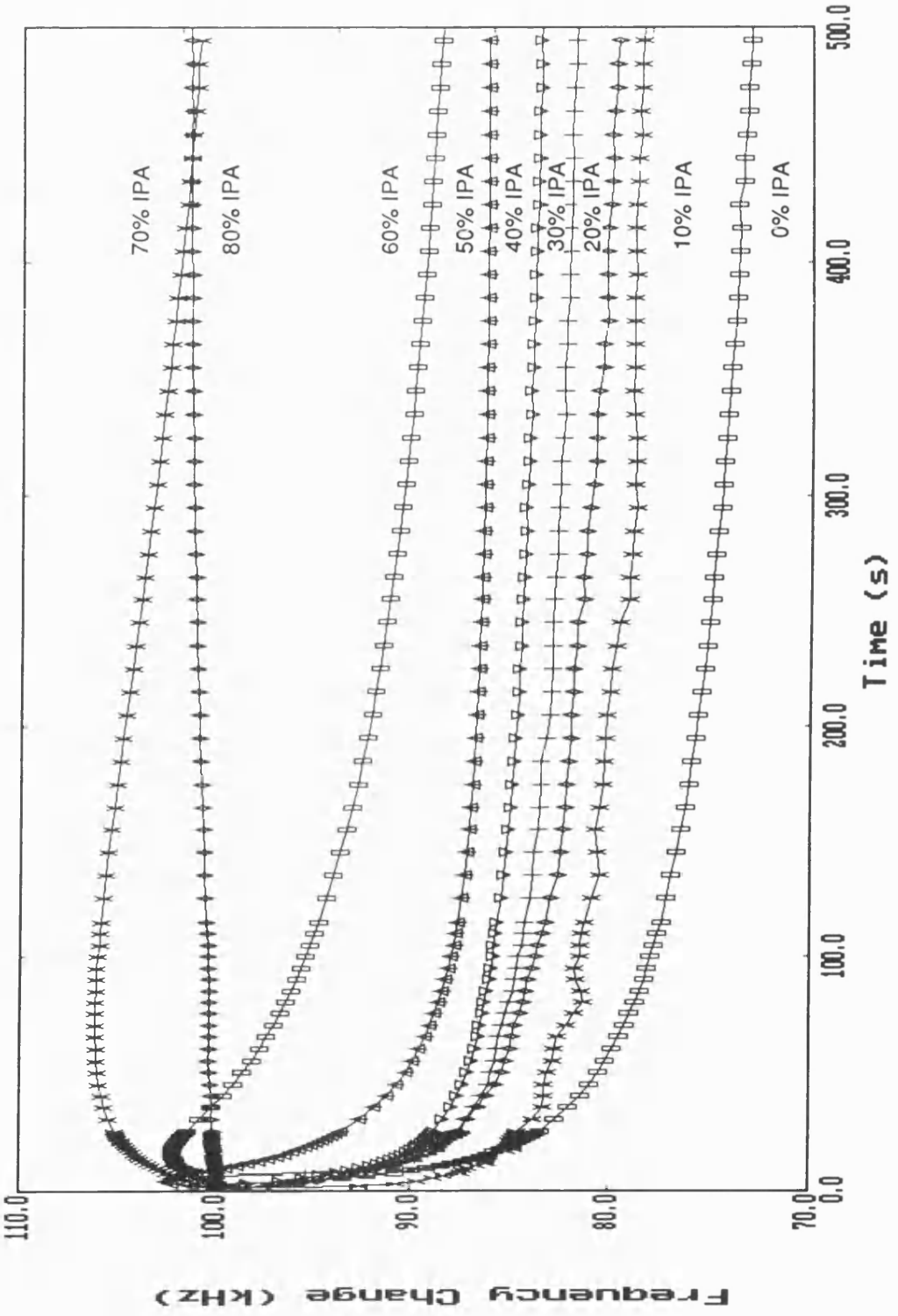

Figure 159: Effect of Composition on the Dissolution of Poly(phenylmethylsilane) in MIBK/IPA at 24.7°C

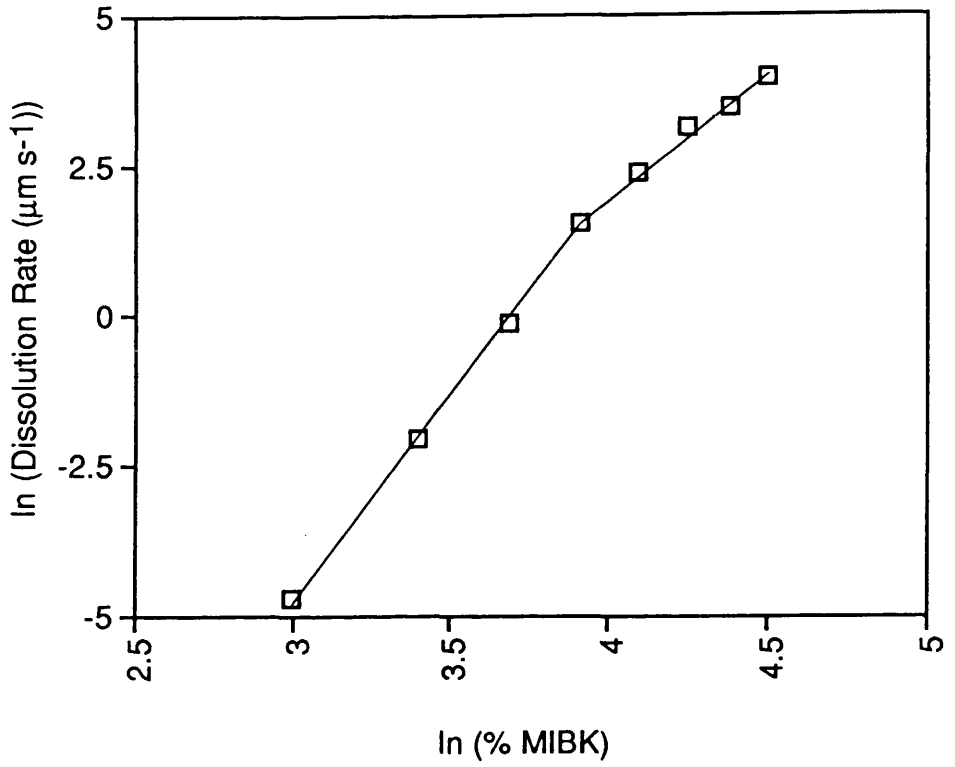

Figure 160: Dissolution of Poly(phenylmethylsilane) at 24.7°C Effect of MIBK/IPA Concentration

This can be more clearly demonstrated when considering the log of dissolution rate versus % MIBK (Figure 161) where a more obvious change in slope can be observed. It appears that there is a greater distinction between dissolution rates with % MIBK when swelling of the films becomes a predominant factor (i.e. at 50% MIBK). Closer observation of Figure 161, indicates an enhancement of the dissolution rate at low concentrations of non-solvent. This is similar to the effect that we have observed in Section 7.1.2 for the dissolution of PMMA in MEK/alcohol mixtures. Further analysis of this polymer/developer system is required to gain a further insight into the dissolution kinetics.

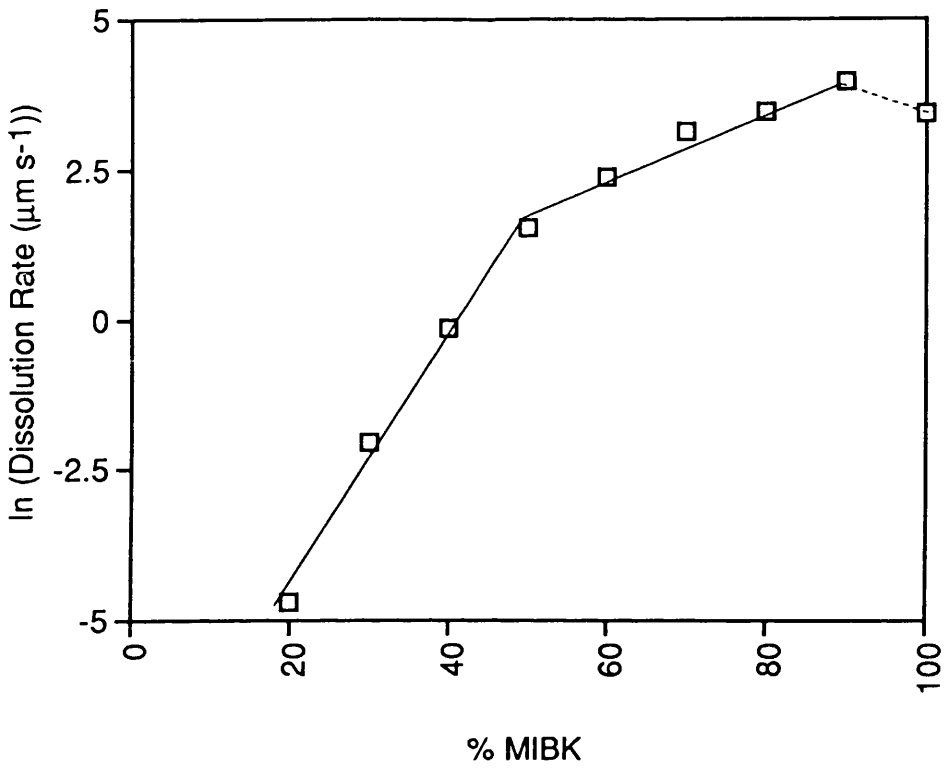

Figure 161: **Dissolution of Poly(phenylmethylsilane) at 24.7°C**
Effect of MIBK/IPA Concentration

We have shown that by the variation of certain solvent/non-solvent compositions, the dissolution/swelling kinetics of polymers can be altered to such an extent that changes in the diffusion mechanisms can be observed.

8.4 Conclusion

In this Chapter, we have attempted to demonstrate the effect of polymer molecular weight, temperature and solvent composition upon the dissolution characteristics of both positive and negative resists. It has been shown for polystyrene and poly(phenylmethylsilane)/solvent systems that the dissolution rate increases with decreasing molecular weight and increasing polydispersity and that these variables must be considered in unison when predicting dissolution behaviour. The log-log plot of molecular weight and dissolution rate for the development of polysilane in MEK/IPA has not shown the break in linearity observed for the PMMA system, while the activation energy is found to increase with molecular weight.

It has been shown that adjustment of the developing temperature of polystyrene in MEK/IPA can moderate the observed polymer swelling and a change in diffusion mechanism with temperature has been indicated for various ratios of solvent/non-solvent. The Arrhenius plots of poly(vinyl cinnamate) in acetone, xylene and toluene have demonstrated the importance of choosing the developing temperature in tandem with the solvent.

Chapter Nine

9.0 Ultraviolet Exposure of Resist Systems

Although the major aim of the work was to measure the parameters important in resist dissolution, as described in the previous chapters, it was also desirable to illustrate the potential of the apparatus under real conditions. Therefore as the final phase of the studies, quartz crystals were coated with a series of polymers and exposed to UV irradiation and their swelling/dissolution rates measured.

9.1 UV Exposure of PMMA

Resists based on PMMA have been widely used for deep UV lithography owing to the polymer's spectral absorption below 240 nm which, as detailed in Section 1.1.2.2, leads to chain scission. The reduction in molecular weight enhances the solubility of the polymer in a particular developing solvent system, to produce faster dissolution rates.

9.1.1 MIBK/IPA Developer Mixtures

Initial studies of the effect of UV exposure on PMMA were performed using both the UVA and Hanovia lamp (see Chapter 2). A series of exposed PMMA coated crystals were developed in a 75:25 v/v MIBK/IPA solvent/non-solvent system at 25.0°C, and the observed dissolution curves for exposure with the UVA lamp can be seen in Figure 162. The rate of dissolution increases and the initial swelling observed gradually diminishes with increased exposure time. The amount of swelling of the polymer film is enhanced by the presence of the IPA with the non-solvent moderating the rate of dissolution. Figure 163 shows there is a linear relationship between log dissolution rate and time.

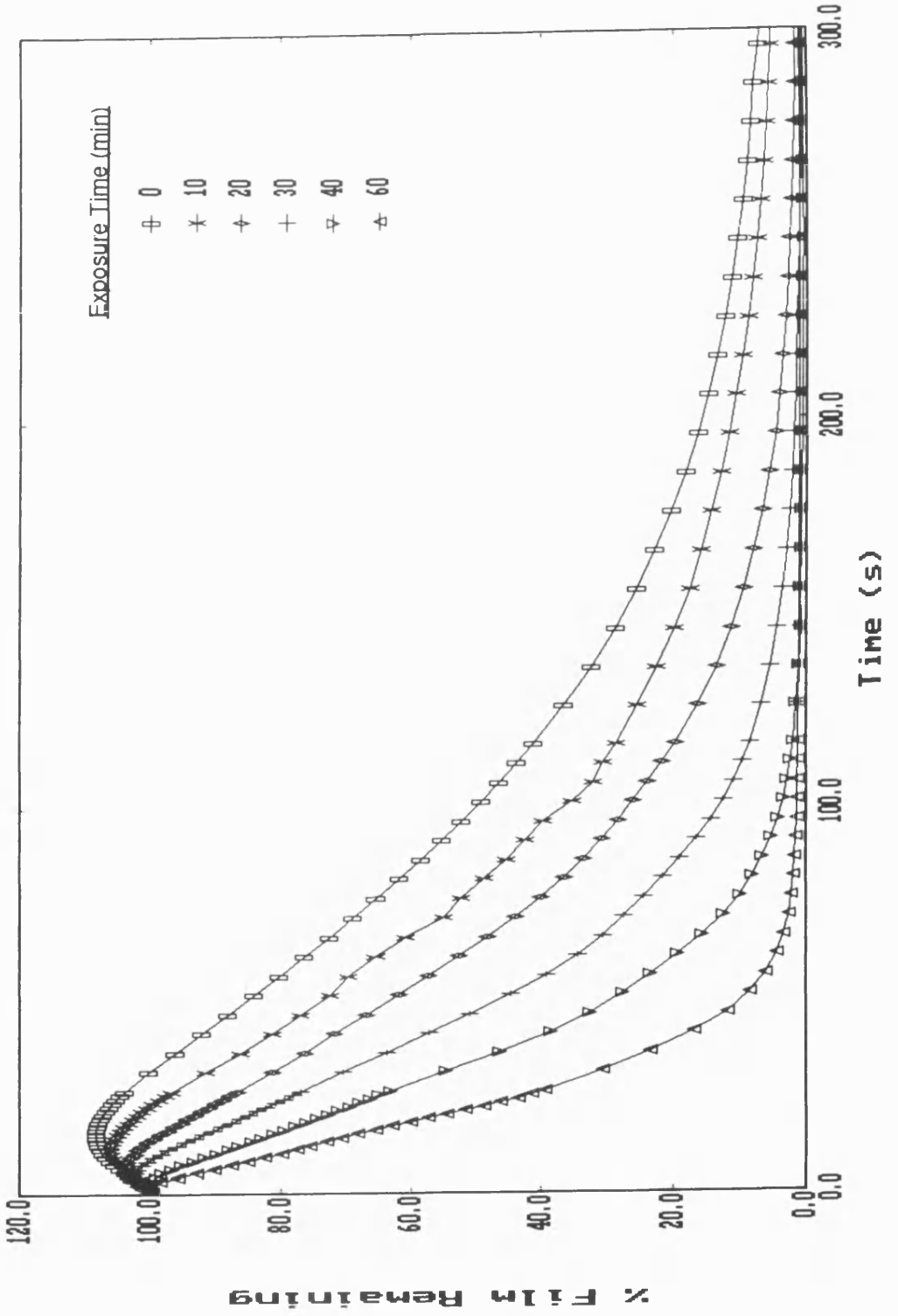

Figure 162: Effect of UV Exposure on the Dissolution of PMMA in 75:25 v/v MIBK/IPA at 25.0°C - UVA Lamp

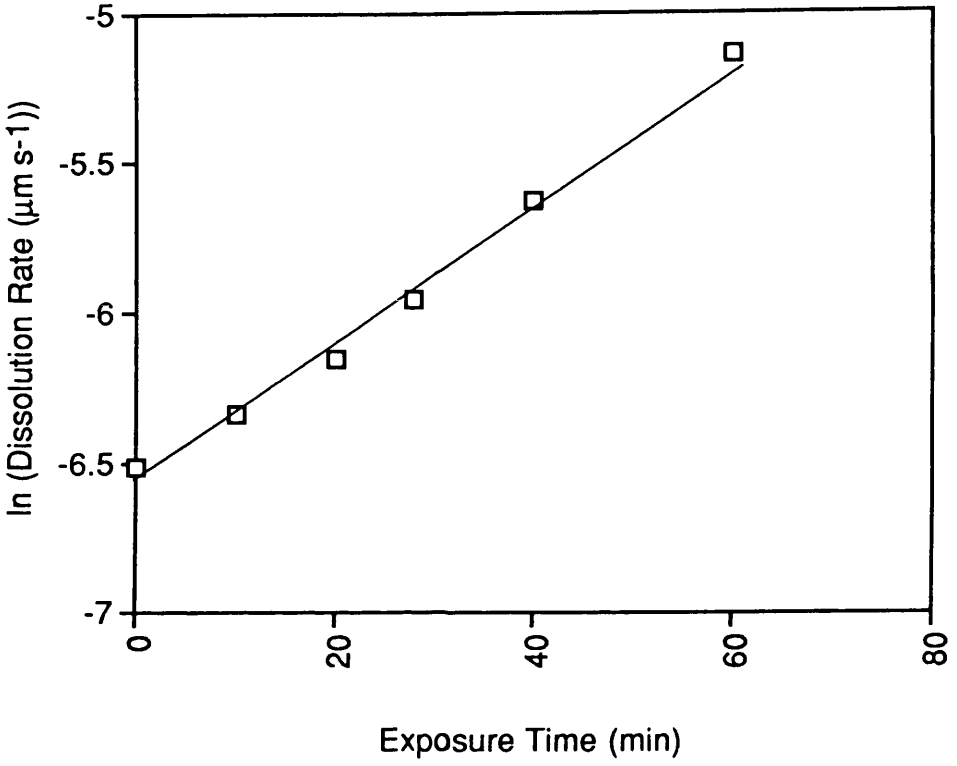

Figure 163: Effect of UV Exposure on the Dissolution of PMMA in 75:25 v/v MIBK/IPA at 25.0°C - UVA Lamp

Another series of PMMA coated crystals were exposed with the Hanovia lamp and developed in the same solvent system at both 25.0 and 18.0°C. No initial swelling of the polymer was found for both developing temperatures and complete dissolution was observed. The effect of UV exposure on the rate of dissolution of PMMA in this solvent system at both temperatures was shown to be a logarithmic function of exposure time (see Figure 164).

There is no difference between the slope of the lines for the respective temperatures, even though the higher temperature shows the expected enhanced dissolution rate.

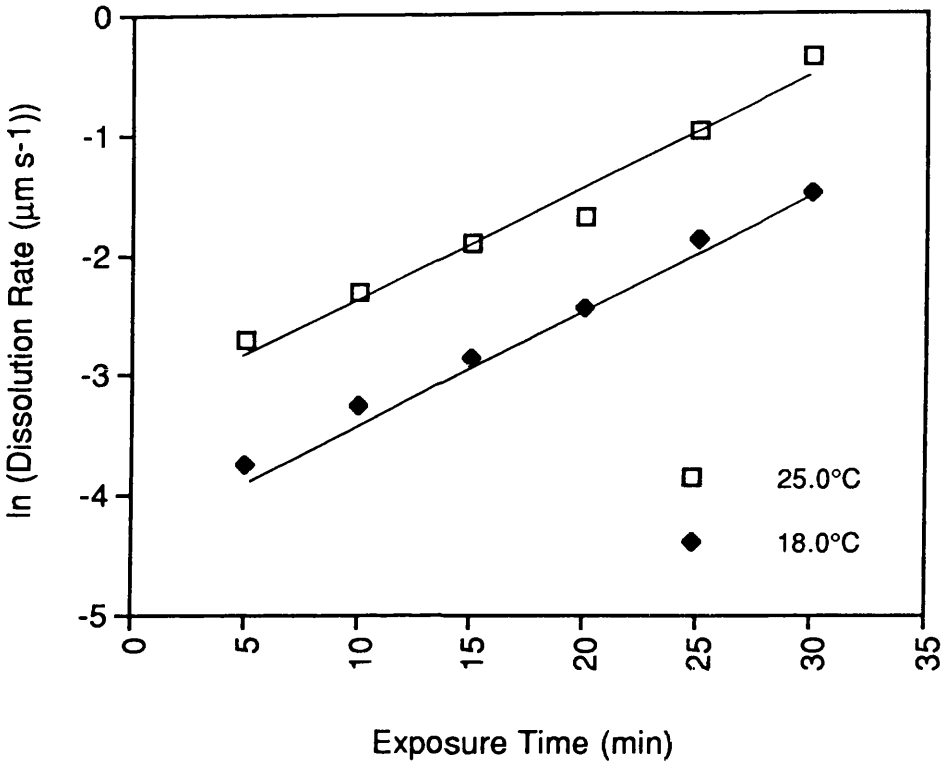

Figure 164: Effect of UV Exposure on the Dissolution of PMMA in 75:25 v/v MIBK/IPA - Hanovia Lamp

Slopes *(linear correlation coefficient)*

25.0°C: y = 0.09x - 3.25 *(0.987)*

18.0°C: y = 0.09x - 4.20 *(0.999)*

Ouano[40] also observed no change in the slope for the electron-beam exposure of PMMA developed in MIBK at three different temperatures. Because of the lower intensity of the UVA lamp, the enhancement of the dissolution rate with respect to exposure time was found to be lower by comparison of the slopes of Figures 163 and 164.

Greeneich[189] performed initial studies on the solubility characteristics of PMMA as an electron beam resist for developer

combinations of MIBK and IPA. The solubility rate was determined in terms of the fragmented molecular weight upon electron-beam exposure and the energy absorbed by the polymer in degrading to the lower molecular weight. An enhancement of dissolution rate was observed with energy absorbed (i.e. exposure), however, complete dissolution curves were not produced as the "Dip and Dry" method (with thicknesses measured by ellipsometry) was the measurement method and hence, only overall dissolution rates are quoted with no information on any swelling phenomena.

9.1.2 MEK/IPA Developer Mixtures

PMMA coated crystals exposed to the UVA lamp were developed in a 50:50 v/v MEK/IPA developer system at 20.5°C. The enhancement in dissolution rate with respect to exposure time followed a logarithmic form, as shown in Figure 165.

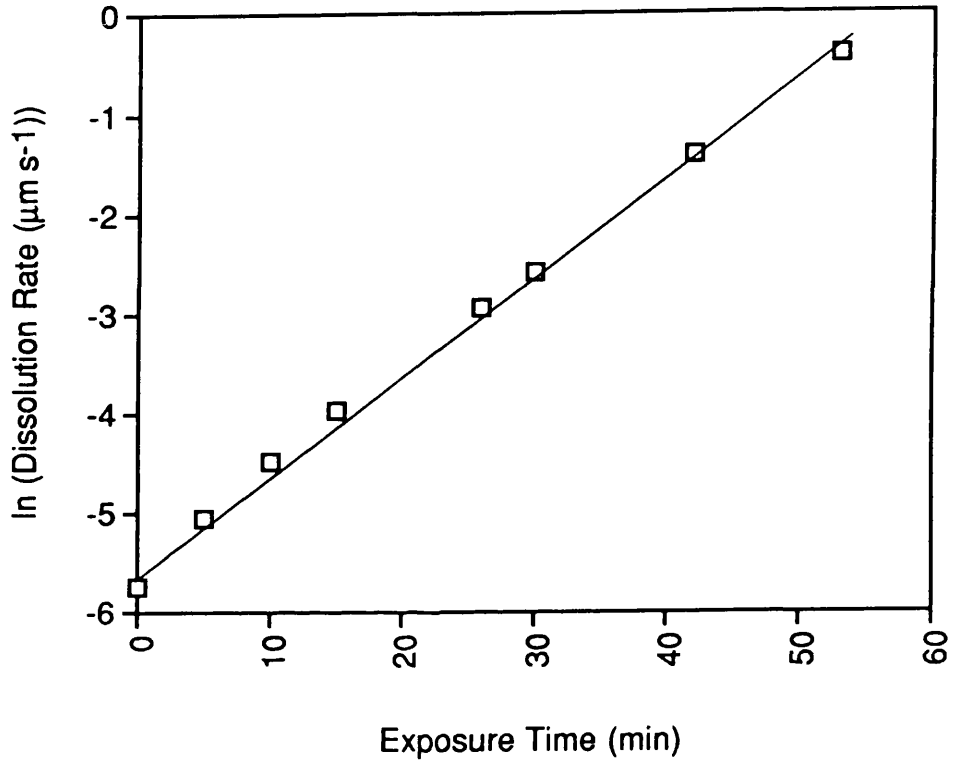

Figure 165: Effect of UV Exposure on the Dissolution of PMMA in 50:50 v/v MEK/IPA at 20.5°C - UVA Lamp

9.1.3 n-Butyl Acetate Developer

An approximate linear relationship was found between the exposure time of PMMA coated crystals and the logarithm of the dissolution rate when developed in butyl acetate (at 20.4 and 25.0°C respectively) using both the Hanovia and UVA lamps (Figures 166 and 167). By consideration of the slopes, the enhancement of dissolution rate was found to be greater when the crystals were exposed by the Hanovia lamp even when the samples had been developed at a lower temperature. This confirmed that the output of the Hanovia lamp was of higher intensity. The dissolution curves of the two systems show a difference in the initial swelling observed for the PMMA (Figures 168 and 169).

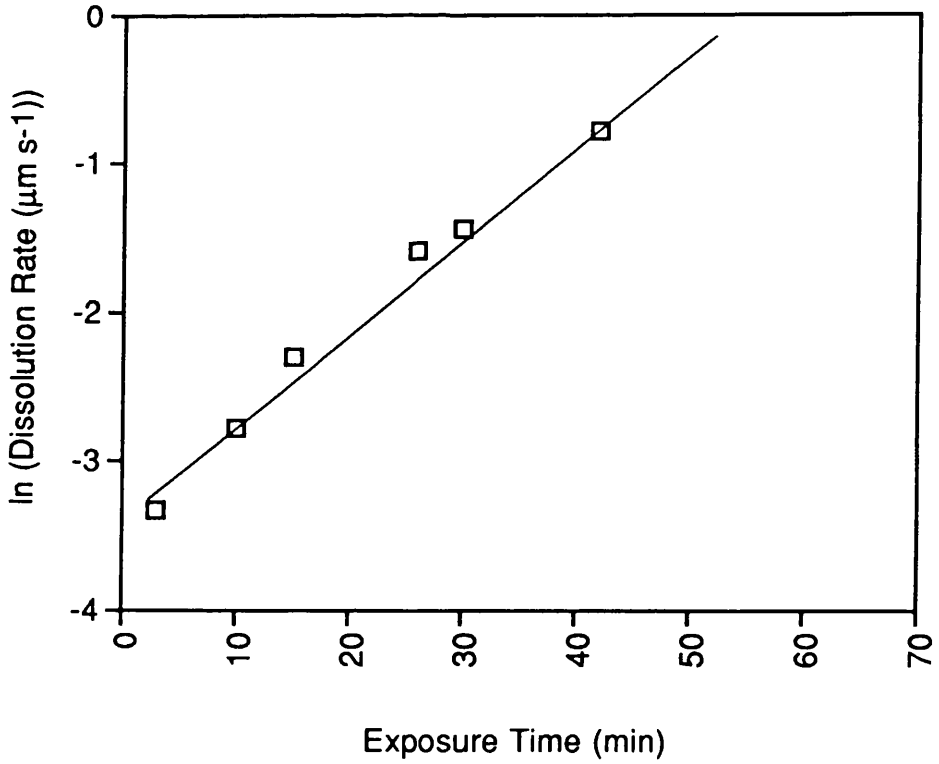

Figure 166: Effect of UV Exposure on the Dissolution of PMMA in n-Butyl Acetate at 20.4°C - Hanovia Lamp

No swelling is observed for UV exposure with the Hanovia lamp even after an exposure of only 3 minutes, whilst initial swelling is observed for exposures up to 40 minutes for the PMMA samples exposed with the UVA lamp. This is a surprising result since, at the higher developing temperature, both higher dissolution rates and less swelling would be expected. It is therefore apparent that when considering developing conditions for a resist system, the intensity and spectral characteristics of the lamp must be considered in conjunction with temperature and solvent systems. The Hanovia lamp has a maximum 500 W output compared with 200 W for the UVA lamp. It would therefore be expected that greater changes in dissolution characteristics would be observed upon exposure with the Hanovia lamp. The distance from the lamps and samples must also be considered, and any effect of temperature fluctuations caused by prolonged exposure.

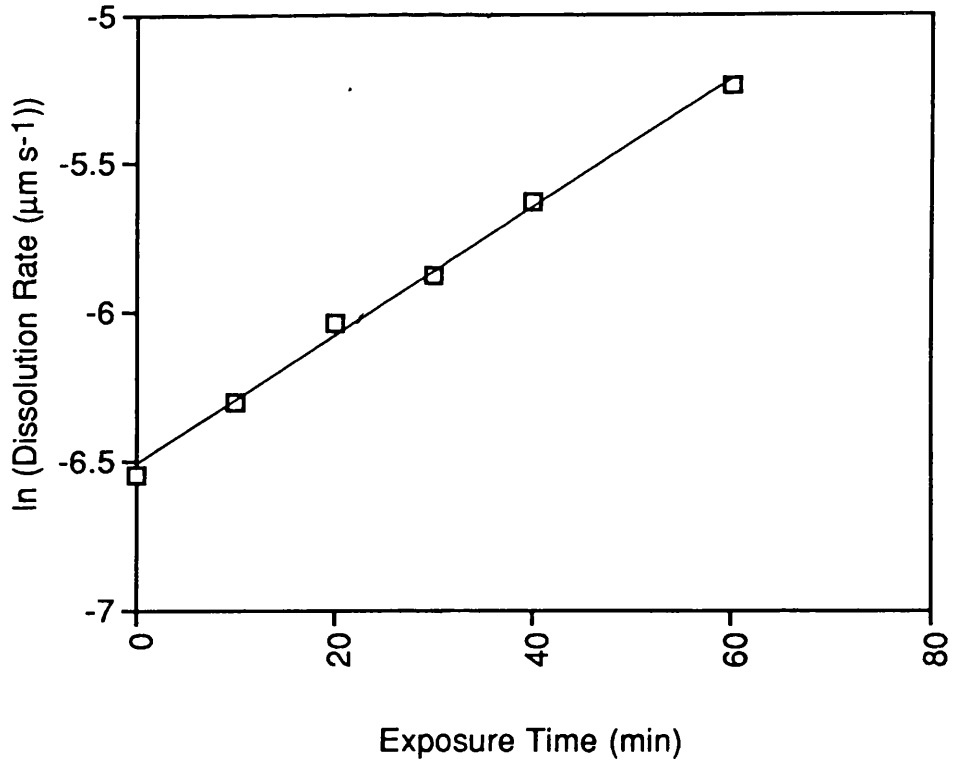

Figure 167: Effect of UV Exposure on the Dissolution of PMMA in n-Butyl Acetate at 25.0°C - UVA Lamp

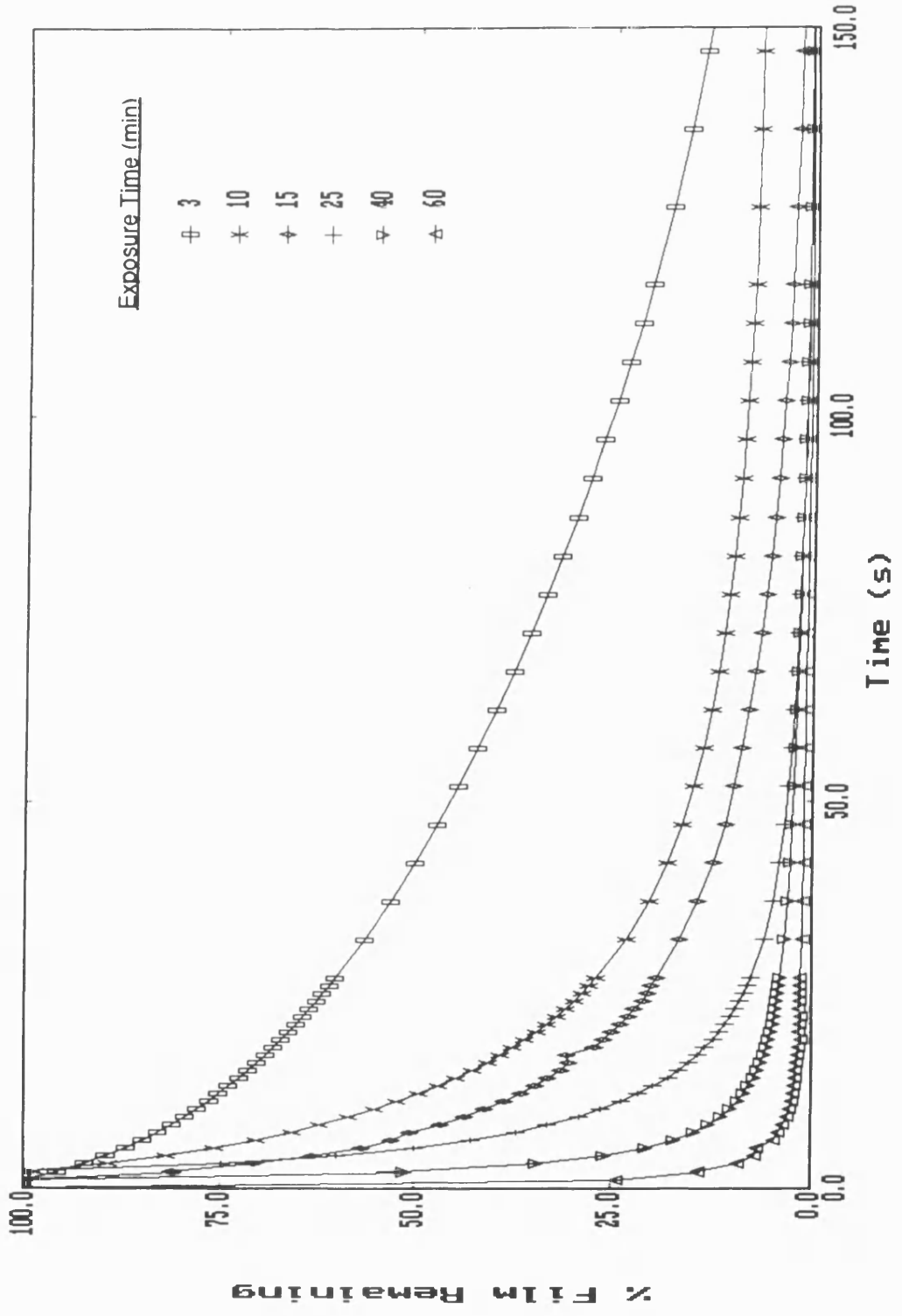

Figure 168: Effect of UV Exposure on the Dissolution of PMMA in n-Butyl Acetate at 20.4°C - Hanovia Lamp

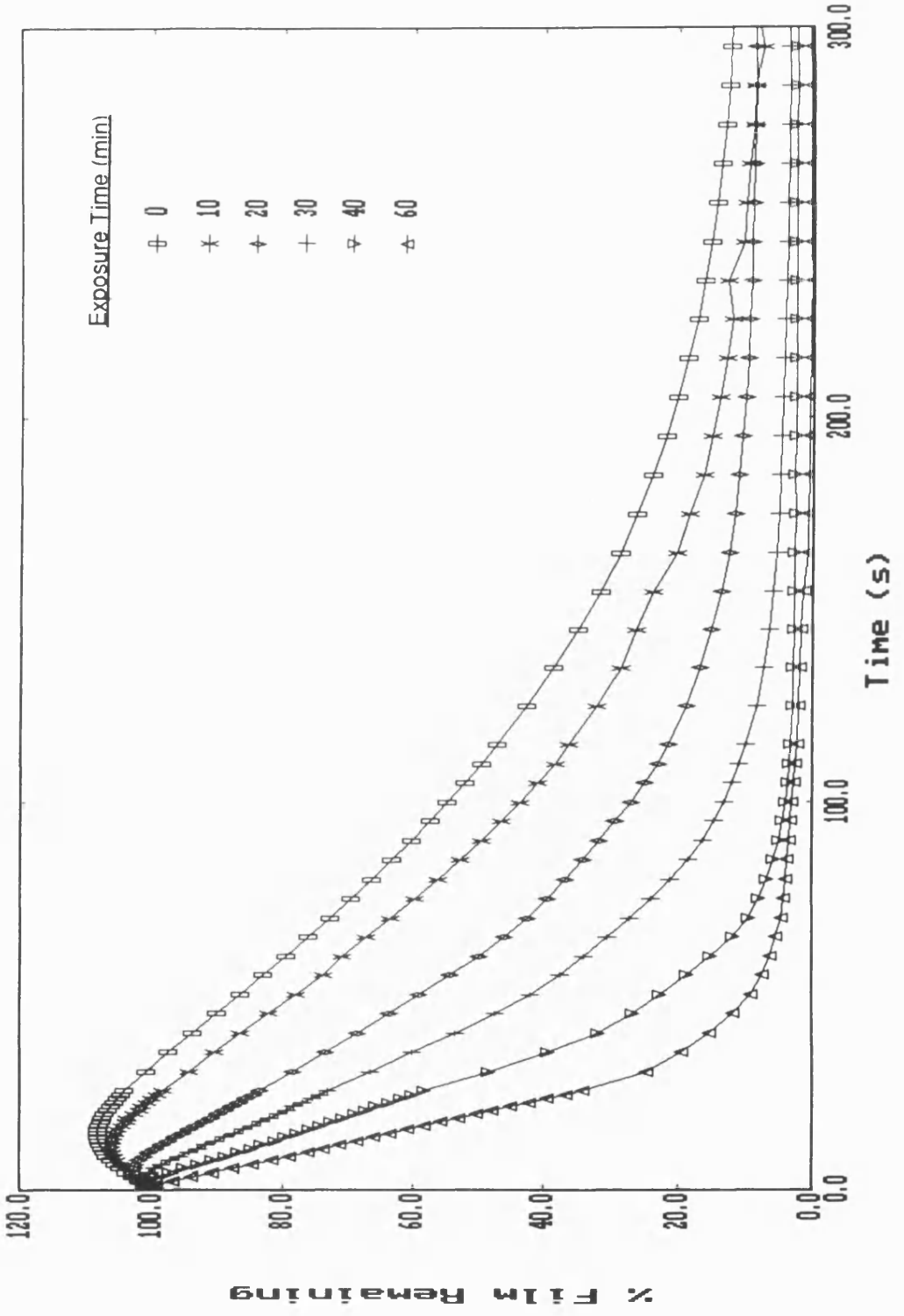

Figure 169: Effect of UV Exposure on the Dissolution of PMMA in n-Butyl Acetate at 25.0°C - UVA Lamp

9.1.4 Change of Film Mass During UV Exposure

The change in frequency for polymer coated quartz crystals was measured before and after UV exposure and prior to development. By assuming uniform coverage of the quartz crystal, a linear relationship was found between the loss of film thickness and exposure time (Figure 170). Ouano[40] observed a similar quantitative relationship between the mass thickness of PMMA and the intensity of X-ray exposure.

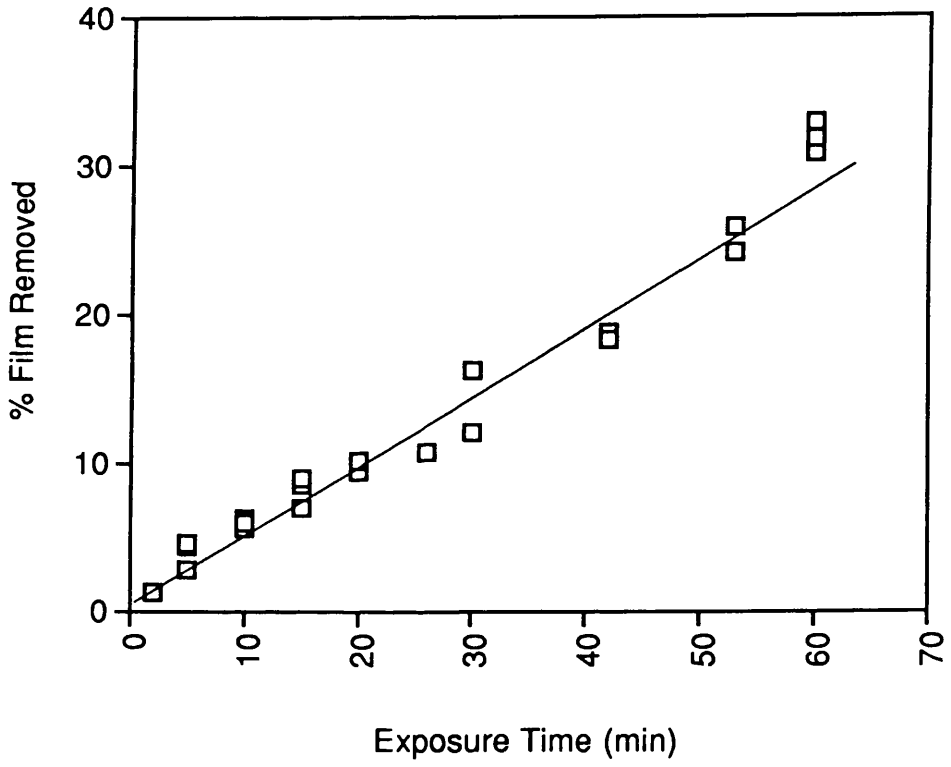

Figure 170: Effect of UV Exposure on the Thickness of PMMA Films Prior to Development - Hanovia Lamp

By consideration of the linear relationship between exposure time and mass change, it would be expected that Figures 166 and 167 would have shown a linear relationship between exposure time and dissolution

rate and not the logarithmic form. Therefore it is evident that another factor is operating in the enhancement of the dissolution rate. In his electron beam study of PMMA, Ouano hypothesised that the large enhancement of dissolution rate suggested that other physical and chemical changes accompanied the molecular weight diminution upon irradiation, which greatly contribute to the solubility rate of the irradiated PMMA. Volatile matter (e.g. CO, CO_2H_2, CH_4 and CH_3OH) is formed upon chain scission of PMMA which, when released, could open up the polymer structure, hence increasing the free volume (i.e. microporosity) of the polymer. The enhanced microporosity of the structure of the polymer would exhibit a higher effective diffusivity for the solvent and hence, an increased solubility rate.

Ouano showed that there were large differences between the slopes of solubility/molecular weight plots of irradiated and unirradiated PMMA, reinforcing the idea that other physical and chemical changes accompanied the molecular weight diminution on irradiation. Stillwagon[206] found a similar effect with poly(butene-1-sulphone) which is known to decompose with the evolution of sulphur dioxide. Likewise Besmann and Greer[207] observed the formation of voids in irradiated polyethylene, and found that the number of voids increased with radiation dosage. Van Pelt[208] found that upon UV irradiation of PMMA, the molecular weight of the polymer decreased by a factor of 10, whilst the solubility rate increased by a factor of 100.

From our study of the change in film thickness due to UV irradiation and our dissolution studies, it appears that the degradation products of PMMA must open up the polymer structure (i.e. increase free volume) to allow more rapid diffusion of the solvent into the polymer film.

9.2 UV Exposure of Poly(vinyl cinnamate)

Poly(vinyl cinnamate) (a negative resist) comprises a cinnamate group attached to polyvinyl alcohol and upon exposure the net photochemical reaction is energy transfer to the cinnamate group followed by dimerization (see Section 1.1.2.1). The increase in polymer molecular weight due to cross-linking decreases the solubility of the polymer.

9.2.1 Acetone Developer

A series of poly(vinyl cinnamate) coated crystals were irradiated with the UVA lamp and developed in acetone at 35.0 and 45.0°C. Figure 171 shows the dissolution curve for the development of the exposed films at 45.0°C. Both the rate of dissolution of the polymer and the final amount of film removed decreased with increased exposure time. A similar effect was observed at 35.0°C with less film removed and slower dissolution rates for the corresponding exposure time. Negligible swelling of the film was observed and, for exposure times greater than 45 minutes, there was no dissolution of the polymer. For all exposure times, the overall dissolution rate was very slow. The dissolution rate of the polymer decreases due to the cross-linking of the film (i.e. increased molecular weight). The rate of change of dissolution slows down with increasing exposure time. As the cross-linking of the film proceeds, the reactive cinnamyl groups become depleted, more quanta are captured in the top layers by non-reactive sites, and the quantum yield of the reaction decreases[208].

The effect of UV exposure on the dissolution rate of poly(vinyl cinnamate) in acetone at 35.0 and 45.0°C is shown to be a logarithmic function of exposure time (Figure 172). The slopes of the lines are negative,

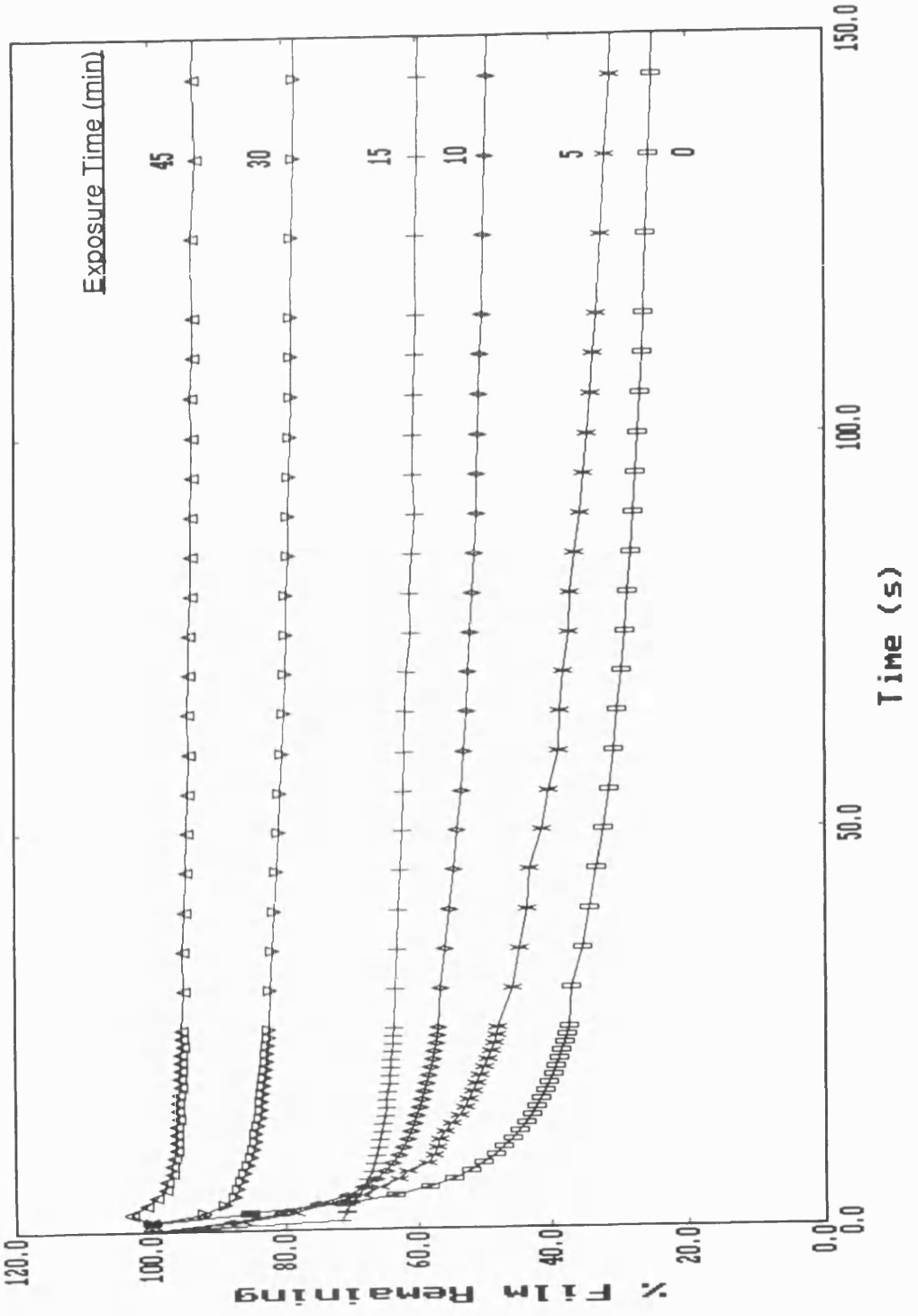

Figure 171: Dissolution of Poly(vinyl cinnamate) in Acetone at 45°C

Effect of UV Exposure - UVA Lamp

indicative of a negative resist where as in the study of the UV exposure of PMMA the slopes had been shown to be positive, indicative of a positive resist. As previously observed in Section 9.1.1, there is no difference in the slope for the dissolution of poly(vinyl cinnamate) at 35.0 and 45.0°C.

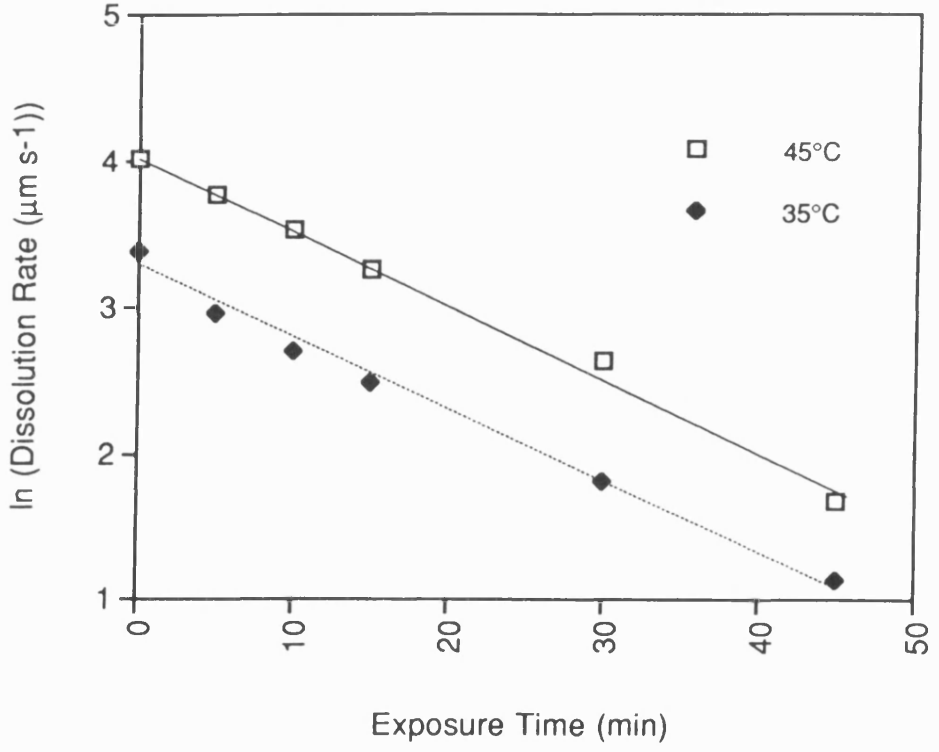

Figure 172: Dissolution of Poly(vinyl cinnamate) in Acetone Effect of UV Exposure - UVA Lamp

Slope *(linear correlation coefficient)*

35.0°C: y = -0.05x - 4.03 *(0.997)*

45.0°C y = -0.05x - 3.25 *(0.996)*

There is a tendency for cross-linked polymeric systems to exhibit swelling in liquids that are solvents for the uncross-linked polymer, and this

can be a great obstacle for the application of negative working polymers where fine line structures in the sub-micrometer range have to be replicated. During the development of the UV exposed poly(vinyl cinnamate), very little swelling was observed, even after the 45 minute exposure, indicating the usefulness of poly(vinyl cinnamate) as a negative resist.

9.3 Conclusion

By the use of our QCM dissolution apparatus, we have been able to make some preliminary investigations into the effect of UV exposure on the dissolution kinetics of polymer films. We have shown for both positive and negative resist systems that there is a logarithmic relationship between the dissolution rate and the exposure time with the developing temperature having little effect on this relationship. For the positive resist, PMMA, positive slopes have been observed whilst the converse has been found for the negative resist, poly(vinyl cinnamate). A linear relationship has been found between the film mass and exposure time prior to development showing loss of the degradation products which facilitate easier penetration of the solvent and hence faster dissolution rates.

Hence, the QCM technique has proved to be an easy and rapid method for the determination of these kinetics, and could therefore prove to have great applicability in the screening of potential UV resist systems.

Chapter Ten

10.0 Conclusions

We have shown the reproducibility of our experimental methods and agreement with literature results. The developed techniques have been used to measure both thermodynamic and dissolution/swelling behaviour for a number of previously unstudied polymer/solvent systems. The piezoelectric sorption technique has been shown to be a quick and reliable method of determining thermodynamic parameters compared with more conventional methods and new data for the PMMA/solvent systems have been presented. Throughout the solubility studies, it has been demonstrated that both initial swelling and overall dissolution kinetics of the polymer films can be monitored using our technique. We have used the data from the thermodynamic studies to aid in the interpretation of the effects encountered during the development of the resist systems.

A series of factors fundamental to the resolution of a resist system have been considered. We have demonstrated that both the polymer molecular weight and its distribution can have a great effect upon the dissolution kinetics of resist systems and the changes in solubility correlated with molecular weight to gain an understanding of the parameters that effect the resolution of a resist.

The development of a series of PMMA standards in a range of solvents has demonstrated clearly that the rate of dissolution decreases with increasing molecular weight. This is an indication of the greater chain entanglement at higher polymer molecular weight which requires a longer development time before the polymer chain can be released into the solvent. The onset of swelling is found to considerably slow the dissolution rate, and the kinetics change greatly with temperature. This increase in the thickness

of the swollen layer can be related to the depth of solvent penetration required before chain disentanglement can occur.

For the PMMA/MEK system, there is some disagreement in the literature for the log-log relationship of molecular weight with dissolution rate and our studies have been able to clarify the situation. Over the complete molecular weight range studied, the system can be represented as two straight lines with the change in slope occurring at approximately M_n 100000 for all the developing temperatures studied. This is in agreement with the UV exposure studies of Ouano[40] and Krasicky and Cooper[71] who suggested that the change in slope was due to the release of radiation products increasing the free volume of the polymer. However, no irradiation has taken place in our studies indicating that their hypothesis was invalid.

Development of the molecular weight series of poly(phenylmethylsilane) in MEK/IPA mixtures has shown a range of dissolution/swelling kinetics with trends similar to those observed for the PMMA/MEK system and with the swelling of the polymer film becoming predominant as the polymer molecular weight is increased. The log-log plot of dissolution rate versus polymer molecular weight for the development of poly(phenylmethylsilane) in MEK/IPA has shown a linear relationship and the break in linearity demonstrated for PMMA in MEK has not been observed. The large differences in polydispersity for the molecular weight series has slightly blurred some of the observed trends, as we have demonstrated for other polymer/solvent systems that differences in polydispersity can have a large contributory effect upon the dissolution characteristics. For example, in the development of polystyrene in MEK/IPA mixtures the wider molecular weight distribution sample has a much faster overall dissolution rate with minimal swelling and much greater film removal than the corresponding

standard. This enhanced rate for wide polydispersity samples has also been observed for poly(phenylmethylsilane) in the MEK/IPA developer.

As the wide distribution samples are made up of a range of molecular weight, in the early stages of dissolution the solvent can remove the low molecular weight polymer chains more quickly that the bulk of the polymer. This opening up of the polymer structure facilitates faster movement of the solvent into the polymer (hence reducing the amount of swelling) and easier removal of the higher molecular weight polymer chains.

Preliminary studies of the UV irradiation of resist systems have shown the utility of the piezoelectric technique. The UV irradiation of a positive resist (e.g. PMMA) and a negative resist (e.g. poly(vinyl cinnamate)) has shown the expected difference in trends of dissolution data. For PMMA, exposure to UV irradiation leads to chain scission and the solubility of the polymer in a number of developer systems was shown to be enhanced to produce faster developing times with reduced initial swelling of the polymer film. Exposure of poly(vinyl cinnamate) leads predominantly to crosslinking and the converse effect upon solubility was observed. The dissolution rates for both polymers is found to be a logarithmic function of exposure time with the slopes positive for PMMA and negative for poly(vinyl cinnamate), whilst the developing temperature has little effect on the relationship despite the enhanced dissolution rates at higher temperatures. This confirms a similar relationship for the electron beam exposure of PMMA reported by Ouano[40].

The intensity and spectral characteristics of the UV lamp upon the dissolution kinetics of PMMA has been considered and as expected was found to have a major effect upon the dissolution characteristics of the resist. The change of the film mass of PMMA during UV irradiation indicates the

release of radiation products, and the logarithmic rather than linear relationship between dissolution rate and exposure time is evidence that the molecular weight diminution upon irradiation is accompanied by the release of these degradation products to enhance the microporosity of the polymer.

The effect of solvent molar volume upon the dissolution kinetics of polymers has been considered for several systems to gain an understanding of the influence of solvent size upon the kinetic polymer/solvent interactions. In mixed solvent/non-solvent systems such as MEK/IPA, dissolution/swelling rates intermediate between those of the single components have been demonstrated for a number of polymer systems. However, interesting effects have been observed upon development with the lower alcohol homologues. Substantial enhancements of the dissolution rates upon addition of methanol or ethanol to MEK with PMMA have been observed and this enhancement had been found greater for wide polydispersity samples. An analogous effect has been observed for water/MEK mixtures. The addition of the higher less mobile alcohols to MEK shows the expected reduction in dissolution rate due to the presence of the non-solvent.

Our thermodynamic studies have aided in our interpretation of the observed phenomena. Firstly, the values of the interaction parameter for the pure alcohols/PMMA systems have indicated the non-solvent character of the alcohols. In the IPA/PMMA system, the values of the interaction parameter indicate decreasing polymer/solvent interaction with increasing solvent fraction confirming the decreased solubility observed as the percentage of non-solvent is increased. Both the methanol and ethanol/PMMA systems have shown different thermodynamic behaviour. The interaction between the polymer and solvent is seen to increase with increasing solvent fraction. The combination of the enhanced thermodynamic interactions and ease of

diffusion of the smaller alcohol molecules influence the observed dissolution kinetics.

The enhancement in dissolution rate can be ascribed to a plasticisation effect as the smaller mobile molecules can diffuse more rapidly into the polymer to open up its structure to allow the solvent to enter at a faster rate and hence give an effectively faster dissolution rate. With the wide polydispersity sample, the release of the shorter polymer chains will also facilitate faster diffusion of the solvent into the polymer. There is a transition between domination of the dissolution rate by kinetic effects for the small non-solvent molecules and by thermodynamic effects of the higher molecules.

Throughout our solvent studies, we have shown the importance of a good choice of developer, as this can have a drastic effect upon the final resolution of the resist. We have demonstrated that with a combination of kinetic and thermodynamic parameters, the factors affecting the dissolution and swelling kinetics can be established and aid in the choice of an appropriate developer.

From the thermodynamic data for the sorption of MEK and IPA on polystyrene, it can be predicted that MEK is a thermodynamically good solvent for the polymer whilst IPA is a poor solvent. In mixtures of MEK/IPA, the proportion of polymer transition to gel state and polymer dissolution has been shown to be dependent upon the ratio of solvent/non-solvent. At a number of MEK/IPA concentrations, it has been demonstrated that with increasing temperature there is a change in diffusion mechanism from Case II to Fickian as the system becomes less controlled by the polymer relaxation. For the development of poly(phenylmethylsilane) in MIBK/IPA mixtures, a

greater distinction between dissolution rates with percentage of MIBK has also been observed when swelling of the films becomes a predominant factor.

From our temperature studies, the calculation of activation energies has enabled the determination of the predominant diffusion mechanism. For example, the activation energy for the dissolution of polystyrene in 60:40 v/v MEK/IPA was found to be 88.1 kJ mol^{-1}, indicative of a Case II diffusion process whilst a substantial increase in the value of the activation energy is found as the level of non-solvent is increased to 60% IPA (177.1 kJ mol^{-1}). The change in the value of activation energy indicates the need for greater swelling of the polymer before dissolution can occur. Comparison of the dissolution kinetics of polystyrene with poly(4-chlorostyrene) in 40:60 v/v MEK/IPA shows differences in the dependence of the swelling kinetics with temperature. For polystyrene, the percentage of swelling increases with developing temperature whilst for poly(4-chlorostyrene), the swelling decreases. This may be due to a combination of factors, such as differences in the polymer molecular weight and the polymer/solvent thermodynamic interactions. Our thermodynamic studies have shown greater solvent interactions for MEK with poly(4-chlorostyrene) than polystyrene. At this developer composition, the increase in temperature may be such as to increase the partial solubility of poly(4-chlorostyrene) and hence reduce the percentage of swelling, whilst the interaction between MEK and polystyrene may not be sufficiently high for dissolution to occur.

In the 75:25 v/v MEK/IPA developer system, a variety of dissolution/swelling behaviour has been observed for poly(phenylmethylsilane). The value of activation energy increases with polymer molecular weight with a distinct break in the trend encountered when swelling of the polymer film becomes predominant (i.e. 32.2 - 91.9 kJ mol^{-1}).

By the use of the QCM technique with the capability of monitoring both swelling/dissolution kinetics, the change of the value of activation energy can be related to the percentage of swelling. The dependence of dissolution upon temperature is found greater for the high polydispersity samples.

The development of poly(vinyl cinnamate) in a series of solvents have shown contrasting values of activation energy. In xylene, there is a large dependence of the dissolution rate with temperature (135.8 kJ mol^{-1}) with the activation energy indicative of Case II diffusion. Whilst in acetone or toluene, much lower values of activation energy are obtained (18.3 and 23.3 kJ mol^{-1} respectively) indicating a Fickian diffusion process. This illustrates the importance of choosing developing temperature when changing solvent systems to ensure no deterioration of the resist's resolution.

Throughout our studies, we have observed that the swelling kinetics of polymer systems are dependent not only upon the type of solvent system but also upon the developing temperature. The kinetics of diffusion of the solvent into both the exposed and unexposed regions of the polymer will influence the ultimate resolution of the resist. The study of the swelling kinetics of PMMA films in methanol has enabled the study of the "solvent" diffusion process without the dissolution of the polymer obscuring the experimental data.

With increasing temperature, a change in diffusion kinetics during swelling from relaxation controlled Case II (110.7 kJ mol^{-1}) to Fickian (57.2 kJ mol^{-1}) is demonstrated. At ambient temperatures, the relaxation of the polymer structure greatly influences the swelling kinetics whilst at higher temperatures, the diffusion of the penetrant lags behind the relaxation boundary of the polymer film and contributes to the swelling kinetics. By the measurement of the swelling kinetics during the course of the "development"

we have resolved the disagreement amongst workers concerning the diffusion kinetics of methanol in PMMA.

The activation energy values for the development of the PMMA standards in MEK range from 85.5 - 107.4 kJ mol^{-1} and indicate Case II to be the controlling diffusion process with the appearance of an induction period confirming this deduction. In Case II, the diffusion is controlled by the relaxation of the polymer i.e. mobility of the polymer segments. The activation energy is found to increase with molecular weight until a limiting weight of 107000 is reached (85.5 - 101.1 kJ mol^{-1}). This correlates with the break in linearity observed at approximately 100000 for the log-log plot of dissolution rate versus polymer molecular weight. This phenomenon may be due to changes in the extent of chain entanglement with the diffusion of the solvent dependent on the polymer free volume and not the chain length.

The dependence of dissolution rate upon solvent size has also been investigated for the PMMA/alkyl acetate solvent series. The log-log plot of dissolution rate versus molecular weight for the dissolution of the PMMA standards in the alkyl acetates solvent series is found to be dependent on the type of alkyl acetates with the slope increasing as the solvent size is increased. The difference in the slopes is greater at temperatures close to ambient. The break in linearity of these plots observed for the dissolution of PMMA in MEK is not as obvious but occurs at approximately M_n 100000 throughout the solvent series, and hence could not be due to the onset of swelling (as this varies with solvent size). At ambient temperatures, the dissolution kinetics of isopropyl acetate are close to those of n-propyl acetate whilst at higher temperatures, the kinetics are closer to that of n-butyl acetate. This indicates the reduction of the dependence of steric effects and polymer molecular weight at higher temperatures. Broadening of the dissolution

curves are observed for IPA on comparison with propyl acetate as the larger cross section of the isopropyl group causing greater disruption for the polymer structure.

The dissolution rate of PMMA decreases whilst the percentage of initial swelling increases with increasing size of the acetate molecule. The mobility of the solvent is affected by the relative size of the free volume of the polymer and the solvent molecule. Similar trends in the dissolution behaviour have been observed for both the PMMA standards and the wide polydispersity sample.

The slopes of the log-log plots of dissolution rate versus solvent molar volume are independent of both temperature and polymer molecular weight and its distribution. Our results contradict the break in linearity at propyl acetate found by other workers[54,57]. By monitoring the swelling of the PMMA films we have demonstrated that this change in slope observed by Ouano and Gipstein[57] occurs at the onset of swelling in the PMMA/alkyl acetate solvent system. The previous workers have used the "Dip and Dry" method in the determination of the dissolution rates and that technique is unable to monitor swelling in situ and has insufficient sensitivity.

The thermodynamic data for the sorption of alkyl acetates on PMMA illustrates the difference in polymer/solvent interactions between methyl acetate and the higher acetate homologues. Methyl acetate has very low polymer/solvent interaction (high χ) and hence the diffusion of the molecule is a major contributory factor to the observed dissolution kinetics. The higher homologues have greater interaction with the polymer and hence swelling of the polymer film is encountered.

A general independence of the slopes of the Arrhenius plots with solvent size and polymer molecular weight and the activation energy indicates Case II diffusion. The greatest variation in activation energy is found for pentyl acetate (121.5 - 148.7 kJ mol^{-1}) with the value increasing with polymer molecular weight.

For investigating solubility in resist systems, the QCM method offers speed, convenience, economy and wide applicability. It has been proven to be a quick and useful method for gathering the necessary data for determining the viability of potential resist systems in terms of optimising conditions for developing. Various types of polymers can be studied and a wide range of solvents, temperatures, irradiation conditions and dissolution/swelling rates can be examined under conditions close to those used for commercial resist development. For example, the selection of the most appropriate molecular weight and distribution to be used, the determination of the necessary irradiation doses to give sufficiently different dissolution rates, the best temperature and solvent composition to speed dissolution whilst inhibiting swelling and to remove all the appropriate parts of the resist can be attained. With a portfolio of the results obtained from the polymer solubility and dissolution studies, the appropriate developing conditions can be determined to enable optimum resolution of the resist.

References

References

1 W. Schnabel and H. Sotobayashi, *Prog. Polym. Sci.* **9**, 297 (1983)

2 W. Kern and C.A. Deckert in *"Thin Film Processes"*, J.L. Voesen and W. Kern, Eds., Academic Press, New York (1978)

3 K.L. Mittal, *Solid State Technol.* **22**, 89 (1979)

4 I. Haller, M. Hatzakis and R. Srinivasan, *I.B.M. J. Res. Dev.* **12**, 251 (1986)

5 E. Reichmanis and L.F. Thompson, *Ann. Rev. Mater. Sci.* **17**, 235 (1987)

6 S.R. Turner in *"Photopolymerisation and Photoimaging Science and Technology"*, N.S. Allen, Ed., Elsevier (1989)

7 F.A. Delzenne, *Encycl. Polym. Sci., Technol. Suppl.* **1,** 401 (1976)

8 M. Hatzakis, *App. Polym. Symp.* **23**, 73 (1974)

9 J.H. Lai, *"Polymers for Electronic Applications"*, C.R.C. Press (1989)

10 R.A. Pethrick in *"High Value Polymers"*, A.H. Fawcett, Ed., R.S.C. Special Pub. **87**, 267 (1991)

11 E.D. Feit, R.D. Heidenreich and L.F. Thompson, *App. Polym. Symp.* **23**, 125 (1974)

12 G.N. Taylor, G.A. Coquin and S. Somekh, *Polym. Eng. Sci.* **19**, 1703 (1979)

13 *"An Introduction to Microlithography"*, L.F. Thompson, C.G. Willson and M.J. Bowden, Eds., A.C.S. Symp. Ser. **219**, (1983)

14 J. Luitkis, M. Hatzakis, J. Shaw and J. Paraszczak, *Polym. Eng. Sci.* **23**(18), 1047 (1983)

15 L.G. Griffiths, R.G. Jones, D.R. Brambley and P. Miller Tate, *Makromol. Chem., Macromol. Symp.* **24**, 201 (1989)

16 R.G. Jones, Y. Matsubayashi and N.J. Haskins, *Eur. Polym. J.* **25**, 701 (1989)

17 K. Tanagaki, Y. Ohnishi and S. Fujiwara, *A.C.S. Symp. Ser.* **242**, 177 (1984)

18 T. Hirai, Y. Hatano and S. Nonogaki, *J. Electrochem. Soc.* **118**, 669 (1971)

19 E.D. Feit, L.F. Thompson and R.D. Heidenreich, *Am. Chem. Soc. Div. Org. Coat. Plast. Chem. Prepr.* 383 (1973)

20 L.F. Thompson, E.D. Feit and R.D. Heidenreich, *Polym. Eng. Sci.* **14**, 529 (1974)

21 L.M. Minsk, *J. App. Polym. Sci.* **2**, 302 (1959)

22 R.C. Daly, R.H. Engebrecht, D.P. Specht and S.Y. Farid in "*Preprints of the International Symposium on Advances in Photopolymer Systems*" Washington D.C. (1978), The Society of Photographic Scientists and Engineers, Springfield, V.A.

23 L.F. Thompson and R.E. Kerwin, *Ann. Rev. Mater. Sci.* **6,** 267 (1976)

24 A.E. Novembre and M.J. Bowden, *Polym. Eng. Sci.* **23**, 975 (1983)

25 M. Hatzakis, *J. Electrochem. Soc.* **116**, 1033 (1969)

26 W.M. Moreau, *Opt. Eng.* **22**, 181 (1983)

27 B. Ranby and J.F. Rabek, *"Photodegradation, Photooxidation and Photostabilisation of Polymers"*, Wiley, New York (1975)

28 R. West, L.D. David, P.I. Djurovich, K.L. Stearley, S.V. Srinivasin and H. Yu, *J. Am. Chem. Soc.* **103**, 7352 (1981)

29 R.D. Miller, D. Hofer, G.N. Fickes, C.G. Willson, E. Marinero, P.T. Trefonas III and R. West, *Polym. Eng. Sci.* **26**, 1129 (1986)

30 R.D. Miller, D. Hofer, D.R. McKean, C.G. Willson, R. West and P.T. Trefonas III, *A.C.S. Symp. Ser.* **266**, 293 (1984)

31 R.D. Miller, G. Wallraff, N. Clecak, R. Sooriyakumaran, J. Michl, T. Karatsu, A.J. McKinley, K.A Klingensmith and J. Downing, *A.C.S. Symp. Ser.* **412**, 115 (1989)

32 R.D. Miller, D. Hofer, J. Rabolt, R. Sooriyakumaran, C.G. Willson, G.N. Fickes, J.E. Guillet and J. Moore, *A.C.S. Symp. Ser.* **346**, 170 (1987)

33 S.V. Babu and S.V. Srinivasan, *S.P.I.E.* **539**, 36 (1985)

34 D.J. Elliot, *"Integrated Circuit Fabrication Technology"*, McGraw Hill (1982)

35 T. Batchelder and J. Piatt, *Solid State Technol.* **26**, 221 (1982)

36 M.J. Bowden, *Solid State Technol.* **24**, 73 (1981)

37 G.N. Taylor, T.M. Wolf and M.R. Goldrick, *J. Electrochem. Soc.* **128**, 361 (1981)

38 S.A. MacDonald, H. Ito and C.G. Willson, *Microelectronic Eng.* **1**, 269 (1983)

39 *"Diffusion in Polymers"*, J. Crank and G.S. Park, Eds., Academic Press, New York (1968)

40 A.C. Ouano, *Polym. Eng. Sci.* **18**, 306 (1978)

41 Y.O. Tu and A.C. Ouano, *I.B.M. J. Res. Dev.* **21**, 131 (1977)

42 K. Ueberreiter and F. Asmussen, *J. Polym. Sci.* **57**, 187 (1962)

43 D.S. Soong, *S.P.I.E.* **539**, 2 (1985)

44 J.S. Vrentas and C.M. Vrentas, *J. Polym. Sci.* **B30**, 1005 (1992)

45 A.H. Windle in *"Polymer Permeability"*, J. Comyn, Ed., Elsevier (1985)

46 N.L. Thomas and A.H. Windle, *Polymer* **21**, 613 (1980)

47 T. Alfrey,Jr., E.F. Gurnee and W.G. Lloyd, *J. Polym. Sci.* **C12**, 249 (1966)

48 N.L. Thomas and A.H. Windle, *Polymer* **19**, 255 (1978)

49 J.S. Vrentas, C.M. Jarzebski and J.L. Duda, *A.I.Ch.E. J.* **21**, 894 (1975)

50 H.B. Hopfenberg, *J. Membrane Sci.* **3**, 215 (1978)

51 F. Asmussen and K. Ueberreiter, *Kolloidzeitschrift* **185**, 1 (1962)

52 P.J. Flory, *"Principles of Polymer Chemistry"*, Cornell University Press, Ithaca, New York (1953)

53 J.H. Lai and L. Shepherd, *J. App. Polym. Sci.* **20**, 2367 (1976)

54 F. Asmussen and K. Ueberreiter, *Kolloid Z.* **223**, 6 (1968)

55 R.A. Harris, *J. Electrochem. Soc.* **120**, 270 (1973)

56 J.S. Papanu, J. Manjkow, D.W. Hess, D.S. Soong and A.T. Bell, *S.P.I.E.* **771**, 93 (1987)

57 E. Gipstein, A.C. Ouano, D.E. Johnson and O.U. Need, *Polym. Eng. Sci.* **17**, 396 (1977)

58 J.S. Greeneich, *J. Electochem. Soc.* **121**, 1669 (1974)

59 A.C. Ouano and J.A. Carothers, *Polym. Eng. Sci.* **20**, 160 (1980)

60 H.W. Deckman and J.H. Dunsmuir, *J. Vac. Sci. Technol.* **B1**(4), 1166 (1983)

61 W.J. Cooper and F. Krasicky, *Polymer* **26**, 1069 (1985)

62 G.C. Berry and T.G. Fox, *Adv. in Polym. Sci.* **5**, 261 (1968)

63 F. Asmussen and K. Ueberreiter, *J. Polym. Sci.* **57**, 199 (1962)

64 A.F.M. Barton, *"Handbook of Solubility Parameters and Other Cohesion Parameters"*, C.R.C. Press, Boca Raton (1983)

65 J. Manjkow, J.S. Papanu, D.S. Soong, D.W. Hess and A.T. Bell, *J. App. Phys.* **62**, 682 (1987)

66 W.J. Cooper, P.D. Krasicky and F. Rodriguez, *J. App. Polym. Sci.* **31**, 65 (1986)

67 F. Rodriguez, P.D. Krasicky and R.J. Groele, *Solid State Technol.* **28**(5), 125 (1985)

68 K. Ueberreiter and F. Asmussen, *Makromol. Chem.* **43**, 324 (1961)

69 K.L. Konnerth and F.H. Dill, *I.E.E.E. Trans. Electron. Dev.* **ED22**, 452 (1975)

70 K.L. Konnerth and F.H. Dill, *Solid State Electron.*, **15**, 371 (1972)

71 W.J. Cooper, P.D. Krasicky and F. Rodriguez, *Polymer* **26**, 1069 (1985)

72 P.D. Krasicky, R.J. Groele, J.A. Jubinsky, K.U. Pohl, F. Rodriguez, Y.M.N. Namaste and S.K. Obendorf, *Proc. S.P.E. Regional Technical Conf.* 237 (1985)

73 W.W. Flack, J.S. Papanu, D.W. Hess, D.S. Soong and A.T. Bell, *J. Electrochem. Soc.* **131**, 2200 (1984)

74 H. Tong and L.T. Nguyen, *"New Characterisation Techniques for Thin Polymer Films"*, Wiley, New York, (1990)

75 P. Maffei, L. Kiene and D. Canet, *Macromolecules* **25**, 7114 (1992)

76 W.D. Hinsberg and K.K. Kanazawa, *Rev. Sci. Instrum.* **60**, 489 (1989)

77 W.D. Hinsberg, C.G. Willson and K.K. Kanazawa, *S.P.I.E.*, **539**, 6 (1985)

78 W.D. Hinsberg, C.G. Willson and K.K. Kanazawa, *J. Electrochem. Soc.*, **137**, 1451 (1986)

79 J. Curie and P. Curie, *Bull. Soc. Min. Paris* **3**, 90 (1880)

80 G.Z. Sauerbrey, *Phys. Verha.* **8**, 113 (1957)

81 P. Oberg and G. Lingensjo, *Rev. Sci. Instrum.* **30**, 1053 (1959)

82 K.H. Behrndt and R.W. Love, *Vacuum* **12**, 1 (1962)

83 A.W. Warner and C.D. Stockbridge in *"Vacuum Microbalance Techniques"* Vol. **2**, Plenum Press, New York (1962)

84 E.P. EerNisse, *I.E.E.E. Trans.* **SU14**, 59 (1967)

85 J.G. Miller and D.I. Bolef, *J. App. Phys.* **39**, 4580 (1968)

86 C. Lu and O. Lewis, *J. App. Phys.* **43**, 4385 (1972)

87 R.A. Heising, *"Quartz Crystals for Electrical Circuits"*, Van Nostrand New York 24 (1946)

88 J.C. Brice, *Rev. Mod. Phys.* **57**, 105 (1985)

89 R. Schumacher, *Angewandte Chemie* **29**, 329 (1990)

90 G.Z. Sauerbrey, *Z. Phys.* **155**, 206 (1959)

91 K.O. Pederson, *Z. Physik. Chem.* **A170**, 41 (1934)

92 D.M. Ullevig, J.F. Evans and M.G. Albrecht, *Anal. Chem.* **54**, 2341 (1982)

93 G.G. Guilbault in *"Applications of Piezoelectric Quartz Crystal Microbalances"*, C. Lu and A.W. Czanderna, Eds., Elsevier (1984)

94 J.F. Alder and J.J. McCallum, *The Analyst* **108**, 1169 (1983)

95 W.H. King, *Res. Dev.* **20**(4), 28 (1969)

96 W.W. Schulz and W.H. King, Jr., *J. Chromatogr. Sci.* **11**, 343 (1973)

97 R.M. Yang and H.M. Tong, *J. Polym. Sci., Polym. Lett. Ed.* **23**(11), 583 (1985)

98 C.R. Moylan, M.E. Best and M. Ree, *J. Polym. Sci.* **B29**, 87 (1991)

99 R. Ognjanovic, C.Y. Hui and E.J. Kramer, *J. Mat. Sci.* **25**, 514 (1990)

100 L.L. Levenson in *"Applications of Piezoelectric Quartz Crystal Microbalances"*, C. Lu and A.W. Czanderna, Eds., Elsevier (1984)

101 J. Hlavey and G.G. Guilbault, *Anal. Chem.* **49**(13), 1890 (1977)

102 L.M. Webber, J. Hlavey and G.G. Guilbault, *Mikrochim. Acta* 351 (1978)

103 G.G. Guilbault, *Anal. Proc.* **19**, 68 (1982)

104 H.K. Pulker, E. Benes, D. Hammer and E. Söllner, *Thin Solid Films* **32**, 27 (1976)

105 P.L. Konash and G.J. Bastiaans, *Anal. Chem.* **52**, 27 (1976)

106 M.R. Deakin and D.A. Buttry, *Anal. Chem.* **61**, 1147 (1989)

107 O. Melroy, K.K. Kanazawa, J.G. Gordon and D. Buttry, *Langmuir* **2**, 697 (1986)

108 S. Bruckenstein and S. Swathirajan, *Electrochim. Acta* **30**, 851 (1985)

109 J.H. Kaufman, K.K. Kanazawa and G.B. Street, *Phys. Rev. Lett.* **52**, 2461 (1984)

110 D. Orata and D.A. Buttry, *J. Am. Chem. Soc.* **109**, 3574 (1987)

111 B.J. Feldman and O. Melroy, *J. Electroanal. Chem.* **234**, 213 (1987)

112 R. Borjas and D.A. Buttry, *J. Electroanal. Chem.* **280**, 73 (1990)

113 S. Servagent and E. Vieil, *J. Electroanal. Chem.* **280**, 227 (1990)

114 M.R. Deakin and O.R. Melroy, *J. Electrochem. Soc.* **136**, 349 (1989)

115 T. Nomura and A. Minemura, *J. Chem. Soc. of Japan* **10**, 1621 (1980)

116 T. Nomura, M. Watanabe and T.S. West, *Anal. Chim. Acta* **175**, 107 (1985)

117 K.K. Kanazawa and J.G. Gordon, *Anal. Chem.* **57**, 1770 (1985)

118 S. Bruckenstein and M. Shay, Abstracts, Pittsburgh Conference and Exposition, Atlantic City, New Jersey (1983)

119 S. Bruckenstein and M. Shay, *Electrochim Acta* **30**, 1295 (1985)

120 Y. Okahata and K. Ariga, *Thin Solid Films* **178**, 465 (1989)

121 M. Thompson, G.K. Dhaliwal, C.L. Arthur and G.S. Calabrese, *I.E.E.E. Transactions on Ultrasonics, Ferroelectric and Frequency Control* **24**(2), 127 (1987)

122 E. Prusak-Sochaczewski and J.H.T. Luong, *Anal. Lett.* **23**(2),183 (1990)

123 K.H. Meyer and R. Lühdemann, *Helv. Chim. Acta* **18**, 307 (1935)

124 R.H. Fowler and G.S. Rushbrooke, *Trans. Faraday Soc.* **33**, 1272 (1937)

125 M.L. Huggins, *J. Chem. Phys.* **9**, 440 (1941)

126 P.J. Flory, *J. Chem. Phys.* **9**, 660 (1941)

127 R.A. Orwoll, *Rubber Chem. Tech.* **50**, 451 (1977)

128 D.C. Bonner, *J. Macromol. Sci.-Revs., Macro.-Mol. Chem.* **C13**(2), 263 (1975)

129 J.H. Baxendale, E.V. Enustun and J. Stern, *Phil. Trans. Roy. Soc. London* **A243**, 169 (1951)

130 R.S. Jessup, *J. Res. Nat. Bur. Stand.* **60**, 47 (1958)

131 C.E.H. Bawn, R.F.J. Freeman and A.R. Kamaliddin, *Trans. Faraday Soc.* **46**, 677 (1950)

132 G. Gee and W.J.C. Orr, *Trans. Faraday Soc.* **42**, 507 (1946)

133 J.H. Van der Waals and J.J. Hermans, *Rec. Trav. Chim. Pays-Bas.* **69**, 971 (1950)

134 D.C. Bonner and J.M. Prausnitz, *J. Polym. Sci., Polym. Phys. Ed.* **12**, 51 (1974)

135 I. Sakwada, A. Nakajima and H. Fujiwara, *J. Polym. Sci.* **35**, 489 (1959)

136 O. Smidsröd and J.E. Guillet, *Macromolecules* **2**, 272 (1969)

137 R.D. Newman and J.M. Prausnitz, *J. Phys. Chem.* **76**, 492 (1972)

138 D. Patterson, Y.B. Tewari, H.P. Schreiber and J.E. Guilllet, *Macromolecules* **4**, 356 (1971)

139 W.E. Hammers and C.L. DeLigny, *Rec. Trav. Chim. Pays-Bas* **90**, 912 (1971)

140 J.E. Guillet, *New Dev. Gas Chromatog.* **11**, 187 (1973)

141 J.R. Conder and J.H. Purnell, *Trans. Faraday Soc.* **64**, 1505 (1968)

142 J.R. Conder and J.H. Purnell, *Trans. Faraday Soc.* **64**, 3100 (1968)

143 J.R. Conder and J.H. Purnell, *Trans. Faraday Soc.* **65**, 824 (1968)

144 N.F. Brockmeier, R.W. McCoy and J.A. Meyer, *Macromolecules* **5**, 130 (1972)

145 N.F. Brockmeier, R.W. McCoy and J.A. Meyer, *Macromolecules* **5**, 464 (1972)

146 N.F. Brockmeier, R.E. Carlson and R.W. McCoy, *Amer. Inst. Chem. Eng.* **19**, 1133 (1973)

147 J.S. Aspler and D.G. Gray, *J. Polym. Sci., Polym. Physics Ed.* **21**, 1675 (1983)

148 W.R. Krigbaum and D.O. Creymer, *J. Am. Chem. Soc.* **81**, 1859 (1959)

149 G. Nehage and H. Meys, *J. Polym. Sci.* **30**, 271 (1958)

150 C. Drucher, *Z. Physik. Chem.* **A180**, 359 (1937)

151 T.F. Young, K.A. Kraus and J.S. Johnson, *J. Chem. Phys.* **22**, 878 (1954)

152 G.V. Schulz, *Z. Physik. Chem.* **A193**, 168 (1944)

153 M. Wales, M. Bender, J.W. Williams and R.H. Ewart, *J. Chem. Phys.* **14**, 353 (1946)

154 H. Fujita, A.M. Linklater and J.W. Williams, *J. Am. Chem. Soc.* **82**, 379 (1960)

155 H.W. Ostertroudt and J.W. Williams, *J. Phys. Chem.* **69**, 1050 (1965)

156 D.A. Albright and J.W. Williams, *J. Phys. Chem.* **71**, 2780 (1967)

157 T.G. Scholte, *J. Polym. Sci.* **A2**(8), 841 (1970)

158 A.J. Ashworth and G.J. Price, *Thermochimica Acta* **82**, 161 (1984)

159 G.J. Price, PhD Thesis, University of Bath (1984)

160 D.C. Bonner and Y.L. Chang, *J. Polym. Sci., Polym. Lett. Ed.* **13**, 259 (1975)

161 S. Saeki, J.C. Holste and D.C. Bonner, J. Polym. Sci. Phys. **19**, 307 (1981); **20**, 805 (1982)

162 J.R. Conder and C.L. Young, *"Physiochemical Measurement by Gas Chromatography"*, Wiley, Chichester (1978)

163 J.L. Lundberg, E.J. Mooney and C.E. Rogers, *J. Polym. Sci.* **A2**, 7, 947 (1969)

164 E.C. Baughan, *Trans. Faraday Soc.* **44**, 495 (1948)

165 R.S. Chahel, W.P. Kao and D. Patterson, *J. Chem. Soc., Faraday Trans.* 1, **69**, 1834 (1973)

166 P.J. Flory and H. Shih, *Macromolecules* **5**, 761 (1972)

167 K. Sugamiya, N. Kuwahara and M. Kanebo, *Macromolecules* **7**, 66 (1974)

168 W.R. Summers, Y.B. Tewari and H.P. Schreiber, *Macromolecules* **5**, 12 (1972)

169 A.J. Ashworth and G.J. Price, *Macromolecules* **19**, 358 (1986)

170 A.J. Ashworth and G.J. Price, *Macromolecules* **19**, 362 (1986)

171 G.J. Price and J.E. Guillet, *J. Macromol. Sci.-Chem.* **A23**(12), 1487 (1986)

172 A.J. Ashworth, C.F. Chien, D.L. Furio, D.M. Hooker, M.M. Kopecni, R.J. Laub and G.J. Price, *Macromolecules* **17**, 1090 (1984)

173 A.R. Schultz and P.J. Flory, *J. Am. Chem. Soc.* **74**, 4760 (1952)

174 C.E.H. Bawn and M.A. Wajid, *Trans. Faraday Soc.* **52**, 1658 (1956)

175 P.J. Flory and H. Hôcker, *Trans. Faraday Soc* **67**, 2258 (1971)

176 R. Corneliussen, S.A. Rice and H. Yamakawa, *J. Chem. Phys.* **38**(7), 1768 (1963)

177 M. Benje, M. Eiermann, U. Pittermann and K.C. Weil, Ber. Bunseges. Phys. Chem. 90, 435 (1986)

178 G.J. Price, Private Communication

179 R.D. Miller, D. Thompson, R. Sooriyakumaran and G.N. Fickes, *J. Polym. Sci., Polym. Chem.* **29**, 813 (1991)

180 C.B. Lin, K.S. Liu and S. Lee, *J. Polym. Sci.* **29**, 1457 (1991)

181 F. Beuche, *"Physical Properties of Polymers"*, Krieger, New York (1979)

182 F.N. Kelly and F. Beuche, *J. Polym. Sci.* **I**, 549 (1961)

183 H. Morawetz in *"Macromolecules in Solution"*, Interscience, New York (1965)

184 F. Bueche, *J. Chem. Phys.* **20**, 1959 (1952)

185 G.V. Schulz, K.V. Gunner and H. Gerrens, *Z. Physik. Chem.* **4**, 192 (1955)

186 P.D. Krasicky, R.J. Greole, J.A. Jubinsky and F. Rodriguez, *Polym. Eng. Sci.* **27**, 282 (1987)

187 J. Manjkow, J.S. Papanu, D.W. Hess, D.S. Soane and A.T. Bell, *J. Electrochem. Soc.* **134**, 2003 (1987)

188 K. Ueberreiter and F. Asmussen, *J. Polym. Sci.* **57**, 199 (1962)

189 J.S. Greeneich, *J. Electrochem. Soc.* **122**, 970 (1975)

190 J.S. Papanu, D.W. Hess, D.S. Soane and A.T. Bell, *J. Electrochem. Soc.* **136**, 3077 (1989)

191 A.C. Ouano, *A.C.S. Symp. Ser.* **242**, 79 (1984)

192 G.C. Sarti, *Polymer* **20**, 827 (1979)

193 H. Fujita, A. Kishimoto and K. Matsumoto, Trans. Faraday Soc. **56**, 424 (1960)

194 E.H. Andrews, G.M. Levy and J. Willis, *J. Mater. Sci.* **8**, 1000 (1973)

195 H.B. Hopfenberg, L. Nicolais and E. Drioli, *Polymer* **17**, 195 (1976)

196 J.S. Papanu, D.W. Hess, D.S. Soane and A.T. Bell, *J. App. Polym.* Sci. **39**, 803 (1990)

197 A. Peterlin, J. Polym. Sci. **B3**, 1083 (1965)

198 A.C. Ouano, *Org. Coat. Appl. Polym. Sci. Proc.* **48**, 42 (1983)

199 *"Selected Values of Properties of Chemical Compounds"*, T.R.C. Data Project, Texas A. and M., Univ. College Station (1965)

200 C.R. Wilke and P. Chang, *A.I.Ch.E. J.* **1**, 264 (1955)

201 F.A. Long and L.J. Thompson, *J. Polym. Sci.* **14**, 321 (1954)

202 A. Sfirakis and C.E. Rogers, *Polym. Eng. Sci.* **21**, 542 (1981)

203 International Critical Tables Vol. **3**, McGraw Hill, New York (1928)

204 Japanese Patent 60,15,636, Marusen; Chem. Abstr. **102**, 212703 (1985)

205 Y. Kamoshida, M. Koshiba, H. Yoshimoto, Y. Harita and K. Harada, *J. Vac. Sci. Technol.* **B1**, 1156 (1983)

206 L. Stillwagon in *"Polymer Materials for Electronic Applications"*, E.D. Feit and C. Williams,Jr,. Eds., *A.C.S. Symp. Ser.* **184**, 19 (1982)

207 T. Besmann and R. Greer, *J. Polym. Sci.* **13**, 537 (1975)

208 P. Van Pelt, S.P.I.E. **275**, 150 (1981)

209 P. Egerton, J. Trigg, E. Hyde and A. Reisser, *Macromolecules* **14**, 100 (1981)

210 I.U.P.A.C. Tables, *Pure App. Chem.* **21**(1), 91 (1970)

211 R. Reid, J.M. Prausnitz and T.K. Sherwood, *"The Properties of Gases and Liquids"*, McGraw-Hill, New York (1977)

212 J.H. Dymond and E.B. Smith, *"The Second Virial Coefficients of Pure Gases and their Mixtures"*, O.U.P., Oxford (1980)

213 S.E. Wood and J.P. Brusie, *J. Am. Chem. Soc.* **89**, 6814 (1967)

214 S. Ohe, *"Computer Aided Data Book of Vapour Pressures"*, Data Pub. Co., Tokyo (1976)

215 S.E. Wood and J.A. Gray, *J. Am. Chem. Soc.* **74**, 3729 (1952)

216 R.A. Orwell and P.J. Flory, *J. Am. Chem. Soc.* **89**, 6814 (1967)

217 G.A. Bottomley and C.G. Reeves, *J. Chem. Soc.* 3794 (1958)

218 87010 E.S.D.U. Engineering Data (1990)

219 B.D. Smith and R. Srivastava, *"Thermodynamic Data for Pure Compounds B"*, Vol. **25** Physical Sciences, Elsevier (1986)

220 N.B. Vargaftik, *"Tables on Thermophysical Properties of Liquids and Gases"*, 2nd edn., Wiley, New York (1975)

221 I. Mertl and J. Polak, *Collection Czechoslav. Chem. Comm.* **30**, 3526 (1965)

222 D. Ambrose, J.H. Ellender, H.A. Grundy, D.A. Lee and R. Townsend, *J. Chem. Thermodyn.* **13**, 795 (1981)

223 M. Usanovich and A. Dembicky, *Zh. Obshch. Khim.* **29**, 1771 (1959)

224 D.W. van Krevelen, "Properties of Polymers", Elsevier (1990)

Appendix One

Appendix 1.0

A1.1 Thermodynamic Data

A1.1.1

Absorption of Benzene by PDMS (M_w 26000) at 303 K - Run 1

Frequency Change (Hz)	Pressure (Torr)	Φ_1	$\ln^{v}\gamma_1$	χ_1
16	6.368	0.0097	1.7215	0.7455
27	10.52	0.0162	1.7060	0.7463
42	15.05	0.0238	1.6790	0.7376
58	20.88	0.0342	1.6450	0.7282
71	25.17	0.0416	1.6369	0.7386
90	30.73	0.0521	1.6099	0.7368
126	40.36	0.0715	1.5659	0.7392
168	49.92	0.0931	1.5135	0.7375
215	59.14	0.1161	1.4613	0.7389
287	70.16	0.1492	1.3805	0.7316
368	79.00	0.1835	1.2911	0.7119
499	89.64	0.2336	1.1753	0.6961
639	97.22	0.2807	1.0720	0.6818

ΔF_o = 1818 Hz

A1.1.2

Absorption of Benzene by PDMS (M_w 26000) at 303 K - Run 2

Frequency Change (Hz)	Pressure (Torr)	Φ_1	$\ln^{v}\gamma_1$	χ_1
29	11.35	0.0174	1.7121	0.7556
55	20.40	0.0325	1.6731	0.7538
87	30.27	0.0505	1.6271	0.7514
121	39.39	0.0688	1.5793	0.7475
163	49.52	0.0905	1.5330	0.7538
213	59.47	0.1151	1.4751	0.7538
273	68.97	0.1429	1.4062	0.7475
367	80.08	0.1831	1.3068	0.7341

ΔF_o = 1818 Hz

A1.1.3

Absorption of Hexane by PDMS (M_w 26000) at 303 K

Frequency Change (Hz)	Pressure (Torr)	Φ_1	$\ln^v\gamma_1$	χ_1
19	10.92	0.0153	1.3662	0.3934
38	20.81	0.0301	1.3320	0.3849
59	30.75	0.0459	1.2980	0.3778
80	40.40	0.0613	1.2816	0.3891
105	50.61	0.0789	1.2529	0.3911
130	60.24	0.0959	1.2311	0.4000
159	69.73	0.1148	1.1962	0.3969
192	80.00	0.1354	1.1675	0.4052
230	89.56	0.1580	1.1252	0.3994
272	99.11	0.1816	1.0862	0.3999
334	110.4	0.2141	1.0281	0.3923
393	119.1	0.2428	0.9775	0.3842
471	128.5	0.2776	0.9185	0.3757

ΔF_0 = 1818 Hz

A1.1.4

Absorption of Chloroform by PDMS (M_w 26000) at 303 K

Frequency Change (Hz)	Pressure (Torr)	Φ_1	$\ln^v\gamma_1$	χ_1
51	24.67	0.0212	1.5882	0.6362
85	39.39	0.0349	1.5584	0.6370
139	60.37	0.0558	1.5141	0.6393
193	79.03	0.0759	1.4755	0.6455
264	99.73	0.1009	1.4210	0.6457
341	118.1	0.1267	1.3619	0.6406
457	140.5	0.1627	1.2835	0.6365
621	160.9	0.2089	1.1678	0.6020

ΔF_0 = 1542 Hz

A1.1.5

Absorption of Benzene by Polystyrene (M_n 430000) at 298K

Frequency Change (Hz)	Pressure (Torr)	Φ_1	$\ln^v\gamma_1$	χ_1
32	9.858	0.0216	1.5801	0.6286
69	19.72	0.0455	1.5290	0.6306
112	29.47	0.0718	1.4735	0.6330
168	39.53	0.1040	1.3961	0.6230
236	48.84	0.1402	1.3082	0.6066
456	68.26	0.2396	1.1055	0.5968
640	76.91	0.3066	0.9774	0.5908
1257	88.74	0.4648	0.7034	0.5875

ΔF_o = 1736 Hz

A1.1.6

Absorption of Benzene by Polystyrene (M_n 430000) at 303K

Frequency Change (Hz)	Pressure (Torr)	Φ_1	$\ln^v\gamma_1$	χ_1
29	9.783	0.0197	1.4376	0.4760
61	19.35	0.0406	1.3968	0.4753
100	29.56	0.0649	1.3511	0.4758
142	39.21	0.0898	1.3090	0.4813
196	49.28	0.1198	1.2480	0.4748
247	56.94	0.1464	1.1913	0.4635
338	68.39	0.1901	1.1124	0.4613
434	77.60	0.2316	1.0406	0.4610
597	88.93	0.2931	0.9405	0.4674

ΔF_o = 1736 Hz

A1.1.7

Absorption of Benzene by Polystyrene (M_n 430000) at 308K

Frequency Change (Hz)	Pressure (Torr)	Φ_1	$\ln^v\gamma_1$	χ_1
25	10.21	0.0175	1.3698	0.4011
50	19.60	0.0343	1.3467	0.4086
79	29.81	0.0531	1.3290	0.4262
118	42.09	0.0774	1.2994	0.4426
146	49.39	0.0940	1.2651	0.4374
182	58.24	0.1145	1.2330	0.4432
234	68.69	0.1426	1.1976	0.4382
295	78.94	0.1733	1.1242	0.4353
369	89.01	0.2077	1.0636	0.4323

ΔF_o = 1736 Hz

A1.1.8

Absorption of Chloroform by Polystyrene (M_n 430000) at 298K

Frequency Change (Hz)	Pressure (Torr)	Φ_1	$\ln^v\gamma_1$	χ_1
221	38.46	0.0661	1.1130	0.2053
344	57.30	0.0992	1.1040	0.2503
503	77.07	0.1386	1.0639	0.2729
688	95.38	0.1804	1.0122	0.2869
939	115.0	0.2311	0.9506	0.3073
1398	140.6	0.3091	0.8588	0.3518

ΔF_o = 2223 Hz

A1.1.9

Absorption of Chloroform by Polystyrene (M_n 430000) at 303K

Frequency Change (Hz)	Pressure (Torr)	Φ_1	$\ln^v\gamma_1$	χ_1
390	78.45	0.1110	1.0779	0.2390
679	114.9	0.1786	0.9861	0.2442
1005	144.1	0.2435	0.9044	0.2584
1381	169.0	0.3067	0.8345	0.2938

ΔF_o = 2223 Hz

A1.1.10

Absorption of Chloroform by Polystyrene (M_n 430000) at 308K

Frequency Change (Hz)	Pressure (Torr)	Φ_1	$\ln^{\nu}\gamma_1$	χ_1
308	77.49	0.0903	1.0953	0.2242
525	116.1	0.1447	1.0254	0.2325
811	154.1	0.2071	0.9471	0.2453
1067	181.5	0.2594	0.8841	0.2616

ΔF_o = 2223 Hz

A1.1.11

Absorption of Cyclohexane by Polystyrene (M_n 430000) at 303K

Frequency Change(Hz)	Pressure (Torr)	Φ_1	$\ln^{\nu}\gamma_1$	χ_1
15	9.850	0.0102	2.0908	1.1237
33	19.79	0.0221	2.0112	1.0805
54	30.02	0.0356	1.9484	1.0581
80	39.89	0.0519	1.8557	1.0096
111	50.22	0.0706	1.7774	0.9816
148	59.90	0.0919	1.6883	0.9462
195	69.81	0.1177	1.5934	0.9134
249	79.40	0.1455	1.5088	0.8962
336	89.46	0.1869	1.3771	0.8530
478	99.52	0.2464	1.2062	0.7969
681	108.9	0.3178	1.0409	0.7707

ΔF_o = 1990 Hz

A1.1.12

Absorption of Hexane by Polystyrene (M_n 430000) at 303K

Frequency Change (Hz)	Pressure (Torr)	Φ_1	$\ln^v\gamma_1$	χ_1
10	11.21	0.0080	2.0350	1.0600
17	20.09	0.0136	2.0925	1.1367
27	30.16	0.0214	2.0431	1.1115
37	39.89	0.0291	2.0145	1.1070
50	50.26	0.0389	1.9535	1.0743
74	69.92	0.0565	1.9080	1.0835
107	92.28	0.0797	1.8393	1.0850
150	115.6	0.1082	1.7558	1.0866
185	130.5	0.1302	1.6907	1.0851
258	150.0	0.1727	1.5454	1.0493

ΔF_o = 1990 Hz

A1.1.13

Absorption of MEK by Polystyrene (M_n 430000) at 303K

Frequency Change (Hz)	Pressure (Torr)	Φ_1	$\ln^v\gamma_1$	χ_1
30	9.940	0.0120	1.9922	1.0288
72	19.92	0.0284	1.8276	0.9067
121	29.85	0.0468	1.7311	0.8561
183	40.25	0.0691	1.6391	0.8171
256	50.48	0.0940	1.5560	0.7920
309	59.80	0.1113	1.5557	0.8446
420	69.91	0.1455	1.4432	0.8063
541	79.93	0.1799	1.3641	0.8088
737	90.63	0.2301	1.2427	0.7975
979	98.40	0.2841	1.1131	0.7752

ΔF_o = 3250 Hz

A1.1.14

Absorption of IPA by Polystyrene (M_n 430000) at 303K

Frequency Change(Hz)	Pressure (Torr)	Φ_1	$\ln^v\gamma_1$	χ_1
39	6.528	0.0193	1.7314	0.7806
51	11.11	0.0251	2.0001	1.0787
62	15.67	0.0303	2.1534	1.2590
71	20.61	0.0346	2.2955	1.4271
81	25.89	0.0393	2.3958	1.5548
93	30.49	0.0448	2.4262	1.6124
103	35.46	0.0494	2.4791	1.6916
119	40.03	0.0567	2.4629	1.7075
134	44.76	0.0634	2.4622	1.7389
158	50.40	0.0739	2.4265	1.7492

ΔF_o = 2670 Hz

A1.1.15

Absorption of Benzene by Poly(4-chlorostyrene) (M_n 60000) at 303K

Frequency Change (Hz)	Pressure (Torr)	Φ_1	$\ln^v\gamma_1$	χ_1
50	9.346	0.0303	0.9627	-0.0075
90	19.50	0.0533	1.1335	0.2084
136	30.38	0.0784	1.1899	0.3159
180	39.12	0.1012	1.1868	0.3565
238	48.80	0.1296	1.1599	0.3821
307	58.90	0.1611	1.1293	0.4127
391	69.81	0.1965	1.0997	0.4589
501	79.20	0.2386	1.0310	0.4651
664	89.66	0.2935	0.9473	0.4822
880	98.78	0.3550	0.8529	0.4999

ΔF_o = 2209 Hz

A1.1.16

Absorption of Cyclohexane by Poly(4-chlorostyrene) (M_n 60000) at 303K

Frequency Change (Hz)	Pressure (Torr)	Φ_1	$\ln^{\nu}\gamma_1$	χ_1
16	9.399	0.0112	1.9485	0.9815
31	19.48	0.0214	2.0253	1.0931
49	29.46	0.0334	1.9926	1.0982
70	39.64	0.0471	1.9459	1.0936
94	49.79	0.0623	1.8941	1.0876
123	59.75	0.0799	1.8257	1.0697
156	68.70	0.0992	1.7480	1.0442
201	79.42	0.1243	1.6667	1.0315
260	89.75	0.1551	1.5664	1.0109
354	100.1	0.2000	1.4201	0.9690
478	107.9	0.2524	1.2621	0.9205

ΔF_o = 2209 Hz

A1.1.17

Absorption of Hexane by Poly(4-chlorostyrene) (M_n 60000) at 303K

Frequency Change (Hz)	Pressure (Torr)	Φ_1	$\ln^v\gamma_1$	χ_1
30	10.25	0.0245	0.8251	-0.1580
42	20.55	0.0339	1.1929	0.2430
49	32.35	0.0393	1.4969	0.5810
58	42.68	0.0462	1.6615	0.7230
64	50.86	0.0508	1.6923	0.8247
72	60.81	0.0567	1.7585	0.9163
80	71.04	0.0627	1.8138	0.9976
86	80.47	0.0670	1.8699	1.0764
95	93.42	0.0735	1.9252	1.1635
102	101.3	0.0785	1.9395	1.1990
115	111.1	0.0877	1.9207	1.2114
128	121.7	0.0966	1.9137	1.2380
143	130.8	0.1067	1.8853	1.2432
162	140.5	0.1192	1.8451	1.2431
192	151.3	0.1382	1.7700	1.2230
232	160.5	0.1624	1.6672	1.1823
328	172.4	0.2151	1.4562	1.0896

ΔF_o = 2209 Hz

A1.1.18

Absorption of MEK by Poly(4-chlorostyrene) (M_n 60000) at 303K

Frequency Change (Hz)	Pressure (Torr)	Φ_1	$\ln^v\gamma_1$	χ_1
86	20.88	0.0555	1.2028	0.2896
130	30.21	0.0816	1.1861	0.3174
176	39.59	0.1074	1.1811	0.3621
238	49.80	0.1399	1.1449	0.3851
318	59.99	0.1786	1.0863	0.3926
407	69.56	0.2177	1.0354	0.4136
524	79.48	0.2638	0.9758	0.4420
675	88.83	0.3158	0.9062	0.4740
899	98.64	0.3807	0.8231	0.5311

ΔF_o = 2209 Hz

A1.1.19

Absorption of IPA by Poly(4-chlorostyrene) (M_n 60000) at 303K

Frequency Change (Hz)	Pressure (Torr)	Φ_1	$\ln^v\gamma_1$	χ_1
15	9.968	0.0104	2.7747	1.8227
24	16.07	0.0165	2.7874	1.8649
32	21.16	0.0219	2.7796	1.8830
39	25.62	0.0265	2.7771	1.9034
48	30.57	0.0325	2.7514	1.9057
58	35.21	0.0390	2.7095	1.8932
69	39.86	0.0460	2.6665	1.8818
82	45.73	0.0542	2.6390	1.8929
96	50.53	0.0629	2.5896	1.8818

ΔF_o = 2209 Hz

A1.1.20

Absorption of Benzene by PMMA (M_n 56000) at 303K

Frequency Change (Hz)	Pressure (Torr)	Φ_1	$\ln^v\gamma_1$	χ_1
25	5.123	0.0112	1.3548	0.3744
52	10.30	0.0231	1.3322	0.3723
107	20.42	0.0464	1.3185	0.4012
167	31.19	0.0706	1.3217	0.4540
224	39.85	0.0924	1.2961	0.4717
294	50.01	0.1179	1.2789	0.5099
393	60.05	0.1516	1.2097	0.5019
505	69.69	0.1867	1.1493	0.5080
678	79.95	0.2356	1.0532	0.4942
911	88.79	0.2928	0.9509	0.4874
1276	99.18	0.3671	0.8236	0.4760

ΔF_o = 2964 Hz

A1.1.21

Absorption of Benzene by PMMA (M_n 56000) at 313K

Frequency Change (Hz)	Pressure (Torr)	Φ_1	$\ln^v\gamma_1$	χ_1
50	19.59	0.0224	1.5824	0.6329
108	39.06	0.0472	1.5266	0.6321
182	59.51	0.0771	1.4560	0.6259
279	79.68	0.1135	1.3594	0.6018
407	100.3	0.1574	1.2607	0.5890
573	119.1	0.2083	1.1516	0.5741
871	139.4	0.2857	0.9915	0.5431

ΔF_o = 2964 Hz

A1.1.22

Absorption of Hexane by PMMA (M_n 56000) at 303K

Frequency Change(Hz)	Pressure (Torr)	Φ_1	$\ln^v\gamma_1$	χ_1
18	20.43	0.0108	2.3301	1.3703
31	32.47	0.0185	2.2563	1.3232
40	41.73	0.0237	2.2567	1.3433
51	50.86	0.0300	2.2171	1.3256
61	60.14	0.0357	2.2106	1.3403
76	71.22	0.0441	2.1674	1.3258
89	80.44	0.0513	2.1378	1.3210
103	90.84	0.0589	2.1202	1.3311
119	100.6	0.0674	2.0858	1.3258
135	111.0	0.0758	2.0661	1.3366
154	120.6	0.0855	2.0269	1.3301
180	129.9	0.0985	1.9585	1.3007
213	141.1	0.1145	1.8896	1.2806
261	152.0	0.1368	1.7851	1.2372

ΔF_o = 2964 Hz

A1.1.23

Absorption of Hexane by PMMA (M_n 56000) at 313K

Frequency Change (Hz)	Pressure (Torr)	Φ_1	$\ln^{v}\gamma_1$	χ_1
12	20.26	0.0073	2.3149	1.3418
26	42.46	0.0157	2.2882	1.3460
41	64.45	0.0246	2.2573	1.3472
52	80.03	0.0310	2.2414	1.3549
70	102.0	0.0412	2.1955	1.3454
95	130.3	0.0552	2.1472	1.3468
117	151.6	0.0671	2.1012	1.3423
140	172.8	0.0792	2.0639	1.3483
171	190.8	0.0951	1.9789	1.3115
204	210.5	0.1114	1.9172	1.3026
268	233.1	0.1414	1.7787	1.2481

ΔF_o =2964 Hz

A1.1.24

Absorption of MEK by PMMA (M_n 56000) at 303K

Frequency Change (Hz)	Pressure (Torr)	Φ_1	$\ln^{v}\gamma_1$	χ_1
32	5.641	0.0156	1.1621	0.1834
59	11.91	0.0285	1.3098	0.3584
77	16.10	0.0368	1.3533	0.4206
97	20.90	0.0460	1.3925	0.4817
140	30.72	0.0650	1.4300	0.5663
184	40.09	0.0838	1.4423	0.6266
237	50.11	0.1053	1.4351	0.6752
298	59.93	0.1289	1.4109	0.7115
381	69.67	0.1591	1.3501	0.7203
489	79.31	0.1954	1.2734	0.7243
659	89.58	0.2466	1.1616	0.7193

ΔF_o = 2964 Hz

A1.1.25

Absorption of MEK by PMMA (M_n 56000) at 313K

Frequency Change (Hz)	Pressure (Torr)	Φ_1	$\ln^v\gamma_1$	χ_1
38	9.844	0.0187	1.1019	0.1253
65	20.23	0.0317	1.2975	0.3510
89	29.95	0.0428	1.3862	0.4683
139	49.25	0.0653	1.4594	0.6006
194	69.72	0.0889	1.4969	0.7056
261	90.06	0.1160	1.4842	0.7681
357	109.7	0.1522	1.4075	0.7787
509	130.3	0.2038	1.2858	0.7722

ΔF_o = 2964 Hz

A1.1.26

Absorption of IPA by PMMA (M_n 56000) at 303K

Frequency Change (Hz)	Pressure (Torr)	Φ_1	$\ln^v\gamma_1$	χ_1
21	5.151	0.0106	2.0983	1.1326
43	10.51	0.0214	2.1049	1.1760
63	15.50	0.0310	2.1206	1.2265
83	20.16	0.0405	2.1168	1.2569
103	25.04	0.0497	2.1266	1.3027
124	30.07	0.0593	2.1334	1.3476
146	34.98	0.0691	2.1310	1.3847
172	40.50	0.0804	2.1249	1.4252

ΔF_o = 2964 Hz

A1.1.27

Absorption of IPA by PMMA (M_n 56000) at 313K

Frequency Change (Hz)	Pressure (Torr)	Φ_1	$\ln^v\gamma_1$	χ_1
29	10.30	0.0146	1.9047	0.9469
54	20.49	0.0269	1.9820	1.0656
76	30.28	0.0375	2.0405	1.1636
98	40.33	0.0478	2.0824	1.2466
124	51.13	0.0598	2.0956	1.3069
151	61.46	0.0718	2.0943	1.3536
183	71.41	0.0858	2.0660	1.3779

ΔF_o = 2964 Hz

A1.1.28

Absorption of Methanol by PMMA (M_n 56000) at 303K

Frequency Change (Hz)	Pressure (Torr)	Φ_1	$\ln^v\gamma_1$	χ_1
17	10.698	0.0085	2.0660	1.0930
29	20.72	0.0144	2.1979	1.2481
41	31.98	0.0203	2.2905	1.3656
52	41.78	0.0256	2.3245	1.4219
62	50.67	0.0303	2.3455	1.4633
76	61.14	0.0369	2.3355	1.4798
91	71.16	0.0439	2.3134	1.4849
106	80.70	0.0508	2.2928	1.4913
143	100.3	0.0673	2.2264	1.4872
198	122.6	0.0909	2.1250	1.4711

ΔF_o = 2964 Hz

A1.1.29

Absorption of Ethanol by PMMA (M_n 56000) at 303K

Frequency Change (Hz)	Pressure (Torr)	Φ_1	$\ln^{\infty}\gamma_1$	χ_1
43	10.42	0.0213	1.8321	0.8909
71	20.74	0.0347	2.0309	1.1434
92	29.76	0.0444	2.1418	1.2991
122	39.85	0.0581	2.1644	1.3780
149	49.05	0.0701	2.1837	1.4497
177	55.06	0.0821	2.1392	1.4497

ΔF_o = 2964 Hz

A1.1.30

Absorption of Methyl Acetate by PMMA (M_n 56000) at 303K

Frequency Change (Hz)	Pressure (Torr)	Φ_1	$\ln^{\infty}\gamma_1$	χ_1
57	20.00	0.0239	1.1582	0.1911
99	41.47	0.0407	1.3510	0.4257
139	63.07	0.0563	1.4454	0.5632
169	80.76	0.0676	1.5077	0.6617
210	104.0	0.0826	1.5573	0.7603
252	124.6	0.0975	1.5706	0.8204
318	150.3	0.1200	1.5485	0.8633
412	175.0	0.1502	1.4744	0.8648
555	199.7	0.1923	1.3571	0.8421
928	234.2	0.2847	1.1209	0.7927

ΔF_o = 2964 Hz

A1.1.31

Absorption of Ethyl Acetate by PMMA (M_n 56000) at 303K

Frequency Change (Hz)	Pressure (Torr)	Φ_1	$\ln^{\nu}\gamma_1$	χ_1
59	9.848	0.0256	1.1857	0.2225
110	20.03	0.0466	1.2935	0.3742
150	29.48	0.0625	1.3855	0.5098
202	40.84	0.0824	1.4340	0.6133
244	50.13	0.0979	1.4660	0.6928
299	60.06	0.1173	1.4641	0.7463
366	69.48	0.1400	1.4325	0.7739
466	79.47	0.1716	1.3617	0.7772
618	89.44	0.2155	1.2509	0.7580
850	98.88	0.2743	1.1092	0.7281
1158	106.3	0.3399	0.9658	0.7015

ΔF_o = 2964 Hz

A1.1.32

Absorption of Propyl Acetate by PMMA (M_n 56000) at 303K

Frequency Change (Hz)	Pressure (Torr)	Φ_1	$\ln^{\nu}\gamma_1$	χ_1
74	4.587	0.0322	1.1826	0.2294
138	9.617	0.0585	1.3264	0.4342
194	14.69	0.0803	1.4320	0.6057
253	19.69	0.1022	1.4827	0.7258
327	24.40	0.1283	1.4693	0.7865
427	29.12	0.1612	1.4171	0.8219
597	34.14	0.2118	1.3023	0.8276
878	39.21	0.2833	1.1493	0.8420

ΔF_o = 2964 Hz

A1.1.33

Absorption of Butyl Acetate by PMMA (M_n 56000) at 303K

Frequency Change (Hz)	Pressure (Torr)	Φ_1	$\ln^v\gamma_1$	χ_1
32	0.980	0.0143	1.7212	0.7570
62	1.912	0.0273	1.7412	0.8123
92	2.848	0.0400	1.7579	0.8657
122	3.839	0.0523	1.7869	0.9346
152	4.869	0.0644	1.8173	1.0072
178	5.801	0.0746	1.8452	1.0740
203	6.798	0.0842	1.8825	1.1526
232	7.839	0.0951	1.9032	1.2189
268	8.879	0.1082	1.8978	1.2650
329	10.51	0.1297	1.8851	1.3396

ΔF_o = 2964 Hz

Solvents	T (K)	P° (Torr)	-B ($dm^3\ mol^{-1}$)	ρ ($g\ cm^{-3}$)	V ($cm^3\ mol^{-1}$)[a]	M. Wt. (g)[b]
Benzene	298	94.52[c]	1.478[d]	0.8738[e]	89.40	78.11
Benzene	303	118.76[c]	1.492[d]	0.8684[e]	89.95	78.11
Benzene	308	147.35[c]	1.357[d]	0.8632[e]	90.50	78.11
Benzene	313	181.65[c]	1.420[d]	0.8576[f]	91.08	78.11
Chloroform	298	193.42[c]	1.227[d]	1.4701[f]	81.21	119.38
Chloroform	303	238.25[c]	1.160[d]	1.4701[f]	81.20	119.38
Chloroform	308	291.14[c]	1.178[d]	1.4603[f]	81.75	119.38
Cyclohexane	303	121.15[g]	1.702[d]	0.7392[h]	109.41	84.16
Hexane	303	185.86[g]	1.845[d]	0.6502[i]	132.54	86.18
Hexane	313	279.42[g]	1.620[j]	0.6408[k]	134.50	86.18
MEK	303	113.94[g]	1.699[l]	0.7946[f]	90.75	72.11
MEK	313	177.65[g]	2.035[l]	0.7830[f]	92.09	72.11
IPA	303	60.38[c]	29.38[l]	0.7769[m]	77.36	60.10
IPA	313	105.95[c]	23.64[l]	0.7681[k]	78.25	60.10
Methanol	303	161.78[f]	18.94[f]	0.7820[f]	40.97	32.04
Ethanol	303	79.21[f]	26.86[f]	0.7808[f]	59.00	46.07
Methyl Acetate	303	268.92[n]	15.50[f]	0.9204[f]	80.49	74.08
Ethyl Acetate	303	119.17[n]	20.40[f]	0.8878[f]	99.24	88.11
Propyl Acetate	303	43.89[o]	30.00[f]	0.8769[f]	116.50	102.13
Butyl Acetate	303	12.31[p]	49.99[f]	0.8718[f]	133.20	116.16

Table A1.2.1: Properties of Pure Solvents for Thermodynamic Studies

Polymer	T (K)	ρ (g cm^{-3})	M_n	V_2 (cm^3 mol^{-1})
PDMS	303	0.9643[q]	26000	26960
Polystyrene	298	1.0482[r]	119628	114130
Polystyrene	303	1.0470[r]	119628	114230
Polystyrene	308	1.0458[r]	119628	114390
Poly(4-chlorostyrene)	303	1.2000[s]	60000	50000
PMMA	303	1.1700[r]	56000	47863
PMMA	313	1.1670[r]	56000	47986

Table A1.2.2: Properties of Polymers

Key to Tables A1.2.1 and A1.2.2

a. The molar volumes were calculated from the molecular weight and density values
b. Ref. 210
c. The S.V.P. was calculated from Antoine vapour pressure coefficients obtained from Ref. 211
d. The second virial coefficients were calculated from data extrapolated from Ref. 212
e. Ref. 213
f. Ref. 199
g. Ref. 214
h. Ref. 215
i. Ref. 216
j. Ref. 217
k. Ref. 218
l. Ref. 219
m. Ref. 220
n. Ref. 221
o. Ref. 222
p. Ref. 223
q. Ref. 159
r. Ref. 224
s. Ref. 176

Appendix Two

Appendix 2.0

2.1 Dissolution Data

A2.1.1

Dissolution of PMMA (M_n 6100, γ 1.11) in 100% MEK

T (°C)	Film Thickness (μm)	Dissn. Rate (μm s^{-1})*10^3	ln (Dissn. Rate)
16.25	0.187	73.936	-2.605
20.25	0.303	126.005	-2.071

A2.1.2

Disssolution of PMMA (M_n 10300, γ 1.06) in 100% MEK

T (°C)	Film Thickness (μm)	Dissn. Rate (μm s^{-1})*10^3	ln (Dissn. Rate)
16.30	0.284	48.103	-3.034
20.40	0.335	75.529	-2.583
25.40	0.371	139.217	-1.972
29.90	0.333	231.401	-1.463
35.10	0.380	345.477	-1.063

A2.1.3

Dissolution of PMMA (M_n 22200, γ 1.07) in 100% MEK

T (°C)	Film Thickness (μm)	Dissn. Rate (μm s^{-1})*10^3	ln (Dissn. Rate)
16.55	0.400	18.660	-3.981
20.30	0.323	30.959	-3.475
25.30	0.347	55.520	-2.891
30.15	0.466	120.563	-2.116
35.15	0.401	195.491	-1.632
40.00	0.402	317.580	-1.147

A2.1.4

Dissolution of PMMA (M_n 34500, γ 1.04) in 100% MEK

T (°C)	Film Thickness (μm)	Dissn. Rate (μm s^{-1})*10^3	ln (Dissn. Rate)
16.50	0.412	11.840	-4.436
20.50	0.344	19.673	-3.928
25.70	0.386	33.991	-3.384
30.15	0.444	68.771	-2.677
35.30	0.382	119.141	-2.127
40.15	0.473	240.520	-1.425

A2.1.5

Dissolution of PMMA (M_n 67000, γ 1.04) in 100% MEK

T (°C)	Film Thickness (μm)	Dissn. Rate (μm s^{-1})*10^3	ln (Dissn. Rate)
16.90	0.342	7.630	-4.876
20.40	0.312	12.533	-4.380
25.35	0.349	26.537	-3.629
30.30	0.404	45.050	-3.100
35.10	0.413	84.768	-2.468
45.20	0.455	282.673	-1.263

A2.1.6

Dissolution of PMMA (M_n 107000, γ 1.10) in 100% MEK

T (°C)	Film Thickness (μm)	Dissn. Rate (μm s^{-1})*10^3	ln (Dissn. Rate)
16.25	0.462	5.082	-5.282
20.55	0.426	9.678	-4.638
25.30	0.484	19.698	-3.927
29.90	0.451	35.000	-3.352
35.20	0.457	67.064	-2.702
40.05	0.461	124.350	-2.085

A2.1.7

Dissolution of PMMA (M_n 330000, γ 1.11) in 100% MEK

T (°C)	Film Thickness (μm)	Dissn. Rate (μm s^{-1})*10^3	ln (Dissn. Rate)
16.30	0.796	3.550	-5.641
20.45	0.748	6.919	-4.973
25.35	0.657	14.697	-4.220
30.40	0.790	31.884	-3.446
34.95	0.816	57.389	-2.858
40.35	0.776	117.276	-2.143

A2.1.8

Dissolution of PMMA (M_n 820000, γ 1.04) in 100% MEK

T (°C)	Film Thickness (μm)	Dissn. Rate (μm s^{-1})*10^3	ln (Dissn. Rate)
16.45	0.720	3.045	-5.794
20.40	0.694	5.822	-5.146
25.30	0.849	13.142	-4.332
29.95	0.803	27.679	-3.587
35.65	0.868	57.617	-2.854
39.85	0.301	90.700	-2.400

A2.1.9

Dissolution of PMMA (M_n 1400000, γ 1.07) in 100% MEK

T (°C)	Film Thickness (μm)	Dissn. Rate (μm s^{-1})*10^3	ln (Dissn. Rate)
16.50	0.422	3.392	-5.686
20.45	0.792	6.684	-5.008
24.95	0.905	11.448	-4.470
30.70	0.242	33.042	-3.410
34.90	0.702	49.982	-2.996
40.25	0.317	89.172	-2.417

A2.1.10

Dissolution of PMMA (M_n 22200 γ 1.07) in Methyl Acetate

T (°C)	Film Thickness (μm)	Dissn. Rate (μm s^{-1})*10^3	ln (Dissn. Rate)
14.90	0.295	44.642	-3.109
20.15	0.273	99.150	-2.311

A2.1.11

Dissolution of PMMA (M_n 34500, γ 1.04) in Methyl Acetate

T (°C)	Film Thickness (μm)	Dissn. Rate (μm s^{-1})*10^3	ln (Dissn. Rate)
15.00	0.279	25.896	-3.654
19.80	0.310	49.851	-2.999

A2.1.12

Dissolution of PMMA (M_n 67000, γ 1.04) in Methyl Acetate

T (°C)	Film Thickness (μm)	Dissn. Rate (μm s^{-1})*10^3	ln (Dissn. Rate)
14.90	0.543	21.394	-3.845
20.15	0.561	42.669	-3.154
25.00	0.424	87.649	-2.434

A2.1.13

Dissolution of PMMA (M_n 107000, γ 1.10) in Methyl Acetate

T (°C)	Film Thickness (μm)	Dissn. Rate (μm s^{-1})*10^3	ln (Dissn. Rate)
14.90	0.531	16.609	-4.098
20.15	0.478	33.746	-3.389
25.00	0.408	70.380	-2.654

A2.1.14

Dissolution of PMMA (M_n 330000, γ 1.11) in Methyl Acetate

T (°C)	Film Thickness (μm)	Dissn. Rate ($\mu m\ s^{-1}$)*10^3	ln (Dissn. Rate)
14.90	0.427	10.623	-4.545
20.15	0.608	22.660	-3.787
25.00	0.571	42.071	-3.168

A2.1.15

Dissolution of PMMA (M_n 22200, γ 1.07) in Ethyl Acetate

T (°C)	Film Thickness (μm)	Dissn. Rate ($\mu m\ s^{-1}$)*10^3	ln (Dissn. Rate)
15.05	0.221	12.908	-4.350
20.10	0.307	23.731	-3.741
24.85	0.202	38.006	-3.270

A2.1.16

Dissolution of PMMA (M_n 34500, γ 1.04) in Ethyl Acetate

T (°C)	Film Thickness (μm)	Dissn. Rate ($\mu m\ s^{-1}$)*10^3	ln (Dissn. Rate)
15.05	0.246	6.494	-5.037
20.10	0.252	13.968	-4.271
24.85	0.170	36.709	-3.305
29.95	0.231	54.680	-2.906

A2.1.17

Dissolution of PMMA (M_n 67000, γ 1.04) in Ethyl Acetate

T (°C)	Film Thickness (μm)	Dissn. Rate ($\mu m\ s^{-1}$)*10^3	ln (Dissn. Rate)
15.05	0.482	4.473	-5.410
20.10	0.468	10.048	-4.600
24.85	0.368	21.310	-3.849
29.95	0.517	44.410	-3.114
34.80	0.608	84.512	-2.471

A2.1.18

Dissolution of PMMA (M_n 107000, γ 1.10) in Ethyl Acetate

T (°C)	Film Thickness (μm)	Dissn. Rate ($\mu m\ s^{-1}$)*10^3	ln (Dissn. Rate)
15.90	0.221	5.794	-5.151
20.55	0.252	9.562	-4.650
25.85	0.329	18.259	-4.003
30.50	0.238	29.626	-3.519
34.85	0.209	44.504	-3.112
39.65	0.275	72.501	-2.624

A2.1.19

Dissolution of PMMA (M_n 330000, γ 1.11) in Ethyl Acetate

T (°C)	Film Thickness (μm)	Dissn. Rate ($\mu m\ s^{-1}$)*10^3	ln (Dissn. Rate)
17.50	0.820	3.239	-5.733
21.40	0.995	6.089	-5.101
25.20	0.673	10.667	-4.541
30.10	0.614	21.717	-3.830
35.10	0.814	42.523	-3.158
39.80	0.612	71.420	-2.639

A2.1.20

Dissolution of PMMA (M_n 22200, γ 1.07) in n-Propyl Acetate

T (°C)	Film Thickness (μm)	Dissn. Rate ($\mu m\ s^{-1}$)*10^3	ln (Dissn. Rate)
15.05	0.238	2.977	-5.817
19.90	0.223	5.798	-5.150
24.90	0.194	11.993	-4.423
29.90	0.216	19.818	-3.921
34.90	0.253	48.411	-3.028
39.95	0.259	86.094	-2.452

A2.1.21

Dissolution of PMMA (M_n 34500, γ 1.04) in n-Propyl Acetate

T (°C)	Film Thickness (μm)	Dissn. Rate (μm s^{-1})*10^3	ln (Dissn. Rate)
15.05	0.349	1.193	-6.731
19.90	0.347	2.560	-5.967
24.90	0.158	6.569	-5.021
29.90	0.219	14.107	-4.261
34.80	0.257	30.081	-3.504
39.95	0.210	62.836	-2.767

A2.1.22

Dissolution of PMMA (M_n 67000, γ 1.04) in n-Propyl Acetate

T (°C)	Film Thickness (μm)	Dissn. Rate (μm s^{-1})*10^3	ln (Dissn. Rate)
15.05	0.257	0.840	-7.082
19.90	0.164	1.801	-6.319
24.90	0.299	4.168	-5.480
29.90	0.322	9.470	-4.660
34.90	0.247	19.194	-3.953
39.95	0.341	43.194	-3.142

A2.1.23

Dissolution of PMMA (M_n 107000, γ 1.10) in n-Propyl Acetate

T (°C)	Film Thickness (μm)	Dissn. Rate (μm s^{-1})*10^3	ln (Dissn. Rate)
15.00	0.491	0.618	-7.388
20.05	0.378	1.387	-6.580
24.90	0.301	3.571	-5.635
29.80	0.464	6.820	-4.988
35.00	0.501	30.012	-4.300
39.80	0.505	44.712	-3.506

A2.1.24

Dissolution of PMMA (M_n 330000, γ 1.11) in n-Propyl Acetate

T (°C)	Film Thickness (μm)	Dissn. Rate ($\mu m\ s^{-1}$)*10^3	ln (Dissn. Rate)
15.00	0.613	0.386	-7.859
20.05	0.631	1.097	-6.814
24.90	0.857	1.893	-6.269
29.80	0.637	4.363	-5.435
34.70	0.746	10.167	-4.589
39.80	0.685	20.419	-3.891

A2.1.25

Dissolution of PMMA (M_n 22200, γ 1.07) in Isopropyl Acetate

T (°C)	Film Thickness (μm)	Dissn. Rate ($\mu m\ s^{-1}$)*10^3	ln (Dissn. Rate)
14.90	0.276	1.214	-6.713
20.10	0.235	2.740	-5.900
25.00	0.309	6.720	-5.003
30.10	0.279	12.761	-4.361
35.00	0.303	20.964	-3.865
40.00	0.297	31.805	-3.448

A2.1.26

Dissolution of PMMA (M_n 34500, γ 1.04) in Isopropyl Acetate

T (°C)	Film Thickness (μm)	Dissn. Rate ($\mu m\ s^{-1}$)*10^3	ln (Dissn. Rate)
15.10	0.321	0.481	-7.639
19.95	0.280	1.279	-6.661
24.90	0.255	2.822	-5.870
29.80	0.308	5.445	-5.213
34.60	0.228	11.646	-4.453

A2.1.27

Dissolution of PMMA (M_n67000, γ 1.04) in Isopropyl Acetate

T (°C)	Film Thickness (μm)	Dissn. Rate (μm s^{-1})*10^3	ln (Dissn. Rate)
14.90	0.345	0.341	-7.985
20.10	0.499	0.968	-6.940
25.00	0.438	2.031	-6.199
30.10	0.423	3.519	-5.650
35.00	0.389	8.733	-4.741
40.00	0.495	18.859	-3.971

A2.1.28

Dissolution of PMMA (M_n 107000, γ 1.10) in Isopropyl Acetate

T (°C)	Film Thickness (μm)	Dissn. Rate (μm s^{-1})*10^3	ln (Dissn. Rate)
14.90	0.516	0.273	-8.206
20.10	0.439	0.676	-7.301
25.00	0.387	1.776	-6.333
30.10	0.361	3.418	-5.679
35.00	0.410	6.970	-4.966
40.00	0.380	12.391	-4.391

A2.1.29

Dissolution of PMMA (M_n 330000, γ 1.10) in Isopropyl Acetate

T (°C)	Film Thickness (μm)	Dissn. Rate (μm s^{-1})*10^3	ln (Dissn. Rate)
14.90	0.513	0.123	-9.002
20.10	0.481	0.351	-7.954
25.00	0.478	0.941	-6.968
30.10	0.574	2.031	-6.199
35.00	0.515	4.063	-5.506
40.10	0.577	8.730	-4.741

A2.1.30

Dissolution of PMMA (M_n 22200, γ 1.07) in n-Butyl Acetate

T (°C)	Film Thickness (μm)	Dissn. Rate ($\mu m\ s^{-1}$)*10^3	ln (Dissn. Rate)
15.10	0.241	0.771	-7.168
20.05	0.369	1.494	-6.506
25.00	0.327	3.116	-5.771
30.00	0.274	8.609	-4.755
34.85	0.291	15.967	-4.137
39.90	0.350	33.362	-3.400

A2.1.31

Dissolution of PMMA (M_n 34500, γ 1.04) in n-Butyl Acetate

T (°C)	Film Thickness (μm)	Dissn. Rate ($\mu m\ s^{-1}$)*10^3	ln (Dissn. Rate)
15.10	0.269	0.422	-7.770
20.05	0.272	1.078	-6.900
25.00	0.291	1.932	-6.249
30.00	0.280	4.701	-5.360
34.85	0.244	9.825	-4.623
40.00	0.232	20.041	-3.910

A2.1.32

Dissolution of PMMA (M_n 67000, γ 1.04) in n-Butyl Acetate

T (°C)	Film Thickness (μm)	Dissn. Rate ($\mu m\ s^{-1}$)*10^3	ln (Dissn. Rate)
15.00	0.264	0.191	-8.560
19.80	0.215	0.416	-7.783
24.80	0.235	0.937	-6.972
29.80	0.213	2.290	-6.079
34.90	0.259	4.475	-5.409
39.80	0.351	8.406	-4.779

A2.1.33

Dissolution of PMMA (M_n 107000, γ 1.10) in n-Butyl Acetate

T (°C)	Film Thickness (μm)	Dissn. Rate (μm s^{-1})*10^3	ln (Dissn. Rate)
16.15	0.316	0.167	-8.693
20.25	0.333	0.384	-7.864
24.85	0.343	0.799	-7.132
29.70	0.285	1.613	-6.429
34.85	0.287	3.544	-5.642
39.50	0.314	6.876	-4.980

A2.1.34

Dissolution of PMMA (M_n 330000, γ 1.11) in n-Butyl Acetate

T (°C)	Film Thickness (μm)	Dissn. Rate (μm s^{-1})*10^3	ln (Dissn. Rate)
17.65	0.798	0.096	-9.254
21.35	0.793	0.206	-8.487
25.15	0.828	0.422	-7.770
30.05	0.794	1.246	-6.687
35.00	0.756	2.729	-5.904
39.90	0.689	5.656	-5.175

A2.1.35

Dissolution of PMMA (M_n 22200, γ 1.07) in n-Pentyl Acetate

T (°C)	Film Thickness (μm)	Dissn. Rate (μm s^{-1})*10^3	ln (Dissn. Rate)
15.00	0.386	0.247	-8.306
20.10	0.429	0.553	-7.499
25.00	0.446	1.208	-6.718
30.05	0.383	3.247	-5.730
34.90	0.473	6.134	-5.094
39.80	0.519	12.715	-4.365

A2.1.36

Dissolution of PMMA (M_n 34500, γ 1.04) in n-Pentyl Acetate

T (°C)	Film Thickness (μm)	Dissn. Rate ($\mu m\ s^{-1}$)*10^3	ln (Dissn. Rate)
15.00	0.441	0.070	-9.559
20.10	0.384	0.203	-8.500
25.00	0.382	0.488	-7.623
30.05	0.340	1.057	-6.852
34.90	0.456	2.649	-5.933
39.80	0.583	4.599	-5.382

A2.1.37

Dissolution of PMMA (M_n 67000, γ 1.04) in n-Pentyl Acetate

T (°C)	Film Thickness (μm)	Dissn. Rate ($\mu m\ s^{-1}$)*10^3	ln (Dissn. Rate)
15.00	0.454	0.040	-10.117
19.90	0.365	0.113	-9.087
24.90	0.358	0.290	-8.143
30.10	0.317	0.716	-7.241
35.00	0.308	1.509	-6.496
39.80	0.283	3.002	-5.808

A2.1.38

Dissolution of PMMA (M_n 107000, γ 1.10) in n-Pentyl Acetate

T (°C)	Film Thickness (μm)	Dissn. Rate ($\mu m\ s^{-1}$)*10^3	ln (Dissn. Rate)
15.00	0.480	0.017	-11.000
19.90	0.360	0.046	-9.970
24.90	0.411	0.152	-8.791
30.10	0.401	0.336	-7.996
35.00	0.419	0.879	-7.036
39.90	0.450	2.268	-6.089

A2.1.39

Dissolution of PMMA (M_n 330000, γ 1.11) in n-Pentyl Acetate

T (°C)	Film Thickness (μm)	Dissn. Rate ($\mu m\ s^{-1}$)*10^3	ln (Dissn. Rate)
15.00	0.482	0.032	-10.333
19.90	0.651	0.089	-9.317
24.90	0.491	0.230	-8.376
30.10	0.698	0.575	-7.461
35.00	0.599	1.183	-6.740
39.90	0.680	3.101	-5.776

A2.1.40

Dissolution of PMMA (M_n 56000, γ 2.0) in Methyl Acetate

T (°C)	Film Thickness (μm)	Dissn. Rate ($\mu m\ s^{-1}$)*10^3	ln (Dissn. Rate)
14.70	1.189	26.918	-3.615
19.85	0.973	53.096	-2.936
24.90	0.989	95.398	-2.350
30.55	1.742	211.443	-1.554
35.10	1.607	330.817	-1.106

A2.1.41

Dissolution of PMMA (M_n 56000, γ 2.0) in Ethyl Acetate

T (°C)	Film Thickness (μm)	Dissn. Rate ($\mu m\ s^{-1}$)*10^3	ln (Dissn. Rate)
14.75	1.333	8.736	-4.740
20.75	0.964	19.704	-3.927
25.45	1.263	38.306	-3.262
30.35	1.343	59.092	-2.829
35.60	1.309	110.309	-2.204
40.65	1.291	239.390	-1.430

A2.1.42

Dissolution of PMMA (M_n 56000, γ 2.0) in Isopropyl Acetate

T (°C)	Film Thickness (μm)	Dissn. Rate ($\mu m\ s^{-1}$)*10^3	ln (Dissn. Rate)
14.40	0.957	0.842	-7.080
20.15	1.208	2.058	-6.186
26.25	1.132	5.220	-5.255
31.20	1.320	9.372	-4.670
36.50	1.193	18.193	-4.007
40.50	1.186	31.274	-3.465

A2.1.43

Dissolution of PMMA (M_n 56000, γ 2.0) in Butyl Acetate

T (°C)	Film Thickness (μm)	Dissn. Rate ($\mu m\ s^{-1}$)*10^3	ln (Dissn. Rate)
14.40	1.041	0.248	-8.299
19.95	0.682	0.845	-7.075
24.75	1.013	2.147	-6.143
30.75	0.894	5.337	-5.233
35.25	1.097	9.894	-4.616
40.15	1.204	18.613	-3.984

A2.1.44

Swelling of PMMA (M_n 56000, γ 2.0) in Methanol

T (°C)	Film Thickness (μm)	Swell. Rate ($\mu m\ s^{-1}$)*10^3	ln (Swell. Rate)
15.00	0.222	0.439	-7.730
20.10	0.212	0.665	-7.315
24.90	0.167	0.941	-6.968
30.10	0.220	1.458	-6.530
34.90	0.179	2.522	-5.983
39.70	0.212	5.603	-5.184

A2.1.45

Dissolution of PMMA (M_n 56000, γ 2.0) in MEK/Methanol at 25.0°C

% Methanol	Film Thickness (μm)	Slope (s^{-1})	Dissn. Rate ($\mu m\ s^{-1}$)*10^3
0	0.531	7.627	40.499
5	0.741	10.118	74.974
10	0.514	17.353	89.194
20	0.842	11.886	100.080
30	0.716	12.945	92.686
40	0.548	14.866	81.465
50	0.530	10.022	53.116
70	0.776	0.057	0.445

A2.1.46

Dissolution of PMMA (M_n 67000, γ 1.04) in MEK/Methanol at 25.0°C

% Methanol	Film Thickness (μm)	Slope (s^{-1})	Dissn. Rate ($\mu m\ s^{-1}$)*10^3
0	0.686	3.211	22.027
5	0.705	3.333	37.597
10	0.712	6.293	44.806
15	0.707	6.797	48.054
20	0.543	9.090	49.358
25	0.407	11.590	47.171
30	0.553	8.565	47.364
35	0.765	5.485	41.960

A2.1.47

Dissolution of PMMA (M_n 107000, γ 1.10) in MEK/Methanol at 25.0°C

% Methanol	Film Thickness (μm)	Slope (s^{-1})	Dissn. Rate ($\mu m\ s^{-1}$)*10^3
0	0.660	2.950	19.470
5	0.296	10.383	30.733
10	0.346	10.738	37.153
15	0.458	8.370	38.334
20	0.408	10.837	44.214
25	0.516	8.582	44.283
30	0.387	9.313	36.041
35	0.495	7.112	35.204
40	0.509	5.950	30.285

A2.1.48

Dissolution of PMMA (M_n 330000, γ 1.11) in MEK/Methanol at 25.0°C

% Methanol	Film Thickness (μm)	Slope (s^{-1})	Dissn. Rate ($\mu m\ s^{-1}$)*10^3
0	0.742	1.947	14.446
5	1.061	2.095	22.227
10	0.853	3.336	28.456
15	0.715	4.312	30.830
20	1.250	2.507	31.337
25	1.088	2.897	31.519
30	1.471	2.096	30.832
35	1.622	1.801	29.212
40	1.016	2.755	27.990

A2.1.49

Dissolution of PMMA (M_n 56000, γ 2.0) in MEK/Ethanol at 25.0°C

% Ethanol	Film Thickness (μm)	Slope (s^{-1})	Dissn. Rate (μm s^{-1})*10^3
0	0.531	7.627	40.499
5	1.191	3.864	46.020
10	0.779	6.607	51.468
20	0.937	5.610	52.565
30	1.421	3.110	44.193
40	1.083	2.444	26.468
50	1.100	1.674	18.414
60	0.971	0.497	4.825

A2.1.50

Dissolution of PMMA (M_n 107000, γ 1.10) in MEK/Ethanol at 25.0°C

% Ethanol	Film Thickness (μm)	Slope (s^{-1})	Dissn. Rate (μm s^{-1})*10^3
0	0.660	2.950	19.470
5	0.329	7.656	25.188
10	0.609	3.768	22.947
15	0.577	3.734	21.545
20	0.571	3.563	20.344
25	0.488	3.838	18.729
30	0.611	2.711	16.564
35	0.619	2.168	13.419
40	0.657	1.786	11.734

A2.1.51

Dissolution of PMMA (M_n 56000, γ 2.0) in MEK/1-Propanol at 25.0°C

% 1-Propanol	Film Thickness (μm)	Slope (s^{-1})	Dissn. Rate (μm s^{-1})*10^3
0	0.531	7.627	40.499
5	0.809	5.390	43.605
10	1.106	3.555	39.318
20	0.515	5.328	27.439
30	1.496	1.630	24.384
40	1.213	1.521	18.449
50	1.497	1.001	14.984

A2.1.52

Dissolution of PMMA (M_n 56000, γ 2.0) in MEK/2-Propanol at 25.0°C

% 2-Propanol	Film Thickness (μm)	Slope (s^{-1})	Dissn. Rate (μm s^{-1})*10^3
0	0.531	7.627	40.499
5	1.523	2.326	35.424
10	1.185	2.738	32.445
20	1.201	2.142	25.725
30	1.270	1.688	21.437
40	1.404	1.188	16.679
50	1.213	0.766	9.291
60	1.132	0.298	3.373
70	1.413	0.048	0.678

A2.1.53

Dissolution of PMMA (M_n 107000, γ 1.10) in MEK/2-Propanol at 25.0°C

% 2-Propanol	Film Thickness (μm)	Slope (s^{-1})	Dissn. Rate (μm s^{-1})*10^3
0	0.660	2.950	19.470
5	0.274	6.269	17.177
10	0.278	5.171	14.375
15	0.217	5.902	12.807
20	0.254	4.159	10.563
25	0.306	3.190	9.761
30	0.234	3.232	7.562
35	0.308	2.030	6.252
40	0.362	1.410	5.104

A2.1.54

Dissolution of PMMA (M_n 56000, γ 2.0) in MEK/1-Butanol at 25.0°C

% 1-Butanol	Film Thickness (μm)	Slope (s^{-1})	Dissn. Rate (μm s^{-1})*10^3
0	0.531	7.627	40.499
5	0.519	7.094	36.817
10	0.547	6.095	33.339
20	0.521	4.824	25.133
30	0.519	3.812	19.784
40	0.490	3.096	15.170
50	0.613	1.612	9.881
60	0.656	0.312	2.046
70	0.906	0.004	0.036

A2.1.55

Dissolution of PMMA (M_n 56000, γ 2.0) in MEK/2-Butanol at 25.0°C

% 2-Butanol	Film Thickness (μm)	Slope (s^{-1})	Dissn. Rate (μm s^{-1})*10^3
0	0.531	7.627	40.499
5	2.034	1.876	38.157
10	1.973	1.746	34.445
20	2.468	1.161	28.653
30	2.529	0.870	22.002
40	2.055	0.759	15.597
50	1.804	0.532	9.597
60	1.322	0.427	5.644

A2.1.56

Dissolution of PMMA (M_n 56000, γ 2.0) in MEK/Water at 25.3°C

% Water	Film Thickness (μm)	Slope (s^{-1})	Dissn. Rate (μm s^{-1})*10^3
0	1.800	2.318	41.724
1	1.120	5.220	58.464
2	1.280	5.297	67.801
3	1.220	6.349	77.457
4	1.640	5.100	83.640
6	1.520	5.837	88.722
7	1.630	5.350	87.205
8	1.170	7.400	86.580
9	1.990	4.354	86.644
10	1.570	5.390	84.623

A2.1.57

Dissolution of PMMA (M_n 56000, γ 2.0) in MEK/Water at 16.0°C

% Water	Film Thickness (μm)	Slope (s^{-1})	Dissn. Rate ($\mu m\ s^{-1}$)*10^3
0	1.911	0.609	11.637
2	2.094	0.974	20.395
4	2.516	0.946	23.801
6	1.970	1.072	21.118
8	1.789	1.185	21.199

A2.1.58

Dissolution of Polystyrene (M_w 430000, γ 3.1) in 60:40 MEK/IPA

T (°C)	Film Thickness (μm)	Dissn. Rate ($\mu m\ s^{-1}$)*10^3	ln (Dissn. Rate)
20.00	0.277	0.628	-7.372
24.90	0.209	1.126	-6.789
30.10	0.378	2.252	-6.096
34.90	0.335	3.309	-5.711
40.50	0.343	6.777	-4.994

A2.1.59

Dissolution of Polystyrene (M_w 430000, γ 3.1) in 40:60 MEK/IPA

T (°C)	Film Thickness (μm)	Dissn. Rate ($\mu m\ s^{-1}$)*10^3	ln (Dissn. Rate)
20.3	0.312	1.244	-6.689
26.4	0.399	5.063	-5.286
31.0	0.351	12.084	-4.416
35.8	0.351	45.226	-3.096
39.8	0.344	114.018	-2.171

A2.1.60

Dissolution of Poly(phenylmethylsilane) (M_n 7500, γ 1.4) in 75:25 MEK/IPA

T (°C)	ΔF (kHz)	(ΔF*Slope) (kHz s^{-1})	ln (ΔF*Slope)
15.00	2.953	23.122	3.141
20.10	2.644	31.511	3.450
24.90	3.340	46.620	3.842
30.10	2.833	57.363	4.049
35.10	2.717	55.709	4.020

A2.1.61

Dissolution of Poly(phenylmethylsilane) (M_n9600, γ 1.2) in 75:25 MEK/IPA

T (°C)	ΔF (kHz)	(ΔF*Slope) (kHz s^{-1})	ln (ΔF*Slope)
15.00	4.123	8.056	2.086
20.20	4.128	11.822	2.470
25.20	3.910	12.958	2.561
29.90	3.259	16.324	2.792
34.80	3.060	23.648	3.163
39.50	3.423	21.859	3.085

A2.1.62

Dissolution of Poly(phenylmethylsilane) (M_n 14500, γ 1.4) in 75:25 MEK/IPA

T (°C)	ΔF (kHz)	(ΔF*Slope) (kHz s^{-1})	ln (ΔF*Slope)
14.90	6.270	0.690	-0.371
20.20	5.697	1.607	0.474
25.00	6.376	2.283	0.825
29.90	6.514	5.979	1.788
34.90	6.362	9.791	2.281
40.20	6.835	14.094	2.646

A2.1.63

Dissolution of Poly(phenylmethylsilane) (M_n 18400, γ 1.4) in 75:25 MEK/IPA

T (°C)	ΔF (kHz)	(ΔF*Slope) (kHz s^{-1})	ln (ΔF*Slope)
15.00	1.907	0.606	-0.500
20.20	1.980	1.005	-0.005
25.20	1.519	2.212	0.794
29.90	1.249	3.617	1.286
34.80	2.493	8.234	2.108
39.50	1.765	10.874	2.386

A2.1.64

Dissolution of Poly(phenylmethylsilane) (M_n 29300, γ 1.9) in 75:25 MEK/IPA

T (°C)	ΔF (kHz)	(ΔF*Slope) (kHz s^{-1})	ln (ΔF*Slope)
15.00	2.211	0.285	-1.254
20.00	1.687	0.616	-0.484
24.80	2.243	1.501	0.406
29.80	2.127	1.887	0.635
35.00	2.244	5.439	1.694
39.90	1.918	8.758	2.170

A2.1.65

Dissolution of Poly(phenylmethylsilane) (M_n 36500, γ 1.9) in 75:25 MEK/IPA

T (°C)	ΔF (kHz)	(ΔF*Slope) (kHz s^{-1})	ln (ΔF*Slope)
15.00	2.632	0.029	-3.542
20.10	2.986	0.054	-2.923
24.90	2.638	0.098	-2.327
30.10	2.805	0.196	-1.628
35.10	2.182	0.482	-0.729
40.10	2.871	1.792	0.583

A2.1.66

Dissolution of Poly(phenylmethylsilane) (M_n 53700, γ 5.8) in 75:25 MEK/IPA

T (°C)	ΔF (kHz)	(ΔF*Slope) (kHz s^{-1})	ln (ΔF*Slope)
15.00	0.003	0.006	-5.153
19.85	0.005	0.012	-4.389
24.90	0.014	0.034	-3.388
30.10	0.053	0.116	-2.157
35.00	0.095	0.275	-1.290
40.00	0.341	0.784	-0.243

A2.1.67

Dissolution of Poly(phenylmethylsilane) (M_n 9600, γ 6.2) in 50:50 MEK/IPA

T (°C)	ΔF (kHz)	(ΔF*Slope) (kHz s^{-1})	ln (ΔF*Slope)
15.0	9.216	4.433	1.489
20.0	3.393	9.053	2.203
25.0	8.274	13.619	2.611
30.0	5.809	19.146	2.952
35.0	9.175	24.341	3.192
40.0	7.724	53.760	3.985

A2.1.68

Dissolution of Poly(phenylmethylsilane) (M_n 9600, γ 6.2) in 50:50 MIBK/IPA

T (°C)	ΔF (kHz)	(ΔF*Slope) (kHz s^{-1})	ln (ΔF*Slope)
15.0	2.142	1.829	0.604
20.0	2.786	2.736	1.006
25.0	3.033	3.934	1.370
30.0	2.944	8.414	2.130
35.0	2.598	13.413	2.596

A2.1.69

Dissolution of Poly(phenylmethylsilane) in MIBK/IPA at 24.7°C

% IPA	ΔF (kHz)	ΔF*Slope ($kHz\ s^{-1}$)	ln (ΔF*Slope)
0	7.684	31.120	3.438
10	7.219	52.843	3.967
20	7.077	32.038	3.467
30	7.259	22.909	3.132
40	6.362	10.822	2.382
50	7.836	4.694	1.546
60	7.215	0.874	-0.134
70	7.384	0.130	-2.041
80	7.561	0.009	-4.702

A2.1.70

Dissolution of Poly(vinyl cinnamate) in Toluene

T (°C)	ΔF (kHz)	(ΔF*Slope) ($kHz\ s^{-1}$)	ln (ΔF*Slope)
15.00	6.725	24.789	3.210
19.90	7.010	27.984	3.332
25.10	4.540	32.629	3.485
29.60	3.568	37.064	3.613
34.60	4.637	39.178	3.668

A2.1.71

Dissolution of Poly(vinyl cinnamate) in Acetone

T (°C)	ΔF (kHz)	(ΔF*Slope) ($kHz\ s^{-1}$)	ln (ΔF*Slope)
15.00	4.513	14.870	2.699
19.80	5.515	17.301	2.851
24.90	4.512	19.880	2.990
30.00	4.531	22.791	3.126

A2.1.72

Dissolution of Poly(vinyl cinnamate) in Xylene

T (°C)	ΔF (kHz)	(ΔF*Slope) (kHz s^{-1})	ln (ΔF*Slope)
15.00	6.458	2.370	0.863
20.00	6.323	6.696	1.902
24.90	6.207	21.321	3.059
29.60	7.249	41.769	3.732
34.30	4.745	79.678	4.377

A2.1.73

Dissolution of PMMA (M_n 56000, γ 2.0) in 75:25 MIBK/IPA at 25.0°C- UV Effect

UVA lamp

Exposure Time (min)	Film Thickness (μm)	Dissn. Rate (μm s^{-1})*10^3	ln (Dissn. Rate)
0	0.204	14.850	-6.512
10	0.257	17.700	-6.336
20	0.200	21.280	-6.152
28	0.193	25.900	-5.956
40	0.210	35.930	-5.629
60	0.215	58.730	-5.137

A2.1.74

Dissolution of PMMA (M_n 56000, γ 2.0) in 75:25 MIBK/IPA at 18.0°C - UV Effect

Hanovia Lamp

Exposure Time (min)	Film Thickness (μm)	Dissn. Rate (μm s^{-1})*10^3	ln (Dissn. Rate)
5	0.965	23.642	-3.745
10	0.913	38.437	-3.259
15	0.653	56.922	-2.867
20	0.802	86.928	-2.443
25	1.102	154.048	-1.870
30	0.782	225.528	-1.489

A2.1.75

Dissolution of PMMA (M_n 56000, γ 2.0) in 75:25 MIBK/IPA at 25.0°C - UV Effect

Hanovia Lamp

Exposure Time (min)	Film Thickness (μm)	Dissn. Rate (μm s^{-1})*10^3	ln (Dissn. Rate)
5	1.231	66.584	-2.709
10	0.687	99.745	-2.305
15	0.919	149.521	-1.900
20	1.028	185.040	-1.687
25	0.800	378.799	-0.971
30	0.844	697.228	-0.361

A2.1.76

Dissolution of PMMA (Mn 56000, γ 2.0) in 50:50 MEK/IPA at 20.5°C - UV Effect

UVA Lamp

Exposure Time (min)	Film Thickness (μm)	Dissn. Rate (μm s^{-1})*10^3	ln (Dissn. Rate)
0	0.963	3.206	-5.742
5	0.739	6.370	-5.056
10	0.975	11.319	-4.481
15	0.909	18.816	-3.973
26	0.779	53.205	-2.934
30	0.756	75.645	-2.582
42	0.746	246.329	-1.401
53	0.787	661.473	-0.413
60	0.951	576.496	-0.551

A2.1.77

Dissolution of PMMA (M_n 56000, γ 2.0) in n-Butyl Acetate at 20.4°C - UV Effect

Hanovia Lamp

Exposure Time (min)	Film Thickness (μm)	Dissn. Rate (μm s^{-1})*10^3	ln (Dissn. Rate)
3	0.841	35.750	-3.331
10	0.845	62.352	-2.775
15	0.617	100.663	-2.296
26	1.025	204.897	-1.585
30	0.856	236.341	-1.442
42	0.933	454.063	-0.790
60	0.797	797.000	-0.227

A2.1.78

Dissolution of PMMA (M_n 56000, γ 2.0) in n-Butyl Acetate at 25.0°C - UV Effect

UVA Lamp

Exposure Time (min)	Film Thickness (μm)	Dissn. Rate (μm s^{-1})*10^3	ln (Dissn. Rate)
0	0.205	1.439	-6.544
10	0.175	1.837	-6.299
20	0.209	2.393	-6.035
30	0.201	2.803	-5.877
40	0.166	3.578	-5.633
60	0.173	5.295	-5.241

A2.1.79

Dissolution of Poly(vinyl cinnamate) in 100% Acetone at 35.0°C - UV Effect

UVA Lamp

Exposure Time (min)	ΔF (kHz)	ΔF*Slope (kHz s^{-1})	ln (ΔF*Slope)
0	3.839	55.666	4.019
5	3.225	43.276	3.768
10	3.186	34.001	3.526
15	4.080	26.006	3.258
30	2.568	14.014	2.640
45	2.369	5.380	1.683

A2.1.80

Dissolution of Poly(vinyl cinnamate) in 100% Acetone at 45.0°C - UV Effect

UVA Lamp

Exposure Time (min)	ΔF (kHz)	ΔF*Slope (kHz s^{-1})	ln (ΔF*Slope)
0	4.405	29.306	3.378
5	2.294	19.341	2.962
10	4.863	14.934	2.704
15	4.963	12.060	2.490
30	2.974	6.159	1.818
45	2.646	3.106	1.133

Appendix Three

Appendix 3.0

A3.0 BASIC Programs

A3.1 "Volume Fraction Activity Coefficients and Flory-Huggins Interaction Parameters" BASIC Programs

A3.1.1 Calculation of Themodynamic Parameters - "FHUGGINS" BASIC Program

```
10    CLS
20    KEY OFF
30    PRINT TAB(8)"* * * *
```

```
270   PRINT:INPUT "Frequency of uncoated crystal at atmospheric
      pressure (Hz) ";H
280   INPUT "Frequency of coated crystal at atmospheric pressure (Hz) ";E
290   INPUT "Frequency of coated crystal at vacuum (Hz) ";J
300   '
310   'Calculation of activity coefficients
320   '
330   CLS
340   L=H-E                'Frequency change due to polymer
350   P0=(PR*133.322)           'Conversion to pascals
360   LOCATE 4,1:COLOR 0,7:PRINT "Enter values of frequency  (Hz) and
      pressure (Torr): ":COLOR 7,0
370   LOCATE 6,1
380   FOR I=1 TO N
390   INPUT K(I),P(I)           'Reading values of frequency and pressure
400   S(I)=J-K(I)               'Frequency change due to solvent
410   PHI(I)=((S(I)/D1)/((S(I)/D1)+(L/(D2)))          'Volume fraction of solvent
420   F(I)=(P(I)*133.322)/(P0*(PHI(I))
430   LGF(I)=LOG(F(I))
440   C1=(V1-B)/(8.314*T)
450   C2=((B*B)/((8.314*T)^2))
460   LNG(I)=LGF(I)+(C1*(P0-(P(I)*133.322)))+((C2*((P0^2)-
      ((P(I)*133.322)^2))/2))
470   'LNG(I) is the logarithm of the activity coefficient of absorbate based on
      volume fraction
480   NEXT I
490   PRINT "Name of run ";E$
500   '
510   'Calculation of Flory-Huggins interaction parameters
520   '
530   R=V2/V1                   'Size ratio of components
540   FOR I=1 TO N
550   PHI(I)=(L/D2)/((L/D2)+(S(I)/D1))       'Volume fraction of polymer
560   U(I)=1-PHI(I)
570   Q(I)=(1-1/R)*PHI(I)
580   KHI(I)=(LNG(I)-Q(I))/(PHI(I)^2)
590   'Flory-Huggins interaction parameter based on volume fraction
600   NEXT I
```

```
610     '
620     'Storing of constants and calculated data
630     '
640     OPEN E$ FOR OUTPUT AS #1        'Opening data file
650     WRITE #1,F$,C$,N,T,PR,D1,B,V1,D2,V2,VV,VS,H,E,J,L
660     FOR I=1 TO N
670     WRITE #1,K(I),P(I),S(I),PHI(I),U(I),LNG(I),KHI(I)
680     NEXT I
690     CLOSE #1
700     CLS
710     PRINT "FREQUENCY     PRESSURE      VOLUME FRACTION
        ACTIVITY      INTERACTION "
720     PRINT "CHANGE (Hz)    (Torr)          POLYMER  SOLVENT
        COEFFICIENT   PARAMETER"
730     PRINT:PRINT
740     FOR I=1 TO N
750     PRINT USING "#######     ##.###     #.####  #.####     #.####
        #.####"  ;S(I),P(I),PHI(I),U(I),LNG(I),KHI(I)
760     NEXT I
770     END
```

A3.1.2 Storage of Constants for "FHUGGINS" - "CONSTANTS"

```
10    CLS
20    PRINT TAB(17) "* * * *
```

```
340     OPEN IP$ FOR OUTPUT AS #1
350     WRITE #1,F$,C$,N,T,PR,D1,B,V1,D2,V2
360     CLOSE #1
370     '
380     LOCATE 10,10:COLOR 0,7:PRINT "Do you wish to view the stored data
        (Y/N)?";:COLOR 7,0
390     A$=INKEY$
400     IF A$="Y" OR A$="y" THEN GOTO 490
410     IF A$="N" OR A$="n" THEN GOTO 660
420     GOTO 390
430     CLS
440     LOCATE 10,10:COLOR 0,7:INPUT "Name of input file: ";IP$:COLOR 7,0
450     OPEN IP$ FOR INPUT AS #1
460     INPUT #1,F$,C$,N,T,PR,D1,B,V1,D2,V2
470     CLOSE #1
480     '
490     'Display of stored data
500     '
510     CLS
520     LOCATE 5,1:COLOR 0,7:PRINT "The following constants have been
        stored in data file: "IP$:COLOR 7,0
530     LOCATE 8,1:PRINT "Name of polymer deposited on crystal: "F$
540     PRINT "Name of vapour used: "C$
550     PRINT "Absolute temperature (K): "T
560     PRINT "S.V.P. OF Vapour (Torr): "PR
570     PRINT "Density of vapour (g cm^-3): "D1
580     PRINT "Second virial coefficient of vapour (m^3 mol^-1): "B
590     PRINT "Molar volume of vapour (m^3 mol^-1): "V1
600     PRINT "Density of polymer (g cm^-3): "D2
610     PRINT "Molar volume of polymer (m^3 mol^-1): "V2
620     PRINT:PRINT
630     '
640     'Printout of constants
650     '
660     PRINT:COLOR 0,7:PRINT "Do you require a printout of the constants
        (Y/N)?";:COLOR 7,0
670     A$=INKEY$
680     IF A$="Y" OR A$="y" THEN GOTO 740
```

```
690     IF A$="N" OR A$="n" THEN GOTO 880
700     GOTO 670
710     '
720     'Printout of stored constants
730     '
740     CLS
750     COLOR 0,7:LPRINT "The following constants have been stored in data
        file: "IP$;: COLOR 7,0
760     LPRINT:LPRINT
770     LOCATE 8,1:LPRINT "Name of polymer deposited on crystal: "F$
780     LPRINT "Name of vapour used: "C$
790     LPRINT "Number of data points: "N
800     LPRINT "Absolute temperature (K): "T
810     LPRINT "S.V.P. OF Vapour (Torr): "PR
820     LPRINT "Density of vapour (g cm^-3): "D1
830     LPRINT "Second virial coefficient of vapour (m^3 mol^-1): "B
840     LPRINT "Molar volume of vapour (m^3 mol^-1): "V1
850     LPRINT "Density of polymer (g cm^-3): "D2
860     LPRINT "Molar volume of polymer (m^3 mol^-1): "V2
870     GOTO 890
880     CLS
890     LOCATE 15,15:COLOR 0,7:PRINT "The constants have been stored in
        data file: "IP$;:COLOR 7,0
900     LOCATE 18,10:PRINT "The stored constants can be used in the
        calculation of activity coefficients and Flory-Huggins"
910     PRINT "interaction parameters by accessing the 'FHUGGINS' program"
920     END
```

A3.2 "Rate of Dissolution of Thin Films" BASIC Program

```
10      CLS
20      KEY OFF
30      PRINT TAB(8) "* * * *
```

```
340   LOCATE 5,1:PRINT "Name of run: "N$
350   PRINT:PRINT "Name of polymer deposited on crystal: "P$
360   PRINT:PRINT "Molecular weight of polymer: "MW
370   PRINT:PRINT "Solvent system to be used (Solvent 1/Solvent 2): "S$
380   PRINT:PRINT "Percentage weight of Solvent 1/Solvent 2: "W%
390   PRINT:PRINT "Stirrer set point: "F
400   PRINT:PRINT "Temperature of system (°C): "T
410   '
420   'To commence program
430   '
440   LOCATE 22,1:COLOR 0,7:PRINT"Press ANY key to continue";:COLOR
      7,0
450   IF INKEY$ = "" GOTO 450
460   SCREEN 0,0,0:WIDTH 80
470   CLS
480   LOCATE 5,1:COLOR 0,7:PRINT "Before commencing the run, please
      ensure that:-":COLOR 7,0
490   LOCATE 8,1:PRINT "1. The Frequency Counter is switched on"
500   PRINT "2. The power supplies and Q.C.M. are functioning"
510   PRINT "3. The stirrer is set to correct r.p.m."
520   '
530   'Initialisation of IEEE card
540   '
550   DIM X(3000),Y(3000),T(3000)
560   DEF SEG=&HC400
570   CMD$="syscon mad=3,cic=1,nob=1,ba0=&h300
580   IE488=0
590   A%=0:FLG%=0:BRD%=0
600   CALL IE488(CMD$,A%,FLG%,BRD%)
610   IF FLG%<>0 THEN PRINT "INSTALLATION ERROR" GOTO 2600
620   CMD$="REMOTE 12"
630   BRD%=0
640   CALL IE488(CMD$, A%, FLG%, BRD%)
650   IF FLG%<>0 THEN PRINT "ERROR ";HEX$(FLG%) GOTO 2600
660   LOCATE 18,15:COLOR 0,7:PRINT"Press ANY key to start collecting
      data";: COLOR 7,0
670   IF INKEY$= "" GOTO 670
680   CLS
```

```
690   LOCATE 2,17:COLOR 0,7:PRINT "To stop collecting data press
      <F10>":COLOR 7,0
700   LOCATE 5,1
710   PRINT "NUMBER OF POINTS     TIME (s)      FREQUENCY (Hz)"
720   LOCATE 7,1
730   CMD$="CLEAR 12"
740   BRD%=0
750   CALL IE488 (CMD$,VAR%,FLG%,BRD%)
760   IF FLG%<>0 THEN PRINT "ERROR" ;HEX$(FLG%) GOTO 2600
770   'To switch back to reading frequency A
780   VAR$="FA"
790   CMD$="OUTPUT 12[$E]"
800   CALL IE488(CMD$,VAR$,FLG%,BRD%)
810   VAR$="AFE"                    'Enable filter on channel A
820   CMD$="OUTPUT 12[$E]"
830   CALL IE488(CMD$, VAR$, FLG%, BRD%)
840   T0=TIMER                      'Starting timer
850   WHILE T8<2970
860   NN=NN+1
870   T9=TIMER:T(NN)=T9-T0
880   IF NN=1 THEN 900
890   IF INT(T(NN))=INT(T(NN-1)) THEN 870
900   DVM$=SPACE$(25)
910   CMD$="ENTER 12[$,0,20]"
920   CALL IE488(CMD$, DVM$, FLG%, BRD%)
930   V$=RIGHT$(DVM$,18)
940   D9=VAL(V$)
950   T8=TIMER-T0
960   IF FLAG%<>0 THEN GOTO 2600
970   X(NN)=T8: Y(NN)=D9
980   PRINT NN,"",X(NN),"",Y(NN)
990   KEY(10) ON: ON KEY(10) GOSUB 1040
1000  IF A$="FIN" THEN 1050
1010  GOTO 850
1020  WEND
1030  GOTO 1050
1040  A$="FIN":RETURN
1050  CLS:LOCATE 5,1:PRINT "Program has been terminated"
```

```
1060  '
1070  'Choose type of file required
1080  '
1090  CLS
1100  LOCATE 5,1:COLOR 0,7:PRINT"The data can be processed as
      follows:-";:COLOR 7,0
1110  LOCATE 8,1:PRINT" <1> - Generate a data file"
1120  PRINT:PRINT" <2> - Display data on screen"
1130  PRINT:PRINT" <3> - Exit to BASIC"
1140  PRINT:PRINT" <4> - Printout constants used"
1150  LOCATE 20,1:COLOR 0,7:PRINT"Enter selection number (1-4):
      ";:COLOR 7,0
1160  A$=INKEY$: IF A$="" GOTO 1160
1170  PRINT A$
1180  IF VAL(A$)=1 THEN GOTO 1240
1190  IF VAL(A$)=2 THEN GOTO 1600
1200  IF VAL(A$)=3 THEN CLS:LOCATE 13,18:COLOR 0,7:PRINT "The
      program has been treminated":COLOR 7,0:END
1210  IF VAL(A$)=4 THEN GOTO 2170
1220  PRINT "[";A$;"] is not a valid entry. Please re-enter selection": GOTO
      1150
1230  '
1240  'Generation of data file
1250  '
1260  CLS
1270  COLOR  0,7:LOCATE 12,15:INPUT"Please type data file name
      [DRIVE]:NAME.EXT";FILX$:COLOR 7,0
1280  OPEN FILX$ FOR OUTPUT AS #1
1290  WRITE #1, P$, MW, S$, W, F, T, NN
1300  K=30
1310  IF NN<30 THEN K=NN
1320  FOR I=1 TO K
1330  WRITE #1, I, X(I), Y(I)
1340  NEXT
1350  IF K<30 THEN 1530
1360  K=120
1370  IF NN<120 THEN K=NN
1380  FOR I = 35 TO K STEP 5
```

```
1390  WRITE #1, I, X(I), Y(I)
1400  NEXT
1410  IF K<120 THEN 1530
1420  K=600
1430  IF NN<600 THEN K=NN
1440  FOR I = 130 TO K STEP 10
1450  WRITE #1, I, X(I), Y(I)
1460  NEXT
1470  IF K<600 THEN 1530
1480  K=2000
1490  IF NN<3000 THEN K=NN
1500  FOR I=630 TO K STEP 30
1510  WRITE #1, I, X(I), Y(I)
1520  NEXT
1530  CLOSE #1
1540  CLS
1550  LOCATE 8,1:PRINT "The data has been stored in data file " FILX$
1560  LOCATE 17,1:COLOR 0,7:PRINT "Press ANY key to return to the main
      menu";:COLOR 7,0
1570  IF INKEY$ = "" GOTO 1570
1580  GOTO 1090
1590  '
1600  'Display of data on screen
1610  '
1620  CLS
1630  LOCATE 10,17:COLOR 0,7:PRINT "-Do you wish to view the constants
      used (Y/N)?-";:COLOR 7,0
1640  A$=INKEY$
1650  IF A$="Y" OR A$="y" THEN GOTO 1670 ELSE IF A$<>"" THEN GOTO
      1780
1660  GOTO 1640
1670  CLS
1680  LOCATE 4,1:COLOR 0,7:PRINT "The following constants were used:-":
      COLOR 7,0
1690  LOCATE 7,1:PRINT "Name of run: "N$
1700  PRINT:PRINT "Name of polymer deposited on crystal: "P$
1710  PRINT:PRINT "Molecular weight of polymer: "MW
1720  PRINT:PRINT "Solvent system used: "S$
```

```
1730  PRINT:PRINT "Percentage weight of Solvent 1/Solvent 2: "W%
1740  PRINT:PRINT "Stirrer set point: "F
1750  PRINT:PRINT "Temperature of system (°C): "T
1760  LOCATE 23,1:COLOR 0,7:PRINT"Press ANY key to view collected
      data";:COLOR 7,0
1770  IF INKEY$ = "" GOTO 1770
1780  CLS
1790  LOCATE 3,1:COLOR 0,7:PRINT "Name of run:- " N$:COLOR 7,0
1800  PRINT:PRINT "The following data has been collected:-"
1810  LOCATE 8,1:PRINT "NUMBER OF POINTS     TIME (s)
      FREQUENCY (Hz)"
1820  FOR I = 0 TO NN
1830  PRINT I, "", X(I), "", Y(I)
1840  A$ = INKEY$
1850  IF A$=CHR$(27) THEN I = NN+3
1860  IF A$<>"" THEN GOTO 2320
1870  NEXT I
1880  IF I = NN+3 GOTO 1070
1890  PRINT:PRINT
1900  '
1910  'Printout of data
1920  '
1930  PRINT:COLOR 0,7:PRINT "Do you require a printout of the data (Y/N)?";
      :COLOR 7,0
1940  A$ = INKEY$
1950  IF A$ = "Y" OR A$ = "y" THEN GOTO 1970 ELSE IF A$<>"" THEN GOTO
      2260
1960  GOTO 1940
1970  CLS
1980  LOCATE 10,15:COLOR 0,7:PRINT "Press any key to start printout of
      collected data";:COLOR 7,0
1990  IF INKEY$ ="" GOTO 1990
2000  CLS
2010  LPRINT "* * * * * * * * * * * * * * * * * * * * * * * * * * * * * * * * * * * * *"
2020  LPRINT "*       Rate of Dissolution of Thin Polymer Films    * "
2030  LPRINT "* * * * * * * * * * * * * * * * * * * * * * * * * * * * * * * * * * * * *"
2040  LPRINT:LPRINT
2050  LPRINT "Name of run:-" N$
```

```
2060  LPRINT "Data of collected:-"
2070  LPRINT:LPRINT
2080  LPRINT "NUMBER OF POINTS     TIME (s)      FREQUENCY (Hz)"
2090  FOR I = 0 TO NN
2100  LPRINT I, "", X(I), "", Y(I)
2110  A$ = INKEY$
2120  IF A$ = CHR$(27) THEN I = NN+3
2130  IF A$<>"" THEN GOTO 2320
2140  NEXT I
2150  IF I = NN+3 GOTO 1070
2160  PRINT:PRINT
2170  '
2180  'Printout of variables
2190  '
2200  CLS
2210  LOCATE 6,10:COLOR 0,7:PRINT "-Do you require a printout of the
      constants used (Y/N)?-";:COLOR 7,0
2220  A$ = INKEY$
2230  IF A$ = "Y" OR A$ = "y" THEN 2350
2240  IF A$ = "N" OR A$ = "n" THEN 2270
2250  GOTO 2220
2260  '
2270  CLS
2280  LOCATE 10,18:COLOR 0,7:PRINT "Press ANY key to return to storage
      menu";: COLOR 7,0
2290  IF INKEY$ = "" GOTO 2290
2300  CLS
2310  GOTO 1070
2320  FOR K = 1 TO 50 :NEXT K                    'delay
2330  IF INKEY$=1 TO 50 :NEXT K
2340  GOTO 1870
2350  LOCATE 17,15:COLOR 0,7:PRINT "Press ANY key to start printout of
      constants";:COLOR 7,0
2360  IF INKEY$="" GOTO 2360
2370  CLS
2380  LOCATE 5,1:PRINT "Name of run: "N$
2390  PRINT:PRINT "Name of polymer deposited on crystal: "P$
2400  PRINT:PRINT "Molecular weight of polymer: "MW
```

```
2410  PRINT:PRINT "Solvent system to be used (Solvent 1/Solvent 2): "S$
2420  PRINT:PRINT "Percentage weight of Solvent 1/Solvent 2: "W%
2430  PRINT:PRINT "Stirrer set point: "F
2440  PRINT:PRINT "Temperature of system(°C): "T
2450  LPRINT
2460  LPRINT:LPRINT "Name of run: "N$
2470  LPRINT:LPRINT "Name of polymer deposited on crystal: "P$
2480  LPRINT:LPRINT "Molecular weight of polymer: "MW
2490  LPRINT:LPRINT "Solvent system to be used (Solvent 1/Solvent 2): "S$
2500  LPRINT:LPRINT "Percentage weight of Solvent 1/Solvent 2: "W%
2510  LPRINT:LPRINT "Stirrer set point: "F
2520  LPRINT:LPRINT "Temperature of system (°C): "T
2530  LPRINT
2540  LOCATE 24,1:COLOR 0,7:PRINT "Press ANY key to return to storage
      menu";:COLOR 7,0
2550  IF INKEY$="" GOTO 2550
2560  CLS
2570  GOTO 1070
2580  CMD$="CLEAR 12"
2590  CALL IE488(CMD$,VAR$,FLG%,BRD%)
2600  CLS
2610  LOCATE 10,15:PRINT"An error has occurred - arrays need to be
      redimensioned"
2620  LOCATE 15,15:COLOR 0,7:PRINT"Please press ANY key to return to
      menu";:COLOR 7,0
2630  LOCATE 15,15:COLOR 0,7:PRINT"Press ANY key to return to
      menu";:COLOR 7,0
2640  GOTO 1090
2650  END
```